

2016

Strategies for Enhanced After-Treatment Performance: Post Injection Characterization and Long Breathing with Low NO_x Combustion

Marko Jeftic
University of Windsor

Follow this and additional works at: <http://scholar.uwindsor.ca/etd>

Recommended Citation

Jeftic, Marko, "Strategies for Enhanced After-Treatment Performance: Post Injection Characterization and Long Breathing with Low NO_x Combustion" (2016). *Electronic Theses and Dissertations*. Paper 5737.

This online database contains the full-text of PhD dissertations and Masters' theses of University of Windsor students from 1954 forward. These documents are made available for personal study and research purposes only, in accordance with the Canadian Copyright Act and the Creative Commons license—CC BY-NC-ND (Attribution, Non-Commercial, No Derivative Works). Under this license, works must always be attributed to the copyright holder (original author), cannot be used for any commercial purposes, and may not be altered. Any other use would require the permission of the copyright holder. Students may inquire about withdrawing their dissertation and/or thesis from this database. For additional inquiries, please contact the repository administrator via email (scholarship@uwindsor.ca) or by telephone at 519-253-3000ext. 3208.

STRATEGIES FOR ENHANCED AFTER-TREATMENT PERFORMANCE:
POST INJECTION CHARACTERIZATION AND LONG BREATHING WITH LOW
NO_x COMBUSTION

by
Marko Jeftić

A Dissertation
Submitted to the Faculty of Graduate Studies
through Mechanical, Automotive, and Materials Engineering
in Partial Fulfillment of the Requirements for
the Degree of Doctor of Philosophy at the
University of Windsor

Windsor, Ontario, Canada

© 2016 Marko Jeftić

Strategies for Enhanced After-Treatment Performance:
Post Injection Characterization and Long Breathing with Low NO_x Combustion

by

Marko Jeftić

APPROVED BY:

Dr. J. G. Hawley, External Examiner
University of Bath, United Kingdom

Dr. X. Chen, Outside Reader
Department of Electrical & Computer Engineering

Dr. D. Ting, Department Reader
Department of Mechanical, Automotive, and Materials Engineering

Dr. J. Tjong, Department Reader
Department of Mechanical, Automotive, and Materials Engineering

Dr. G. T. Reader, Advisor
Department of Mechanical, Automotive, and Materials Engineering

Dr. M. Zheng, Advisor
Department of Mechanical, Automotive, and Materials Engineering

3 May 2016

AUTHOR'S DECLARATION OF ORIGINALITY

I hereby certify that I am the sole author of this thesis and that the framework and the details of the technical core of the thesis have not been published. The proof of the majority of findings has mostly been refereed and produced to original research publications in journals and professional conferences with myself being the first author.

I certify that, to the best of my knowledge, my thesis does not infringe upon anyone's copyright nor violate any proprietary rights and that any ideas, techniques, quotations, or any other material from the work of other people included in my thesis, published or otherwise, are fully acknowledged in accordance with the standard referencing practices. Furthermore, to the extent that I have included copyrighted material that surpasses the bounds of fair dealing within the meaning of the Canada Copyright Act, I certify that I have obtained a written permission from the copyright owner(s) to include such material(s) in my thesis and have included copies of such copyright clearances to my appendix.

I declare that this is a true copy of my thesis, including any final revisions, as approved by my thesis committee and the Graduate Studies office, and that this thesis has not been submitted for a higher degree to any other University or Institution.

ABSTRACT

A novel long breathing technique was created to achieve ultra-low NO_x emissions with reduced supplemental fuel consumption compared to conventional strategies. Long breathing refers to the use of in-cylinder NO_x reduction to prolong the NO_x storage (breathing) cycle of a lean NO_x trap (LNT). Exhaust gas recirculation (EGR) was used with conventional diesel fuel and steady-state experimental tests identified that engine-out NO_x emissions of 0.4 to 0.8 g/kW·hr were suitable for long breathing operation. The results indicated that the reduced engine-out NO_x emissions significantly prolonged the NO_x storage cycle and decreased the supplemental fuel consumption penalty of the LNT for all of the tested conditions.

However, the long breathing strategy was mainly suitable for low and medium loads, below 10 bar indicated mean effective pressure (IMEP), because the supplemental fuel savings of the long breathing LNT were offset by increased fuel consumption from the engine and increased smoke emissions at higher loads. Long breathing was also developed with neat n-butanol for in-cylinder NO_x reduction. However, the long breathing strategy with neat n-butanol was primarily suitable for low load operation (below 6 bar IMEP) under the tested conditions because of increased engine fuel consumption and increased NO_x emissions at higher loads.

Post injection strategies were developed for active control of the exhaust gas temperature for enhanced LNT performance. The results indicated that active management of the exhaust gas temperature was achieved by using relatively high intake oxygen, 16.5 to 20.8 percent by volume (%V), and by controlling the duration of early post injections, 20 to 60 degrees crank angle after top dead centre (°CA ATDC). Post injection strategies were also implemented for increased in-cylinder production of desirable NO_x reducing agents like hydrogen to benefit the LNT NO_x conversion efficiency. Engine tests demonstrated that the combination of very low intake oxygen (<10%V), low temperature combustion, and an early post injection exponentially increased the yields of hydrogen (0.76%V), carbon monoxide (1.96%V), and ethylene (0.19%V) despite the relatively low in-cylinder temperatures. However, the same conditions also undesirably increased the methane emissions up to 0.30%V.

DEDICATION

This work is dedicated to my mom, dad, and sister.

ACKNOWLEDGEMENTS

The primary person whom I would like to acknowledge is my thesis supervisor, Dr. Ming Zheng. Under Dr. Zheng's guidance, I was able to grow and develop my research abilities and I consider these experiences to be of extremely high value to my past and future career development. I would also like to give special acknowledgement to my co-adviser Dr. Graham T. Reader. I consider it a privilege to have been able to interact with and learn from such a distinguished individual.

Furthermore, I would like to thank all of the current and the past members of the Clean Diesel Engine Laboratory at the University of Windsor, including Dr. Shui Yu, Dr. Meiping Wang, Dr. Xiaoye Han, Dr. Tadanori Yanai, Dr. Xiao Yu, Tongyang Gao, Kelvin Xie, Prasad Divekar, Qingyuan Tan, Shouvik Dev, Zhenyi Yang, Geraint Bryden, Chris Aversa and Mark Ives. We each have our individual strengths and, through our daily interactions, I was able to learn from my colleagues and absorb some of their strengths and integrate them to my own abilities.

I would also like to thank the following University of Windsor faculty and staff members: Dr. Jimi Tjong, Dr. David S-K Ting, Dr. Edwin Tam, Dr. Daniel Green, Dr. Jerry Sokolowski, Dr. Vladimir Bajic, Dr. Nader Zamani and Bruce Durfy. I would like to thank the following organizations which have provided funding support: the Natural Sciences and Engineering Research Council of Canada; the Ontario Ministry of Training, Colleges, and Universities; the University of Windsor; Auto21; the Canada Research Chairs program; Canada Foundation for Innovation; Ontario Innovation Trust; the Ford Motor Company, and the AVL University Partnership Program. Finally, I would like to thank my parents and my sister for all their love and support throughout my life.

TABLE OF CONTENTS

AUTHOR’S DECLARATION OF ORIGINALITY	iii
ABSTRACT	iv
DEDICATION	v
ACKNOWLEDGEMENTS	vi
LIST OF TABLES	xi
LIST OF FIGURES	xiv
LIST OF ABBREVIATIONS.....	xxii
MAJOR RESULTS.....	xxv
CHAPTER 1: INTRODUCTION AND LITERATURE REVIEW	1
1.1 Dissertation Outline	1
1.2 Research Objective	3
1.3 Research Motivation	4
1.4 Formation of NO _x Emissions in Internal Combustion Engines	8
1.5 In-Cylinder NO _x Emission Reduction Literature Review	10
1.6 Post Injection Emission Reduction Literature Review	16
1.7 Lean-Burn After-Treatment NO _x Emission Reduction Literature Review	18
1.8 Chapter Summary	24
CHAPTER 2: RESEARCH PLAN.....	25
2.1 General Research Outline	25
2.2 Long Breathing Lean NO _x Trap	26
2.3 Long Breathing LNT with EGR and Diesel Fuel	33
2.4 Long Breathing LNT with Neat Butanol Fuel	35
2.5 Post Injection Strategies for the Active Control of the Exhaust Gas	37

CHAPTER 3: RESEARCH TOOLS	40
3.1 Experimental Setup for Engine Tests	40
3.2 Experimental Setup for After-Treatment Flow Bench Tests	44
CHAPTER 4: LONG BREATHING USING DIESEL FUEL AND EGR	48
4.1 Engine Test Conditions for the EGR Tests.....	48
4.2 NO _x Reduction with EGR	50
4.3 Effect of EGR on Emissions and Engine Fuel Consumption	52
4.4 Chapter Summary for Long Breathing using EGR and Diesel Fuel.....	59
CHAPTER 5: LONG BREATHING USING NEAT BUTANOL FUEL	61
5.1 Ultra-Low NO _x Emissions with Neat Butanol Fuel	61
5.2 Strategies to Mitigate the Peak Pressure Rise Rate of Neat Butanol	67
5.3 Increased Engine Load with a Post Injection of Neat Butanol Fuel	85
5.4 High Load Operation with Neat Butanol Fuel.....	93
5.5 Chapter Summary for Long Breathing using Neat Butanol Fuel	104
CHAPTER 6: LONG BREATHING LEAN NO _x TRAP	107
6.1 Setup of the Lean NO _x Trap Numerical Model.....	107
6.2 LNT Numerical Model Validation	111
6.3 Quantification of Energy Savings for Long Breathing with Diesel and EGR...	115
6.4 Quantification of Energy Savings for Long Breathing with Neat Butanol.....	128
6.5 Chapter Summary for Supplemental Fuel Savings with Long Breathing	135
CHAPTER 7: ACTIVE CONTROL OF THE EXHAUST GAS TEMPERATURE AND COMPOSITION TO AID LNT PERFORMANCE	139
7.1 The Purpose of Exhaust Gas Management	139

7.2 Effects of Post Injection Duration and Timing on Exhaust Temperature and Composition.....	141
7.3 Effects of Engine Load and Combustion Phasing on Exhaust Temperature and Composition.....	155
7.4 Effects of Intake Oxygen and Low Temperature Combustion on Exhaust Temperature and Composition.....	165
7.5 Chapter Summary for Exhaust Gas Management.....	177
CHAPTER 8: CONCLUSIONS AND FUTURE WORK.....	179
8.1 Long Breathing LNT with Diesel Fuel and EGR	179
8.2 High Load Operation with Neat Butanol Fuel.....	180
8.3 Long Breathing LNT with Neat Butanol Fuel	180
8.4 Active Control of the Exhaust Gas Temperature and Composition	181
8.5 Recommendations for Future Work	182
REFERENCES	184
APPENDIX A: DERIVATION OF THE HEAT RELEASE RATE EQUATION.....	197
APPENDIX B: ADDITIONAL NEAT BUTANOL TEST RESULTS	200
APPENDIX C: ADDITIONAL EXHAUST GAS MANAGEMENT RESULTS	207
APPENDIX D: ADDITIONAL FIGURES FOR EXPERIMENTAL SETUP.....	214
APPENDIX E: PROPORTIONALITY FACTOR CALCULATION	215
APPENDIX F: DEFINITION OF TERMS	217
APPENDIX G: TRIPLE POST INJECTION STRATEGY WITH NEAT BUTANOL FUEL.....	218
APPENDIX H: EFFECTS OF FUEL INJECTION PRESSURE ON EXHAUST TEMPERATURE AND COMPOSITION.....	223

LIST OF AUTHORED AND CO-AUTHORED PUBLICATIONS.....	229
VITA AUCTORIS	233

LIST OF TABLES

Table 2-1: Operating Conditions for Preliminary Flow Bench Test.....	31
Table 2-2: Properties of n-Butanol Fuel Compared to Conventional Diesel Fuel.....	36
Table 3-1: Test Engine and Fuel Injection System Specifications	42
Table 3-2: Pressure Transducer Specifications.....	42
Table 4-1: Test Conditions for Low Load EGR Sweep.....	49
Table 4-2: Test Conditions for Medium Load EGR Sweep	49
Table 4-3: Test Conditions for High Load EGR Sweep.....	49
Table 4-4: Upper Limit for Intake Oxygen for Long Breathing LNT Operation	51
Table 4-5: Lower Limit for Intake Oxygen for Long Breathing LNT Operation.....	53
Table 4-6: Summary of Fuel Consumption Penalties at Different Engine Loads	59
Table 5-1: Test Conditions for Comparison of Butanol and Diesel	62
Table 5-2: Test Conditions for Single Shot Injection Timing Sweep.....	68
Table 5-3: Test Conditions for Butanol Pilot Injection Timing Sweep	73
Table 5-4: Test Conditions for Butanol Post Injection Timing Sweep.....	78
Table 5-5: Test Conditions for Butanol Post Injection Duration Sweep	85
Table 5-6: Test Conditions for a Modified Butanol Single Post Injection Strategy.....	94
Table 5-7: Test Conditions for a Butanol Double Post Injection Strategy	98
Table 5-8: Representative Exhaust Gas Conditions with Neat Butanol	105
Table 6-1: Thermal and Physical Properties of the Numerical Model Catalyst	108
Table 6-2: Physical Properties of the Experimental Flow Bench Catalyst.....	109
Table 6-3: Operating Conditions for Experimental Flow Bench Test.....	113
Table 6-4: Exhaust Gas Conditions for Diesel Combustion with EGR.....	116
Table 6-5: Stored NO _x Mass for Low Load Diesel Conditions	120

Table 6-6: Supplemental LNT Fuel Consumption for Low Load Diesel Conditions.....	120
Table 6-7: Supplemental Fuel Penalty for Low Load Diesel Conditions.....	120
Table 6-8: Regeneration Duration as a Function of Storage Duration	121
Table 6-9: Stored NO _x Mass for Mid Load Diesel Conditions	124
Table 6-10: Supplemental LNT Fuel Consumption for Mid Load Diesel Conditions ...	124
Table 6-11: Supplemental Fuel Penalty for Mid Load Diesel Conditions.....	124
Table 6-12: Stored NO _x Mass for High Load Diesel Conditions.....	126
Table 6-13: Supplemental LNT Fuel Consumption for High Load Diesel Conditions ..	126
Table 6-14: Supplemental Fuel Penalty for High Load Diesel Conditions	126
Table 6-15: Exhaust Conditions for Neat Butanol Combustion	129
Table 6-16: Stored NO _x Mass for Low Load Butanol.....	130
Table 6-17: Supplemental LNT Fuel Consumption for Low Load Butanol.....	130
Table 6-18: Supplemental Fuel Penalty for Low Load Butanol	130
Table 6-19: Stored NO _x Mass for Mid & High Load Butanol	134
Table 6-20: Supplemental LNT Fuel Consumption for Mid & High Load Butanol	134
Table 6-21: Supplemental Fuel Penalty for Mid & High Load Butanol.....	134
Table 6-22: Long Breathing Results for Combustion with Diesel Fuel and EGR.....	137
Table 6-23: Summary of Long Breathing Results for Neat n-Butanol Combustion	138
Table 7-1: Diesel Post Injection Duration Test Matrix.....	142
Table 7-2: Test Conditions for Post Injection Timing Sweep at 6.1 bar IMEP	148
Table 7-3: Test Conditions for Engine Load and Combustion Phasing Study	155
Table 7-4: Test Conditions for the Intake Oxygen Study	166
Table 7-5: Test Conditions for Intake Oxygen Sweep Study	172
Table 7-6: Test Conditions for LTC Post Injection Sweep Study	175

Table B-1: Test Conditions for Broad Range Butanol Post Injection Timing Sweep	200
Table F-1: Definition of Different Load Levels	217
Table F-2: Definition of Post Injection Timing Descriptions.....	217
Table G-1: Test Conditions for Butanol Triple Post Injection Duration Sweep.....	218
Table G-2: Tabulated Data for Butanol Multiple Post Injection Strategies.....	222
Table H-1: Test Conditions for Injection Pressure Study.....	223

LIST OF FIGURES

Figure 1-1: Dissertation Outline	2
Figure 1-2: Space Filling Diagram for NO (Left) and NO ₂ (Right)	5
Figure 1-3: US EPA Heavy Duty Diesel On-Highway Emission Standards [9]	6
Figure 1-4: Corporate Average Fuel Economy Standards in USA [13]	7
Figure 1-5: 1999-2011 Diesel Passenger Car Market Share in Western Europe [15]	8
Figure 1-6: Air Composition by Volumetric Fraction	9
Figure 1-7: Low Pressure (Left) and High Pressure (Right) EGR Loop	11
Figure 1-8: SCR System with Upstream DOC and Urea Mixer	19
Figure 1-9: LNT NO _x Storage (Left) and Regeneration (Right) Processes	23
Figure 2-1: Outline of Proposed Research Topics	26
Figure 2-2: Conventional LNT Fuel Injection Frequency	27
Figure 2-3: Long Breathing LNT Fuel Injection Frequency	27
Figure 2-4: Methodology for Supplemental Fuel Savings with the Long Breathing Strategy.....	28
Figure 2-5: Effect of NO _x Level on NO _x Storage Efficiency	29
Figure 2-6: NO _x Storage Efficiency for a Fixed NO _x Storage Duration	30
Figure 2-7: LNT Adsorption Duration as a Function of Feed Gas NO _x	31
Figure 2-8: LNT Supplemental Energy Consumption as a Function of Feed Gas NO _x ..	32
Figure 2-9: Effect of EGR on NO _x and Smoke	33
Figure 2-10: Effect of EGR on THC and CO	34
Figure 3-1: Schematic Diagram of the Experimental Setup for the Engine Tests.....	41
Figure 3-2: Photo of the After-treatment Flow Bench Setup.....	46
Figure 4-1: Effect of Intake Oxygen on NO _x Emissions for Long Breathing LNT	50

Figure 4-2: Effect of Intake Oxygen on Smoke Emissions	52
Figure 4-3: Effect of Intake Oxygen on THC Emissions	54
Figure 4-4: Effect of Intake Oxygen on CO Emissions	55
Figure 4-5: Effect of EGR on ISFC at Low Load Conditions	56
Figure 4-6: Effect of EGR on ISFC at Medium Load Conditions	57
Figure 4-7: Effect of EGR on ISFC at High Load Conditions	58
Figure 4-8: Summary for EGR Sweep Tests for Long Breathing LNT	60
Figure 5-1: Butanol vs. Diesel: Effect of Load on NO _x and Smoke	63
Figure 5-2: Comparison of Ignition Delay for Butanol and Diesel	64
Figure 5-3: Butanol vs. Diesel: Effect of Load on PRR and COV _{IMEP}	66
Figure 5-4: Butanol vs. Diesel: In-Cylinder Pressure Comparison	66
Figure 5-5: Butanol vs. Diesel: Heat Release Rate Comparison	67
Figure 5-6: Butanol Single Shot Fuel Injection Timing vs. PRR, Efficiency, and COV _{IMEP}	69
Figure 5-7: Effect of Butanol Single Shot Injection Timing on In-Cylinder Pressure	69
Figure 5-8: Effect of Butanol Single Shot Injection Timing on the Heat Release Rate ...	70
Figure 5-9: Effect of Butanol Single Shot Injection Timing on NO _x and Smoke	71
Figure 5-10: Effect of Butanol Single Shot Injection Timing on CO and Hydrocarbons	72
Figure 5-11: Effect of Butanol Pilot Injection Timing on PRR, Efficiency, and COV _{IMEP}	74
Figure 5-12: Effect of Butanol Pilot Injection Timing on In-Cylinder Pressure	74
Figure 5-13: Effect of Butanol Pilot Injection Timing on Heat Release Rate	75
Figure 5-14: Effect of Butanol Pilot Injection Timing on Bulk Gas Temperature	76
Figure 5-15: Effect of Butanol Pilot Injection Timing on NO _x and Smoke	76

Figure 5-16: Effect of Butanol Pilot Injection Timing on CO and Hydrocarbons	77
Figure 5-17: Effect of Butanol Post Injection Timing on PRR, Efficiency, COV_{IMEP}	79
Figure 5-18: Effect of Butanol Post Injection Timing on Heat Release Rate.....	80
Figure 5-19: Effect of Butanol Post Injection Timing on In-Cylinder Pressure.....	80
Figure 5-20: Effect of Butanol Post Injection Timing on NO_x and Smoke Emissions	81
Figure 5-21: Effect of Butanol Post Injection Timing on Bulk Gas Temperature.....	82
Figure 5-22: Effect of Butanol Post Injection Timing on CO and Hydrocarbons	83
Figure 5-23: Comparison of Different Butanol Injection Strategies for PRR Reduction	84
Figure 5-24: Effect of Butanol Post Injection Duration on IMEP and PRR.....	86
Figure 5-25: Effect of Butanol Post Injection Duration on In-Cylinder Pressure	86
Figure 5-26: Effect of Butanol Post Injection Duration on Heat Release.....	87
Figure 5-27: Effect of Butanol Post Injection Duration on Logarithmic Pressure	88
Figure 5-28: Effect of Butanol Post Injection Duration on Bulk Gas Temperature	88
Figure 5-29: Effect of Butanol Post Injection Duration on COV_{IMEP} and Efficiency	89
Figure 5-30: Effect of Butanol Post Injection Duration on NO_x and Smoke Emissions..	90
Figure 5-31: Effect of Butanol Post Injection Duration on CO and THC Emissions.....	91
Figure 5-32: Effect of Butanol Post Injection Duration on Hydrocarbon Speciation.....	91
Figure 5-33: Comparison of Butanol Single Shot Injection and Post Injection	92
Figure 5-34: Effect of Modified Butanol Single Post Injection Strategy on PRR, IMEP, and COV_{IMEP}	94
Figure 5-35: Effect of Modified Butanol Single Post Injection Strategy on HRR	95
Figure 5-36: Effect of Modified Butanol Single Post Injection Strategy on In-Cylinder Pressure.....	96
Figure 5-37: Effect of Modified Butanol Single Post Injection Strategy on Efficiency...	96

Figure 5-38: Effect of Modified Butanol Single Post Injection Strategy on Bulk Gas Temperature	97
Figure 5-39: Effect of Butanol Double Post Injection Strategy on PRR, IMEP, COV_{IMEP}	98
Figure 5-40: Effect of Butanol Double Post Injection Strategy on Heat Release.....	99
Figure 5-41: Effect of Butanol Double Post Injection Strategy on In-Cylinder Pressure	99
Figure 5-42: Effect of Butanol Double Post Injection Strategy on Efficiency and Exhaust Temperature	100
Figure 5-43: Effect of Butanol Double Post Injection Strategy on Indicated NO_x and Smoke Emissions	101
Figure 5-44: Effect of Butanol Double Post Injection Strategy on Bulk Gas Temperature	102
Figure 5-45: Effect of Butanol Double Post Injection Strategy on CO and THC	102
Figure 5-46: Effect of Butanol Double Post Injection Strategy on Light Hydrocarbons	103
Figure 6-1: Three Dimensional LNT Mesh	108
Figure 6-2: Validation Tests for the Numerical Models.....	112
Figure 6-3: Repeatability Tests for the Empirical Flow Bench Tests.....	114
Figure 6-4: Comparison of 1D Model and Empirical Data	114
Figure 6-5: NO_x Storage Efficiency for Low Load Diesel Conditions	117
Figure 6-6: LNT Saturation for Low Load Diesel Conditions	117
Figure 6-7: Required NO_x Conversion Efficiency for Low Load Diesel.....	118
Figure 6-8: Storage Duration & Required NO_x Conversion Efficiency at Low Load ...	119
Figure 6-9: Long Breathing Energy Savings for Low Load Diesel Conditions	122

Figure 6-10: Storage Duration & Required NO _x Conversion Efficiency at Mid Load..	123
Figure 6-11: Long Breathing Energy Savings for Mid Load Diesel Conditions	125
Figure 6-12: Storage Duration & Required NO _x Conversion Efficiency at High Load.....	127
Figure 6-13: Long Breathing Energy Savings for High Load Diesel Conditions.....	127
Figure 6-14: NO _x Storage Duration for Low Load Butanol.....	131
Figure 6-15: LNT Fuel Consumption Penalty for Low Load Butanol	131
Figure 6-16: NO _x Storage Duration for Mid and High Load Butanol	133
Figure 6-17: LNT Fuel Consumption Penalty for Mid and High Load Butanol	133
Figure 7-1: Comparison between Baseline Single Shot Injection and Post Injection	141
Figure 7-2: Effect of Post Injection Timing on Heat Release Rate	143
Figure 7-3: Effect of Post Injection Duration at 30°C CA ATDC on the HRR	143
Figure 7-4: Effect of Post Injection Duration at 100°C CA ATDC on the HRR	144
Figure 7-5: Post Injection Quantity and Timing vs. Exhaust Temperature (9.9 bar)	145
Figure 7-6: Post Injection Quantity and Timing vs. Exhaust Temperature (5.8 bar)	147
Figure 7-7: Effect of Post Injection Timing on Exhaust Temperature (6.1 bar).....	148
Figure 7-8: Exhaust Temperature Control via Post Injection Duration & Timing	149
Figure 7-9: Optimal Post Injection Timing for Exhaust Temperature Control	150
Figure 7-10: Effect of Post Injection on the Formation of NO _x Reducing Agents (9.9 bar)	151
Figure 7-11: Effect of Post Injection on Hydrocarbon Speciation (9.9 bar).....	152
Figure 7-12: Effect of Post Injection Quantity and Timing on NO _x (9.9 bar)	153
Figure 7-13: Optimal Post Injection Timing for NO _x Reducing Agents.....	154
Figure 7-14: In-cylinder Pressure for Post Injection at 30°C CA ATDC.....	156

Figure 7-15: HRR Comparison for Post Injection at 50° & 70°CA ATDC	157
Figure 7-16: Effect of Engine Load on IMEP and Exhaust Temperature	158
Figure 7-17: Effect of Engine Load on NO _x and Smoke Emissions	159
Figure 7-18: Engine Load & Combustion Phasing vs. Post Bulk Gas Temperature	161
Figure 7-19: Effect of Engine Load and Combustion Phasing on CO Emission.....	161
Figure 7-20: Effect of Engine Load and Post Timing on THC Emission.....	162
Figure 7-21: Exhaust Gas Speciation for Low Engine Load	163
Figure 7-22: Exhaust Gas Speciation for High Engine Load (14.7 bar IMEP)	165
Figure 7-23: Effect of Intake Oxygen on IMEP and Exhaust Temperature	167
Figure 7-24: Effect of Oxygen on NO _x and Smoke Emissions	168
Figure 7-25: Effect of Oxygen on Carbon Monoxide Emissions	169
Figure 7-26: Effect of Oxygen on Hydrocarbon Speciation.....	170
Figure 7-27: Effect of Intake Oxygen Sweep on H ₂ , CO, and THC.....	173
Figure 7-28: Effect of Intake Oxygen Sweep on Hydrocarbon Speciation	174
Figure 7-29: Effect of LTC Post Injection Timing Sweep on H ₂ , CO, and THC.....	175
Figure 7-30: Effect of LTC Post Injection Timing Sweep on Hydrocarbon Speciation.....	176
Figure B-1: Comparison of Butanol Main and Post Injection Ignition Delay	200
Figure B-2: Butanol Post Injection Timing vs. PRR, COV _{IMEP} , and Efficiency	201
Figure B-3: Effect of Butanol Post Injection Timing on NO _x and Smoke Emissions ...	201
Figure B-4: Effect of Butanol Post Injection Timing on CO and THC Emissions.....	202
Figure B-5: Effect of Butanol Post Injection Timing on Hydrocarbon Speciation	202
Figure B-6: Effect of Butanol Post Injection Timing on Heat Release Rate	203
Figure B-7: Effect of Butanol Post Injection Duration on NO _x and Smoke Fractions ..	203

Figure B-8: Effect of Butanol Post Injection Duration on Indicated CO and THC.....	204
Figure B-9: Effect of Modified Butanol Single Post Injection Strategy on Indicated NO _x and Smoke Emissions.....	204
Figure B-10: Effect of Modified Butanol Single Post Injection Strategy on Raw NO _x and Smoke Emissions	205
Figure B-11: Effect of Modified Butanol Single Post Injection Strategy on CO and THC.....	205
Figure B-12: Effect of Modified Butanol Single Post Injection Strategy on Light Hydrocarbons	206
Figure B-13: Effect of Butanol Double Post Injection Strategy on NO _x and Smoke	206
Figure C-1: Duration of Early Post Injection vs. HRR (5.8 bar)	207
Figure C-2: Duration of Late Post Injection vs. HRR (5.8 bar).....	207
Figure C-3: Post Injection Duration and Timing vs. NO _x Reducing Agents (5.8bar) ...	208
Figure C-4: Post Injection Duration & Timing vs. Hydrocarbon Speciation (5.8 bar) ..	209
Figure C-5: Effect of Post Injection Quantity and Timing on NO _x (5.8bar).....	210
Figure C-6: Effect of Post Injection Timing on THC, CO, H ₂ (6.1 bar)	210
Figure C-7: Effect of Post Injection Timing on Hydrocarbon Speciation (6.1 bar)	211
Figure C-8: Effect of Intake Oxygen on Total Hydrocarbon Emissions	211
Figure C-9: Effect of Intake Oxygen Sweep on NO _x and Smoke Emissions	212
Figure C-10: Effect of Intake Oxygen Sweep on the Exhaust Temperature	212
Figure C-11: Effect of LTC Post Injection Timing Sweep on NO _x and Smoke	213
Figure D-1: Schematic Diagram of the After-treatment Flow Bench.....	214
Figure G-1: Effect of Butanol Third Post Injection Timing on IMEP, PRR, p _{MAX}	218
Figure G-2: Effect of Butanol Third Post Injection Timing on Heat Release	219
Figure G-3: Effect of Butanol Third Post Injection Timing on In-Cylinder Pressure	219

Figure G-4: Effect of Butanol Third Post Injection Timing on Bulk Gas Temperature	220
Figure G-5: Effect of Butanol Third Post Injection Timing on Exhaust Temperature and Efficiency	220
Figure G-6: Effect of Butanol Third Post Injection Timing on Indicated NO _x and Smoke.....	221
Figure G-7: Effect of Butanol Third Post Injection Timing on CO and THC	221
Figure G-8: Comparison of Butanol Multiple Post Injection Strategies.....	222
Figure H-1: Effect of Injection Pressure on IMEP and Exhaust Temperature	224
Figure H-2: Repeatability Test for Effect of Injection Pressure on IMEP	224
Figure H-3: Effect of Injection Pressure on CO and THC Emissions	225
Figure H-4: Effect of Injection Pressure on Hydrocarbon Speciation (14.7 bar)	226
Figure H-5: Effect of Injection Pressure on Hydrocarbon Speciation (6 bar)	227
Figure H-6: Effect of Injection Pressure on NO _x and Smoke Emissions.....	228

LIST OF ABBREVIATIONS

Uppercase

1D	one dimensional	[-]
3D	three dimensional	[-]
AFR	air to fuel ratio	[-]
ATDC	after compression top dead centre	[-]
BDC	bottom dead centre	[-]
BMEP	brake mean effective pressure	[bar]
BSFC	brake specific fuel consumption	[g/kW·hr]
BTDC	before compression top dead centre	[-]
CA	crank angle	[°]
CA50	crank angle of 50% cumulative heat released	[°]
CAI	California Analytical Instruments	[-]
CI	compression ignition	[-]
COV	coefficient of variation	[%]
DI	direct injection	[-]
DPF	diesel particulate filter	[-]
EGR	exhaust gas recirculation	[-]
EPA	Environmental Protection Agency	[-]
FPGA	field programmable gate array	[-]
FSN	filter smoke number	[-]
FTIR	Fourier transform infrared spectroscopy	[-]
GHSV	gas hourly space velocity	[1/h]
HCCI	homogeneous charge compression ignition	[-]

HRR	apparent heat release rate	[J/°CA]
HTC	high temperature combustion	[-]
IMEP	indicated mean effective pressure	[bar]
ISFC	indicated specific fuel consumption	[g/kW·hr]
LHV	lower heating value	[MJ/kg]
LNT	lean nitrogen oxide trap	[-]
LTC	low temperature combustion	[-]
NI	National Instruments	[-]
NO _x	nitrogen oxides	[-]
PCCI	partially premixed charge compression ignition	[-]
PM	particulate matter	[-]
PO _x	partial oxidation	[-]
PRR	pressure rise rate	[bar/°CA]
Q	apparent heat release	[J]
RT	real-time	[-]
SCR	selective catalytic reduction	[-]
SI	spark ignition	[-]
SOC	start of combustion	[-]
SOI	start of injection	[-]
SR	steam reforming	[-]
STP	standard temperature and pressure	[-]
T	temperature	[°C], [K]
TDC	top dead centre	[-]
THC	total hydrocarbon	[-]

TWCC	three way catalytic converter	[-]
V	volume	[m ³], [L]
WGS	water gas shift	[-]

Lowercase

hr	hour	[hr]
p	absolute pressure	[Pa]
ppmV	parts per million by volume	[ppmV]
rpm	revolutions per minute	[rpm]

Greek

γ	heat capacity ratio	[-]
λ	excess air ratio	[-]
μ	mean value	[-]
η	indicated thermal efficiency	[%]
σ	standard deviation	[-]
τ_{ID}	ignition delay	[ms]

Subscripts

MAX	maximum	[-]
-----	---------	-----

Other Symbols

%V	percent by volume	[%V]
----	-------------------	------

MAJOR RESULTS

- A novel long breathing technique was created that utilized a combination of in-cylinder and after-treatment NO_x reduction for reduced supplemental fuel consumption of a lean NO_x trap (LNT).
- The long breathing method employed in-cylinder strategies, such as the use of exhaust gas recirculation (EGR) with diesel fuel, to reduce the engine-out NO_x emissions to a range of 0.4 to 0.8 g/kW·hr. Consequently, the reduced engine-out NO_x emissions prolonged the NO_x storage cycle, reduced the regeneration frequency, and resulted in supplemental energy savings for the LNT at all of the tested conditions.
- Extensive tests and analysis suggested that the long breathing strategy with EGR and diesel fuel was more suitable for low and medium load conditions (6 to 10 bar IMEP) because of increased engine fuel consumption and increased smoke emissions at high load conditions (14 bar IMEP).
- The long breathing technique was also developed with the use of neat n-butanol in a compression ignition engine. The results indicated that the long breathing method provided supplemental fuel savings at low and medium load conditions. Long breathing was primarily suitable at low load since the supplemental fuel savings of the long breathing strategy were outweighed by the increased fuel consumption of the engine at medium load.
- High load operation, at 14 bar IMEP, was demonstrated for neat n-butanol combustion in a compression ignition engine. Multiple post injection strategies were used to attain tolerable peak pressure rise rates, lower than 15°C/CA/bar. However, long breathing was not suitable at the tested conditions since the exhaust contained a relatively high amount of NO_x emissions that were incompatible with the long breathing method.
- Active control of the exhaust gas temperature was implemented with the use of early post injections to improve the performance of a lean NO_x trap. An optimal post injection timing was identified which allowed for effective management of the exhaust gas temperature with reduced impacts on the exhaust emissions.

- Strategies for increased in-cylinder production of desirable NO_x reducing agents like hydrogen, carbon monoxide, and light hydrocarbons were developed to enhance the NO_x conversion efficiency of an LNT. Increased yields of light hydrocarbons were achieved with the use of a post injection and medium intake oxygen levels (16.5%V). The results demonstrated that the yield was sensitive to the post injection timing.
- The combination of an early post injection, very low intake oxygen (<10%V) and low temperature combustion was implemented to obtain an amplified yield of hydrogen (0.76%V), carbon monoxide (1.96%V), and ethylene (0.19%V). However, the same conditions also resulted in a substantial methane emission penalty of 0.30%V. Nonetheless, the results demonstrated that low temperature combustion conditions exponentially increased the in-cylinder formation of desirable NO_x reducing agents like hydrogen despite the relatively low in-cylinder temperatures.

CHAPTER 1: INTRODUCTION AND LITERATURE REVIEW

This chapter gives the dissertation outline and presents the research objectives. The main engineering challenges associated with the research objectives will be presented; the background information will be provided to place the research within the present-day and the near-future context. A literature review will outline the current research trends and the state of currently available technologies.

1.1 Dissertation Outline

The dissertation consists of eight chapters as illustrated in Figure 1-1. The dissertation structure is categorized into four broad categories. The first three chapters provide an introduction to the dissertation. Chapter 1 gives a literature review and outlines the research motivation and the research objectives. Chapter 2 presents the research plan and introduces the long breathing technique. The research tools and the experimental setup for the proposed research are described in Chapter 3.

Chapters 4 through 7 represent the main body of the dissertation. Chapters 4 to 6 focus on the long breathing lean NO_x trap (LNT) strategy. Long breathing with exhaust gas recirculation and diesel fuel is demonstrated in Chapter 4. The engine test results are used to identify suitable engine operating conditions and potential fuel consumption and emission penalties for the long breathing method. Chapter 5 applies the use of neat n-butanol fuel with long breathing. The advantages of neat n-butanol fuel, compared to diesel fuel, are discussed with regards to the long breathing method. Butanol high load operation¹ is demonstrated with the use of multiple post injection strategies. The exhaust gas conditions at low, medium, and high load operation with neat n-butanol are summarized. Chapter 6 combines the engine test data from Chapters 4 and 5 with results from a numerical LNT model to quantify the supplemental energy savings of the long breathing LNT method. The results in Chapter 6 lead to recommendations regarding the use of the long breathing technique at different engine operating conditions.

¹ The terms low load, mid load, and high load are used throughout the text and are defined in Appendix F. The terms early and late post injection are also defined in Appendix F.

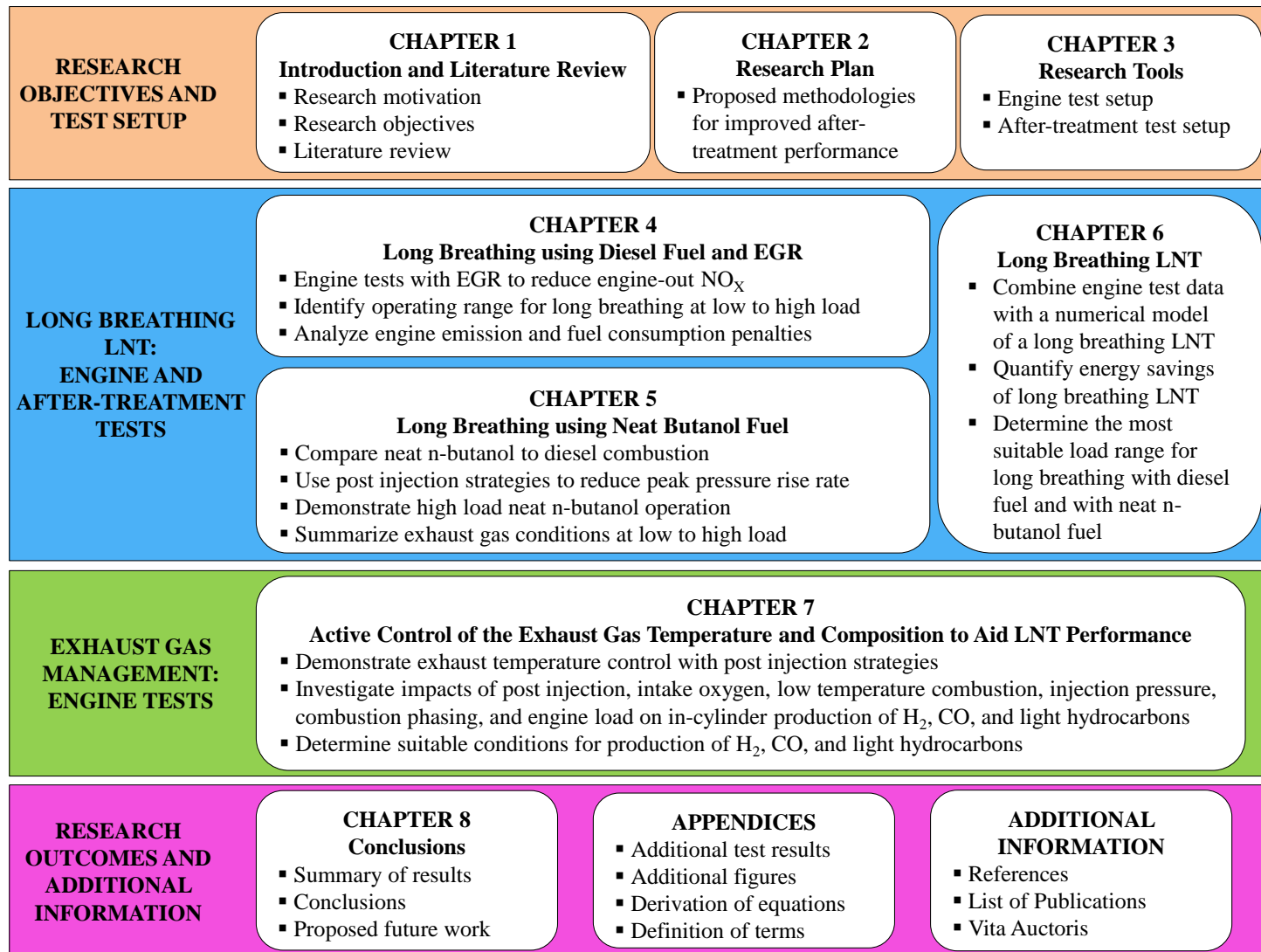


Figure 1-1: Dissertation Outline

In Chapter 7, strategies are developed for the use of post injections for active control of the exhaust gas to improve LNT performance. The effects of the post injection timing, the post injection duration, the intake oxygen, the engine load, the combustion phasing, and low temperature combustion on the exhaust gas temperature and speciation are analyzed. The critical parameters for exhaust gas temperature control and for the in-cylinder production of suitable NO_x reducing agents are identified. A post injection strategy is implemented for generating a high yield of hydrogen, carbon monoxide, and light hydrocarbons.

Chapter 8 gives a summary of the major findings and conclusions from Chapters 4 to 7. Recommendations for future work are also given. Additional information is given in the form of references, list of publications, and appendices. The appendices provide additional figures and test results for Chapters 4 to 7.

1.2 Research Objective

The main objective of the research was to demonstrate strategies for ultra-low NO_x emissions with reduced supplemental fuel penalties compared to traditional methods. A novel long breathing technique was proposed² that significantly extends the NO_x storage (breathing) cycle of an LNT. The long breathing method aimed to accomplish the aforementioned objective by combining the use of in-cylinder NO_x emission control with the use of a lean NO_x trap. The in-cylinder emission control strategies included the use of exhaust gas recirculation with diesel fuel and the use of neat n-butanol. The in-cylinder strategies were used to reduce the engine-out NO_x emissions to extend the NO_x adsorption cycle of the LNT. A longer adsorption cycle would consequently reduce the regeneration frequency³ and the supplemental fuel consumption of the LNT.

Engine tests were proposed to demonstrate and to quantify the in-cylinder NO_x emission reduction with the use EGR and diesel fuel and the use of neat n-butanol for low

² The long breathing method is described in detail in section 2.2.

³ The LNT regeneration process is detailed in section 1.7.

to high load conditions. Numerical modelling was applied to simulate the operation of a lean NO_x trap. The aim was to combine the engine test data with the numerical modelling results to quantify the energy savings and to determine suitable operating conditions for the long breathing method.

The NO_x storage and NO_x conversion efficiencies of an LNT are sensitive to the exhaust temperature and composition⁴. Therefore, a second objective was to develop post injection strategies to control the exhaust gas temperature and composition. Engine tests were proposed to investigate the effects of the post injection timing and duration, the engine load, the combustion phasing, the intake oxygen, and low temperature combustion on the exhaust gas temperature and composition. A detailed measurement of hydrogen and light hydrocarbon species was conducted since the presence of these species can benefit the NO_x reduction performance of an LNT. The goal was to identify a suitable post injection strategy for active control of the exhaust temperature and for in-cylinder formation of hydrogen, carbon monoxide, and light hydrocarbons.

1.3 Research Motivation

The reduction of nitrogen oxide (NO_x) emissions from lean-burn compression ignition (CI) engines is a major contemporary engineering challenge. Nitrogen oxides consist of various compounds of nitrogen and oxygen but, with regards to on-road vehicles and internal combustion engines, engine-out NO_x emissions mainly consist of nitric oxide (NO) and a minor portion of nitrogen dioxide (NO_2) as illustrated in Figure 1-2 [1,2]. Nitric oxide is a molecule composed of one nitrogen and one oxygen atom. It is a colourless gas at standard temperature and pressure (STP) [3,4]. Although it has been medically administered as a clinical treatment, the toxicology of inhaled nitric oxide is not fully understood [5]. However, nitric oxide readily reacts with molecular oxygen to form nitrogen dioxide according to Equation 1-1. To convert 20 ppm of NO in air to 5 ppm of NO_2 , the reaction time is over 1 hour but 80 ppm of NO in air can convert to 5 ppm of NO_2 in about 3 minutes [5].

⁴ The desired exhaust temperature and composition for an LNT are described in section 7.1.

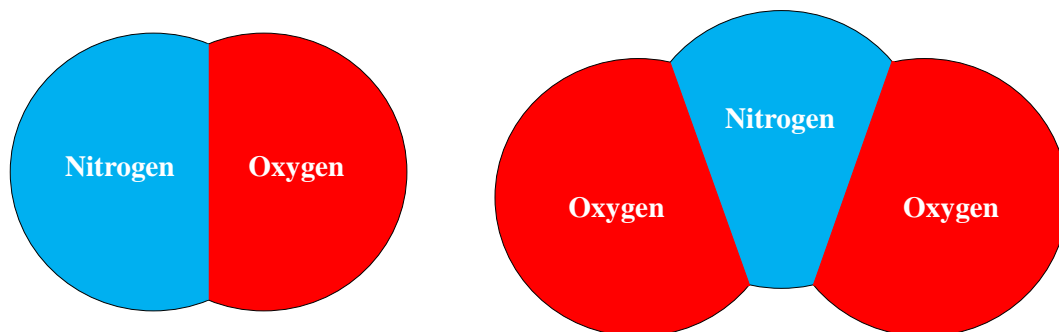
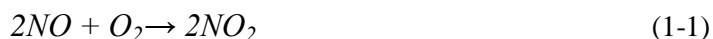


Figure 1-2: Space Filling Diagram for NO (Left) and NO₂ (Right)



Nitrogen dioxide is a brownish-red gas with a pungent odor [5,6]. It consists of two oxygen atoms and one nitrogen atom as shown in Figure 1-2. It is toxic to humans in concentrations as low as 5 ppm over an eight hour exposure period [7]. Human exposure to nitrogen dioxide is associated with numerous pulmonary diseases. Acute effects of nitrogen dioxide exposure may include coughing, shortness of breath, and irritation of the eyes, the nose, the skin, and the lungs [8]. Chronic health effects include genetic mutations and permanent lung damage and high exposures can lead to pulmonary edema and even death [8]. Nitrogen dioxide can also have seriously adverse effects on the environment. Nitrogen dioxide can react in the atmosphere to form nitric acid which can contribute to acid rain and it can react to form ground-level ozone and photochemical smog [8].

Due to the adverse effects of nitrogen dioxide, numerous regulating agencies, such as Environment Canada and the United States Environmental Protection Agency (EPA), have implemented strict standards to regulate the release of nitrogen oxides from motor vehicles. For the purposes of NO_x emission regulations, the common practice is to treat all nitrogen oxides that are released from vehicle exhaust as nitrogen dioxide because of the detrimental effects of NO₂ and the fact that nitric oxide readily converts to nitrogen dioxide in the earth's atmosphere. Increased awareness of the harmful impacts

of vehicle exhaust emissions led to the enforcement of progressively more stringent emission regulations, particularly with respect to NO_x and particulate matter (PM) as highlighted by the 97% reductions from 1988 to 2010 for the on-road heavy duty vehicles shown in Figure 1-3.

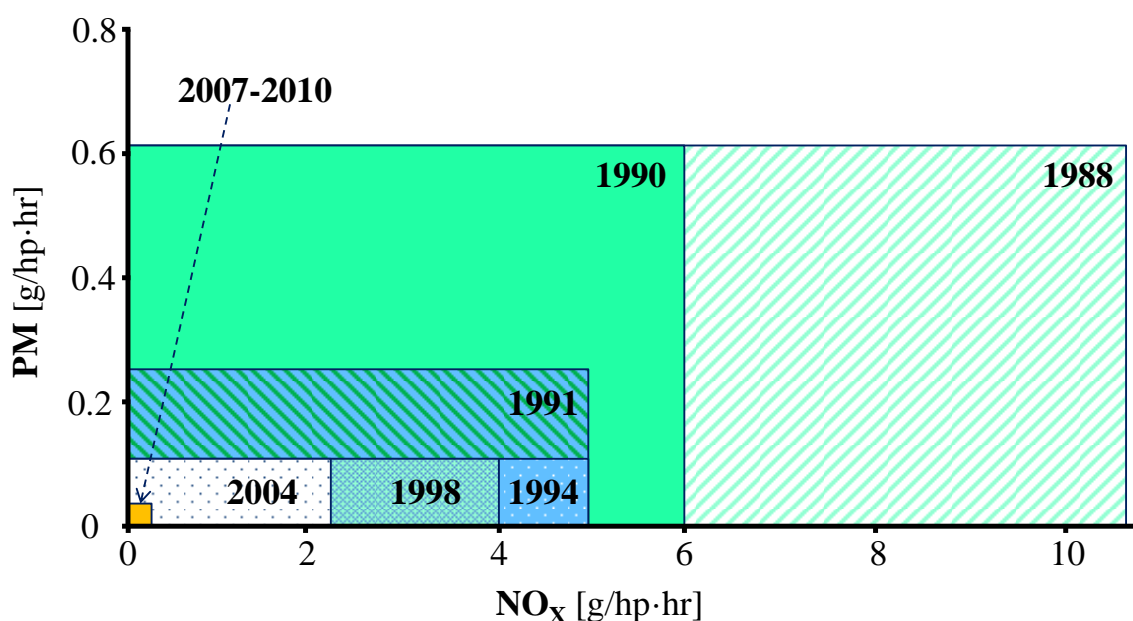


Figure 1-3: US EPA Heavy Duty Diesel On-Highway Emission Standards [9]

There are indications that future vehicle emission standards will continue this trend because the California Air Resources Board has investigated the potential for further NO_x emission reductions of at least 75% for heavy duty on-road vehicles [10-12]. Furthermore, the implementation of more rigorous emission testing procedures and the regulation of particle number emissions, in addition to the particle mass, are expected [10]. At the same time, corporate average fuel economy (CAFE) standards have been implemented which intend to promote fuel efficient vehicles as shown in Figure 1-4. These regulations have compelled engine and vehicle manufacturers to develop new technologies to satisfy the nitrogen oxide emission requirements while also improving the fuel efficiency of the vehicle.

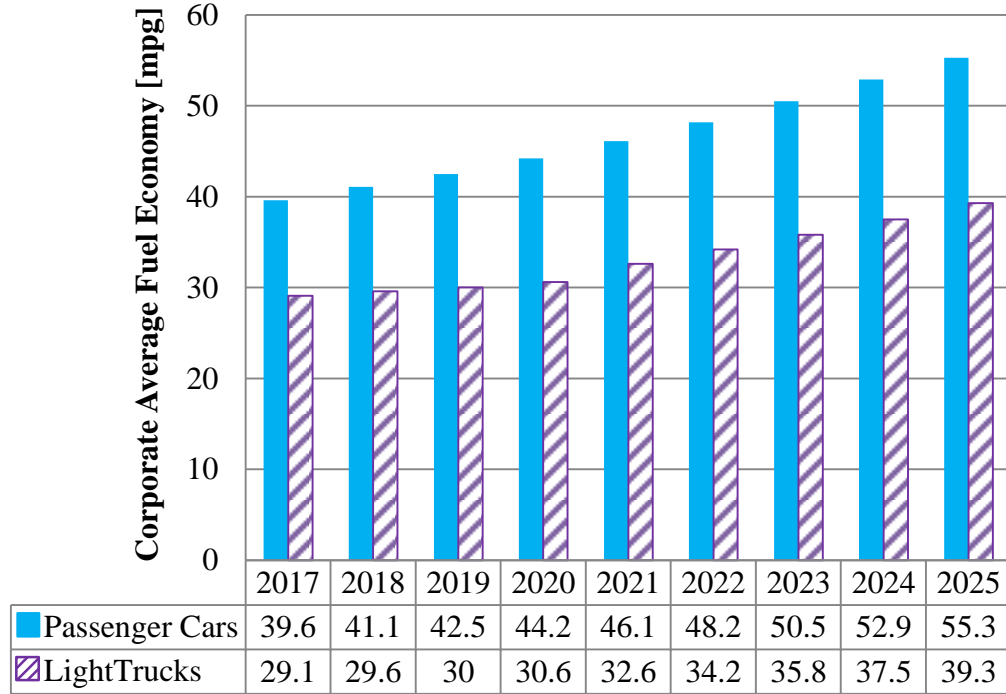
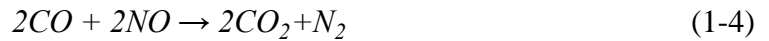
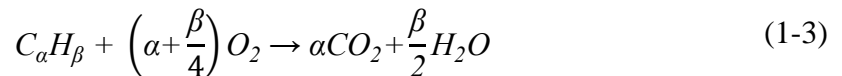
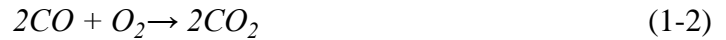


Figure 1-4: Corporate Average Fuel Economy Standards in USA [13]

The three-way catalytic converter (TWCC) has been successfully implemented for the reduction of NO_x emissions from passenger cars with stoichiometric spark ignition (SI) engines [14]. The TWCC functions by oxidizing carbon monoxide and hydrocarbons to carbon dioxide and water under fuel-lean exhaust conditions and by reducing nitrogen oxides to nitrogen under fuel-rich exhaust conditions. Alteration of fuel-lean and fuel-rich exhaust gas conditions of an SI engine can be achieved without undesirable effects to the engine drivability, the fuel consumption, and the emissions. Examples of the global reactions of a TWCC are shown in Equations 1-2 to 1-4.



Lean-burn compression ignition engines, such as diesel engines, are generally more suitable than SI engines for heavy duty transportation due to their superior fuel efficiency and torque output. With the recent implementation of strict fuel consumption standards for passenger cars and light duty trucks, lean-burn CI engines are also becoming more common in these sectors, particularly in Western Europe as shown in Figure 1-5. However, the three-way catalytic converter is not suitable for NO_x reduction in lean-burn CI engines due to the relative abundance of oxygen in the exhaust gas. Diverse technologies have been developed for NO_x reduction in lean-burn CI engines but most come with penalties and trade-offs as will be discussed in more detail in the ensuing sections of this chapter. Thus, in the present and, at least, the near future, the reduction of nitrogen oxide emissions from lean-burn compression ignition engines will continue to be a key engineering challenge.

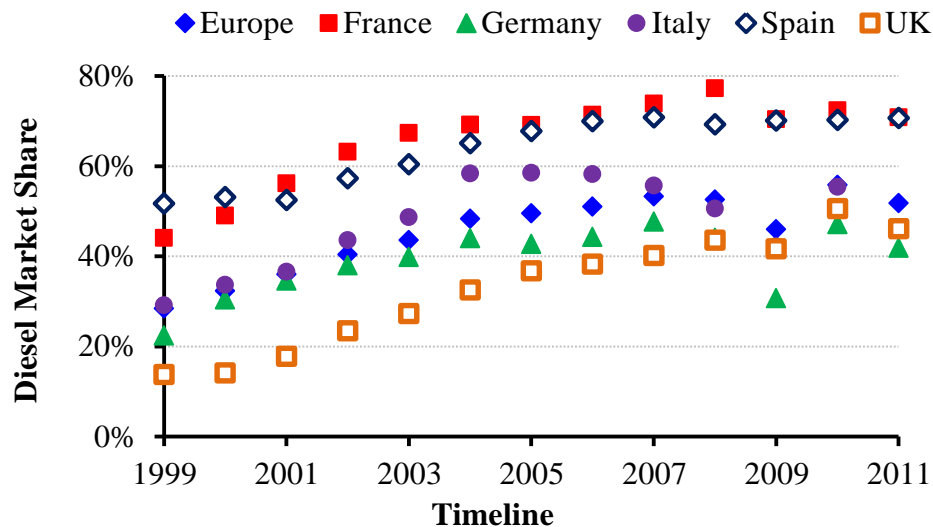


Figure 1-5: 1999-2011 Diesel Passenger Car Market Share in Western Europe [15]

1.4 Formation of NO_x Emissions in Internal Combustion Engines

Before discussing the NO_x emission reduction technologies, it would be beneficial to explain the formation of NO_x emissions in internal combustion engines. Internal combustion engines require a mixture of a combustible fuel, an oxidizing agent,

and a method of ignition to achieve combustion. For on-road vehicles, air is currently the most readily available and the most economic oxidizing agent. Air approximately consists of 78% diatomic nitrogen (N_2) and 21% diatomic oxygen (O_2) by volumetric fraction as shown in Figure 1-6. The remainder is mostly argon gas with only trace amounts of other species. The mass-based stoichiometric air to fuel ratio (AFR) is generally in the range of 14:1 to 15:1 for most gasoline and diesel fuels, the two most common fuels for on-road vehicles. Furthermore, lean burn CI engines typically operate with excess air and the air to fuel ratio can be much higher, such as 35:1 under partial load conditions [16,17]. This signifies that the combustion chamber is predominantly filled with air before combustion.

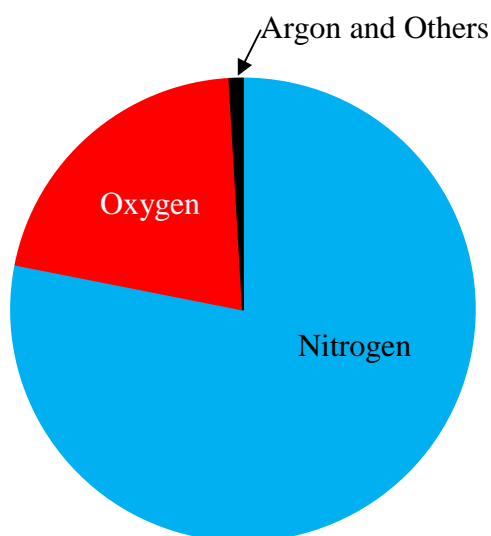


Figure 1-6: Air Composition by Volumetric Fraction

The formation of NO from O_2 and N_2 in internal combustion engines has been studied extensively and is generally acknowledged to proceed according to the extended Zeldovich mechanism as shown in Equations 1-5 to 1-8 [1,2]. A possible pathway for the formation of NO_2 is given in Equation 1-9 but it may also be possible to convert the formed NO_2 back to NO through the mechanism shown in Equation 1-10 [1]. The reaction shown in Equation 1-10 may be a reason for the relatively low NO_2 to NO ratio since the formed NO_2 can convert back to NO unless it is quenched by cooler fluid [1].



The flame and the in-cylinder temperatures are critical parameters for the formation of NO and NO₂. Flynn et al. suggested that NO_x formation increased dramatically at flame temperatures exceeding 2000 K for residence times of 1 to 5 milliseconds [18]. All other aspects being equal, an earlier combustion phasing will generally generate higher flame temperatures and result in increased formation of NO_x. The NO_x chemistry slows down significantly during the early part of the expansion stroke because of the rapidly cooling in-cylinder temperature [1]. In addition to temperature, the oxygen concentration and the air to fuel ratio are important factors for NO_x formation. High flame temperatures, high oxygen content, and near stoichiometric mixtures usually lead to high NO_x formation rates [1,2]. Generally, the peak NO_x formation occurs when the air excess ratio (λ) is in the range of 1.0 to 1.2 [1,2].

1.5 In-Cylinder NO_x Emission Reduction Literature Review

Numerous technologies and strategies have been developed for the reduction of NO_x from lean-burn compression ignition engines. These technologies can be split into two broad categories: in-cylinder NO_x reduction and exhaust after-treatment NO_x reduction. The general goal of the in-cylinder strategies is to suppress the formation of nitrogen oxides while the goal of the exhaust after-treatment is to reduce the NO_x that

were formed in the combustion chamber. The in-cylinder strategies generally aim to reduce the in-cylinder NO_x formation by lowering the flame temperature or by reducing the in-cylinder oxygen concentration. The most established in-cylinder NO_x reduction strategies include the use of exhaust gas recirculation, delayed combustion phasing, highly volatile fuels like butanol, and advanced combustion modes like low temperature combustion (LTC) and homogenous charge compression ignition (HCCI).

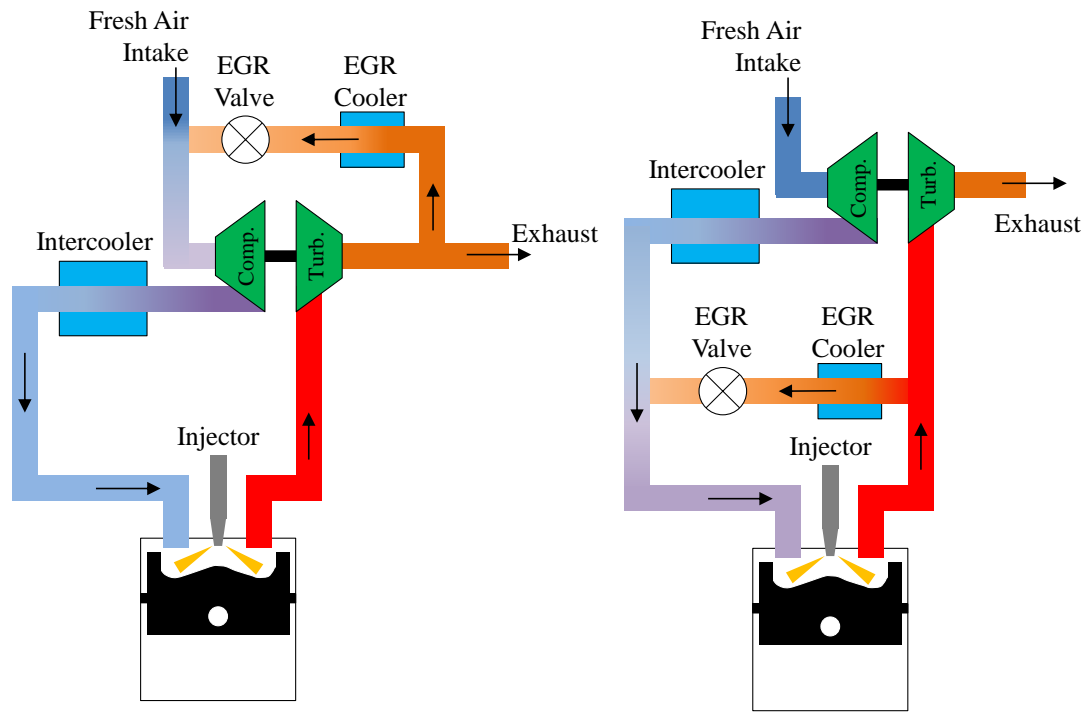


Figure 1-7: Low Pressure (Left) and High Pressure (Right) EGR Loop

Exhaust gas recirculation delivers a portion of the exhaust gas back to the intake stream. The EGR loop can either be a low pressure or high pressure loop as shown in Figure 1-7. High-pressure EGR loop systems are generally more preferred as they have less concern regarding the fouling of the compressor and intercooler. EGR gas primarily consists of nitrogen, carbon dioxide, and water vapour. Oxygen is also present, particularly if very lean mixtures are used. Studies have indicated that EGR has three main effects: a dilution effect, a thermal effect, and a chemical effect [19-22]. The

dilution effect is responsible for reducing the oxygen concentration by replacing it with nitrogen, carbon dioxide, and water vapour. The thermal effect refers to the lowered specific heat capacity ratio of the intake charge due to the presence of carbon dioxide and water vapour. The chemical effect involves the endothermic dissociation of water vapour and carbon dioxide at high temperatures.

Ladomatos et al. indicated that the dilution effect was the most effective for NO_x reduction [20,21]. However, the reduction of the intake oxygen increased the smoke and the total hydrocarbon emissions [19]. The smoke emissions can be controlled by the use of a diesel particulate filter (DPF) but higher engine-out smoke emissions would require more frequent DPF regeneration cycles and could lead to increased supplemental fuel consumption. The thermal and the chemical effects resulted in NO_x reduction due to reduced combustion temperatures but their combined effect was less significant than the dilution effect [20,21].

Other research publications also indicated that EGR can be effective for NO_x reduction [23-27]. Kohketsu et al. found that a high pressure EGR system with a variable geometry turbine was more effective and practical than a low pressure system for certain applications [24]. The study demonstrated that EGR was able to reduce the NO_x emissions from about 800 to 100 ppm [24]. However, the NO_x reduction was accompanied by a dramatic increase in the smoke emissions and a 12% increase in the break specific fuel consumption (BSFC) [24]. The tests indicated that only a 22% NO_x emission reduction was possible without an increase in the smoke emissions or the fuel consumption [24].

A different study investigated a variety of exhaust system designs, including the use of a variable nozzle turbine and a Venturi mixer [25]. At most engine operating conditions, the application of EGR led to a trade-off between NO_x and BSFC and between NO_x and PM, regardless of the exhaust system design [25]. Verbeek et al. [26] suggested implementing an EGR control algorithm to optimise the EGR to reduce NO_x without a significant impact on the PM emissions. The conclusions of these studies cannot be generically applied to all systems since the experimental outcomes were dependant on the hardware limitations of the respective experimental setups.

Numerous studies have established that diesel low temperature combustion was effective for the simultaneous reduction of NO_x and smoke emissions [28-35]. Alriksson and Denbratt conducted single cylinder research experiments on a 2.0 L heavy duty direct injection engine and utilized high EGR levels to achieve low temperature combustion [28]. Simultaneously low NO_x and soot levels were achieved at 50% engine load with EGR rates as high as 65% [28]. However, the results showed that LTC caused increased fuel consumption and increased emissions of CO and total hydrocarbons (THC) [28]. Simultaneously low NO_x and low soot operation with a single shot of fuel and heavy EGR was also demonstrated by Zheng et al. [29]. The study indicated that LTC operation significantly increased the hydrocarbon and carbon monoxide emissions and decreased the thermal efficiency relative to conventional high temperature combustion (HTC) [29]. Further experiments were carried out with multiple injection strategies and the results suggested that the fuel efficiency was improved compared to single shot LTC operation [29].

Low temperature combustion was achieved by de Ojeda et al. with two different fuel injection strategies: an early injection of fuel during the compression stroke and an injection of fuel close to top dead centre (TDC) with heavy EGR [30]. The study suggested that the early injection strategy resulted in higher unburned hydrocarbon emissions because of poor fuel vaporization during the early compression stroke [30]. Han et al. investigated the effect of fuel injection pressure and the air intake pressure on low temperature combustion [31]. A higher fuel injection pressure and a higher air intake pressure improved air and fuel mixing and reduced the THC and CO emissions [31]. Zheng and Kumar also confirmed that CO emissions were reduced by increased air intake pressure and that hydrocarbon emissions were reduced by avoiding early injections which could lead to wall impingement [32].

Picket and Siebers utilized an optically-accessible constant volume combustion chamber with synthetic gas to simulate the use of heavy EGR by reducing the oxygen concentration to as low as 10% [33]. The tests indicated that the combustion flame was non-sooting at temperatures as low as 1980 K [33]. The lack of soot formation was attributed to a “high degree of fuel-air mixing upstream of the lift-off length and the

increase of the lift-off length with decreasing oxygen concentration” [33]. Asad and Zheng explained that the use of LTC with heavy EGR resulted in a longer ignition delay and increased cycle-to-cycle variations and combustion instability [34]. Zheng et al. suggested that catalytic EGR can be used to partially reform the exhaust gas into a gaseous fuel to improve the LTC cycle-to-cycle stability [35]. The study also indicated that the catalytic EGR reduced the NO_x emissions compared to raw EGR [35].

NO_x emissions can also be reduced by controlling the fuel injection timing. Hountalas et al. conducted tests on a single cylinder, turbocharged diesel engine at three different engine loads and two different engine speeds and demonstrated that retarding the injection timing lowered the peak cylinder pressure and reduced the NO_x emissions at all three operating conditions [36]. However, a corresponding increase in the soot emissions was observed [36].

The same trend was observed by Fulton and Leviticus for tests with a six cylinder 7.8 L diesel engine [37]. The NO_x reduction was attributed to reduced peak flame temperatures [37]. An optimal injection timing, at about 9°CA before top dead centre (BTDC) for the tested conditions, was found at which the BSFC and the THC emissions were minimized [37]. Delaying the post injection timing beyond this value continued to reduce NO_x but the BSFC and THC were increased [37]. The authors also explained that the benefits of retarded injection timing were outweighed by the penalties at reduced engine loads because the NO_x emission reduction was not as significant [37]. Hardy and Reitz performed a similar experiment but delayed the injection timing to after top dead centre [38]. Their results showed that the NO_x emissions dropped but the smoke emissions, the carbon monoxide emissions, and the BSFC increased when the injection timing was delayed after top dead centre [38]. The data revealed that there was a slight reduction of the peak pressure rise rate when the fuel injection timing was delayed after top dead centre [38].

Researchers have investigated the effect of alternate fuels on NO_x emission reduction in lean-burn compression ignition engines [39-44]. Zheng et al demonstrated ultra-low NO_x and soot combustion with direct injection of neat butanol without using EGR [39]. However, excessive peak pressure rise rates and unstable combustion placed

limits on the operating range of the engine [39]. Yanai et al. conducted neat butanol tests which showed that very low NO_x emissions were achieved at an indicated mean effective pressure (IMEP) of 6.5 bar but the NO_x emissions significantly increased when the engine load was increased to 8 bar IMEP [40]. Excessive peak pressure rise rates were observed for butanol combustion, narrowing the operating range of the engine, but the test results demonstrated that the peak pressure rise rate was reduced by lowering the fuel injection pressure and delaying the fuel injection timing [40].

Liu et al. blended diesel fuel with n-butanol and the results showed a minimal effect on NO_x emissions but a significant reduction of soot emissions was observed compared to conventional diesel fuel [41]. The soot reduction was attributed to the presence of molecular oxygen in butanol fuel and to improved air and fuel mixing due to the lower cetane number of butanol [41]. Chen et al. investigated the use of n-butanol as a dual fuel in a diesel CI engine [42]. The results revealed that simultaneously low NO_x and soot emissions were achieved with port injection of butanol and direct injection of diesel [42]. However, the hydrocarbon and carbon monoxide emissions increased for higher butanol to diesel ratios [42]. Furthermore, the results indicated that the hydrocarbon emissions were higher when butanol was used as a dual fuel with diesel compared to a blended fuel of butanol and diesel [42]. The study also stated that the peak in-cylinder pressure and the peak heat release rate both increased when the ratio of butanol to diesel was increased with low EGR rates and that the opposite trend was observed with high EGR rates [42].

Ethanol port injection was used by Maurya and Agarwal to achieve homogeneous charge compression ignition [43]. Very low NO_x emissions were achieved but there were relatively high hydrocarbon and carbon monoxide emissions [43]. The combustion and the peak in-cylinder pressure were relatively sensitive to the air to fuel ratio and the air intake temperature [43]. A study by Han et al. revealed that port injection of ethanol with direct injection of diesel was suitable for low temperature combustion operation at high engine loads [44].

The aforementioned studies highlighted the major in-cylinder NO_x control strategies. Each strategy was found to have benefits and challenges. In general, the use

of EGR was effective for the reduction of the NO_x emissions but at the cost of fuel consumption and PM emission penalties. Low temperature combustion and HCCI were suitable for NO_x and smoke emission reduction but generally increased CO and THC emissions and the fuel consumption. Combustion instability was also occasionally reported to be an issue. The use of oxygenated fuels was normally beneficial for the reduction of NO_x and PM emissions. However, there were trade-offs with high in-cylinder pressures, high peak pressure rise rates, or high carbon monoxide and total hydrocarbon emissions.

1.6 Post Injection Emission Reduction Literature Review

Numerous studies investigated the effects of a diesel post injection on the exhaust emissions [45-49]. Researchers demonstrated that meaningful soot emission reductions were achieved with a post injection [45,46,49]. Lee et al. showed that a piston with a two-staged bowl and an injector with a twelve hole double-row nozzle reduced the carbon monoxide, the total hydrocarbon, and the PM emissions with a close-coupled post injection and high EGR rates [45]. The smoke reduction was attributed to the increased in-cylinder temperatures and to the increased turbulence caused by the injection of the post injection fuel [46].

For partially premixed charge compression ignition, de Ojeda et al. indicated that a diesel post injection, in combination with a pilot and a main injection, was useful for soot reduction at high engine loads (brake mean effective pressure of 16.5 bar) [51]. For constant BSFC and NO_x emission levels, the results by Hardy and Reitz suggested that the use of a close-coupled post injection resulted in only a slight reduction of the PM emissions [38]. The PM reduction was attributed to the disturbance caused by the momentum of the post injection fuel that enhanced the mixing of the in-cylinder gases [38]. However, Nimodia et al. indicated that the use of a post injection resulted in increased brake specific fuel consumption [49].

Desantes et al. compared the emission and combustion characteristics of close-coupled and remote post injections [47]. The study suggested that smaller close-coupled

injections increased the acceleration of the final stages of combustion and were more suitable for PM reduction [47]. Conversely, remote post injections produced a split flame which did not affect PM emissions and any PM reduction was attributed to the shortening of the main injection [47]. The PM emissions also increased with the use of relatively large and relatively early post injections [47]. Other studies indicated that the dwell time between the main and the post injection affected the particle size distribution [48]. Test results showed that close-coupled injections reduced the count of the nucleation mode particles and increased the count of the accumulation mode particles [48]. These trends were consistent for tests with a single and with a double post injection [48].

Park et al. investigated the use of a post injection to reduce hydrocarbon and carbon monoxide emissions for diesel partially premixed charge compression ignition (PCCI) [50]. The authors found that the post injection significantly reduced the carbon monoxide and hydrocarbon emissions compared to a single-shot injection [50]. However, the NO_x emissions increased for relatively early post injections [50]. The use of a double post injection was also investigated and, although the same trends were observed, the double post injection had a slightly higher reduction of carbon monoxide and hydrocarbon emissions [50]. Yao et al. studied post injections of butanol and diesel fuel blends [54]. A post injection of the blended fuel reduced the soot and carbon monoxide emissions compared to a single shot injection [54]. The soot emission reduction was more pronounced as the fuel ratio of butanol to diesel was increased [54].

Hydrocarbon speciation studies with diesel post injections were carried out by Storey et al. [52]. A post injection timing sweep, from 40° crank angle (CA) to 100°CA after compression top dead centre (ATDC), was conducted. The test results indicated that light hydrocarbons increased when the post injection timing was delayed while the change in heavy hydrocarbons was negligible [52]. The authors observed that a post injection generally produced more alkenes compared to an injection of fuel directly into the exhaust that mostly produced longer chain alkanes [52]. These results suggested that a post injection was more suitable for the production of light and reactive hydrocarbons species, such as propylene, for NO_x after-treatment. Other studies also showed that a post injection can contribute to in-cylinder hydrogen production [53,55].

Overall, the literature survey indicated that a post injection was useful for the reduction of PM emissions. However, the PM reduction was sensitive to the post injection timing and duration [47]. For combustion modes like PCCI, the addition of a post injection was beneficial for the reduction of CO and THC emissions. Speciation studies indicated that increased light hydrocarbons, such as alkenes, were generated by the use of a post injection. However, the effects of the post injection on the NO_x emissions were generally negligible or adverse under conventional high temperature combustion.

1.7 Lean-Burn After-Treatment NO_x Emission Reduction Literature Review

The after-treatment strategies utilize a catalytic reactor and NO_x reducing agents to reduce the NO_x that were formed in the combustion chamber. A high surface area reactor is typically utilized to increase the contact between the NO_x molecules and the catalytic surface. The two predominant NO_x after-treatment systems are selective catalytic reduction (SCR) and the lean NO_x trap. Selective catalytic reduction utilizes a catalytic reactor that promotes the reduction of NO_x with ammonia. The catalyst is often a zeolite, such as an iron or copper zeolite, or a base metal oxide like vanadia (V₂O₅) or titania (TiO₂) [56-58]. A urea solution, (NH₂)₂CO·H₂O, is generally injected into the exhaust stream to generate ammonia since ammonia is not typically found in diesel engine exhaust. Additional hardware, such as a heated storage tank and a urea injector, are required for the storage and the injection of the urea solution [59].

Once the urea is injected into the high temperature exhaust, the solution will undergo thermal decomposition and hydrolysis to form ammonia as shown in Equation 1-11 [61]. A urea mixer is commonly installed slightly downstream of the urea dispersion location to promote homogeneous radial distribution of ammonia to the SCR catalyst [59,60]. Inside the catalyst, ammonia will react with NO and NO₂ to produce nitrogen and water according to Equations 1-12 to 1-14. Diesel exhaust usually contains a high ratio of NO to NO₂ and this promotes NO_x reduction according to Equation 1-12 [61]. However, the reaction path of Equation 1-13 tends to be faster than that of Equations 1-12 and 1-14, especially at low exhaust temperatures [61,62]. Thus, studies have been

carried out to purposely increase the exhaust NO_2 concentration to obtain a 1:1 ratio of $\text{NO}:\text{NO}_2$ to promote the fast SCR reaction [62]. The most common method is to use an upstream oxidation catalyst to oxidize the NO to NO_2 as shown in Equation 1-15 and Figure 1-8 [62]. However, the oxidation catalyst must be sized and designed properly to avoid over-producing NO_2 and promoting the slower NO_2 reaction path shown in Equation 1-14 [62].

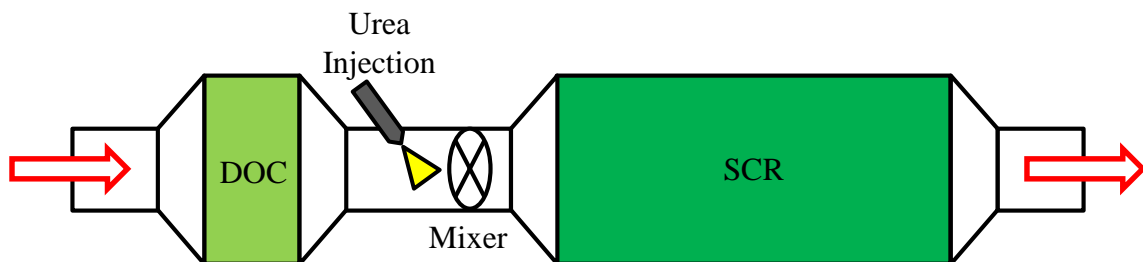
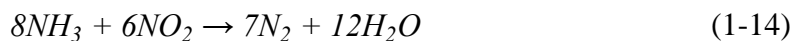
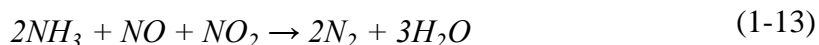


Figure 1-8: SCR System with Upstream DOC and Urea Mixer

There are several challenges related to the use of SCR catalysts. The urea dosing must be monitored and tightly controlled to avoid over-dosing and causing ammonia slip through the catalyst [63]. Urea dosing algorithms must be developed and implemented to

optimize the urea dosing for highest NO_x conversion efficiency while avoiding ammonia slip [63]. To prevent ammonia release into the environment, an ammonia slip catalyst (ASC) is sometimes implemented immediately downstream of the SCR to oxidize ammonia to nitrogen and water as shown in Equation 1-16 [64].

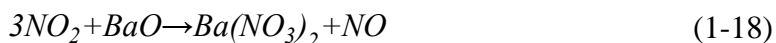
Chemical deactivation of the SCR can occur if hydrocarbons adsorb onto the catalyst surface [58]. The hydrocarbon adsorption on the SCR surface reduced the NO_x conversion efficiency with copper and iron zeolite catalysts [58]. A study by Smith et al. concluded that exposure to hydrocarbons had a negative impact on the SCR performance but exposure to CO and hydrogen did not have a meaningful effect [69]. Platinum contamination of the SCR surface can also be an issue if platinum migrates to the SCR from an upstream DOC that is exposed to high temperatures [65-67]. Studies have found that platinum contamination of the SCR significantly reduced the NO_x conversion efficiency [66,67]. Chen et al. found that platinum contamination of the SCR significantly increased the formation of nitrous oxide (N₂O) at low temperatures [65].

The formation of nitrous oxide (N₂O) is another challenge of SCR systems. Nitrous oxide is a very potent greenhouse gas whose effect is almost 300 times stronger than the effect of carbon dioxide. Kamasamudram et al. showed that the N₂O formation from SCR systems was the highest at a temperature of 300°C and that it increased as the NO₂ to NO_x ratio approached unity [68]. Advanced SCR catalytic formulations must be designed to prevent or mitigate the platinum contamination, hydrocarbon adsorption, and N₂O formation effects.

There are also practical issues concerning the use of SCR in the field. Urea is a solid at room temperature and it has a melting point of 133°C [73]. For more convenient use, urea is generally dissolved in deionized water and the solution typically contains 32.5% urea by weight to produce the lowest freezing point of -12°C [70,72]. Heaters must be employed to heat the urea tank to prevent the solution from freezing [71,72]. The use of a heated urea tank can consume some power from the engine and add to the weight and the cost of the vehicle. The urea level in the tank must also be monitored since the SCR reactor will not function if the urea solution is not refilled. A method must be implemented to ensure that the user will refill the urea tank and to safeguard that the

tank is not filled with a non-urea liquid [70-72]. Despite all of the aforementioned challenges, the urea SCR system is currently the most common NO_x after-treatment solution for heavy duty on-highway diesel vehicles since it provides a relatively high conversion efficiency across a relatively broad range of exhaust temperatures [65,72,74].

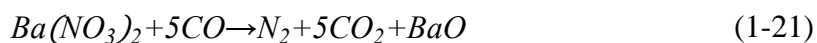
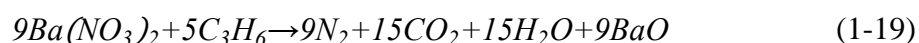
A lean NO_x trap is a lean-burn NO_x after-treatment device which periodically cycles NO_x storage and NO_x reduction. The LNT is commonly coated with a precious metal catalyst, such as platinum, to help oxidize the incoming NO to NO₂ under typical oxygen-rich exhaust conditions as shown in Equation 1-17 [75]. The LNT catalyst formulation also contains a NO_x storage species, typically an alkali or an alkaline earth metal oxide (henceforth barium oxide will be used as an example) [76,77]. Under oxygen-rich exhaust conditions, the barium oxide will react with NO₂ to form a barium nitrate as shown in Equation 1-18, effectively storing the NO_x within the LNT reactor [75,76]. The NO_x storage cycle is also commonly called the trapping or the adsorption cycle. Some NO₂ molecules will not be able to find a barium storage site and will slip through the reactor and get released into the atmosphere. For a fresh and clean catalyst, the NO_x storage efficiency is relatively high but, after prolonged exposure to NO_x, the barium storage sites will approach saturation and the NO_x storage efficiency will deteriorate [78]. Thus, there is a periodic need to desaturate the LNT by purging the stored nitrates from the LNT and converting them to more environmentally friendly substances.



The purging process, commonly called “LNT regeneration”, is triggered when the LNT reaches a predetermined saturation threshold and involves temporarily generating fuel-rich exhaust conditions via in-cylinder post injections or injections of fuel directly into the exhaust gas [79-81]. The fuel used for regeneration is typically the hydrocarbon

fuel used for combustion since it is readily available on-board a vehicle. Under fuel-rich conditions and with the help of a precious metal catalyst, such as rhodium, the stored nitrates are ideally released and reduced to nitrogen gas while the barium compound is regenerated to barium oxide [82]. The LNT regeneration is a complex chemical process involving numerous reactions but the overall global reaction is shown in Equation 1-19, using propene as a representative hydrocarbon [82]. However, some of the released nitrates will fail to react with a reducing agent and will release into the atmosphere as NO_x , resulting in a NO_x emission spike [83].

The NO_x reduction efficiency at optimal conditions can exceed 90% but it can be less than 50% if the exhaust temperature is too low or too high [78]. Due to the presence of a precious metal catalyst, the hydrocarbon fuel can react with water to form carbon monoxide and hydrogen according to the steam reforming reaction shown in Equation 1-20 [82]. The generated carbon monoxide and hydrogen can promote the regeneration process by reducing the released nitrates to nitrogen as shown in Equations 1-21 and 1-22 [82]. A simple illustration of the LNT NO_x storage and regeneration processes is provided in Figure 1-9. More detailed NO_x storage and regeneration chemical kinetic models can be found in literature [75,82,84,85].



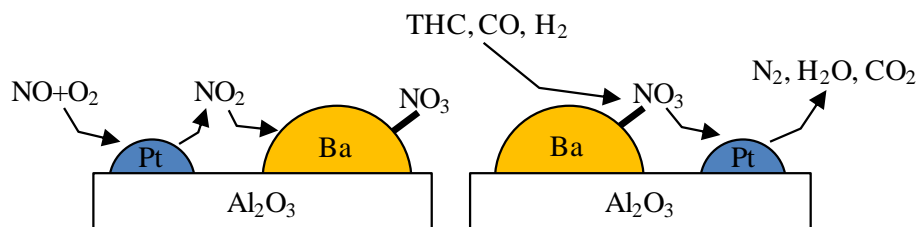


Figure 1-9: LNT NO_x Storage (Left) and Regeneration (Right) Processes

There are numerous challenges related to the use of an LNT. Conventional diesel combustion can produce hundreds to thousands of ppm of NO_x . These levels of NO_x can quickly saturate the NO_x storage sites and reduce the storage efficiency of the LNT. Thus, the NO_x storage cycle is typically limited to the order of one minute followed by a fuel-rich regeneration cycle of approximately ten seconds, although shorter storage cycles have also been proposed [80]. Frequent fuel-rich regeneration can result in a fuel consumption penalty of about 3% but fuel consumption penalties over 10% have also been reported [86,87]. Therefore, the use of an LNT results in a fuel economy penalty because of the requirement for fuel-rich regeneration.

Another challenge is associated with the exposure of the LNT to sulfates. Diesel fuel and lubricating oil may contain traces of sulfur and sulfur compounds which can oxidize during the combustion process to form sulfates [91]. Like nitrates, sulfates can adsorb onto the LNT surface to form a barium sulfate compound [88]. Thus, sulfates will occupy the sites intended for NO_x storage within the LNT and will reduce the NO_x storage efficiency [88,89]. Sulfates can form very strong and stable bonds with an LNT catalyst and a special regeneration procedure, called desulfation, is required to purge the sulfates from the LNT [91]. The desulfation procedure requires fuel-rich conditions, temperatures generally exceeding 500°C , and the presence of species such as hydrocarbons, water, carbon dioxide, and hydrogen [90,91].

Recent regulations have reduced the sulfur limits from 500 of 15 ppmV for diesel fuel [92]. The reduced content of sulfur within the fuel should significantly slow down the adsorption rate of sulfur onto the LNT surface. Nevertheless, the periodic

requirement for the high temperature desulfation process remains. The exposure to high temperatures can result in thermal deactivation of the catalyst. High temperatures can cause the precious metal particles to become unstable and to bond with adjacent precious metals, effectively reducing the available precious metal surface area and deteriorating the performance of the LNT [91]. Research has been carried out to mitigate this issue by utilizing specialized catalytic formulations, such as the use of perovskite crystals, to prevent precious metal grain growth [93]. The research by Kaneeda et al. demonstrated that the thermal resistance can be enhanced by improved formulations of the precious metal catalysts [94]. However, more complex catalytic formulations typically lead to higher cost catalysts.

1.8 Chapter Summary

The literature review outlined that strict NO_x emission regulations have been implemented that led to the development of NO_x emission control strategies and technologies like exhaust gas recirculation, low temperature combustion, delayed fuel injections, selective catalytic reduction, and lean NO_x trap catalysts. However, as outlined in the literature review, these strategies have potential penalties like increased break specific fuel consumption, increased PM emissions, increased CO and THC emissions, or the requirement for additional hardware or secondary fluids like urea. As a result, the overall objective for the proposed research was to develop a strategy for attaining ultra-low NO_x emissions while reducing the impacts on the associated penalties, particularly the fuel consumption and emissions. The methodology for achieving this objective is presented in the following chapter.

CHAPTER 2: RESEARCH PLAN

The purpose of the proposed research is provided in this chapter. A detailed outline of the proposed strategies for enhanced NO_x reduction from lean-burn engines is presented. The methodologies and the principles of each strategy are described and the expected results are discussed.

2.1 General Research Outline

The main goal of the proposed research was to implement the use of a novel long breathing LNT strategy to achieve ultra-low NO_x emissions while simultaneously and significantly reducing the supplemental fuel consumption of the LNT. To achieve the aforementioned objective, the long breathing technique utilized a combination of in-cylinder and after-treatment emission control strategies. The long breathing strategy utilized two independent in-cylinder strategies to reduce the engine-out NO_x emissions: the use of neat n-butanol fuel for enhanced premixed combustion and the use of exhaust gas recirculation with diesel fuel. The use of a lean NO_x trap was proposed to further reduce the tailpipe NO_x emissions.

Moreover, post injection strategies were proposed for the active control of the exhaust gas temperature and composition to improve the performance of an LNT. The aim of the post injection strategies was to control the exhaust gas temperature and to produce suitable NO_x reducing agents for an LNT, including hydrogen and light hydrocarbons like propylene. A detailed exhaust speciation analysis was proposed to determine the effects of different parameters on the production of desired NO_x reducing agents and to identify the conditions which generated the highest yield. A more comprehensive explanation for each strategy is provided in the subsequent subsections of this chapter. Although, many of the strategies may be inter-related, as shown in Figure 2-1, a separate section has been dedicated to each sub-topic.

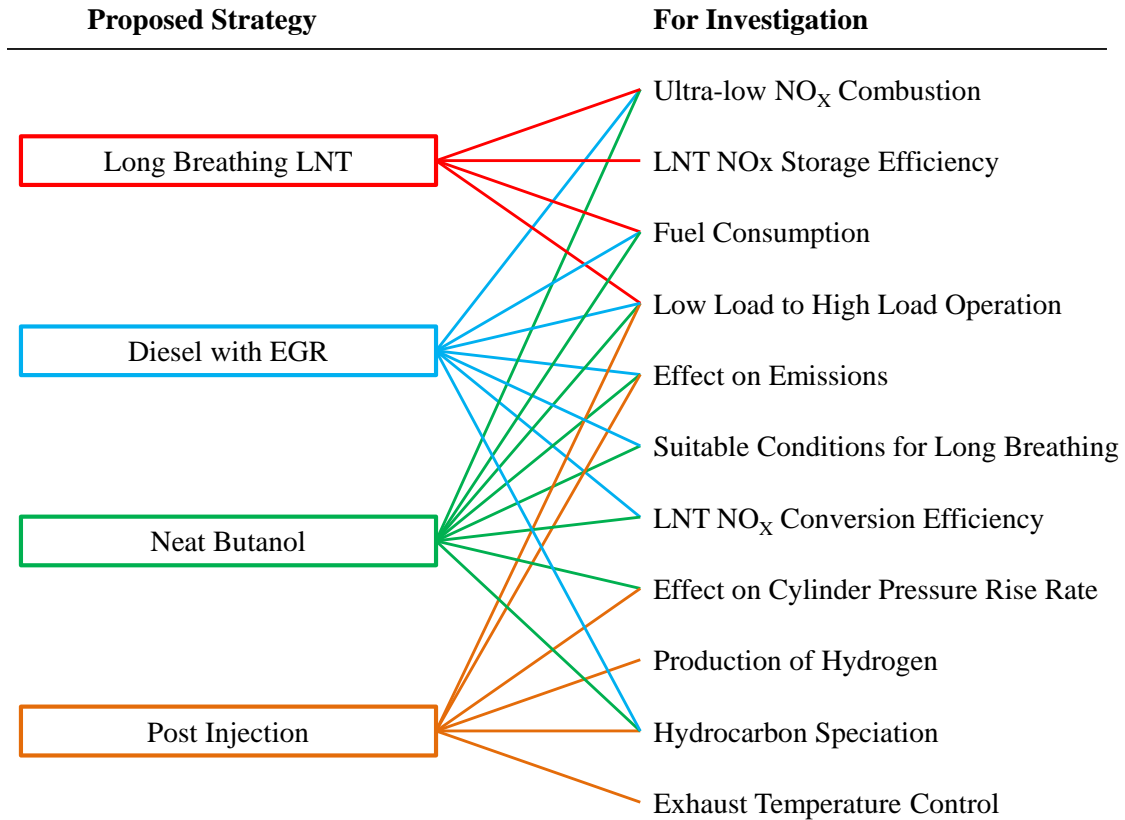


Figure 2-1: Outline of Proposed Research Topics

2.2 Long Breathing Lean NO_x Trap

The long breathing LNT strategy is a novel technique proposed by Jeftić and Zheng that significantly extends the NO_x storage (breathing) cycle [95,96]. The long breathing method was founded on the idea of combining the use of in-cylinder NO_x reduction with an LNT after-treatment system to reduce the tailpipe NO_x emissions. For in-cylinder NO_x reduction, the use of EGR with diesel fuel and the use of neat n-butanol are proposed. The use of in-cylinder NO_x reduction has a double benefit for the long breathing lean NO_x trap. The first benefit is the reduced saturation rate of the LNT during the NO_x storage cycle. Conventional lean-burn combustion of diesel fuel generally produces hundreds to thousands of ppm of NO_x which can quickly saturate an LNT. To maintain a high NO_x storage and conversion efficiency, this generally results in

an LNT storage cycle of approximately one minute followed by a fuel-rich regeneration of about ten seconds as illustrated in Figure 2-2.

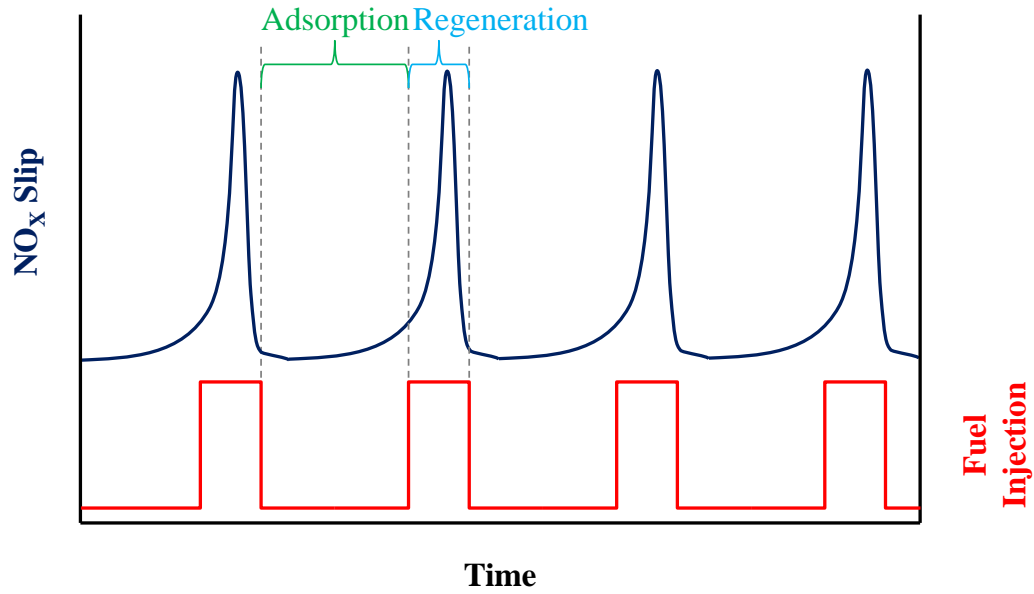


Figure 2-2: Conventional LNT Fuel Injection Frequency

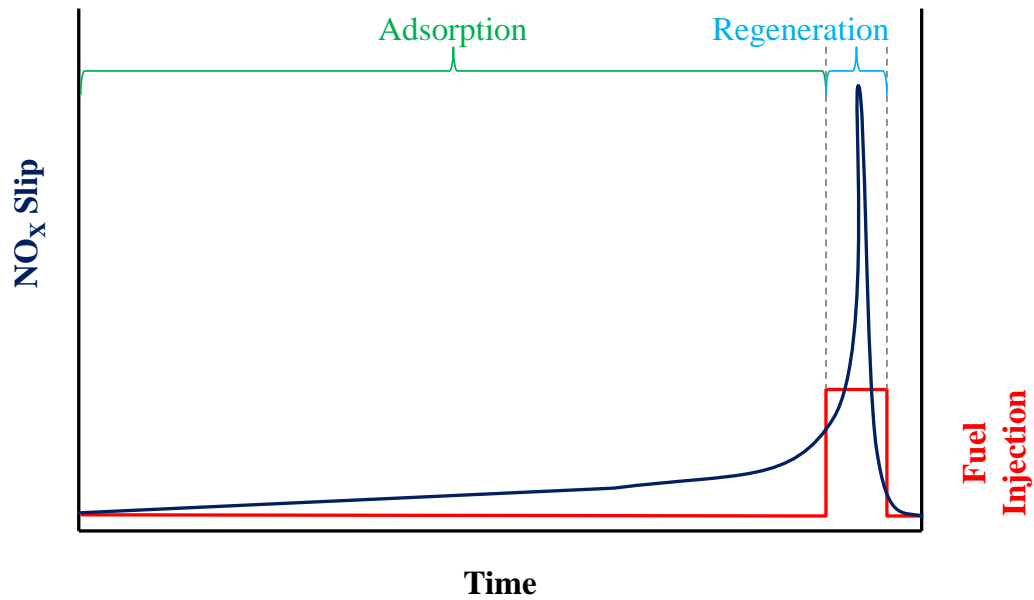


Figure 2-3: Long Breathing LNT Fuel Injection Frequency

As mentioned in the literature review, such frequent fuel-rich regenerations can reduce the fuel economy by 3% or more [86,87]. By reducing the engine-out NO_x with in-cylinder strategies, the LNT saturation rate can be considerably slowed down and the NO_x storage cycle can be substantially extended. An extended NO_x storage cycle results in less frequent fuel-rich regenerations, as shown in Figure 2-3, and offers the potential for supplemental fuel savings.

The second benefit of reducing the engine-out NO_x emissions with in-cylinder strategies is the reduction of the required NO_x conversion efficiency from the after-treatment system. The long breathing method uses a combination of in-cylinder and after-treatment strategies to meet the tailpipe NO_x emission target. By reducing more NO_x with in-cylinder strategies, less NO_x have to be reduced with the LNT after-treatment system. As a result, the LNT can tolerate reduced NO_x storage efficiencies and higher saturation rates. Thus, the NO_x storage process can be prolonged and this can lead to further supplemental fuel savings. The overall methodology of the long-breathing strategy is illustrated in Figure 2-4.

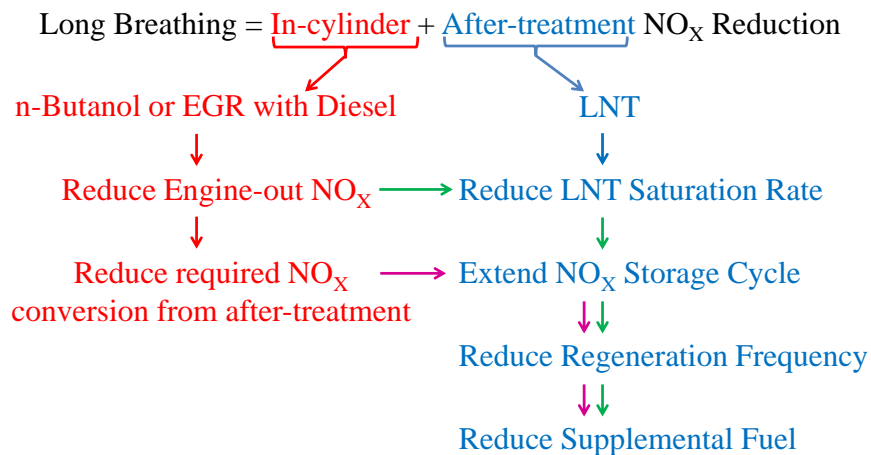


Figure 2-4: Methodology for Supplemental Fuel Savings with the Long Breathing Strategy

Preliminary numerical investigations⁵ were carried out to demonstrate the benefits of the long breathing strategy. The engine-out NO_x quantity was reduced from 1000 to 50 ppmV and the effect on the NO_x storage efficiency was investigated. The numerical calculations were carried out at a catalyst temperature of 315°C and a gas hourly space velocity (GHSV) of 46170 volumes per hour. In addition to NO_x, the feed gas consisted of 8.3%V carbon dioxide, 13.7%V oxygen, and balance nitrogen. The results are shown in Figure 2-5. For all cases, the NO_x storage efficiency declined when the storage time was longer. However, the NO_x storage efficiency dropped very rapidly when the engine-out NO_x level was 250 ppmV or more. The NO_x storage efficiency dropped below 80% after 20 to 80 seconds of storage.

Conversely, the NO_x storage efficiencies were above 80% even after 400 seconds of operation when the engine-out NO_x were reduced to 50 ppmV. The high storage efficiency for low engine-out NO_x levels was caused by a reduced saturation rate of the NO_x storage sites in the LNT. Thus, a reduction of the engine-out NO_x levels to the region of 50 to 100 ppmV may be suitable for the long breathing strategy since it can extend the NO_x storage cycle, while maintaining a high storage efficiency, and thereby reduce the fuel rich regeneration frequency and the supplemental fuel consumption.

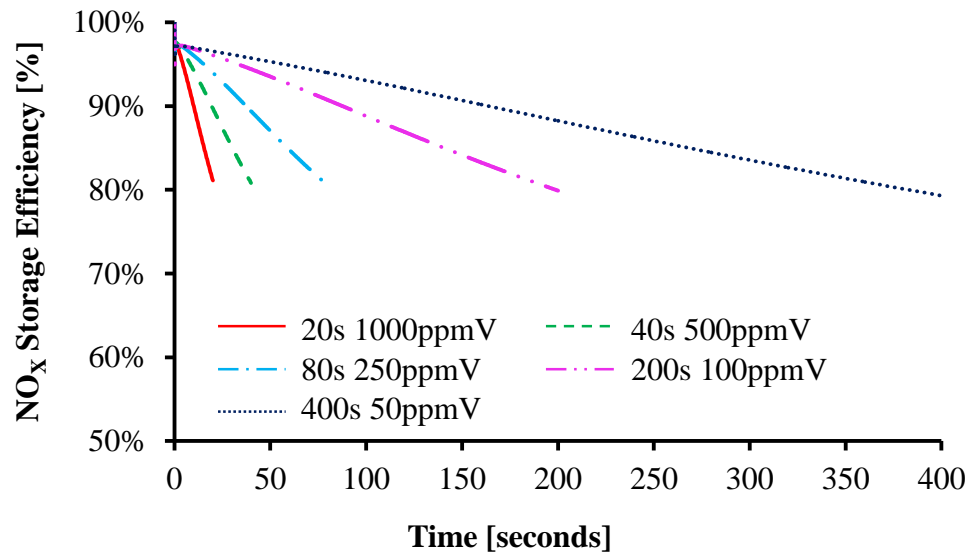


Figure 2-5: Effect of NO_x Level on NO_x Storage Efficiency

⁵ Details of the numerical model are given in section 6.1.

Furthermore, the long breathing strategy maintained a significantly higher NO_x storage efficiency for a fixed storage duration. For an LNT storage cycle of 80 seconds, the data in Figure 2-6 shows that the NO_x storage efficiency was 53% when the LNT was exposed to a feed gas of 1000 ppmV of NO_x while the storage efficiency was 94% when the NO_x level was reduced to 50 ppmV. Thus, for short storage cycles, the long breathing LNT strategy can also provide benefits since its high storage efficiency can reduce the required NO_x conversion efficiency for the LNT regeneration cycle. This could also potentially reduce the fuel consumption penalty and/or the catalyst cost.

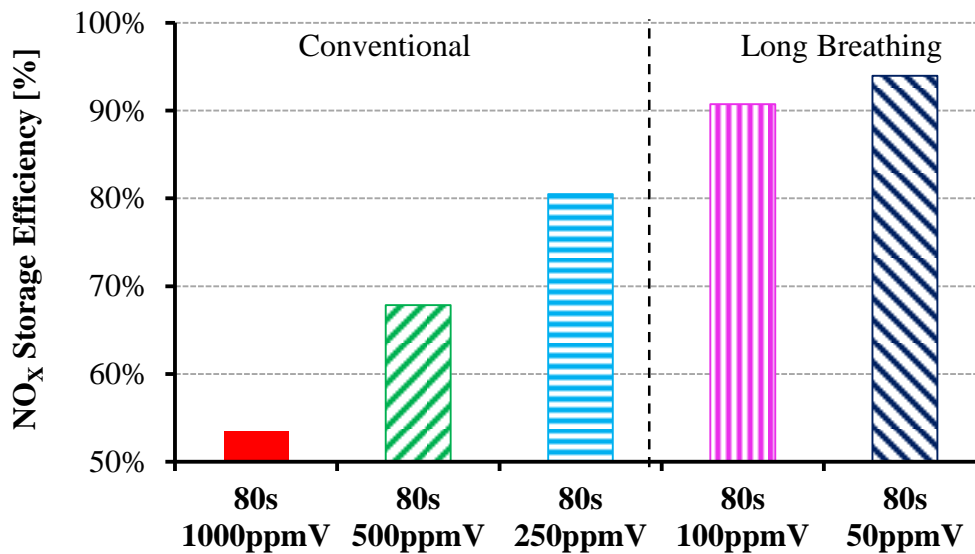


Figure 2-6: NO_x Storage Efficiency for a Fixed NO_x Storage Duration

A preliminary experimental investigation of the long breathing strategy was also previously conducted by the author on an after-treatment flow bench⁶ [96]. The tests were conducted to empirically demonstrate the effect of the reduced engine-out NO_x (feed gas NO_x) on the LNT adsorption duration. The adsorption duration was defined as the time duration required to reach a tolerated NO_x slip limit of 20 ppmV. Details of the test conditions are given in Table 2-1. The tests revealed that the adsorption duration was

⁶ Details of the heated after-treatment flow bench setup are provided in section 3.2.

significantly increased from 11 to 51 minutes when the feed gas NO_x was reduced from 110 to 50 ppmV as shown in Figure 2-7. The extended NO_x adsorption cycle resulted in less frequent LNT regenerations that led to supplemental fuel consumption savings of over 70% as illustrated in Figure 2-8.

Table 2-1: Operating Conditions for Preliminary Flow Bench Test

Average Catalyst Temperature [°C]	300
Gas Hourly Space Velocity [1/h]	75000
Feed Gas NO_x [ppmV]	50-110
Feed Gas O_2 [%V]	17.0
Feed Gas CO_2 [%V]	8.3
Feed Gas H_2O [%V]	6.0
Regeneration Excess Air Fuel Ratio	0.82
Regeneration Duration [s]	15

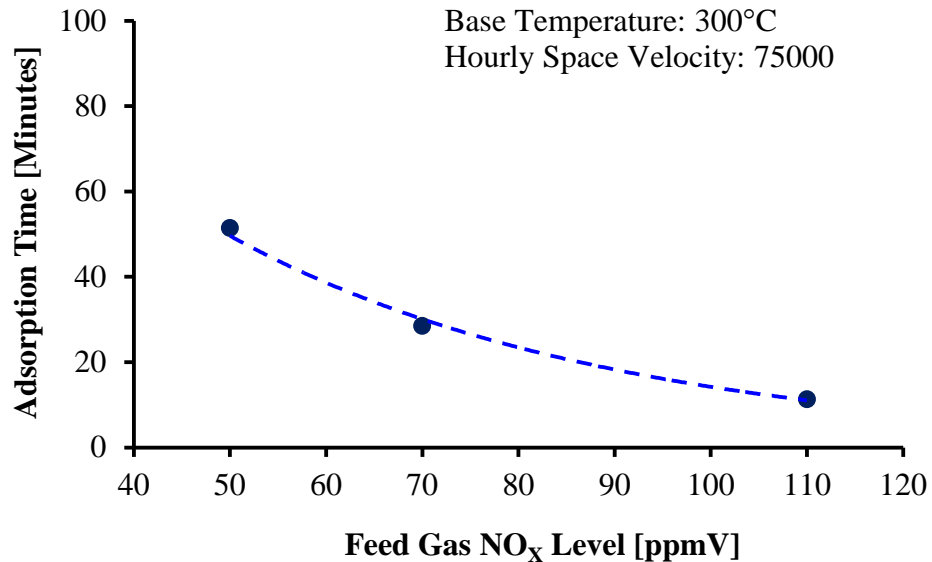


Figure 2-7: LNT Adsorption Duration as a Function of Feed Gas NO_x

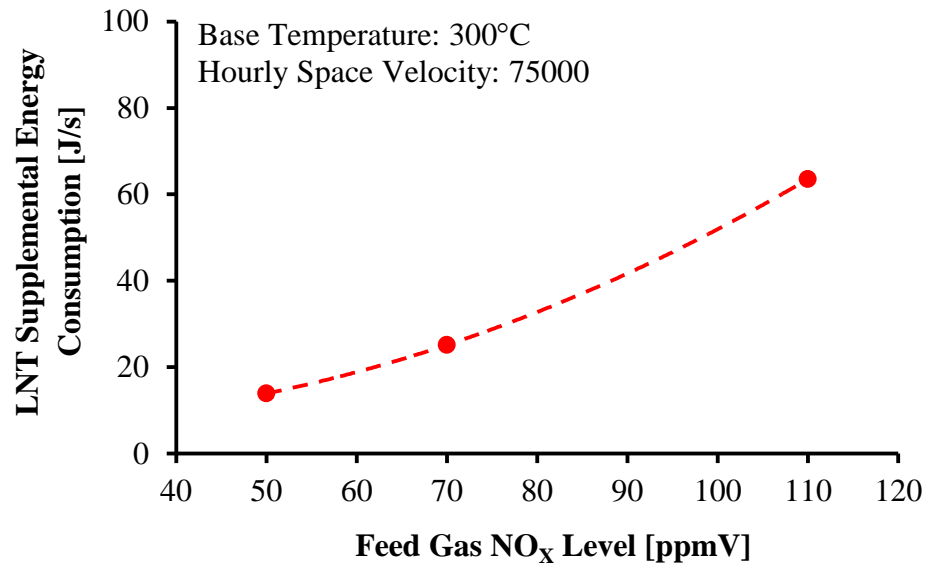


Figure 2-8: LNT Supplemental Energy Consumption as a Function of Feed Gas NO_x

However, the preliminary investigations were conducted as proof of concept studies and were limited to a single set of operating conditions, representative of low load operation. The present research aimed to conduct a more detailed analysis of the long breathing technique to determine the effects of the long breathing LNT strategy on the supplemental fuel consumption, the NO_x storage efficiency, and the required NO_x conversion efficiency at engine operating conditions ranging from low to high load.

The expectation was that the long breathing strategy would provide significant fuel consumption savings while providing a similar NO_x storage efficiency compared to conventional LNT operation. The use of the long breathing LNT strategy was also expected to reduce the required NO_x conversion efficiency due to lower engine-out NO_x emissions. These potential benefits of the long breathing strategy were necessary to quantify to determine if long breathing operation was suitable across a broad range of engine operating conditions. Engine tests were proposed in conjunction with heated after-treatment flow bench tests and numerical modelling to provide a comprehensive analysis of the long breathing strategy. The purpose of the engine tests was to investigate the effects of the in-cylinder NO_x control strategies on the emissions and the engine fuel consumption and to identify suitable exhaust conditions for long breathing operation.

The engine exhaust conditions were used as input parameters for the numerical LNT model to analyze the supplemental fuel consumption of the LNT and the combined fuel consumption of the engine and the LNT. The after-treatment flow bench tests were used to validate the numerical LNT model.

2.3 Long Breathing LNT with EGR and Diesel Fuel

As discussed in the previous section, the long breathing technique utilizes in-cylinder strategies to reduce the engine-out NO_x and to extend the NO_x storage cycle of the LNT. Exhaust gas recirculation is an effective method for in-cylinder NO_x reduction as discussed in the literature review. This method was previously utilized to reduce the engine-out NO_x from 250 to below 100 ppmV to enable long breathing LNT operation as shown in Figure 2-9 [96]. For the selected operating conditions, the long breathing range was identified to be in the region of 16-17.5 percent by volume (%V) intake oxygen.

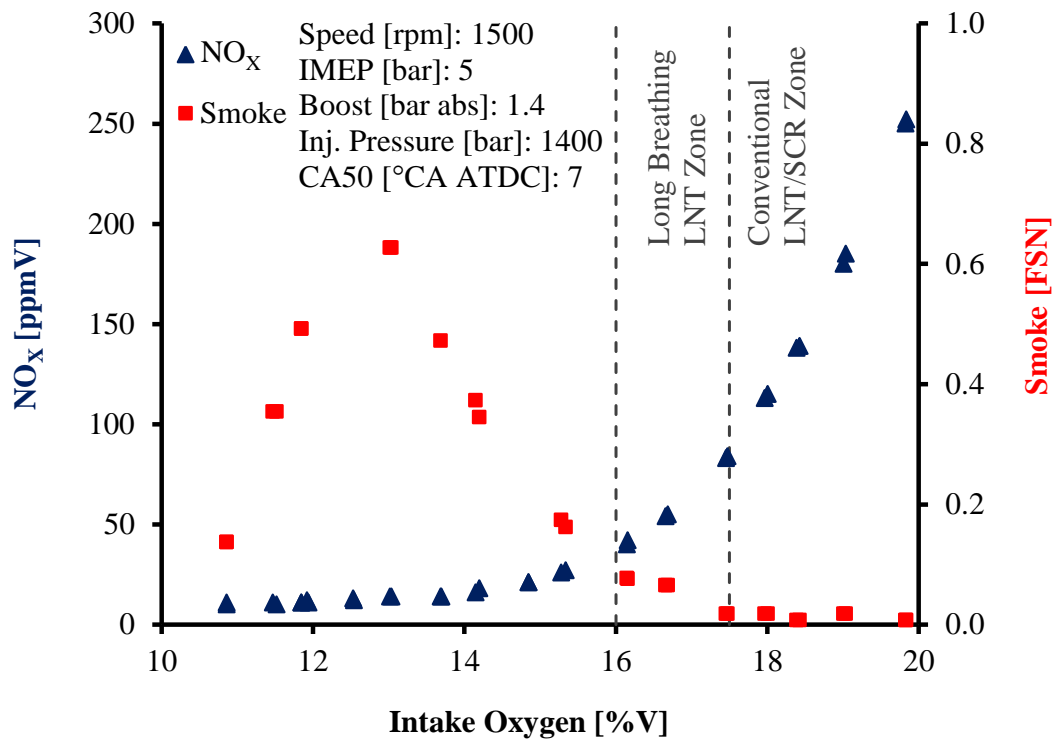


Figure 2-9: Effect of EGR on NO_x and Smoke

This region was selected based on the reduced engine-out NO_x level, 50-100 ppmV, and the minimal impact on the smoke emissions as shown in Figure 2-9. Further reduction of the intake oxygen resulted in an increase in the smoke emissions with a limited reduction of the NO_x emissions. The smoke emission increase was limited to 0.6 FSN because the tests were conducted at a relatively low load, 5 bar IMEP. Also, the fuel injection pressure and the air intake pressure were moderately high, 1400 bar and 1.4 bar absolute respectively, for this load level. The smoke emissions would be expected to increase at higher load levels or if lower fuel injection or air intake pressures were used at this load level.

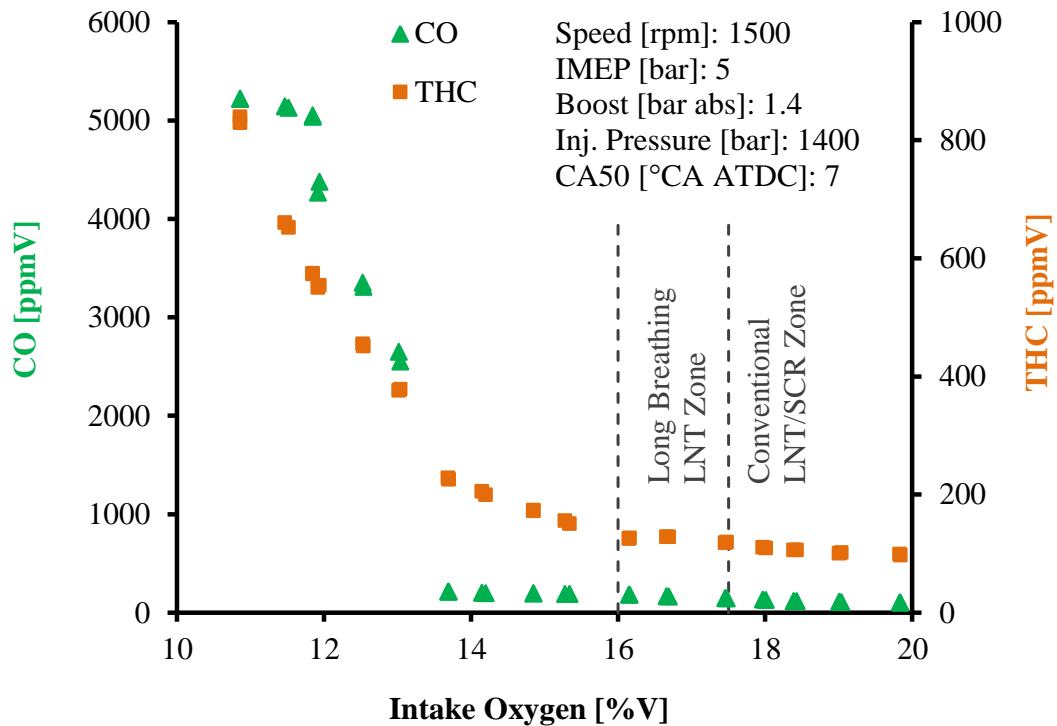


Figure 2-10: Effect of EGR on THC and CO

On the other hand, the low temperature combustion region, with intake oxygen less than 11% as shown in Figure 2-9, had ultra-low NO_x and smoke emissions but was not selected for long breathing because of the very high carbon monoxide and total hydrocarbon emissions as illustrated in Figure 2-10. The data showed that the THC and

CO emissions were relatively low within the selected long breathing region, an indication that there was a negligible fuel penalty for long breathing operation at this engine condition.

The previous work was limited to the engine operating conditions shown in Figure 2-9 and Figure 2-10. Additional EGR tests were proposed at a broader range of engine conditions, ranging from low to high load. The purpose was to utilize EGR to reduce the engine-out NO_x and to determine if there were corresponding penalties for the smoke, CO, and THC emissions and the fuel consumption of the engine. The goal was to utilize the emission and fuel consumption data to identify a suitable engine-out NO_x level for long breathing operation at a broad range of engine loads. Furthermore, the engine data at each operating condition was utilized in combination with the after-treatment data to determine the combined fuel consumption of the engine and the LNT. The combined engine test and numerical modelling results were expected to help determine whether long breathing operation was advantageous for all load conditions or if there were emission or engine fuel consumption penalties that restricted long breathing operation to a limited range of engine loads.

2.4 Long Breathing LNT with Neat Butanol Fuel

The use of neat n-butanol fuel can have beneficial effects on the in-cylinder NO_x and smoke emission reduction as outlined in the literature review. Thus, in addition to the use of diesel fuel with EGR, the use of long breathing with neat n-butanol was proposed. The fuel properties of n-butanol are compared to those of a conventional diesel fuel in Table 2-2. The table shows that n-butanol has a much higher oxygen content and a much lower cetane number than conventional diesel fuel. The cetane number of n-butanol is a key property because, unlike with ethanol, it is high enough to achieve auto-ignition as a neat fuel in a conventional compression ignition engine.

Table 2-2: Properties of n-Butanol Fuel Compared to Conventional Diesel Fuel

Fuel	n-Butanol	Diesel
Chemical Formula	C ₄ H ₉ OH	C _n H _{1.77n}
Hydrogen to Carbon Ratio	2.5	1.77
Oxygen Content by Mass [%]	21.6	0
Cetane Number	25	46.5
Boiling Temp. at 1 bar [°C]	118	288-339
Heat of Vaporization [kJ/kg]	595	317
Stoichiometric Air to Fuel Ratio	11.2	14.4
Density [kg/m ³]	810	858
LHV [MJ/kg]	33.1	42.1

Furthermore, the lower cetane number can extend the ignition delay and the lower boiling point temperature can promote the fuel evaporation process to enhance the premixing of air and fuel. Under lean-burn conditions, the enhanced premixing can result in low temperature combustion with ultra-low NO_x and smoke emissions. The smoke emissions are also suppressed by the presence of oxygen within the butanol molecule [41]. These properties are potentially suitable for long breathing LNT operation. The ultra-low NO_x combustion of neat n-butanol signifies that EGR may not be necessary for in-cylinder NO_x reduction and all of the potential penalties associated with EGR, such as increased smoke emissions, may not be of concern.

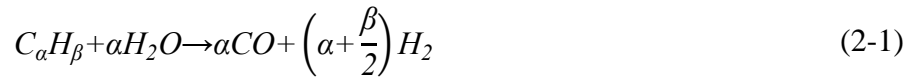
Engine tests with neat n-butanol were proposed without the application of EGR. The goal was to demonstrate suitable exhaust conditions for long breathing LNT operation at low to high load operating conditions. However, previous studies reported that neat n-butanol operation resulted in excessive peak pressure rise rates that limited the engine operation to low load conditions [39]. Therefore, the use of single shot, pilot, and post injection strategies were investigated as a means to overcome the challenges associated with high peak pressure rise rates at mid and high load conditions. The objective was to demonstrate low, mid, and high load neat n-butanol operation. The engine test data was combined with after-treatment modelling to quantify the combined fuel consumption of the LNT and the engine and to determine if long breathing LNT operation with neat n-butanol was feasible at all load conditions.

2.5 Post Injection Strategies for the Active Control of the Exhaust Gas

The NO_x storage cycle of the LNT is the main focus of the long breathing technique. However, the LNT regeneration cycle is also important for achieving a high NO_x conversion efficiency. The LNT regeneration can be sensitive to the exhaust gas temperature and the type of NO_x reducing agents that can range from hydrocarbon fuel to hydrogen. Diesel combustion is traditionally overall lean and generally results in relatively low concentrations of exhaust gas hydrocarbons, carbon monoxide, and hydrogen. Furthermore, the lean NO_x trap generally achieves the highest NO_x conversion efficiency within a narrow temperature range, such as 250 to 450°C [77,78,83]. Diesel exhaust gas can have a very broad temperature range from low to high load conditions. These exhaust gas characteristics of lean-burn CI engines may lead to unfavourable conditions for LNT regeneration. Thus, a strategy is required to manage the exhaust gas temperature and composition to ensure that the LNT is exposed to suitable exhaust conditions.

In particular, studies have shown that the presence of hydrogen in diesel exhaust can be beneficial for NO_x after-treatment devices [79,84,90,97-99]. West et al. investigated the use of hydrogen as a NO_x reducing agent during an LNT regeneration process [79]. The results indicated that the location within the LNT that had the largest NO_x reduction coincided with the highest hydrogen consumption [79]. Kong et al. compared the use of hydrogen with the use of diesel as a NO_x reducing agent in an LNT and observed that a higher NO_x conversion efficiency was achieved with hydrogen [98]. The use of hydrogen enabled high NO_x conversion efficiencies at low exhaust temperatures, as low as 145°C, at which the diesel reducing agent was not effective [98]. Poulsten and Rajaram also demonstrated the low-temperature benefits of hydrogen and showed that utilizing hydrogen as a NO_x reducing agent consistently resulted in higher NO_x conversion efficiencies for thermally aged catalysts [99]. Monroe and Li reported that the presence of hydrogen during the LNT desulfation was of critical importance for sulfur removal [90]. The study demonstrated that the desulfation was only effective if either water or hydrogen were present (water was capable of producing hydrogen via the water gas shift reaction) [90].

Hydrogen is not typically found in large concentrations in lean-burn exhaust but researchers have investigated on-board hydrogen generation [100,101]. Catalytic reactors can be placed in the exhaust stream to generate hydrogen via various reaction mechanisms such as steam reforming (SR), partial oxidation (POx), the water gas shift reaction (WGS), and dry reforming as shown in Equations 2-1 to 2-4 respectively. Each reaction requires certain exhaust gas conditions, such as temperature and species concentration, for optimal performance [102-106]. The exhaust gas must be carefully managed to ensure a high hydrogen yield from these reactions. The hydrogen yield can also heavily depend on the catalytic formulation of the exhaust reactor. On the other hand, hydrogen can also be generated inside the cylinder during combustion.



Thus, post injection strategies were implemented for the active management of the exhaust gas temperature and the production of suitable NO_x reducing agents such as hydrogen, carbon monoxide, and reactive light hydrocarbon species like propylene. The effects of the post injection timing and quantity, the combustion phasing, the intake oxygen, and low temperature combustion on the exhaust gas composition and temperature were investigated. The results of the investigation expected to identify and develop a post injection strategy for generating a high yield of desirable NO_x reducing agents and for active control of the exhaust gas temperature. A further objective was to

quantify the potential emission penalties associated with post injection strategies for active management of the exhaust gas.

CHAPTER 3: RESEARCH TOOLS

This chapter provides a description of the research tools for the proposed studies. Details are given for the set-up of the engine tests and the after-treatment flow bench tests. The various physical instruments, sensors, and devices that were used for the experimental testing are outlined. Schematic diagrams and photos of the experimental set-up are provided.

3.1 Experimental Setup for Engine Tests

All of the tests were carried out at the Clean Diesel Engine Laboratory at the University of Windsor. A Ford Duratorq internal combustion engine was utilized for the in-cylinder NO_x reduction tests, with neat n-butanol and diesel fuel, and for the post injection characterization tests. The engine was a four stroke, four cylinder, compression ignition engine with an 18.2:1 geometric compression ratio. The engine utilized a direct injection (DI), common rail fuel injection system with high pressure solenoid injectors. The fuel injection system was capable of delivering injection pressures up to 1800 bar.

EFS 8232 solenoid injector power drivers (iPoD) [107] were used to power and drive the injectors but the fuel injection was controlled through LabVIEW software and National Instruments (NI) real-time (RT) and field programmable gate array (FPGA) hardware. NI PXI 8110 real time controllers were used with NI PXI 7853R and PXI 7813R FPGA modules and NI LabVIEW 2010 [108,109]. The engine was coupled to a Schenck WS230 eddy-current dynamometer and a DyneSystems Dyn-Loc IV controller was utilized to control the dynamometer. The dynamometer had power adsorption functionality but it lacked engine motoring capabilities. The four cylinder engine was modified into an arrangement of one research cylinder and three non-research cylinders as shown in Figure 3-1. The three non-research cylinders were operated and utilized to motor the research cylinder when necessary. Further details of the engine and the injection system are given in Table 3-1.

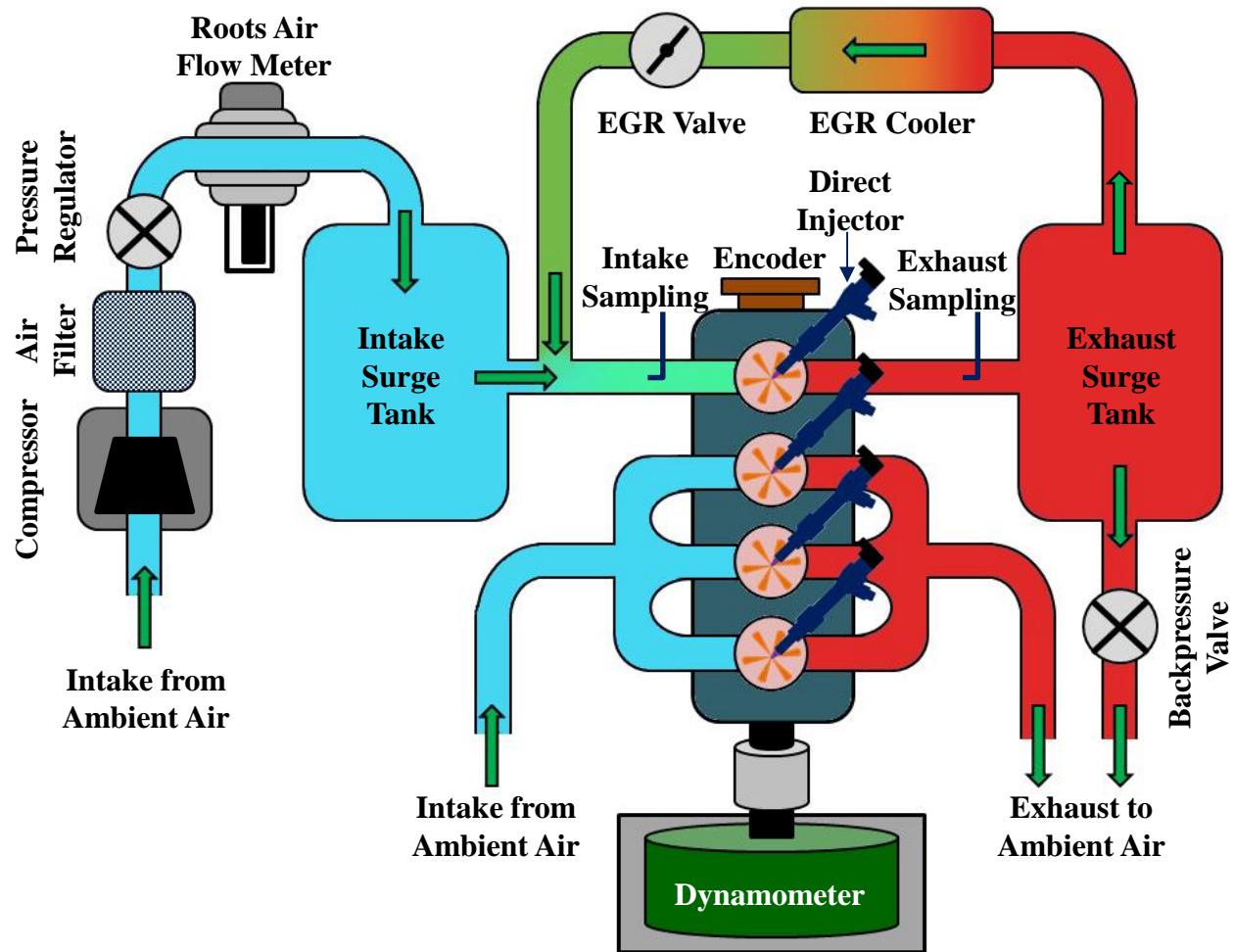


Figure 3-1: Schematic Diagram of the Experimental Setup for the Engine Tests

Table 3-1: Test Engine and Fuel Injection System Specifications

Number of Cylinders	4
Displacement per Cylinder [L]	0.5
Bore [mm]	86
Stroke [mm]	86
Compression Ratio	18.2
Peak Cylinder Pressure [bar]	180
Number of Injector Holes	6
Injector Nozzle Diameter [mm]	0.13

The research cylinder was isolated from the three non-research cylinders by independent intake and exhaust manifolds and by independent fuel injection control. The intake air for the research cylinder was provided by an off-engine compressor that was also utilized to simulate boost conditions. An SMC E/P ITV3051-31N4S5 electronically controlled pressure regulator was used to control the intake air pressure [112]. A high pressure EGR loop was implemented for the research cylinder. A Parker Sinclair Collins 316SS control valve [113] was installed downstream of the exhaust surge tank to control the exhaust backpressure. Large volume surge tanks were utilized to dampen out intake and exhaust gas fluctuations and to provide steady intake and exhaust conditions. The engine tests were conducted under steady operation and all of the data was recorded and reported under stable operating conditions.

Table 3-2: Pressure Transducer Specifications

Model	AVL GU13P
Measuring Range [bar]	0-200
Sensitivity [pC/bar]	15
Linearity [% FSO]	< ± 0.3

The in-cylinder pressure of the research cylinder was measured and recorded by an AVL piezoelectric pressure transducer that was mounted via a glow plug adapter. The specifications of the transducer are given in Table 3-2. The pressure transducer was coupled to a Kistler Type5010 B charge amplifier [110]. The engine speed was measured

with a Gurley Precision Instruments 9125S optical encoder [111]. The recorded pressure was synchronized with the piston position through TDC alignment of the encoder. The cycle-to-cycle pressure traces were recorded but the pressure and the heat release traces were analyzed and reported as averaged values of two hundred consecutive cycles⁷.

Modifications to the fuel injection delivery system were made for the neat n-butanol tests. A stand-alone fuel injection module with an independent high pressure fuel pump was utilized to store and deliver neat n-butanol to the research cylinder. For the neat n-butanol tests, the research cylinder was fuelled with butanol while the non-research cylinders operated on diesel fuel. To prevent potential damage to the fuel injection components, 500 ppmV of a lubricity improver, OLI-9070.x [114], were added to the butanol fuel. The effects of the lubricity improver on the ignition, combustion, and emissions characteristics were not investigated. The impacts of the lubricity improver were expected to be insignificant because of its relatively low volumetric fraction but definite conclusions cannot be made. The butanol high pressure injection system was limited to an injection pressure of 1200 bar to avoid vaporization of butanol within the fuel system. The properties of the diesel and the butanol test fuels were previously given in Table 2-2.

The intake gas was sampled at the intake manifold downstream of the EGR loop and the exhaust gas was sampled at the exhaust manifold upstream of the EGR loop. A variety of emission analyzers were employed to analyze the composition of the intake and the exhaust gases. The measured data from the emission analyzers was synchronized with the engine data through a local area network (LAN) connection and the use of the network published shared variables function in LabVIEW [115].

Exhaust hydrogen was a prime species of interest due to its aforementioned benefits to the lean NO_x trap. Thus, a V&F H-Sense mass spectrometer [116] was used to measure the quantity of hydrogen in the exhaust. The particulate matter emissions were measured by an AVL 415S smoke meter [117] and reported in terms of the AVL

⁷ Two hundred cycles were chosen to increase the fidelity and confidence of the data, as shown by the fairly narrow 95% confidence interval for the results in section 5.2, while maintaining a reasonable data file size.

filter smoke number (FSN). Consequently, the PM emissions were presented as smoke emissions in the results section. A set of California Analytical Instruments (CAI) non-dispersive infrared analyzers were used to measure the intake and the exhaust carbon dioxide and the exhaust carbon monoxide. A CAI chemiluminescence detector was utilized for the measurement of the exhaust nitrogen oxides while a CAI heated flame ionization detector (FID) measured the total hydrocarbons in the exhaust. The noise, zero drift, repeatability, and linearity uncertainties for the CAI emission analyzers were each less than 1% of the full scale operating range.

An MKS 2030 DS Fourier transform infrared (FTIR) analyzer [118] was used for hydrocarbon speciation and for a supplementary measurement of the exhaust NO_x and CO emissions. The measurement of the total hydrocarbons from the FID generally followed the same trends as the aggregate total hydrocarbon emissions from the FTIR measurement. However, there were noticeable differences under operating conditions which generated a high quantity of unburned hydrocarbons. These differences were mostly attributed to the use of a fully heated sampling line for the FTIR measurement and a mostly unheated sampling line for the FID measurement. Furthermore, the FTIR measurements represented wet gas analysis while the FID measurement represented dry gas analysis since a chiller was used upstream of the FID to remove water from the sample gas. For these reasons, the THC emissions were reported based on the FTIR measurements. The THC emission values were presented based on carbon atom counting (ppmV C_1). The emission measurements were taken as time-averaged values over a ten second steady-state sampling period for the CAI analyzers and a five second sampling period for the FTIR measurements.

3.2 Experimental Setup for After-Treatment Flow Bench Tests

A heated after-treatment flow bench was used for experimental testing of the lean NO_x trap. A photo of the after-treatment setup is given in Figure 3-2 and a schematic diagram of the flow bench setup is shown in Figure D-1 in Appendix D. The flow bench utilized compressed gas cylinders from Praxair and externally compressed air to simulate the diesel exhaust gas composition at different operating conditions. The compressed air

provided the supply of oxygen while bottled nitrogen gas diluted the oxygen concentration as necessary. Furthermore, bottled carbon dioxide, carbon monoxide, and nitrogen oxides were employed to simulate diesel exhaust conditions. The simulated exhaust did not contain any particulate matter to prevent damage to system components. The gas flow was controlled by manually adjusting the pressure regulators of each compressed gas cylinder.

The feed gas was sampled upstream of the LNT catalyst and the outlet gas was sampled downstream of the LNT catalyst as shown in Figure 3-2. The composition of the feed gas and the outlet gas was analyzed by the gas analyzers previously described in the experimental setup for the engine tests. The feed gas composition from the gas analyzers was used as feedback information for adjusting the flow pressure of each gas. National Instruments LabVIEW software was employed to monitor and record the measured gas composition. The mass flow rate of the feed gas was measured by a Bosch mass air flow (MAF) sensor, model 0281002619, that was installed upstream of the heater.

The simulated exhaust was heated by a Leister Hot Air Tool 10000S in-line gas heater to simulate diesel exhaust temperatures at different operating conditions. The heater was controlled by an Omron E5CK control panel. The heater was rated for a maximum output temperature of 650°C with a minimum flow rate of 500 standard litres per minute. A thermocouple was installed downstream of the heater for feedback control of the heater outlet temperature.

Water injection was installed downstream of the heater. The water was injected by a fuel injector designed for port fuel injection of gasoline. A second gasoline port fuel injector was installed upstream of the LNT catalyst to dose diesel fuel directly into the feed gas for LNT regeneration. The water and fuel injections were controlled by in-house programming codes developed in NI LabVIEW software. The injections were implemented by a National Instruments cRIO-9002 real-time controller and a cRIO-9474 digital output module.

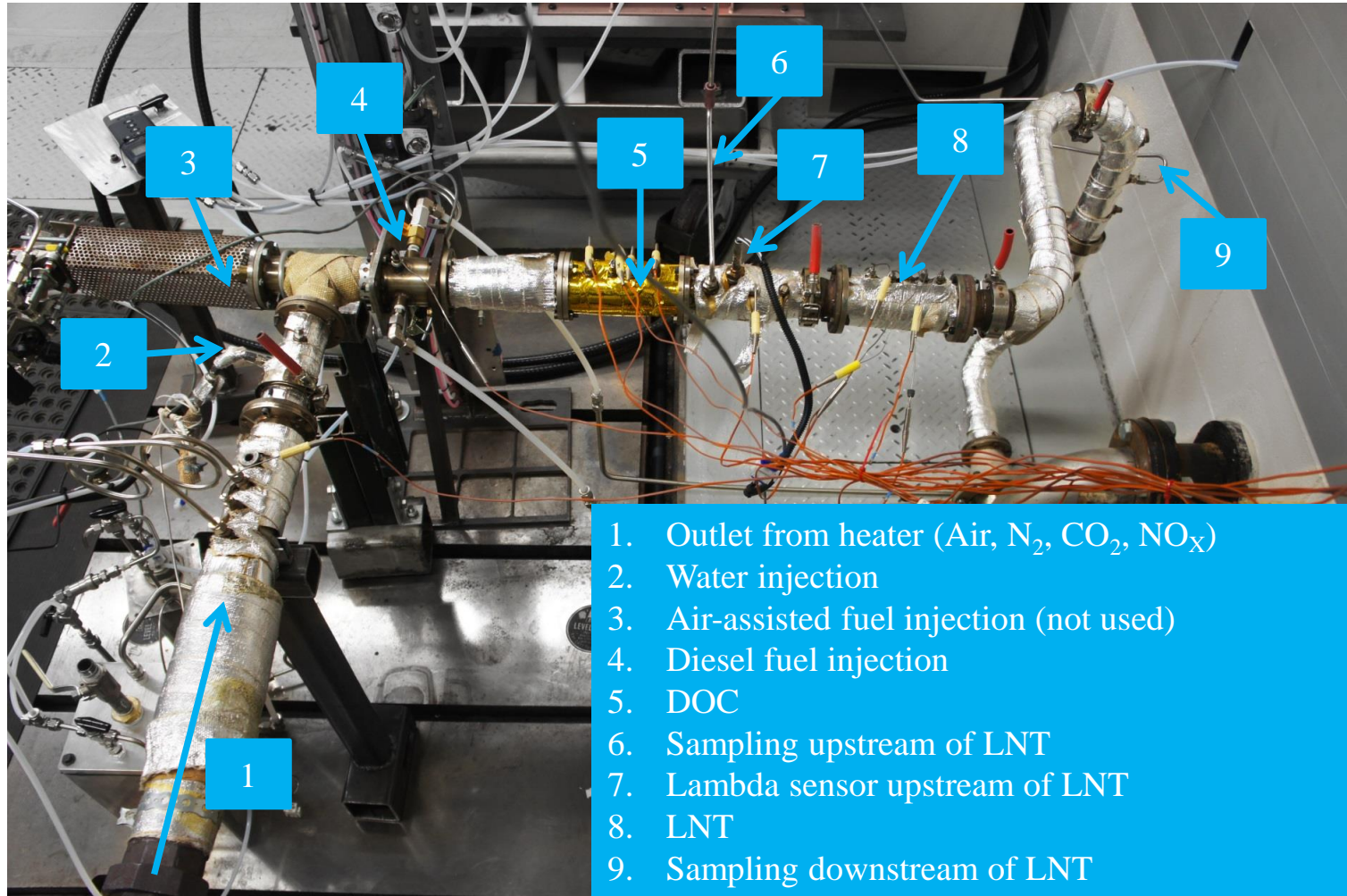


Figure 3-2: Photo of the After-treatment Flow Bench Setup

The lean NO_x trap catalyst was purchased as a commercially available product from Volkswagen with product code 1KO-254-401-T. The purchased catalyst was a ceramic honeycomb substrate but the catalyst coating and the precious metal composition information were not available. The purchased catalyst was designed for use with passenger car diesel engines that are similar in on-road application to the test engine. The catalyst substrate was a cylindrical monolith with a 5.66 inch diameter and a 6 inch length. For proper sizing on the after-treatment flow bench, a 44 mm diameter core with a 152.4 mm length was cut out from the purchased sample. The substrate channel density was measured to be 400 cells per square inch (cpsi). Four equally spaced Omega K-type thermocouples were placed along the centerline of the longitudinal axis of the catalyst for measurement of the catalyst temperature.

CHAPTER 4: LONG BREATHING USING DIESEL FUEL AND EGR

This chapter presents the results for in-cylinder NO_x reduction with diesel fuel and exhaust gas recirculation. EGR tests for NO_x reduction have been previously carried out by other researchers [19-27] but the primary purpose of the present tests is to utilize EGR to identify a suitable engine-out NO_x level for long breathing operation at conditions ranging from low to high load. The emission and fuel consumption penalties are also analyzed at each condition and recommendations are made regarding the feasibility of utilizing long breathing with diesel fuel and EGR at each operating condition. Finally, the exhaust gas conditions at each load level are characterized for the purpose of replicating the conditions for the after-treatment studies.

4.1 Engine Test Conditions for the EGR Tests

Several exhaust gas recirculation tests were conducted to characterize the effect on NO_x emissions and to determine a suitable intake oxygen and engine-out NO_x range for the long breathing strategy. All of the tests were conducted on the Ford Duratorq engine described in the previous chapter. The EGR sweep tests were conducted over a broad span of engine loads, ranging from low to high load as shown in Table 4-1 to Table 4-3. Multiple sets of tests were conducted at each load level to improve the fidelity of the data and the trends. The engine speed was maintained constant at 1500 rpm for all tests.

The intake air pressure was constant throughout the EGR sweep at each load but was increased at higher loads to help mitigate the impact of higher flame temperatures on the smoke emissions. The fuel injection pressure was also increased when the engine load was increased as shown in Table 4-1⁸. This was done to improve the fuel atomization and to prevent excessive smoke emissions at higher load conditions. The injection duration and the injection timing for the EGR sweep at each load are given in Table 4-1. All of the EGR sweeps utilized a single shot injection near the end of the cylinder compression cycle. The fuel injection duration and timing given in Table 4-1

⁸ The air intake pressure and the fuel injecting pressure were controlled through dedicated hardware and software, as described in Chapter 3, and the engine control unit was not used in any of the engine tests.

represent the values for the condition without EGR. Micro adjustments were made to the fuel injection timing and duration throughout the EGR sweep to maintain a near constant engine load and combustion phasing.

Table 4-1: Test Conditions for Low Load EGR Sweep

IMEP [bar]	6.1	6.2
Engine Speed [rpm]	1500	1500
Air Intake Pressure [bar absolute]	1.3	1.3
Test Fuel	Diesel	Diesel
Injection Pressure [bar]	1100	1100
Commanded Injection Duration [μ s]	465	420
Commanded Injection Timing [$^{\circ}$ CA ATDC]	-4.0	-2.0

Table 4-2: Test Conditions for Medium Load EGR Sweep

IMEP [bar]	10.1	10.2
Engine Speed [rpm]	1500	1500
Air Intake Pressure [bar absolute]	1.9	1.9
Test Fuel	Diesel	Diesel
Injection Pressure [bar]	1400	1400
Commanded Injection Duration [μ s]	605	580
Commanded Injection Timing [$^{\circ}$ CA ATDC]	-1.6	-1.0

Table 4-3: Test Conditions for High Load EGR Sweep

IMEP [bar]	14.7	15.2
Engine Speed [rpm]	1500	1500
Air Intake Pressure [bar absolute]	2.5	2.5
Test Fuel	Diesel	Diesel
Injection Pressure [bar]	1400	1400
Commanded Injection Duration [μ s]	800	860
Commanded Injection Timing [$^{\circ}$ CA ATDC]	2.0	0.5

4.2 NO_x Reduction with EGR

The effect of exhaust gas recirculation on the NO_x emissions is illustrated in Figure 4-1. The data was plotted with regards to the intake oxygen quantity where lower intake oxygen represented a higher EGR rate. The effect of EGR on the NO_x emissions was found to be consistent across all engine load levels. There was a significant reduction in NO_x when EGR was applied. The NO_x reduction was mostly attributed to the reduction of the intake oxygen rather than the thermal and chemical effects of EGR application [19-22]. The biggest decline in NO_x was encountered when the intake oxygen was initially lowered from 20 to 16.5% by volume. Further reduction of the intake oxygen resulted in a lower rate of NO_x reduction as demonstrated by the reduced slope in Figure 4-1. These results were consistent with data reported in literature [20-21,24-27].

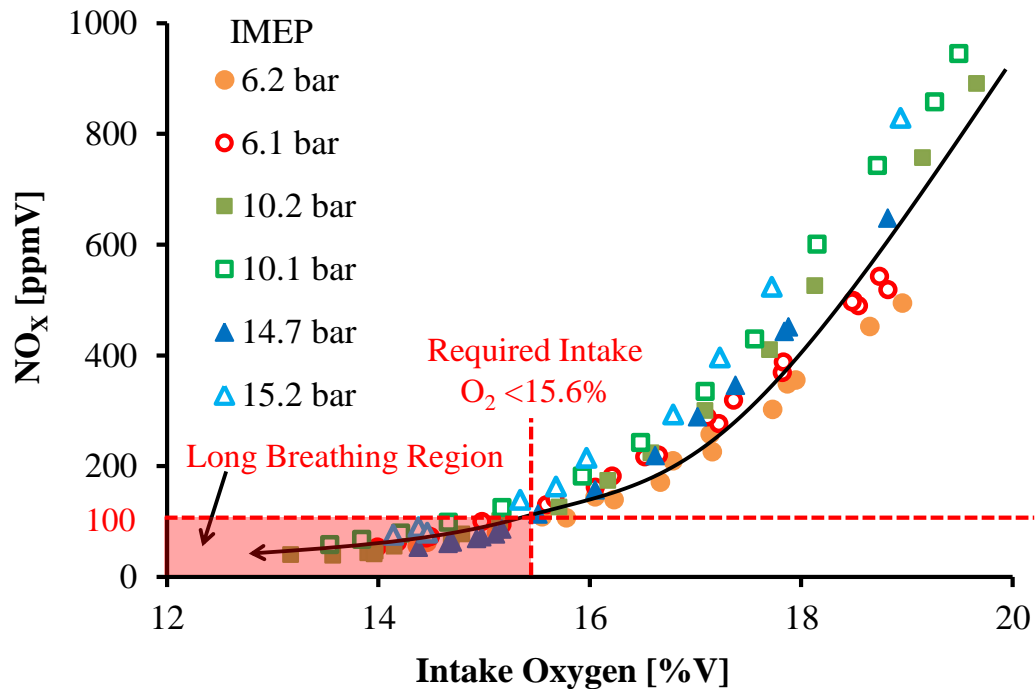


Figure 4-1: Effect of Intake Oxygen on NO_x Emissions for Long Breathing LNT

For long breathing LNT operation, a NO_x target of 100 ppmV was suggested as the upper limit. This value was chosen based on previous work [96] and numerical calculations, previously shown in Figure 2-5 and Figure 2-6, which indicated that the NO_x storage cycle was significantly extended when the NO_x was reduced to 100 ppmV or lower. The engine test data was analyzed to determine the required intake oxygen quantity to achieve the 100 ppmV NO_x emission target at each test condition. The results are summarized in Table 4-4. The NO_x value given in the table represents the data point in the EGR sweep which was closest to 100 ppmV NO_x.

Table 4-4: Upper Limit for Intake Oxygen for Long Breathing LNT Operation

IMEP [bar]	Intake O₂ [%V]	NO_x [ppmV]	NO_x [g/kW·hr]
6.1	15.2	94	0.74
6.2	15.6	104	0.79
10.1	14.7	99	0.68
10.2	15.2	101	0.70
14.7	15.3	99	0.66
15.2	14.4	90	0.57

The data indicated that the required intake oxygen was consistently within the range of 14.4% to 15.6 % by volume. Thus, this was the range selected as the upper limit for the maximum allowable intake oxygen quantity for long breathing operation. As shown in Table 4-4, the upper limit for indicated engine-out NO_x emissions for long breathing did not exceed 0.8 g/kW·hr. The lower limits for the intake oxygen and the engine-out NO_x for long breathing operation were difficult to determine from Figure 4-1 since the data showed that the NO_x emissions continued to decrease as the intake oxygen was reduced. However, reduction of the intake oxygen concentration was expected to eventually result in emission or fuel consumption penalties. Thus, the effects of the EGR sweep on the fuel consumption, the smoke, the total hydrocarbon, and the carbon monoxide emissions were investigated.

4.3 Effect of EGR on Emissions and Engine Fuel Consumption

An analysis of the exhaust emissions of smoke, THC, and CO was carried out to help identify the emission penalties for long breathing LNT operation. The effect of EGR application on the smoke emissions is demonstrated in Figure 4-2. The results showed that the smoke emissions constantly increased as the intake oxygen was reduced. In these tests, the intake oxygen was not reduced to the extent to reach low temperature combustion. The data established that the smoke emission penalty was higher at higher load conditions. The peak smoke at low load conditions did not exceed 1.5 FSN but it exceeded 3.0 FSN for mid and high load conditions. For the mid and high load conditions, the peak smoke emissions exceeded the targeted smoke limit of 2.0 FSN that was selected based on an equivalent indicated PM emission of 0.1 to 0.2 g/kW·hr. This smoke emissions level would require a reasonable filtration efficiency of approximately 90% to 95% from the DPF to meet the current PM emission regulation requirement.

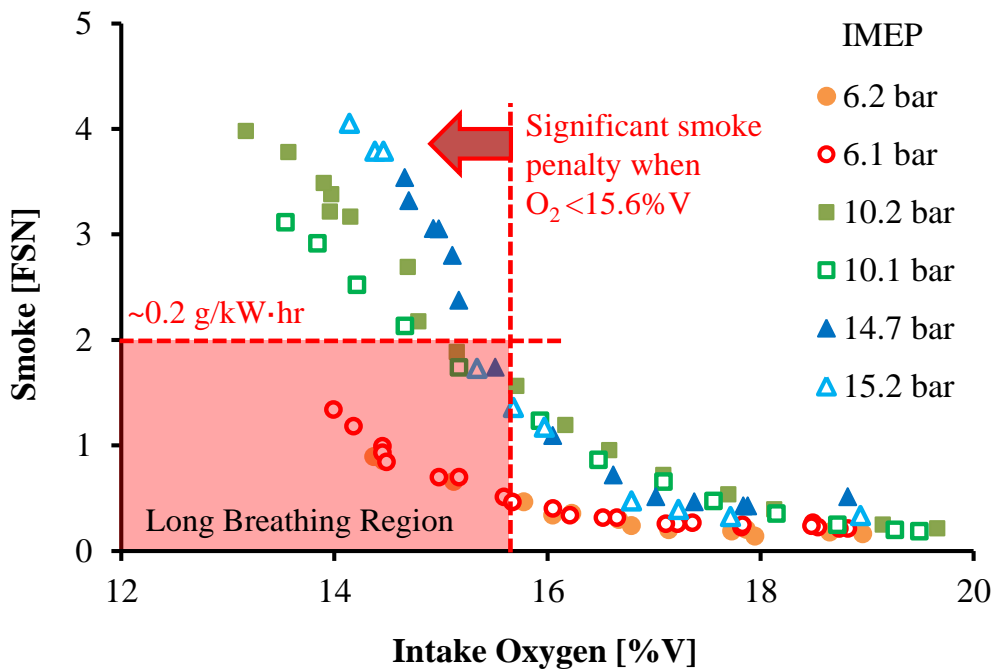


Figure 4-2: Effect of Intake Oxygen on Smoke Emissions

The data in Figure 4-2 was analyzed and the lower limit for the intake oxygen for long breathing operation was selected based on the NO_x emission target of 100 ppmV and the smoke emission target of 2.0 FSN. Based on these criteria, the intake oxygen and the corresponding engine-out NO_x emissions were summarized for each test condition as shown in Table 4-5. The data indicated that the engine-out NO_x emissions were not lower than 0.39 g/kW·hr. Thus, the test results in Table 4-4 and Table 4-5 suggested that a suitable engine-out NO_x level for long breathing operation was in the range of 0.4 to 0.8 g/kW·hr.

Table 4-5: Lower Limit for Intake Oxygen for Long Breathing LNT Operation

IMEP [bar]	Intake O ₂ [% V]	Smoke [FSN]	NO _x [g/kW·hr]
6.1	14.4	0.9	0.41
6.2	14.0	1.3	0.39
10.1	14.7	2.1	0.68
10.2	14.8	2.2	0.52
14.7	15.2	2.4	0.56
15.2	15.2	2.0	0.85

The data in Table 4-4 and Table 4-5 also revealed that the intake oxygen and engine-out NO_x ranges for long breathing were the widest at low load conditions and the narrowest at high load conditions. This observation suggested that long breathing may be more suitable for low load and mid load conditions. In fact, for the high load condition at 15.2 bar IMEP, there was not a single data point which met the required NO_x and smoke emission criteria. Thus, for this condition, the lower limit for the intake oxygen was higher than the upper limit which signified that long breathing was not possible at high load under the selected emission targets. This was an indication that long breathing LNT operation may not be suitable with EGR application at high load conditions. It may be possible to increase the fuel injection pressure and the intake air pressure to reduce the smoke emissions at high load but additional tests are required to investigate the impact of these parameters.

The effect of the EGR sweep on the total hydrocarbon emissions is shown in Figure 4-3. The results showed that the use of EGR consistently increased the THC emissions for all of the tested operating conditions. The highest THC emissions were observed at low load conditions which were two to three times higher than at mid and high load conditions throughout the EGR sweep. This appeared to indicate that the THC penalty was the highest at low load conditions. However, the relative effect of EGR on the THC was approximately the same at all conditions. For all engine loads, the THC emissions increased two to three times when the intake oxygen was reduced from 20% V to the long breathing LNT region. Furthermore, the THC emissions were below 100 ppmV throughout the test for all load conditions and the implementation of a diesel oxidation catalyst would be enough to reduce the THC emissions below the emission regulation requirement. Overall, the data demonstrated that the THC emission penalty was not a major concern for long breathing LNT operation over a broad range of engine load conditions.

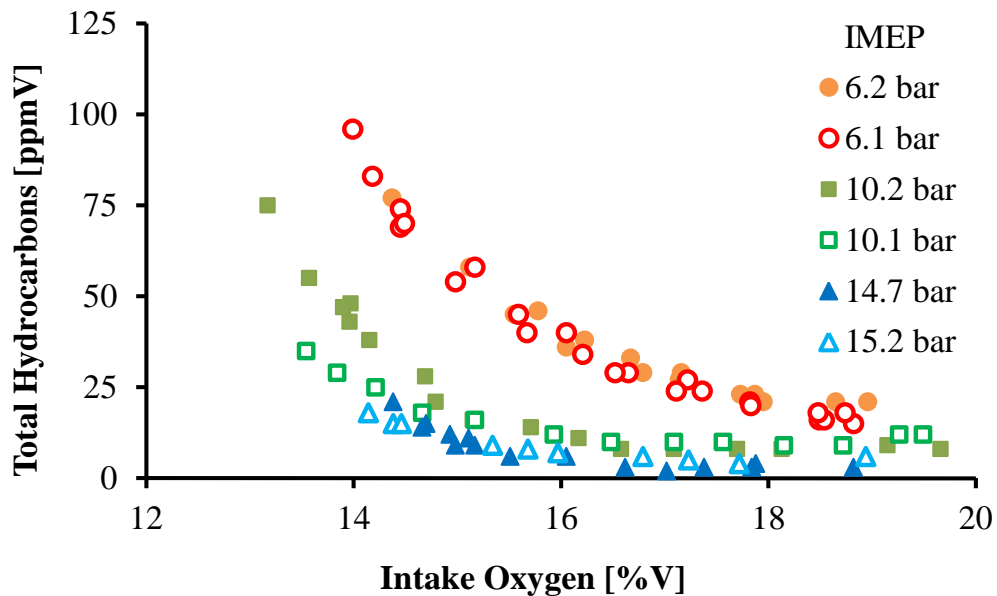


Figure 4-3: Effect of Intake Oxygen on THC Emissions

The carbon monoxide emissions were also affected by the application of EGR as shown in Figure 4-4. Just like THC emissions, the CO emissions continually increased throughout the EGR sweep. However, for the CO emissions, there was not a distinct difference at different engine load levels. The low load conditions generally produced the highest CO emissions but not throughout the entire EGR sweep. The data also showed that the relative CO emission penalty was the highest at high load conditions. For operation in the long breathing LNT range, the use of EGR led to more than a tenfold increase in the CO emissions at high load but only a threefold increase at low load.

The CO emissions were significantly higher than the THC emissions. For most conditions, the CO emissions exceeded 1000 ppmV when the intake oxygen was reduced below 15%V while the THC emissions remained below 100 ppmV. Therefore, there was a significant CO emission penalty for long breathing LNT operation but that was not a major concern since the absolute level of CO emissions was within the working range of a diesel oxidation catalyst. Overall, the results indicated that smoke was the primary emission of concern for long breathing operation, particularly at high load conditions.

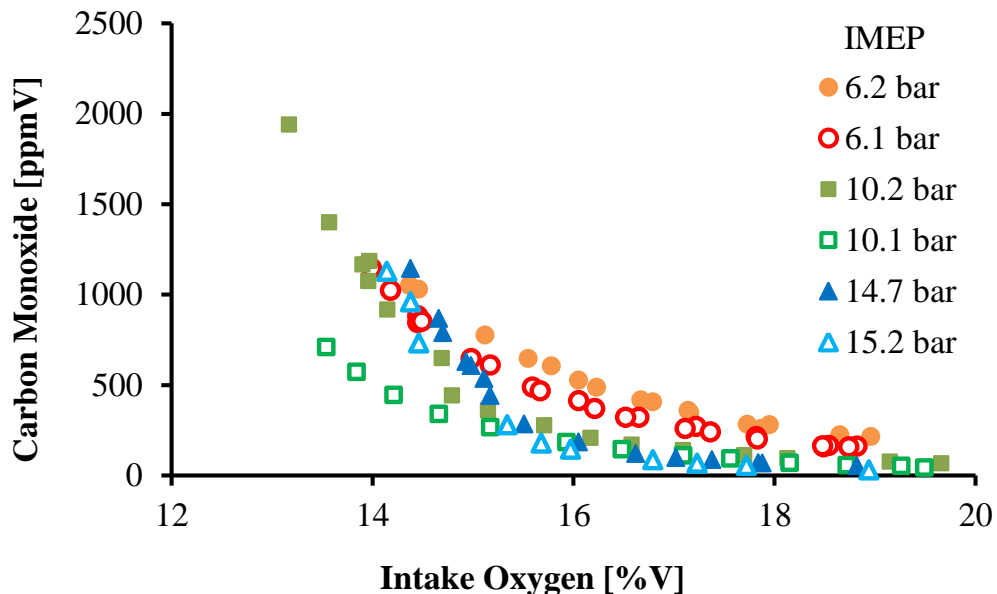


Figure 4-4: Effect of Intake Oxygen on CO Emissions

The effect of the EGR sweep on the indicated specific fuel consumption (ISFC) was also investigated. The ISFC was calculated from the measured fuel flow rate and the indicated power of the research cylinder as shown in Equation 4-1. The main goal was to determine the potential fuel consumption penalty for the long breathing with EGR method. The fuel consumption penalty was calculated at each load condition by comparing the indicated specific fuel consumption of conventional and long breathing operation. The conventional operation was defined as having a very high intake oxygen, above 18% by volume, while the long breathing region was identified according to the intake oxygen values shown in Table 4-4 and Table 4-5.

$$ISFC [g/kW\cdot hr] = \frac{Fuel\ Flow\ Rate [g/s] \times 3600 [s/hr]}{Indicated\ Power [kW]} \quad (4-1)$$

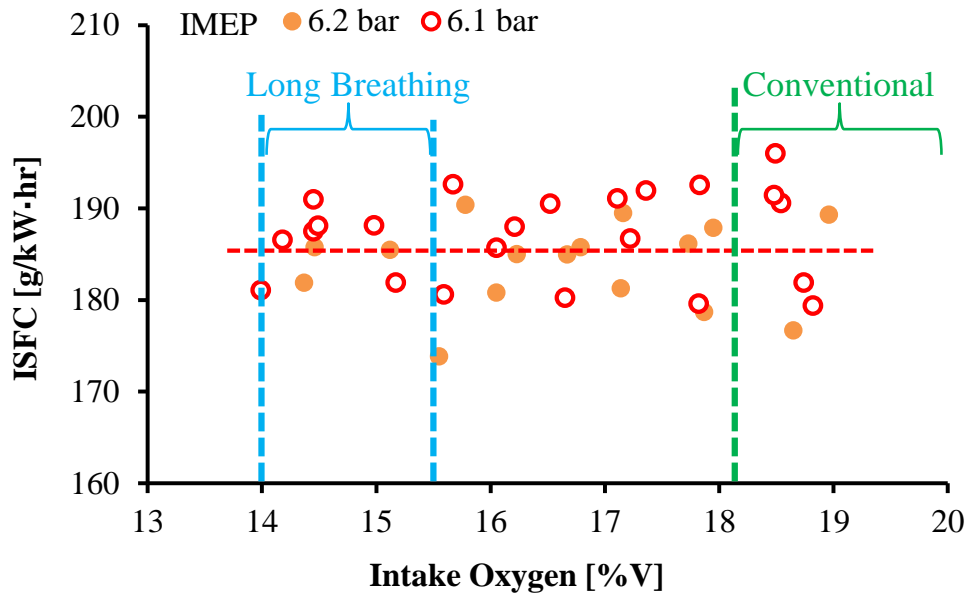


Figure 4-5: Effect of EGR on ISFC at Low Load Conditions

The effect of the EGR sweep on the ISFC at low load conditions is shown in Figure 4-5. Two sets of EGR sweeps were done and the overall trends showed that the

use of EGR had an indeterminate effect on the ISFC. Averaged values of the ISFC for the conventional and the long breathing regions were calculated and compared to determine the overall fuel consumption penalty. The average ISFC was 186.4 g/kW·hr for the conventional operation region and 185.3 g/kW·hr for the long breathing region. Thus, there was actually a 0.6% decrease in the fuel consumption when the engine was operated in the long breathing region at low load conditions. The decreased fuel consumption may not be maintained at all low load conditions but the result was a good indication that the use of long breathing with EGR did not cause an apparent engine fuel consumption penalty at low load conditions.

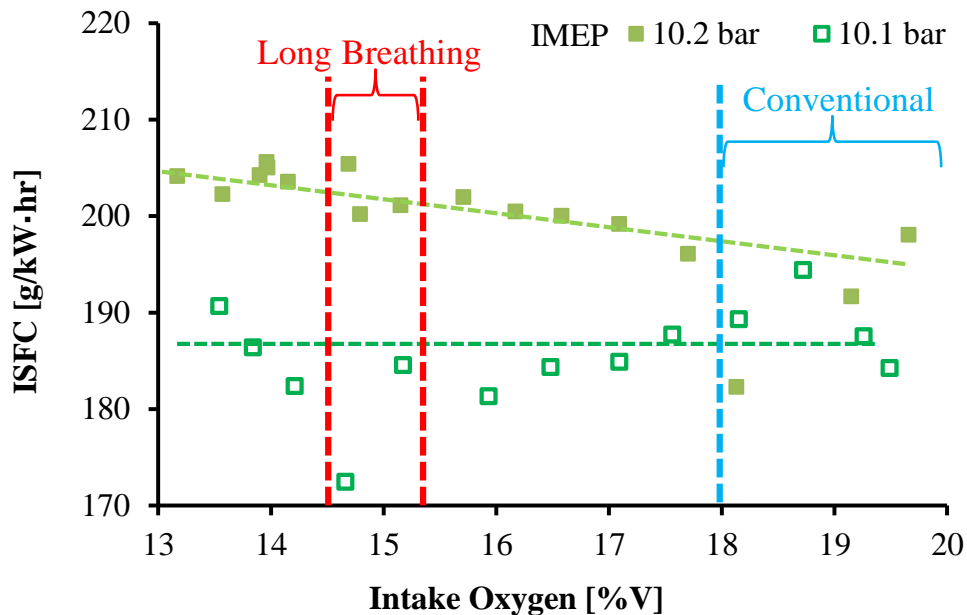


Figure 4-6: Effect of EGR on ISFC at Medium Load Conditions

There was a different outcome when EGR was applied at medium load conditions as shown in Figure 4-6. The two different EGR sweeps showed different trends. For the EGR sweep at 10.2 bar IMEP, there was a consistent increase in the ISFC as the intake oxygen was reduced. For the EGR sweep at 10.1 bar IMEP, the effect of EGR on the ISFC was generally negligible but there were a few outlier points which made it difficult to determine the overall trend. Nevertheless, averaging the ISFC in the conventional

operation region resulted in an ISFC of 189.7 g/kW·hr and in the long breathing region an ISFC of 192.7 g/kW·hr. This resulted in a relative fuel consumption penalty of 1.5%. Thus, at mid load conditions, long breathing LNT operation could only be justified if the fuel consumption savings of the long breathing LNT were high enough to offset the engine fuel consumption penalty of 1.5%. Analysis of the combined fuel consumption of the engine and the LNT is presented in Chapter 6.

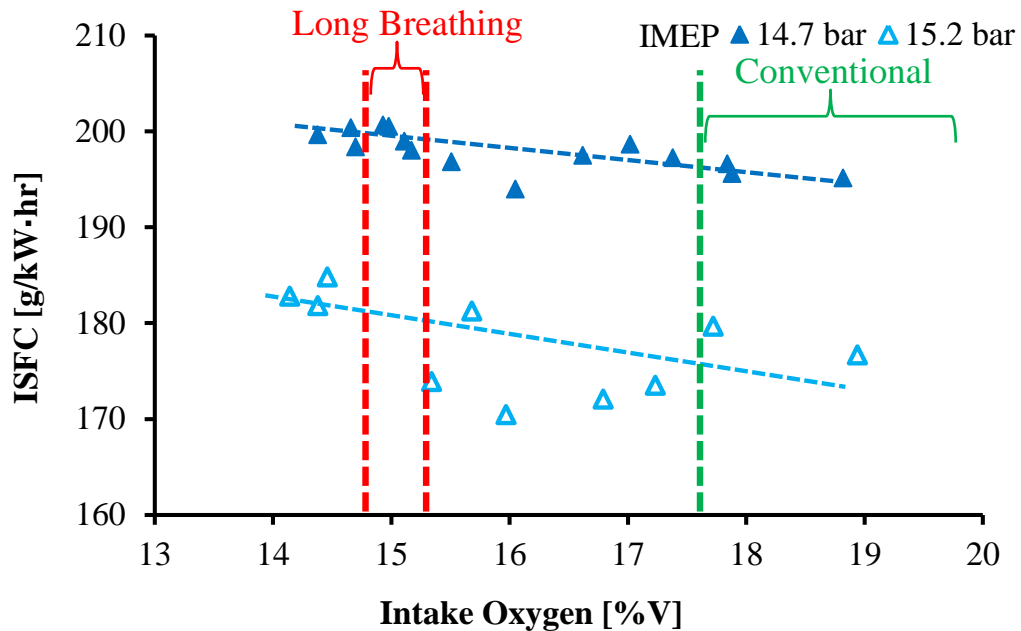


Figure 4-7: Effect of EGR on ISFC at High Load Conditions

At high load conditions, there was an even larger fuel consumption penalty. It should be noted that, due to the lack of data within the long breathing limits as specified in Table 4-4 and Table 4-5, the lower limit for the intake oxygen was extended to include data for smoke emissions up to 3.0 FSN. Also, the conventional operation region was extended to include data with intake oxygen as low as 17.8%. With these limits, the ISFC was 191.0 g/kW·hr for the conventional operation region and 194.4 g/kW·hr for the long breathing region. The overall relative fuel consumption penalty was calculated to be 1.8%. This implied that the fuel consumption savings of the long breathing LNT must be

higher than 1.8% to offset the engine fuel consumption penalty. The engine fuel consumption data was combined with the after-treatment data in Chapter 6 to determine the combined fuel consumption of the engine and the LNT and to determine the suitability of long breathing with EGR at high load conditions. A summary of the average fuel consumption values and the fuel consumption penalty at each load level is shown in Table 4-6.

Table 4-6: Summary of Fuel Consumption Penalties at Different Engine Loads

	IMEP Range [bar]	Average ISFC Conventional [g/kW·hr]	Average ISFC Long Breathing [g/kW·hr]	Relative Fuel Penalty [%]
Low Load	6.1 - 6.2	186.5	185.3	-0.6
Mid Load	10.1 - 10.2	189.7	192.7	1.5
High Load	14.7 -15.2	191.0	194.4	1.8

4.4 Chapter Summary for Long Breathing using EGR and Diesel Fuel

Exhaust gas recirculation was utilized to reduce the engine-out NO_x emissions to enable long breathing operation. The tests were carried out at a broad span of engine load conditions, ranging from 6 to 15 bar IMEP. An overall comparison between conventional operation and long breathing operation is illustrated in Figure 4-8. The required intake oxygen and engine-out NO_x levels for long breathing LNT operation at each condition were identified by utilizing 100 ppmV of NO_x and 2.0 FSN of smoke as the emission targets.

To achieve the aforementioned NO_x and smoke emissions targets, the engine test results indicated that long breathing operation generally required the intake oxygen to be reduced to 14.0 to 15.5%. The corresponding indicated engine-out NO_x emissions were 0.4 to 0.8 g/kW·hr. The use of this intake oxygen level provided significantly reduced engine-out NO_x emissions, compared to operation without EGR, for long breathing operation while mitigating the impacts on the smoke emissions and the engine fuel consumption. A further reduction of the intake oxygen had a diminished effect on the

NO_x emissions but increased the smoke emissions and the engine fuel consumption. The smoke emission penalty was found to be the highest at high load conditions and, consequently, long breathing operation at high load may not be justifiable under the tested conditions and hardware constraints.

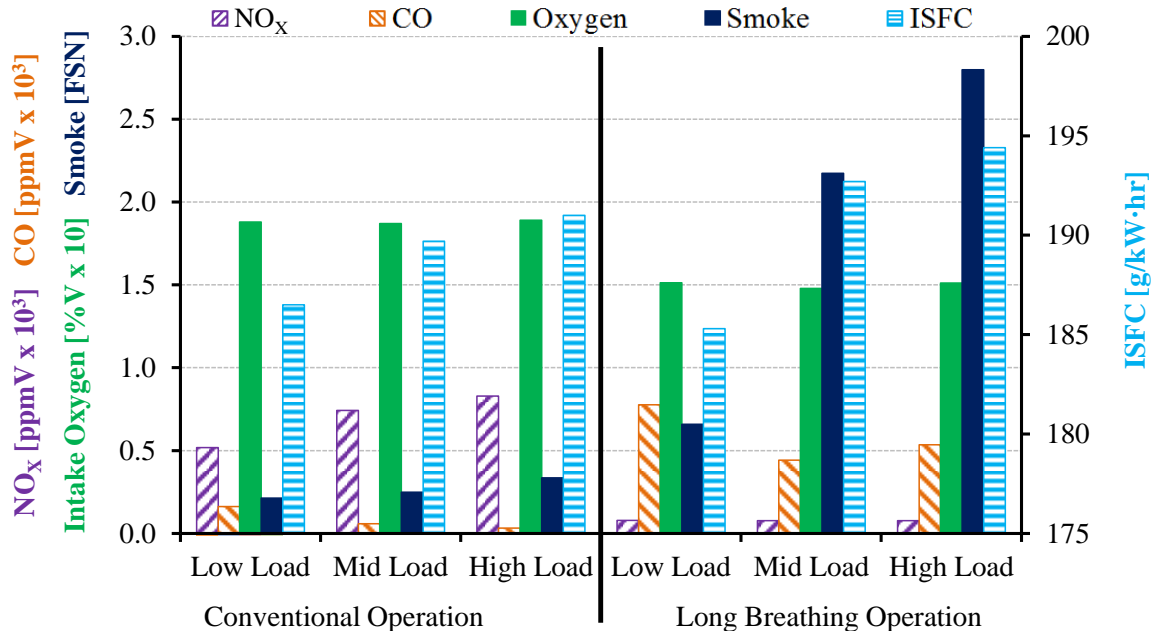


Figure 4-8: Summary for EGR Sweep Tests for Long Breathing LNT

A bigger concern was the fuel consumption penalty at medium and high load conditions as shown in Figure 4-8. The average fuel consumption penalty for long breathing operation was 1.8% at high load conditions. Further after-treatment analysis was required to determine if the supplemental fuel savings of the long breathing LNT outweighed the fuel consumption penalty of the engine at medium and high load conditions. At low load, the engine fuel consumption penalty was negligible. Thus, the overall results indicated that low load conditions appeared to be well-suited for long breathing operation due to the negligible smoke and fuel consumption penalties.

CHAPTER 5: LONG BREATHING USING NEAT BUTANOL FUEL

This chapter presents the results for in-cylinder NO_x reduction with neat n-butanol fuel. The primary purpose of these tests is to achieve ultra-low NO_x combustion, at conditions ranging from low to high loads, which is suitable for long breathing LNT operation. The tests are conducted without EGR since the greater volatility of n-butanol is suitable to attain highly premixed and ultra-lean combustion to reduce NO_x . Literature research and initial tests indicated that neat n-butanol combustion has challenges with extremely high peak pressure rise rates which limited the engine operation to low load conditions. Thus, various fuel injection strategies are investigated to achieve reduced peak pressure rise rates at each load level. Analysis is presented to examine the emission and fuel efficiency penalties at each load condition. This analysis leads to conclusions regarding the feasibility of each injection strategy at each load condition. Furthermore, the exhaust gas conditions at each load level are characterized for the purpose of replicating the conditions for exhaust after-treatment studies.

5.1 Ultra-Low NO_x Emissions with Neat Butanol Fuel

The previous chapter showed that the smoke emissions were one of the main penalties for long breathing LNT operation with diesel fuel, particularly at high load conditions. The smoke penalty was attributed to the use of EGR for in-cylinder NO_x reduction. Subsequently, a solution for in-cylinder NO_x reduction without the use of EGR was sought. Previous studies revealed that the use of neat n-butanol in a compression ignition engine enabled simultaneously low NO_x and smoke emissions [39]. However, the studies also indicated that excessive peak pressure rise rates can limit the engine operation to low load conditions [39]. Thus, tests were conducted to determine if the use of neat n-butanol was suitable for long breathing LNT operation and if it had any advantages compared to the use of diesel fuel with EGR.

The first set of tests directly compared the use of diesel fuel and the use of n-butanol at similar operating conditions to determine the advantages and disadvantages of n-butanol and to identify the limits of neat n-butanol combustion in a CI engine. For the

initial comparison, an engine load sweep was carried out with each fuel. The Ford Duratorq test engine, previously described in Chapter 3, was used for all of the tests. For the butanol tests, an off-engine fuel cart was utilized to deliver high pressure n-butanol fuel to the research cylinder. The experimental setup was previously described in more detail in Chapter 3 and the details of the test fuels were previously given in Table 2-2. The fuel n-butanol was used but, henceforth, for brevity, the term “n-butanol” will be utilized interchangeably with the term “butanol”.

The test conditions for the load sweep comparison are shown in Table 5-1. All of the parameters were the same for both diesel and butanol load sweeps except for the fuel injection timing. The fuel injection timing for the n-butanol test was always earlier compared to the diesel test due to the longer ignition delay of n-butanol. The injection timing for the n-butanol test was fixed throughout the load sweep (-22°CA ATDC) while the fuel injection timing for the diesel load sweep was adjusted throughout the sweep to try to match the combustion phasing with the butanol tests. The combustion phasing was characterized according to the crank angle of 50% heat released (CA50) and was in the range of 5 to 10°CA ATDC throughout the sweep.

Table 5-1: Test Conditions for Comparison of Butanol and Diesel

Fuel	n-Butanol	Diesel
Engine Speed [rpm]	1500	1500
IMEP [bar]	Sweep	Sweep
Air Intake Pressure [bar absolute]	1.9	1.9
Injection Pressure [bar]	900	900
Injection Strategy	Single Shot	Single Shot
Intake Oxygen [% V]	20.8	20.8

A comparison of the NO_x and the smoke emissions for butanol and diesel is shown in Figure 5-1. The results demonstrated the inherent advantage of neat butanol combustion as the NO_x and the smoke emissions were ultra-low throughout the load sweep. The smoke emissions were below 0.02 FSN and the NO_x emissions were below 15 ppmV. In terms of indicated power, the smoke emissions did not exceed 0.005

g/kW·hr and the NO_x did not exceed 0.06 g/kW·hr. This was significantly lower compared to the diesel tests at the same conditions. For diesel, the NO_x emissions were significantly higher throughout the sweep and reached 650 ppmV at 6 bar IMEP compared to 8 ppmV for butanol at the same IMEP. The smoke emissions were relatively low, less than 0.1 FSN, for the diesel test because of the high intake oxygen, but were consistently higher than the smoke emissions for butanol. These results suggested that n-butanol was more suitable than diesel fuel for low NO_x and low smoke combustion in a compression ignition engine.

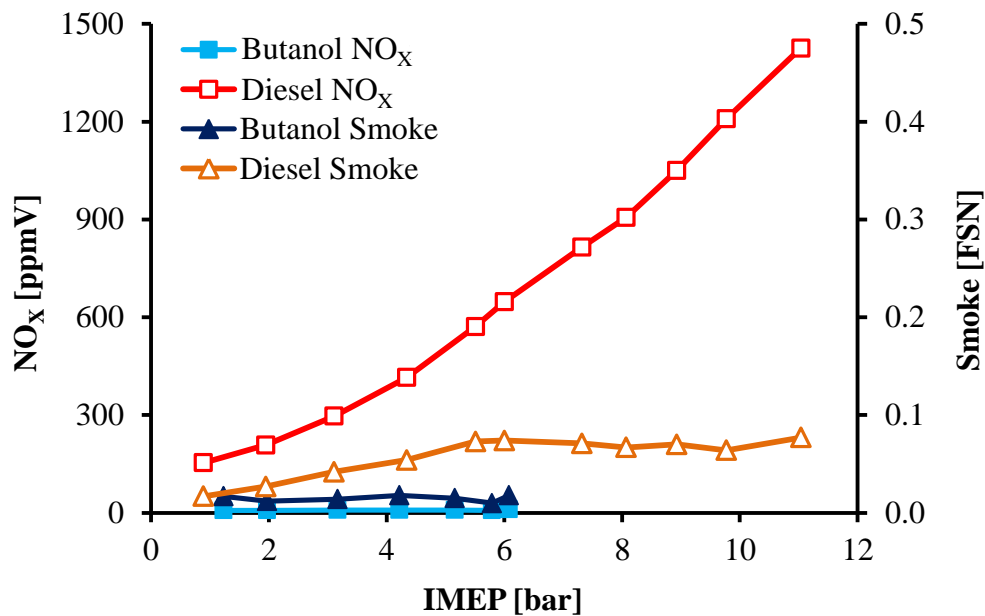


Figure 5-1: Butanol vs. Diesel: Effect of Load on NO_x and Smoke

The ultra-low NO_x and smoke emissions for butanol were attributed to its lower cetane number and higher volatility. The cetane number was 46.5 for the diesel test fuel and 25 for n-butanol. The average ignition delay⁹ was calculated as 2.6 ms for butanol and 0.5 ms for diesel as shown in Figure 5-2. The longer ignition delay, the lower boiling

⁹ The ignition delay (τ_{ID}) was calculated as shown in Equation 5-1. In this equation, the start of injection (SOI) was defined as the commanded fuel injection timing. The start of combustion (SOC) was defined as the crank angle at which the heat release exceeded 5 J/°CA.

point temperature, and overall very lean conditions, excess air to fuel ratio (λ) of 4 to 7, for butanol promoted the pre-mixing of the air and the fuel and resulted in low temperature combustion of butanol with ultra-low NO_x and smoke emissions. Additionally, the oxygen atoms present within the n-butanol molecules contributed to mitigating the smoke emissions. The relatively short ignition delay for diesel fuel resulted in a non-homogeneous air to fuel distribution with a mix of locally lean, stoichiometric, and rich regions that led to traditional diesel high temperature combustion and very high NO_x emissions.

$$\tau_{ID} [ms] = \frac{(SOC [^\circ CA] - SOI [^\circ CA]) \times 60000 [ms/min]}{Engine\ Speed [rpm] \times 360 [^\circ CA/revolution]} \quad (5-1)$$

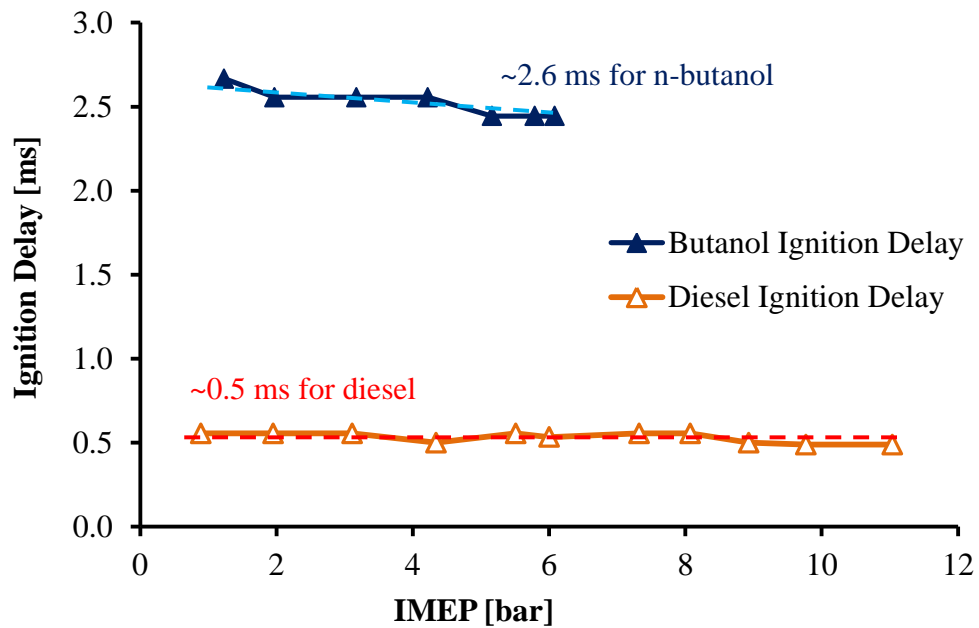


Figure 5-2: Comparison of Ignition Delay for Butanol and Diesel

The high NO_x emissions were an obvious disadvantage for diesel combustion because of the need for in-cylinder NO_x reduction, such as with EGR, to enable long breathing operation. The use of EGR with diesel increased the smoke emissions and

placed limitations to the use of long breathing for high load diesel operation. Conversely, the ultra-low NO_x and smoke emissions with neat butanol fuel implied that EGR was not required to reduce the engine-out NO_x. Thus, the use of long breathing with butanol can potentially avoid the smoke penalty which occurred with diesel fuel and EGR.

However, the results showed that there were load limitations for butanol due to the peak pressure rise rate (PRR) and the coefficient of variation of the IMEP (COV_{IMEP}). The results in Figure 5-3 illustrated that butanol low load operation was limited by extremely high COV_{IMEP}, above 20%, at around 1 bar IMEP and further reduction of the IMEP was not explored. The COV_{IMEP} was calculated according to Equation 5-2 where σ_{IMEP} represented the standard deviation of the IMEP of 200 consecutive cycles and μ_{IMEP} represented the mean value of the IMEP of 200 consecutive cycles. The results also showed that the COV_{IMEP} was much lower for the diesel fuel test at low load conditions. These results implied that there may be challenges related to unstable combustion with very low load neat butanol operation, such as at idle conditions. However, the results suggested that the high load limit was of bigger concern.

$$COV_{IMEP} = \frac{\sigma_{IMEP}}{\mu_{IMEP}} \quad (5-2)$$

The data in Figure 5-3 to Figure 5-5 showed rapid combustion and excessive peak pressure rise rates, exceeding 17 bar/°CA, for butanol at 6 bar IMEP. The load sweep was aborted at this load level to prevent potential damage to the engine. Conversely, the PRR was below 6 bar/°CA for the diesel test even when the IMEP was increased to 11 bar. These results highlighted a major disadvantage for neat butanol combustion, namely the restriction of the high load limit to 6 bar IMEP. Such a load limit would not be suitable in practice and there was a need to demonstrate high load operation as was achieved with diesel fuel. Thus, an objective was set to demonstrate high load operation with neat butanol, up to 14 bar IMEP, while maintaining the peak pressure rise rate below 17 bar/°CA, a level which was not expected to cause damage to the engine.

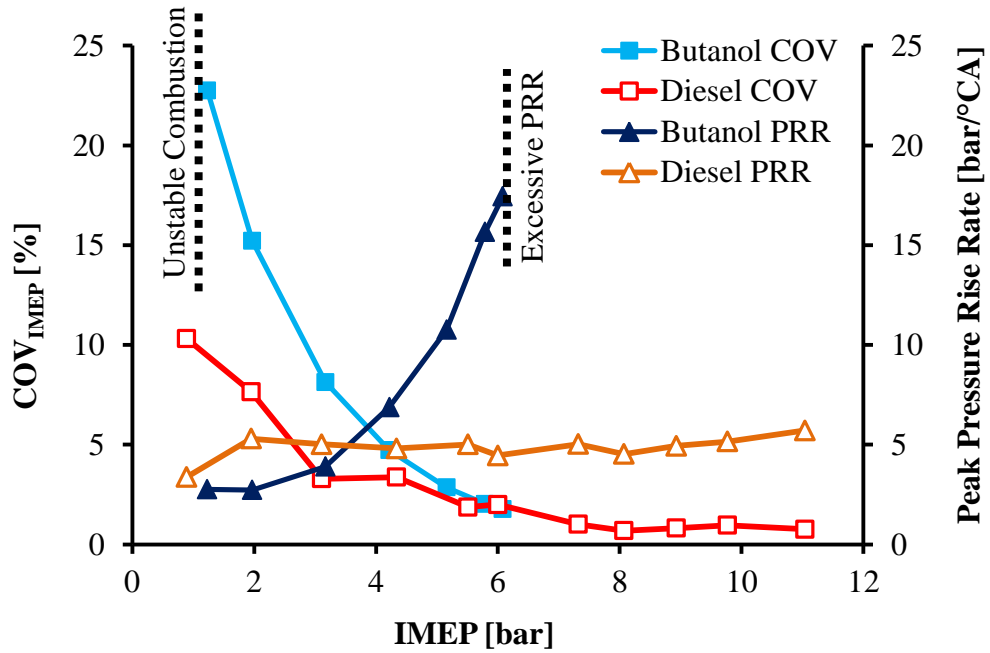


Figure 5-3: Butanol vs. Diesel: Effect of Load on PRR and COV_{IMEP}

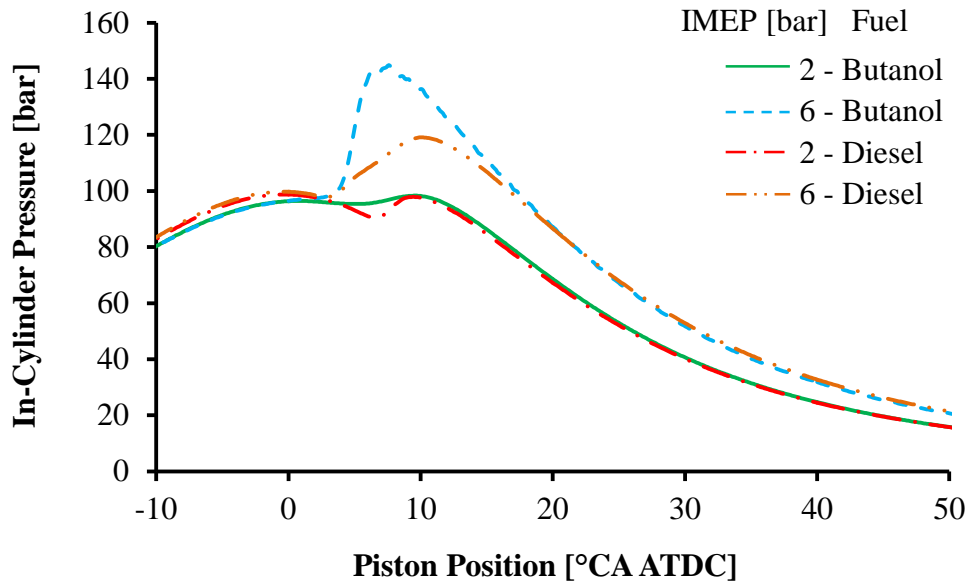


Figure 5-4: Butanol vs. Diesel: In-Cylinder Pressure Comparison

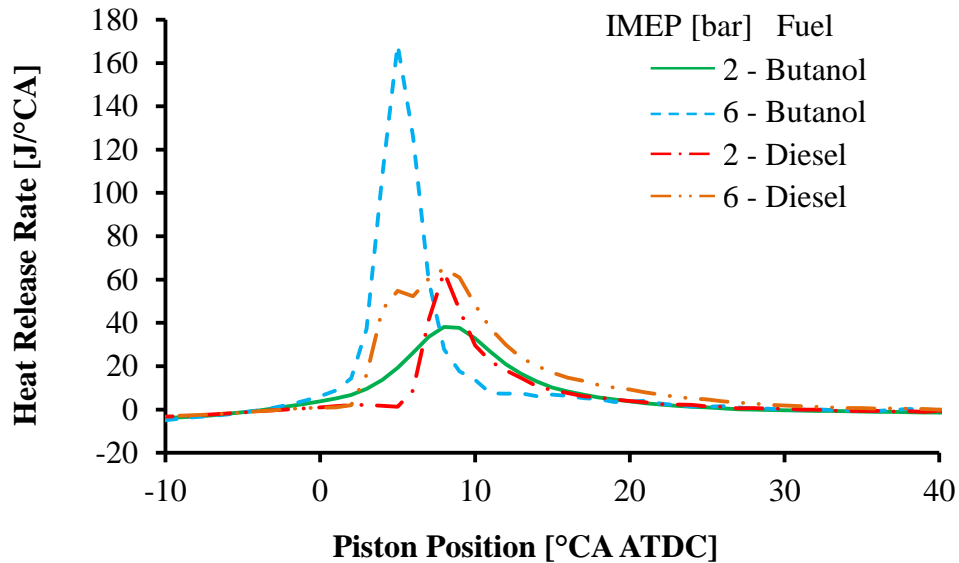


Figure 5-5: Butanol vs. Diesel: Heat Release Rate Comparison

5.2 Strategies to Mitigate the Peak Pressure Rise Rate of Neat Butanol

Three different fuel injection strategies for the direct injection of neat butanol were investigated for the reduction of the peak pressure rise rate: a delayed single shot injection, a pilot injection with a main injection, and a main injection with a post injection. The aim was to reduce the peak pressure rise rate while minimizing the impacts on the efficiency and the emissions. All three fuel injection tests were carried out at a nominal constant load of 6 bar IMEP that represented a low load condition relative to the full load of the production engine. However, the engine was designed to be used with diesel fuel and not with n-butanol fuel. Therefore, the investigation was conducted at a partial load of 6 bar IMEP to avoid excessive peak pressure rise rates that could occur with the use of neat n-butanol at higher load conditions. The methodology was to identify the fuel injection strategy that provided the largest reduction in the PRR at a constant load condition before attempting to use the strategy at higher load conditions.

The conditions for the delayed single shot fuel injection strategy are shown in Table 5-2. The delayed single shot tests were conducted at a fixed fuel injection duration of 670 μ s, which generated a 6 bar IMEP when the fuel injection timing was -24°CA

ATDC. The load was allowed to slightly fluctuate as the fuel injection timing was gradually delayed from -24 to -16°CA ATDC¹⁰. The engine speed, the intake air pressure, the fuel injection pressure, and the intake oxygen were fixed and EGR was not used in any of the neat butanol tests. The reduction in the PRR, the associated impacts on the fuel efficiency and the exhaust emissions were quantified for each injection strategy.

Table 5-2: Test Conditions for Single Shot Injection Timing Sweep

Nominal IMEP [bar]	6.0
Engine Speed [rpm]	1500
Air Intake Pressure [bar absolute]	1.9
Intake Oxygen [% V]	20.7
Test Fuel	n-Butanol
Fuel Injection Pressure [bar]	900
Fuel Injection Duration [μ s]	670
Fuel Injection Timing [°CA ATDC]	-24 to -16

The effect of the single shot fuel injection timing on the peak pressure rise rate is illustrated in Figure 5-6. The results showed that the PRR reduced from 17.1 to 3.1 bar/°CA when the injection timing was delayed from -24 to -16°CA ATDC. The PRR reduction was attributed to the longer and less rapid combustion as shown by the pressure traces in Figure 5-7 and the heat release traces¹¹ in Figure 5-8. Figure 5-8 illustrated that the heat release was relatively short and its peak was high for early injections, resulting in a rapid pressure rise at the onset of combustion as exemplified in Figure 5-7. When the single shot injection timing was delayed, the heat release was longer and the peak was lower, causing a more gradual pressure increase.

$$\frac{dQ}{dCA} = \left[\frac{1}{\gamma-1} \right] \left[V \frac{dp}{dCA} + p\gamma \frac{dV}{dCA} \right] \quad (5-3)$$

¹⁰ The fuel injection timing and duration values in Table 5-2, and throughout the thesis, represented the commanded input values.

¹¹ The heat release figures throughout the text represent the apparent heat release rate (HRR) as calculated by Equation 5-3, which was derived as shown in Appendix A.

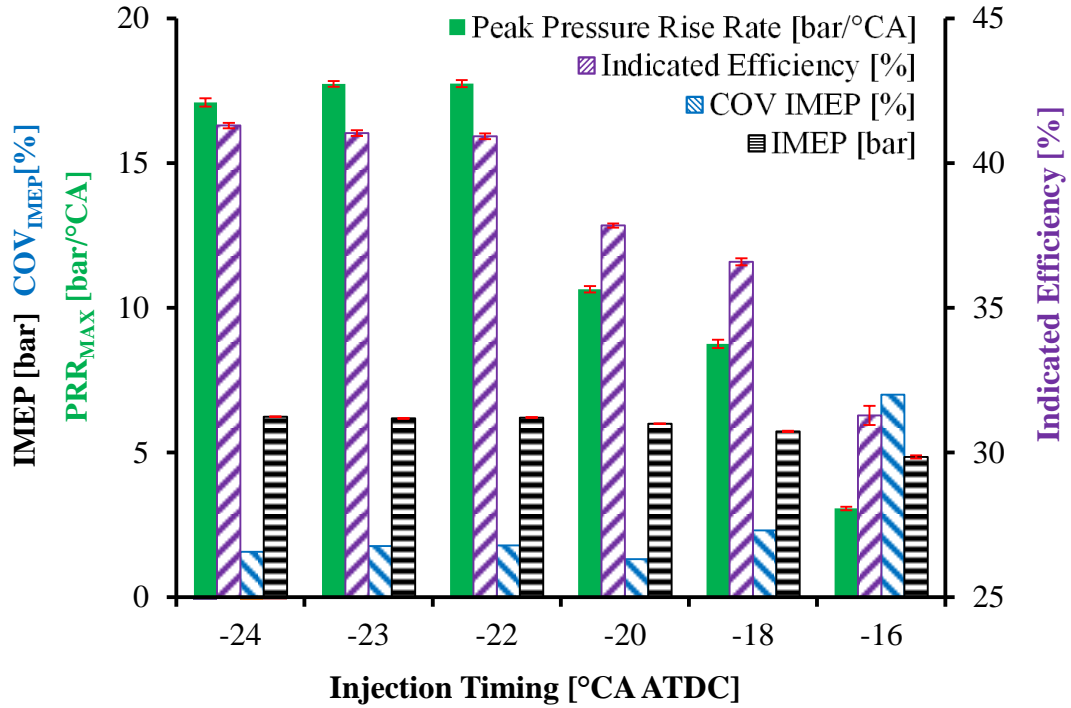
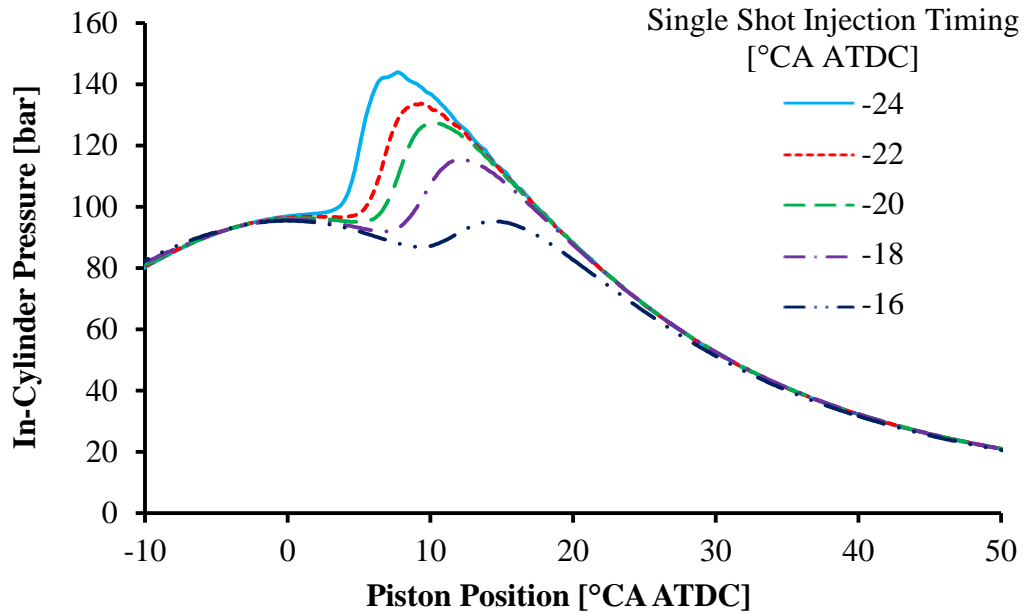
Figure 5-6: Butanol Single Shot Fuel Injection Timing vs. PRR, Efficiency, and COV_{IMEP} 

Figure 5-7: Effect of Butanol Single Shot Injection Timing on In-Cylinder Pressure

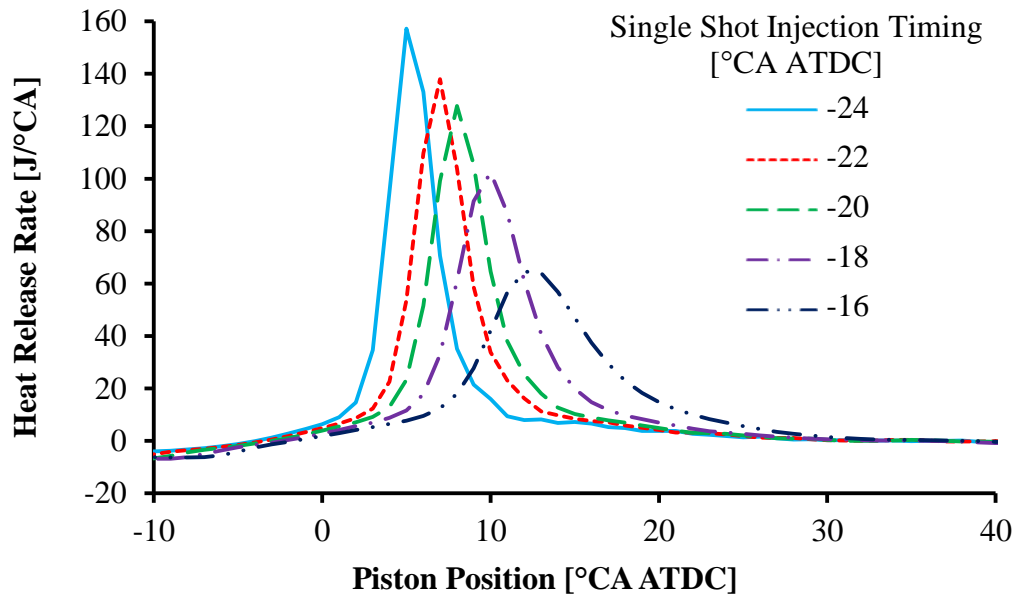


Figure 5-8: Effect of Butanol Single Shot Injection Timing on the Heat Release Rate

However, the use of a delayed fuel injection timing was restricted by unstable combustion and relatively low thermal efficiency. The cycle-to-cycle variations increased when the single shot injection was delayed to $-16^{\circ}\text{CA ATDC}$, as characterized by an increase of the COV_{IMEP} from 2.3 to 7.0%. The indicated thermal efficiency was calculated according to Equation 5-4 and the results presented in Figure 5-6 revealed that the efficiency dropped from 36.6% to 31.3% when the post injection timing was retarded from -18 to $-16^{\circ}\text{CA ATDC}$. The IMEP also declined to 4.9 bar. The error bars illustrated in Figure 5-6 and throughout this section of the chapter represented the 95% confidence interval¹². The data showed that the 95% confidence intervals for the peak pressure rise rate and the indicated efficiency were relatively narrow, indicating that the values given in Figure 5-6 were a good representation of the true values. Thus, the fuel injection timing of $-18^{\circ}\text{CA ATDC}$ was determined to provide the lowest PRR, 8.8 $\text{bar}/^{\circ}\text{CA}$, while maintaining a reasonable efficiency and relatively low cycle-to-cycle variations.

¹² The 95% confidence interval was calculated according to Equation 5-5 where μ represented the sample mean value, σ represented the sample standard deviation, n was the sample size, and t was the coefficient determined by the Student's t -distribution table.

$$\eta_{thermal} = \frac{Indicated\ Power\ [kW]}{Fuel\ Flow\ Rate\ [g/s] \times LHV\ [MJ/kg]} \quad (5-4)$$

$$95\% \text{ confidence interval} = \mu \pm t \left(\frac{\sigma}{\sqrt{n}} \right) \quad (5-5)$$

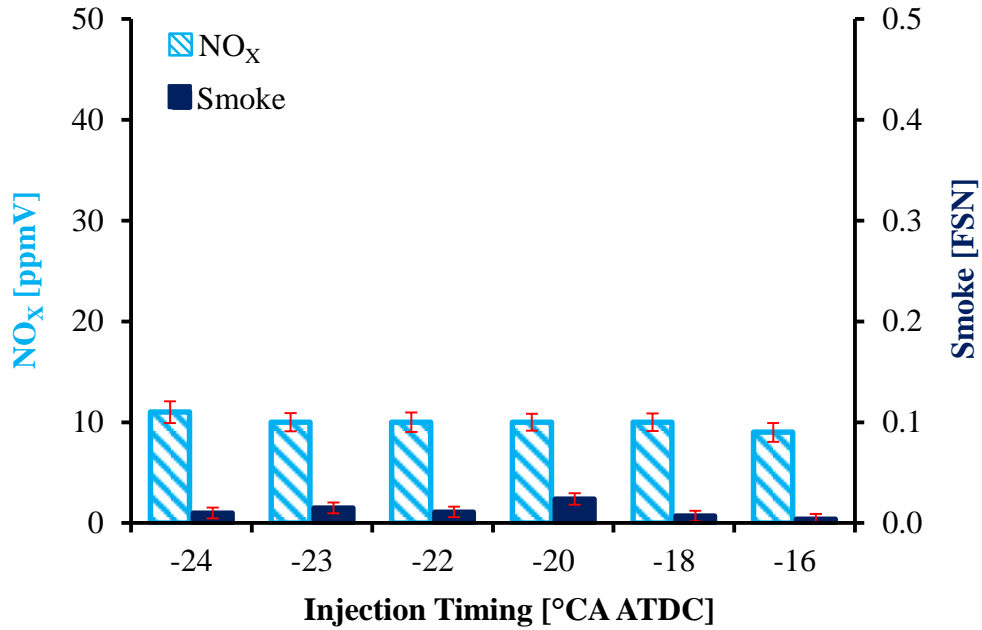


Figure 5-9: Effect of Butanol Single Shot Injection Timing on NO_x and Smoke

Further analysis was carried out to explore the effect of the single shot injection timing on the exhaust emissions. Figure 5-9 shows that the injection timing had a negligible effect on the NO_x and the smoke emissions. The NO_x and smoke emissions were ultra-low throughout the timing sweep. On the other hand, the delay of the single shot injection timing led to a clear penalty for the carbon monoxide, the light hydrocarbon, and the unburned butanol emissions as shown in Figure 5-10. The increased CO and light hydrocarbon emissions were attributed to the lower combustion temperature that led to increased incomplete combustion for delayed injections. Furthermore, the unstable combustion and the high cycle-to-cycle variations at -16°CA ATDC resulted in a high quantity of unburned butanol hydrocarbons. Thus, the single

shot injection timing sweep showed that a significant reduction of the peak pressure rise rate was achieved when the timing was delayed but at the cost of increased THC and CO emissions and a reduced indicated thermal efficiency.

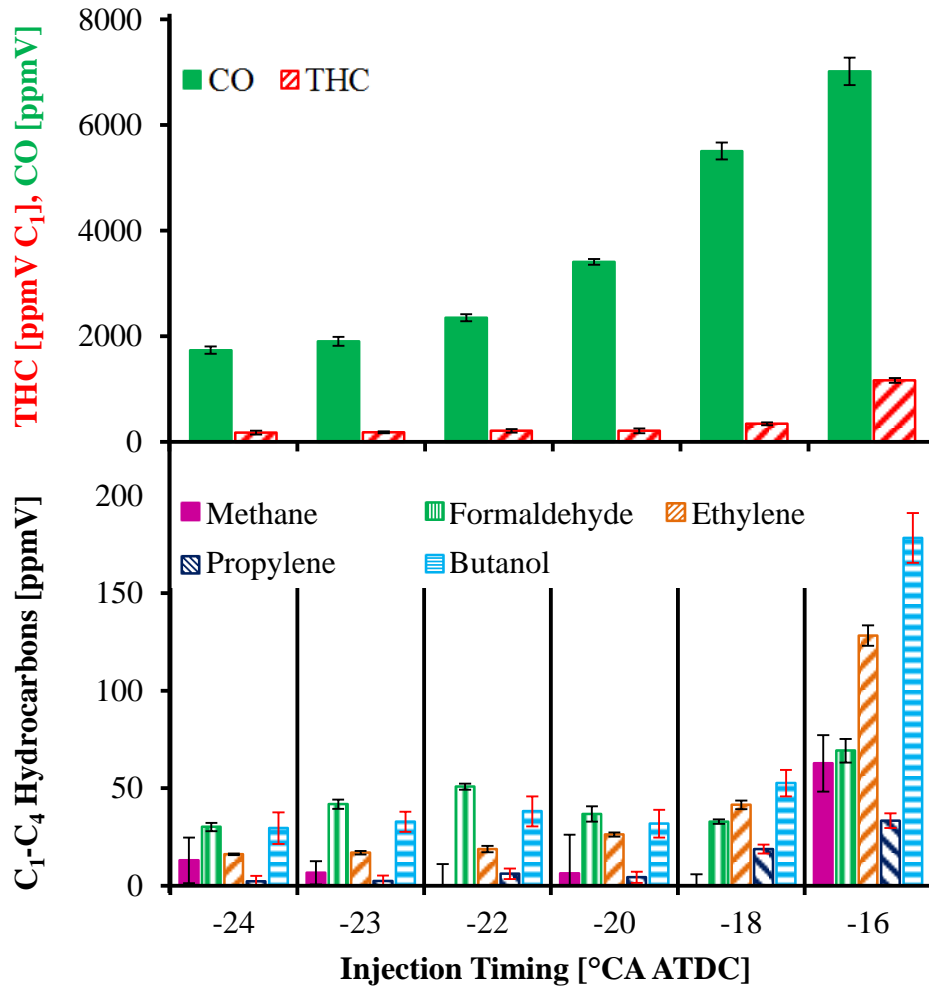


Figure 5-10: Effect of Butanol Single Shot Injection Timing on CO and Hydrocarbons

Tests with diesel fuel by other researchers indicated that a diesel pilot injection can reduce the combustion noise and the PRR of diesel combustion [121,122]. Thus, a butanol pilot injection was used with a butanol main injection to investigate if the use of a pilot injection provided a lower PRR compared to the delayed single shot injection strategy. The pilot injection duration was fixed at 300 μ s and a pilot injection timing

sweep was carried out from -52 to -36°CA ATDC. The main injection timing was fixed at -20°CA ATDC because the previous results in Figure 5-6 indicated that this injection timing had a significantly reduced PRR compared to earlier injections and a moderately higher thermal efficiency compared to delayed injections. The main injection duration was adjusted throughout the sweep to maintain a constant engine load of 6.0 bar IMEP. Further details of the test conditions are provided in Table 5-3.

Table 5-3: Test Conditions for Butanol Pilot Injection Timing Sweep

Nominal IMEP [bar]	6.0
Engine Speed [rpm]	1500
Air Intake Pressure [bar absolute]	1.9
Intake Oxygen [% V]	20.7
Test Fuel	n-Butanol
Fuel Injection Pressure [bar]	900
Main Injection Duration [μs]	Moderated
Main Injection Timing [$^{\circ}\text{CA}$ ATDC]	-20
Pilot Injection Duration [μs]	300
Pilot Injection Timing [$^{\circ}\text{CA}$ ATDC]	-52 to -36

Figure 5-11 and Figure 5-12 showed that the addition of the butanol pilot injection prompted an increased PRR and maximum in-cylinder pressure compared to a single shot injection. The PRR and the maximum pressure also increased when the pilot injection timing was delayed and the dwell between the main and the pilot injections was shortened. The apparent heat release rate curves in Figure 5-13 illustrated that the pilot injection did not auto-ignite and did not generate a visible heat release. Instead, the pilot injection ignited simultaneously with the main injection, shortly after top dead centre when the conditions for butanol auto-ignition were adequate, and led to an increased PRR. The pilot injection timing sweep was aborted at -36°CA ATDC because of excessive PRR.

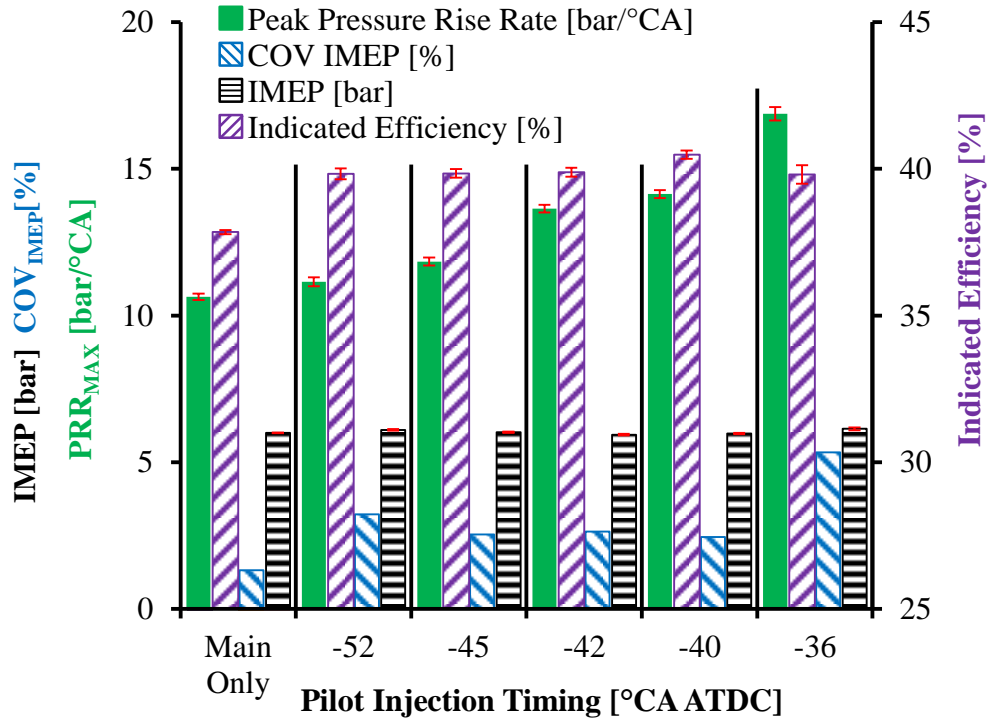


Figure 5-11: Effect of Butanol Pilot Injection Timing on PRR, Efficiency, and COV_{IMEP}

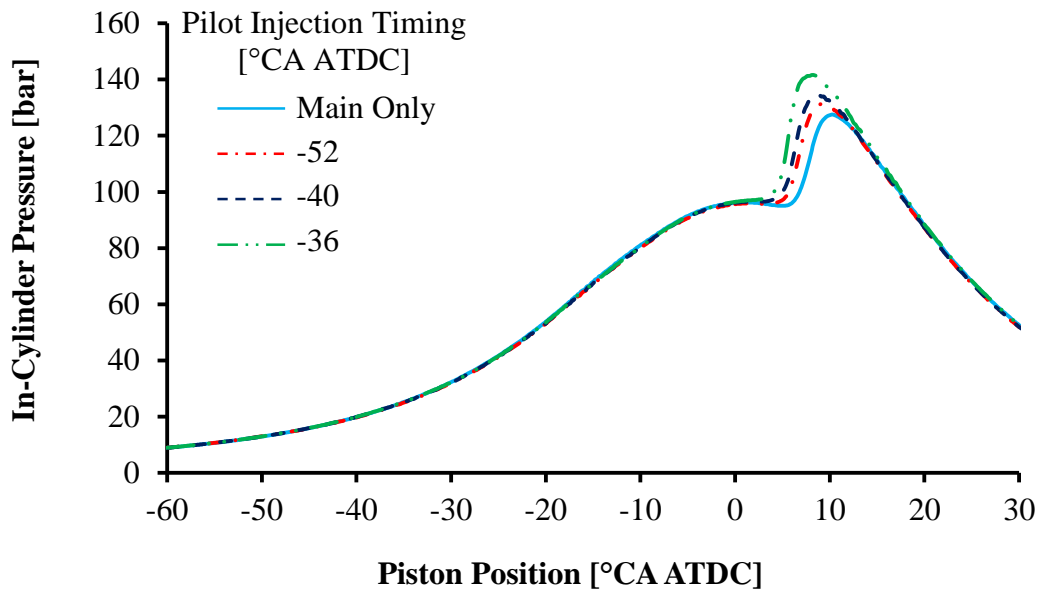


Figure 5-12: Effect of Butanol Pilot Injection Timing on In-Cylinder Pressure

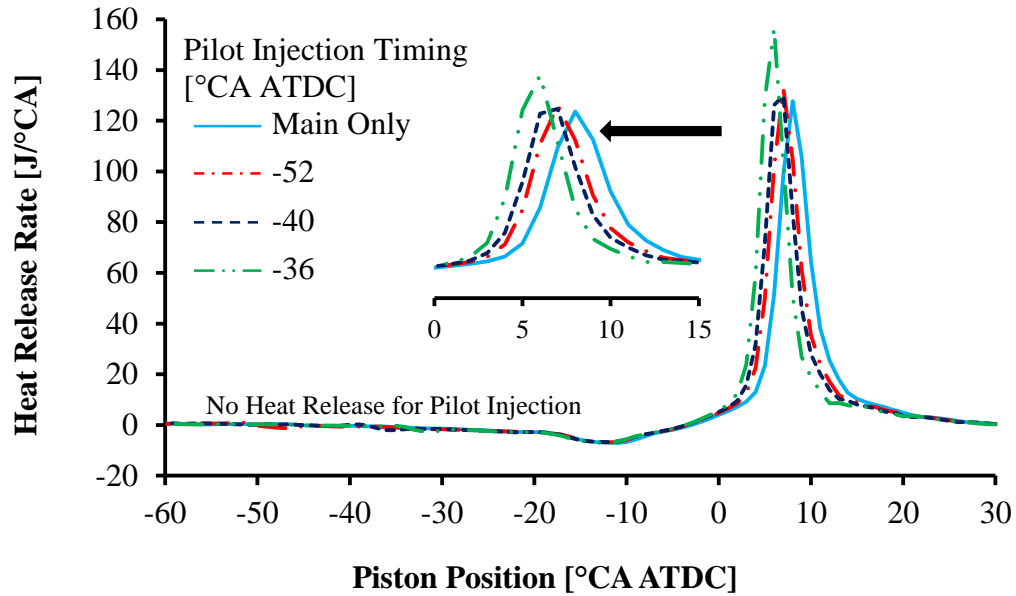


Figure 5-13: Effect of Butanol Pilot Injection Timing on Heat Release Rate

The efficiency and the emissions were analyzed to further judge the impact of the butanol pilot injection. The results in Figure 5-11 showed that the use of a pilot injection increased the indicated efficiency from 37.8% up to 40.5%. The increased indicated efficiency was likely caused by increased combustion temperatures, as suggested by the increased mean bulk gas temperatures¹³ shown in Figure 5-14. The improved indicated efficiency suggested that the application of a pilot injection may be suitable for low load conditions where peak pressure rise rates are less of a concern.

$$\frac{p_2 V_2}{T_2} = \frac{p_1 V_1}{T_1} \quad (5-6)$$

¹³ The bulk gas temperatures were calculated using the measured in-cylinder pressure and volume as shown in Equation 5-6. Ideal gas was assumed as the working fluid and the measured intake temperature was used as an initial value.

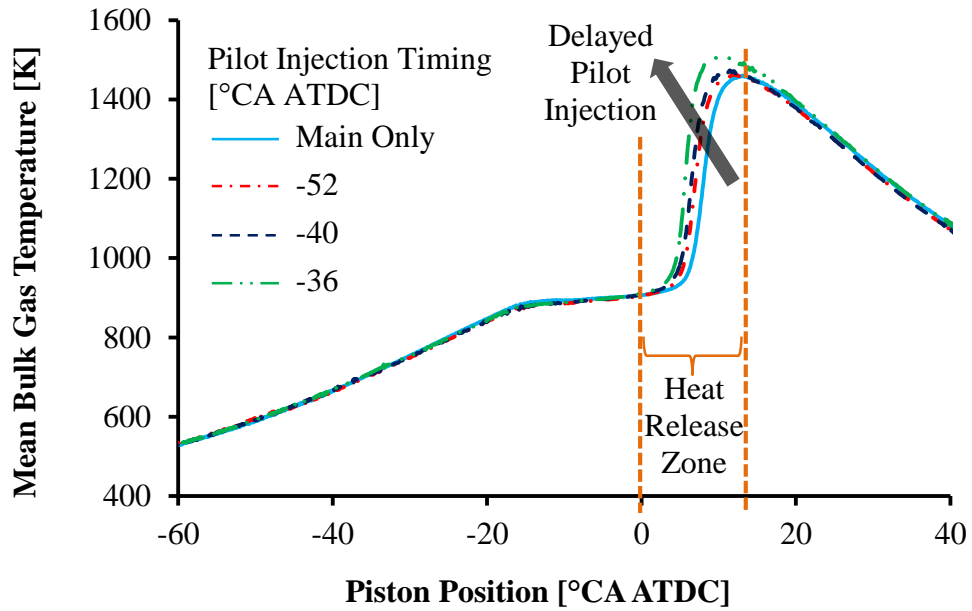


Figure 5-14: Effect of Butanol Pilot Injection Timing on Bulk Gas Temperature

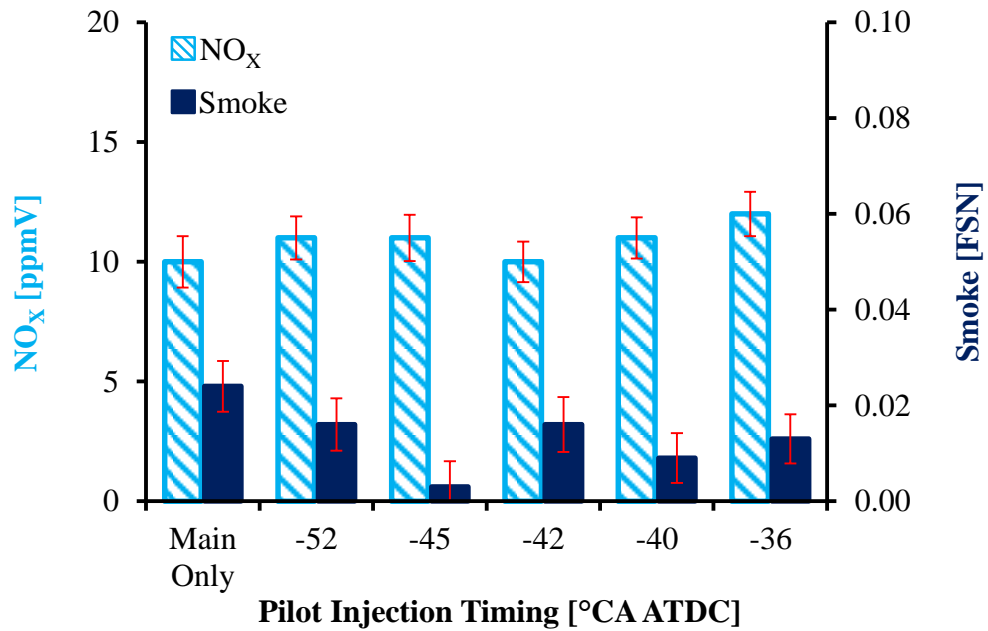


Figure 5-15: Effect of Butanol Pilot Injection Timing on NO_x and Smoke

The pilot injection did not have a meaningful effect on the NO_x emissions as shown in Figure 5-15. The smoke emissions were slightly reduced when a pilot injection

was used and the lowest smoke emissions were observed at a pilot timing of -45°CA ATDC. However, the absolute smoke emission values were ultra-low and the relative change (0.008 FSN) was considered to be insignificant.

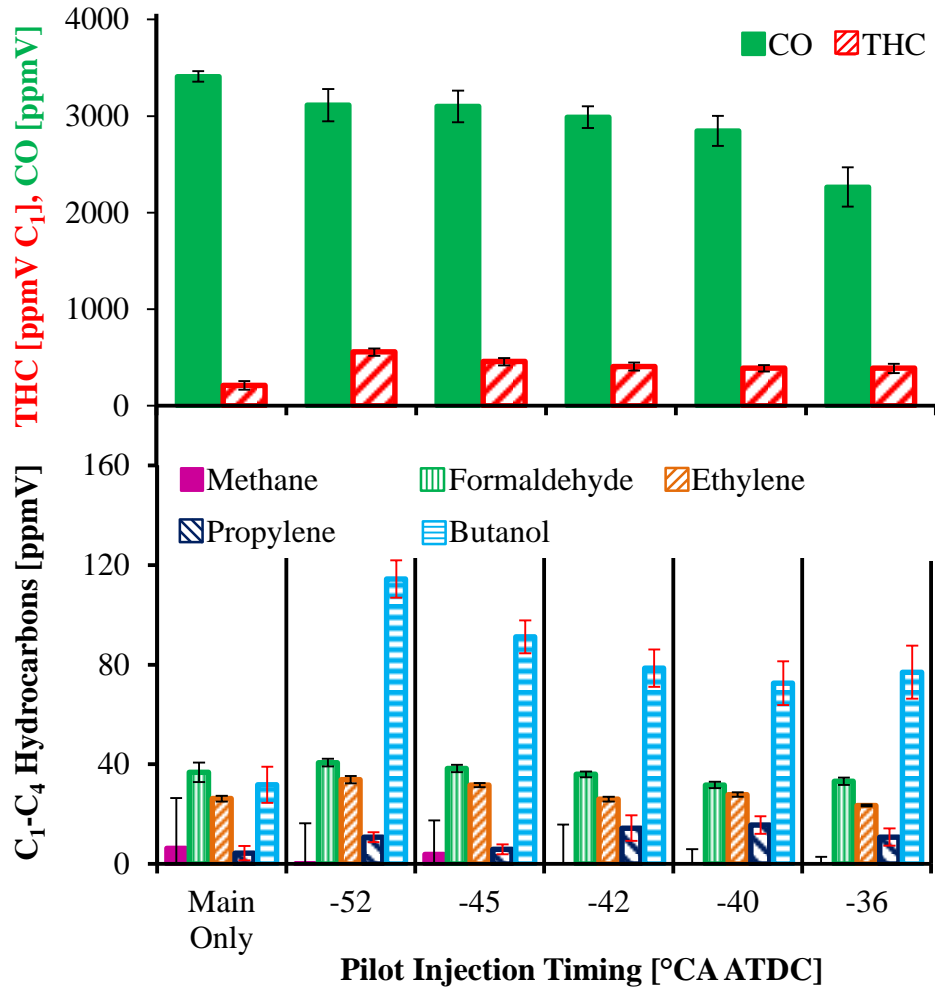


Figure 5-16: Effect of Butanol Pilot Injection Timing on CO and Hydrocarbons

Figure 5-16 showed that the carbon monoxide emissions decreased when the pilot injection was added and when the pilot was delayed. This pattern was consistent with the slightly increased bulk gas temperatures and the increased indicated thermal efficiency. Conversely, the addition of the pilot injection considerably increased the total hydrocarbon emissions, although the THC emissions dropped as the pilot injection was

postponed. A hydrocarbon speciation analysis revealed that the light hydrocarbons were unaffected by the pilot injection while there was a substantial increase in the unburned butanol hydrocarbons. Furthermore, the unburned butanol emissions generally decreased as the pilot timing was delayed. These observations implied that the increased THC and unburned butanol emissions were caused by wall impingement and flame quenching near the cylinder walls, particularly for earlier pilot injections where these effects were expected to be more pronounced due to a higher degree of premixing. The increased unburned butanol emissions reasoned against the use of early pilot injections.

A butanol post injection strategy was investigated for the purpose of reducing the peak pressure rise rate. The premise was that the post injection would generate power without increasing the PRR because it takes place during the expansion stroke. A post injection timing sweep was carried out from 10 to 30°CA ATDC with a fixed post injection duration. The main injection timing was fixed at -18°CA ATDC¹⁴ and the main injection duration was adjusted to maintain a constant load of 6.0 bar IMEP. Further details are provided in Table 5-4.

Table 5-4: Test Conditions for Butanol Post Injection Timing Sweep

Nominal IMEP [bar]	6.0
Engine Speed [rpm]	1500
Air Intake Pressure [bar absolute]	1.9
Intake Oxygen [% V]	20.7
Test Fuel	n-Butanol
Fuel Injection Pressure [bar]	900
Main Injection Duration [μ s]	Moderated
Main Injection Timing [°CA ATDC]	-18
Post Injection Duration [μ s]	330
Post Injection Timing [°CA ATDC]	10 to 30

¹⁴ The injection timing for the main injection was chosen based on previous tests with a single shot strategy that showed a reduced PRR compared to earlier post injections while avoiding very high COV_{IMEP} as with later injections as shown in Figure 5-6.

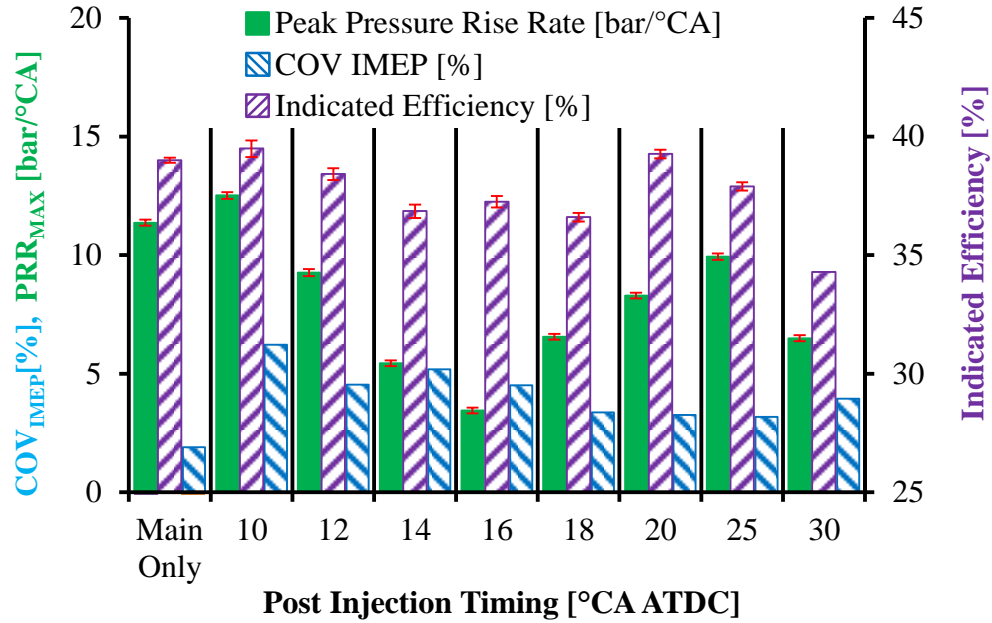


Figure 5-17: Effect of Butanol Post Injection Timing on PRR, Efficiency, COV_{IMEP}

The results shown in Figure 5-17 revealed that the use of a post injection reduced the peak pressure rise rate from 11.4 bar/°CA to a minimum of 3.5 bar/°CA. The heat release curves in Figure 5-18 established that the post injection produced a noticeable heat release, indicating power generation from the post injection. The reduction of the PRR was primarily attributed to the power generated by the post injection that allowed the main injection to be reduced to maintain a constant load. The reduced main injection resulted in a more gradual pressure rise as illustrated in Figure 5-19.

Figure 5-17 also revealed that the PRR was sensitive to the post injection timing. The minimal PRR was obtained when the post timing was at 16°CA ATDC. Earlier injections resulted in a reduced heat release and a larger main injection was required to maintain a constant load. Post injections beyond 16°CA ATDC had a much lower effective expansion ratio, illustrated in Figure 5-18, that led to reduced power output and required a larger main injection to maintain a constant load. The increased main injection resulted in an increased PRR in both instances.

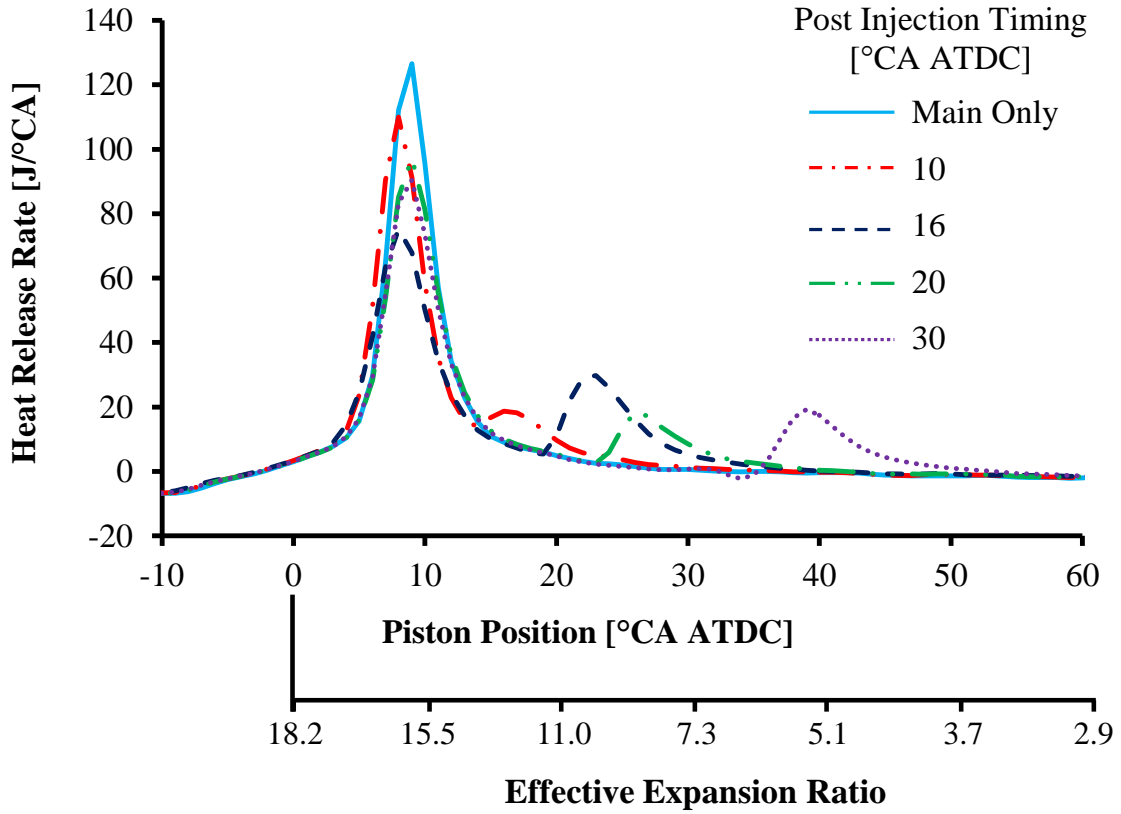


Figure 5-18: Effect of Butanol Post Injection Timing on Heat Release Rate

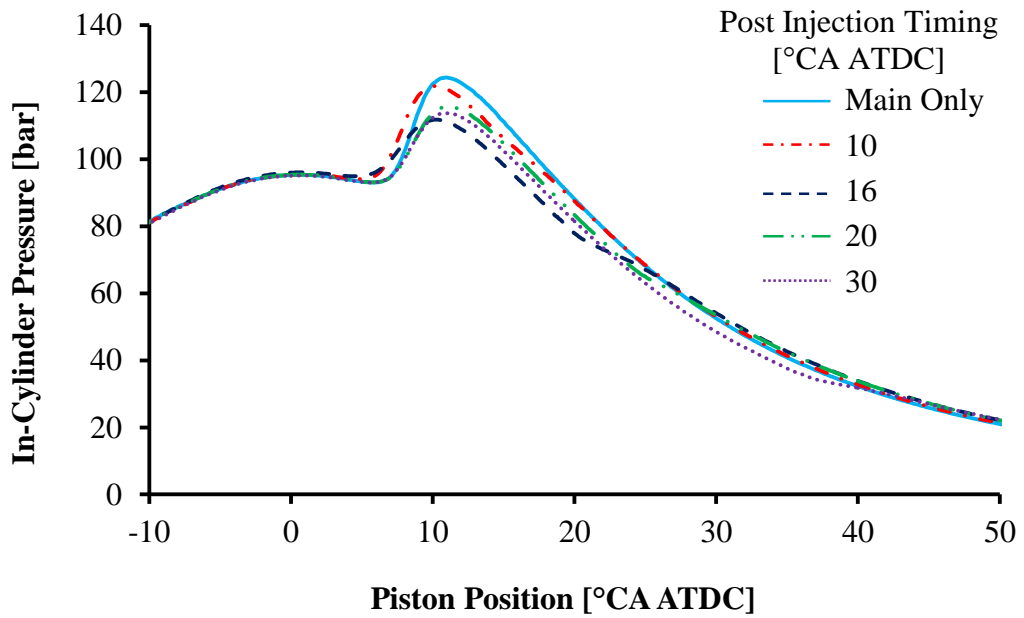


Figure 5-19: Effect of Butanol Post Injection Timing on In-Cylinder Pressure

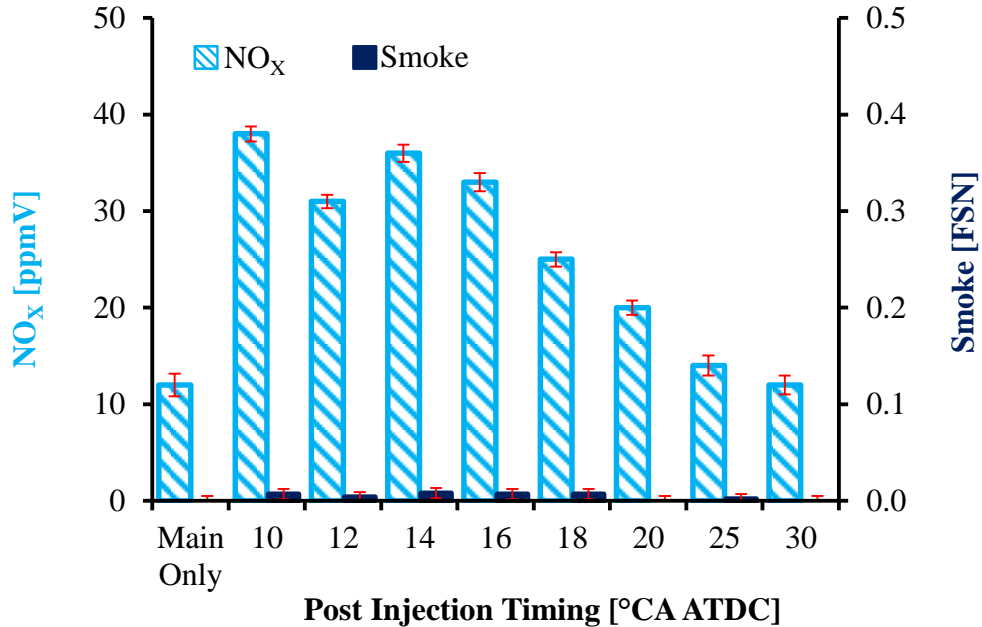


Figure 5-20: Effect of Butanol Post Injection Timing on NO_x and Smoke Emissions

The effects of the post injection on the efficiency and the emissions were also examined. Figure 5-17 and Figure 5-18 showed that the use of a post injection reduced the indicated efficiency because of a shorter effective expansion ratio of the post injection combustion. The results in Figure 5-20 demonstrated that the use of a post injection significantly raised the NO_x emissions. The earliest post injections produced the highest NO_x emissions and there was a steady reduction as the post injection timing was delayed. The increased NO_x formation was accredited to the relatively short ignition delay of the post injection, shown in Figure B-1 in Appendix B, which led to insufficient mixing of air and fuel and resulted in locally near-stoichiometric air to fuel ratios. The NO_x emissions dropped as the post injection was delayed because the expanding cylinder reduced background temperatures, as suggested by the plot of the bulk gas temperatures in Figure 5-21. Despite the significant NO_x emission penalty, the NO_x emissions were within a suitable range, below 38 ppmV (0.76 g/kW·hr), for long breathing operation. The smoke emissions remained ultra-low throughout the test.

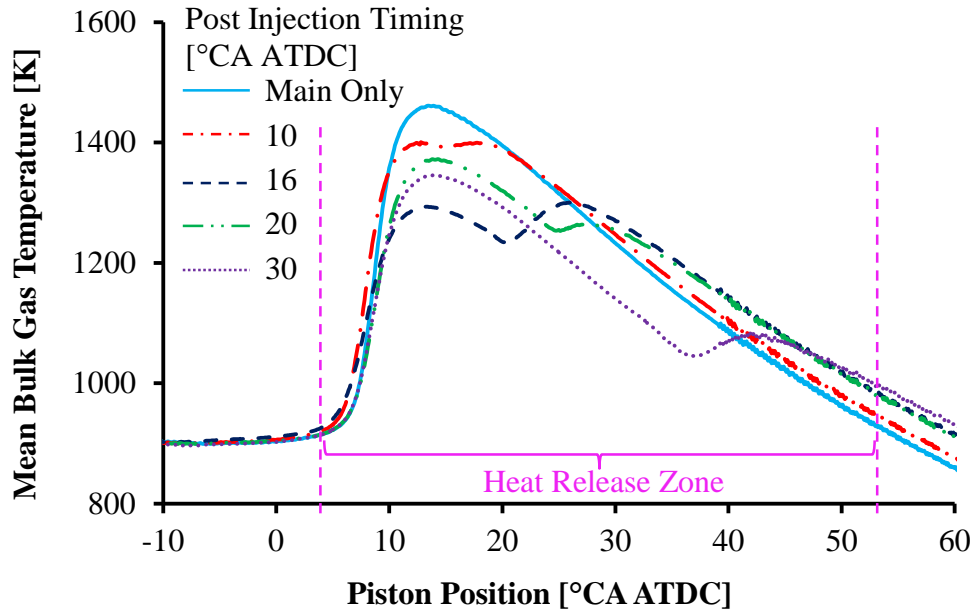


Figure 5-21: Effect of Butanol Post Injection Timing on Bulk Gas Temperature

The use of a post injection produced slightly increased carbon monoxide emissions as shown in Figure 5-22. The CO emissions exceeded 3000 ppmV and consistently increased as the post injection timing was delayed. The increased CO emissions were attributed to rapidly cooling in-cylinder temperatures from cylinder expansion that opposed the complete oxidation of carbon monoxide to carbon dioxide. The effect of the post injection on the total hydrocarbon emissions was less pronounced. The hydrocarbon speciation results established that the light hydrocarbons were relatively low and mostly unaffected by the use of a post injection. The unburned n-butanol emissions were reduced by the use of early post injections but increased for late post injections because of significantly reduced in-cylinder temperatures. Further delaying the post injection beyond 30°CA ATDC was not explored in this set of tests but a broader post injection timing sweep was carried out under similar test conditions. The additional results are shown in the appendix in Table B-1 and Figure B-2 to Figure B-6.

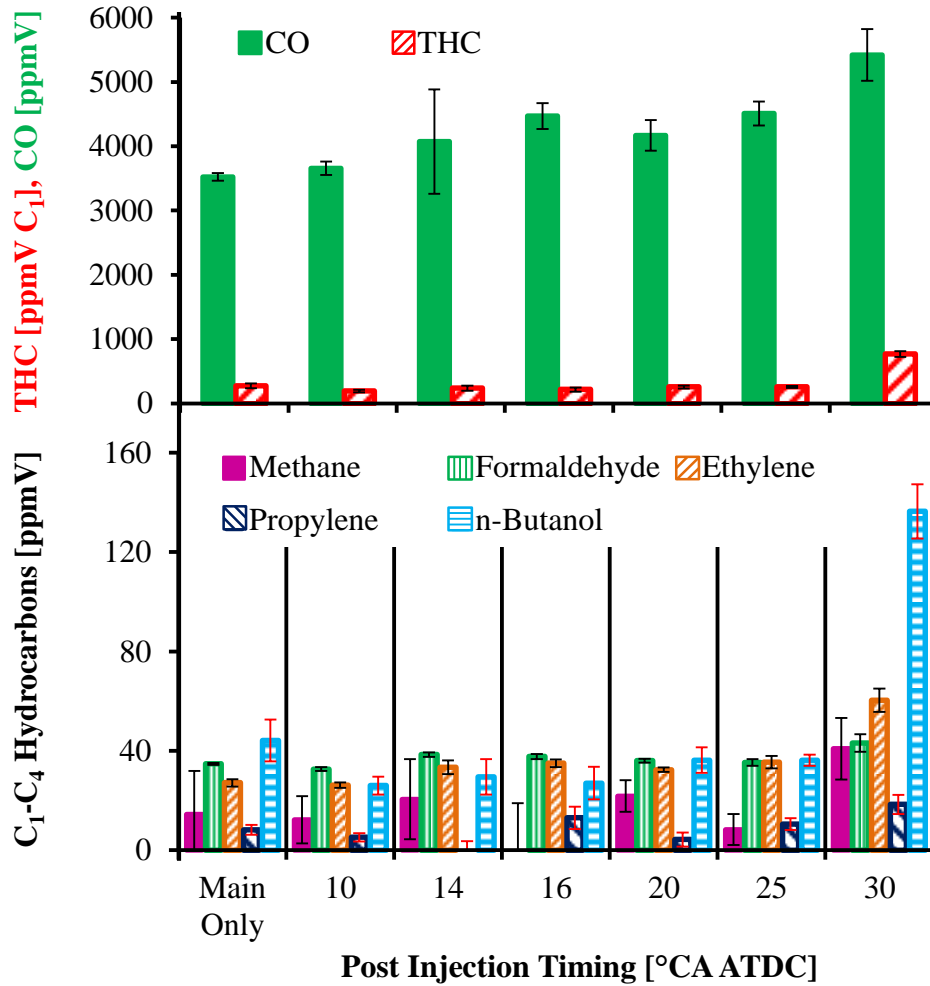


Figure 5-22: Effect of Butanol Post Injection Timing on CO and Hydrocarbons

Representative conditions from each fuel injection strategy were selected and a comparison was made with regards to the effects on the peak pressure rise rate, the indicated efficiency, and the emissions as shown in Figure 5-23. The “early main” strategy denoted a single shot injection at $-24^{\circ}\text{CA ATDC}$, the “late main” strategy represented a single shot injection at $-16^{\circ}\text{CA ATDC}$, the “pilot with late main” signified the condition with a pilot injection at $-40^{\circ}\text{CA ATDC}$, and the “early post with late main” represented the test condition with a post injection at 16°CA ATDC . All four conditions had an IMEP of 6.0 to 6.2 bar and ultra-low smoke emissions.

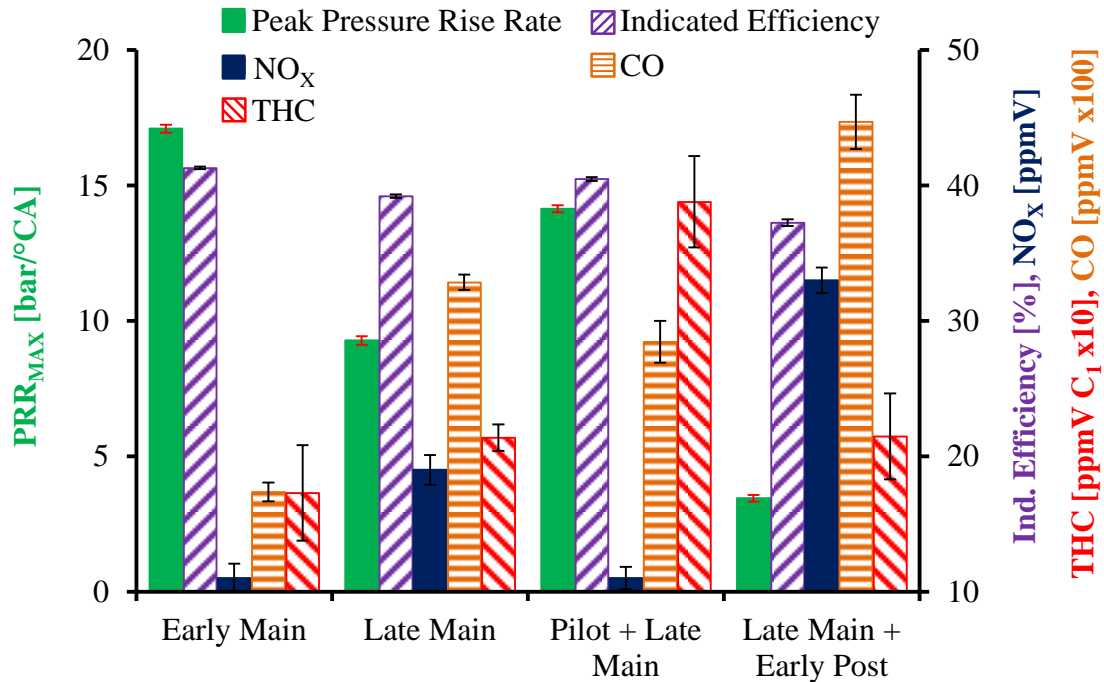


Figure 5-23: Comparison of Different Butanol Injection Strategies for PRR Reduction

The comparison revealed that the lowest pressure rise rate was achieved with the post injection strategy but at the cost of reduced indicated efficiency and increased NO_x and CO emissions. Nevertheless, the NO_x emissions were below 35 ppmV, which was significantly lower compared to the NO_x levels with diesel fuel at similar operating conditions, and this NO_x range was suitable for long breathing operation. The late single shot injection strategy also produced a considerable reduction of the PRR compared to the early single shot injection but there were also penalties in efficiency, NO_x and CO emissions. Meanwhile, the pilot injection strategy failed to provide a meaningful reduction of the PRR and the early main injection had the highest PRR.

Further analysis of the different strategies showed that the early single shot strategy had the highest indicated efficiency and the lowest emissions. This observation suggested that the early single shot strategy was more suitable for very low load conditions, below 4 bar IMEP for the test engine, where the PRR was of less concern as indicated in Figure 5-3. At slightly higher loads, like the conditions presented in Figure 5-23, the delayed single shot injection strategy seemed to offer a reasonable compromise

between the PRR, efficiency, and emissions. For higher loads, above 7 bar IMEP for the test engine, the post injection strategy appeared to be a better choice because the peak pressure rise rate was of much greater concern at these conditions as shown in Figure 5-3.

5.3 Increased Engine Load with a Post Injection of Neat Butanol Fuel

Tests were carried out to investigate increased load operation of neat butanol fuel in a CI engine. The previous tests demonstrated that the post injection strategy significantly reduced the peak pressure rise rate at constant load conditions. Therefore, additional tests were conducted to demonstrate higher load operation by enlarging the post injection duration compared to previous tests. The main injection duration and timing were fixed as shown in Table 5-5. The post injection timing was also fixed and the post injection duration was gradually increased until the peak pressure rise rate exceeded the limit of 17 bar/°CA.

Table 5-5: Test Conditions for Butanol Post Injection Duration Sweep

IMEP [bar]	Sweep
Engine Speed [rpm]	1500
Air Intake Pressure [bar absolute]	1.9
Intake Oxygen [% V]	20.6
Test Fuel	n-Butanol
Fuel Injection Pressure [bar]	900
Main Injection Duration [μ s]	530
Main Injection Timing [°CA ATDC]	-16
Post Injection Duration [μ s]	Sweep
Post Injection Timing [°CA ATDC]	20

The results of the post injection load sweep are illustrated in Figure 5-24. The IMEP gradually increased from 3.5 to 8.9 bar as the post injection was added and the duration was increased from 400 to 530 μ s. At the same time, the PRR increased from 3.1 to 15.1 bar/°CA. The heat release and in-cylinder pressure profiles were plotted and the results revealed the cause of the PRR increase. Figure 5-25 showed that the pressure

rise was negative during the post injection event and that the peak pressure rise occurred during the main injection combustion. Despite the fixed fuel injection timing and fuel injection duration of the main injection, the pressure rise slope during the main injection combustion consistently increased when the post injection duration was increased.

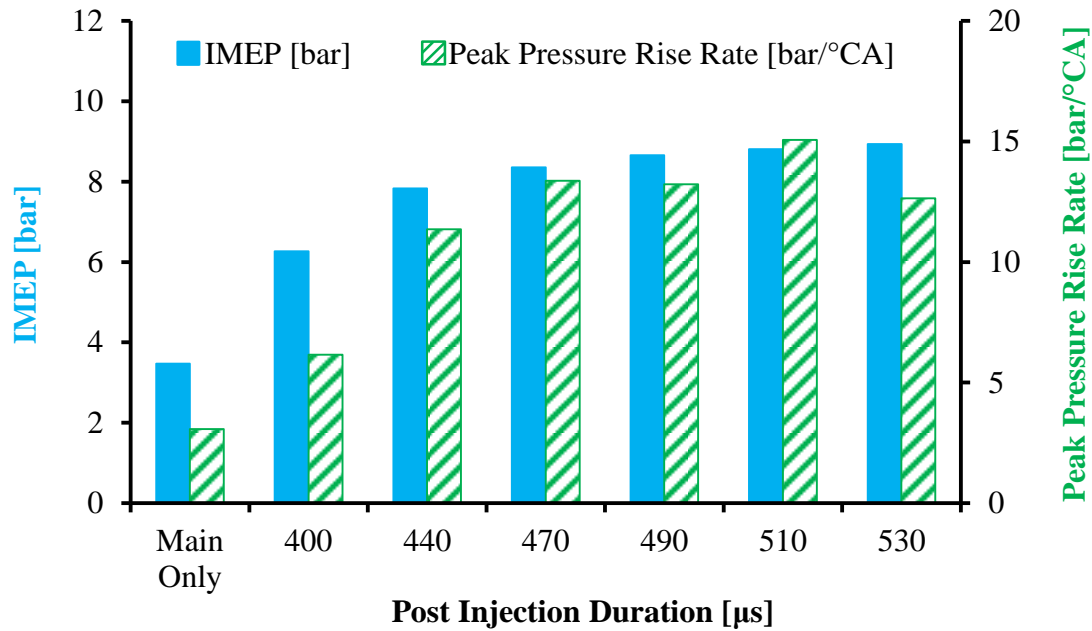


Figure 5-24: Effect of Butanol Post Injection Duration on IMEP and PRR

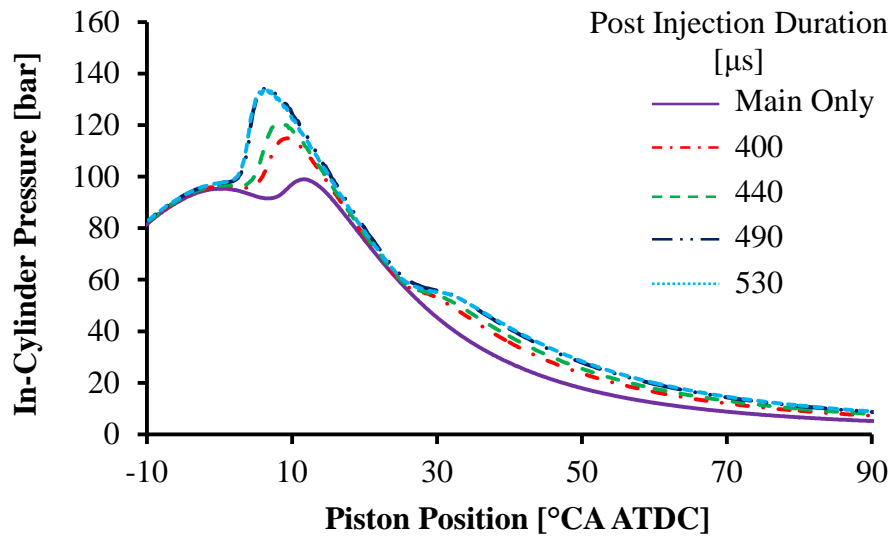


Figure 5-25: Effect of Butanol Post Injection Duration on In-Cylinder Pressure

As shown in Figure 5-26, the addition of the post injection caused an advanced combustion phasing for the main injection. The main injection's combustion phasing consistently advanced as the post injection duration was increased and this caused the increased PRR from the main injection as shown by the pressure traces in Figure 5-25 and Figure 5-27. The use of a larger post injection resulted in a slightly higher residual gas and cylinder surface temperatures as suggested by the plot of bulk gas temperatures in Figure 5-28. The higher residual gas and surface temperatures may have caused an earlier auto-ignition for the main injection on the following cycle. Future work is recommended to further investigate the reasons for the advanced combustion phasing of the main injection.

The PRR limit of 17 bar/°CA was breached when the post injection duration was increased beyond 530 μs and this condition was quickly aborted for laboratory safety purposes. Therefore, the maximum load was limited to 8.9 bar IMEP under these operating conditions. The maximum in-cylinder pressure was not a limiting factor for these tests since the results in Figure 5-25 indicated that the maximum value was below the rated limit of 180 bar for the test engine. The 8.9 bar IMEP load level was an improvement compared to a single shot injection strategy which was limited to a load of 6 bar IMEP. However, the strategy did not attain the targeted load level of 14 bar IMEP.

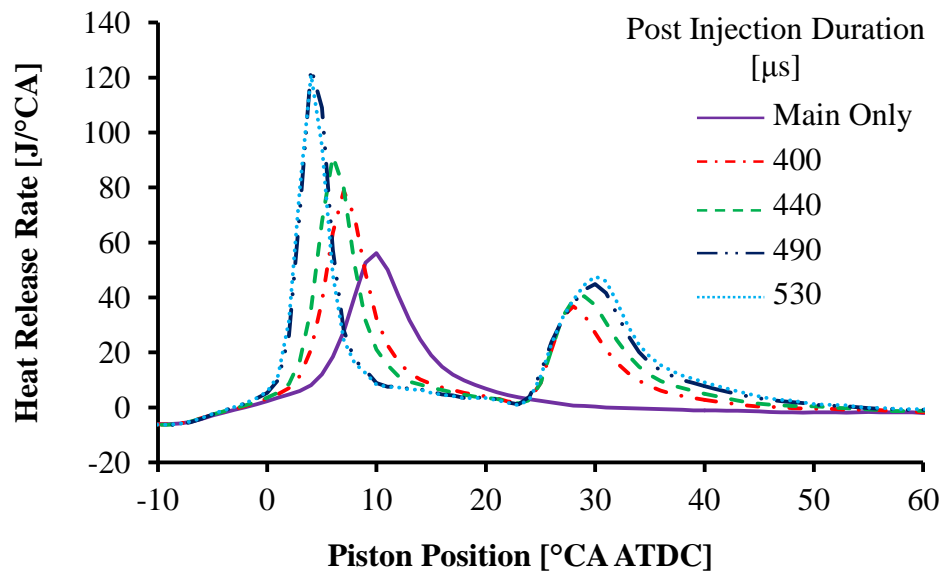


Figure 5-26: Effect of Butanol Post Injection Duration on Heat Release

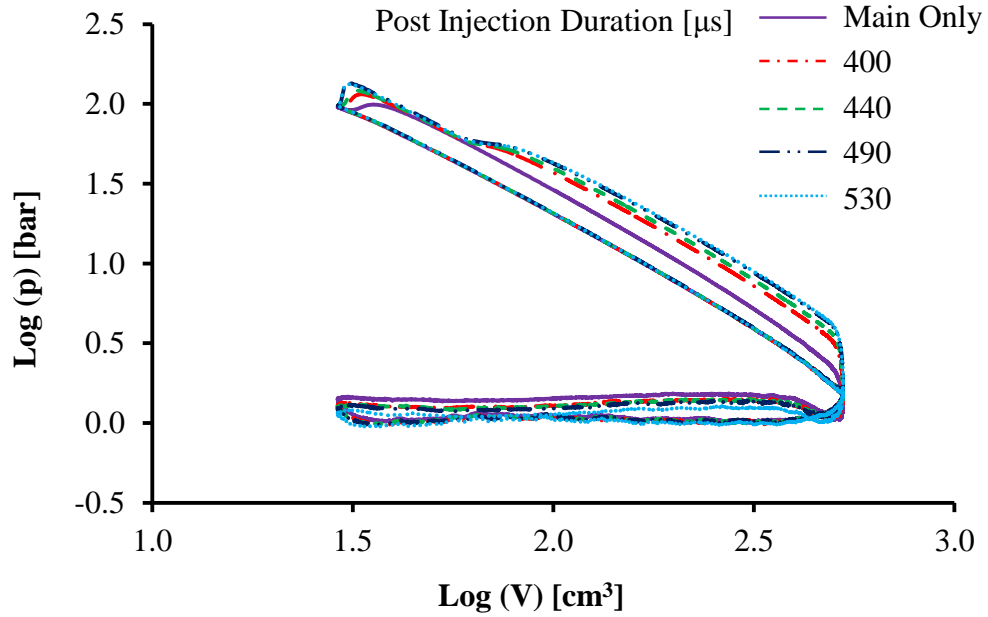


Figure 5-27: Effect of Butanol Post Injection Duration on Logarithmic Pressure

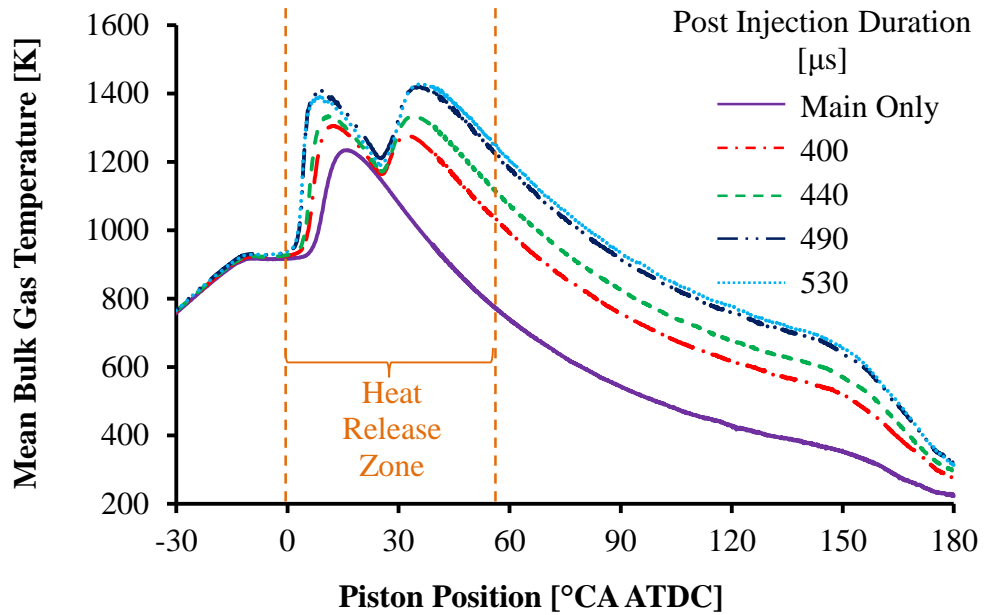


Figure 5-28: Effect of Butanol Post Injection Duration on Bulk Gas Temperature

Further analysis was carried out to determine the effect of the post injection duration on the indicated thermal efficiency, the cycle-to-cycle variations, and the exhaust emissions. The data in Figure 5-29 showed that the indicated efficiency generally increased and that the COV_{IMEP} generally decreased as the post injection duration was increased. The cycle-to-cycle variations were not a major concern and were below 2% when the post was increased to 470 μs and beyond. The indicated efficiency was 36.0% for the shortest post injection and gradually increased to 37.6% for the largest post injection. Thus, the use of a post injection to extend the high load limit did not result in an efficiency penalty. These trends were mainly attributed to the increased engine load which led to higher combustion temperatures.

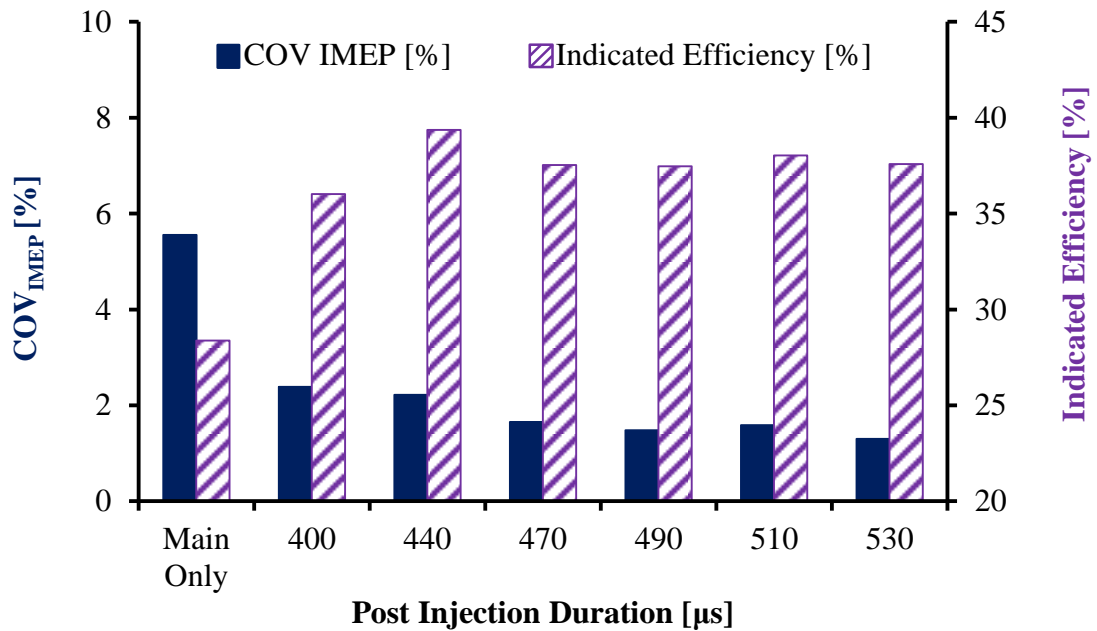


Figure 5-29: Effect of Butanol Post Injection Duration on COV_{IMEP} and Efficiency

Larger post injections led to increased indicated NO_x and smoke emissions as demonstrated in Figure 5-30. The raw NO_x and smoke emissions followed the same trends and are shown in Figure B-7 in the appendix. The increased NO_x emissions were attributed to the higher flame temperatures caused by higher load conditions and the

advanced combustion phasing of the main injection. On the other hand, the increased smoke emissions were attributed to the relatively short ignition delay and the increased combustion temperatures of the post injection. The advanced combustion phasing of the main injection had a negligible effect on the smoke emissions due to the enhanced premixed nature of the main injection combustion. Overall, the NO_x emissions were below $0.8 \text{ g/kW}\cdot\text{hr}$ (60 ppmV) and the smoke emissions were below $0.011 \text{ g/kW}\cdot\text{hr}$ (0.11 FSN) even at 8.9 bar IMEP . The NO_x were much lower compared to conventional diesel combustion at similar conditions, as previously illustrated in Figure 5-1, and were suitable for the application of a long breathing LNT.

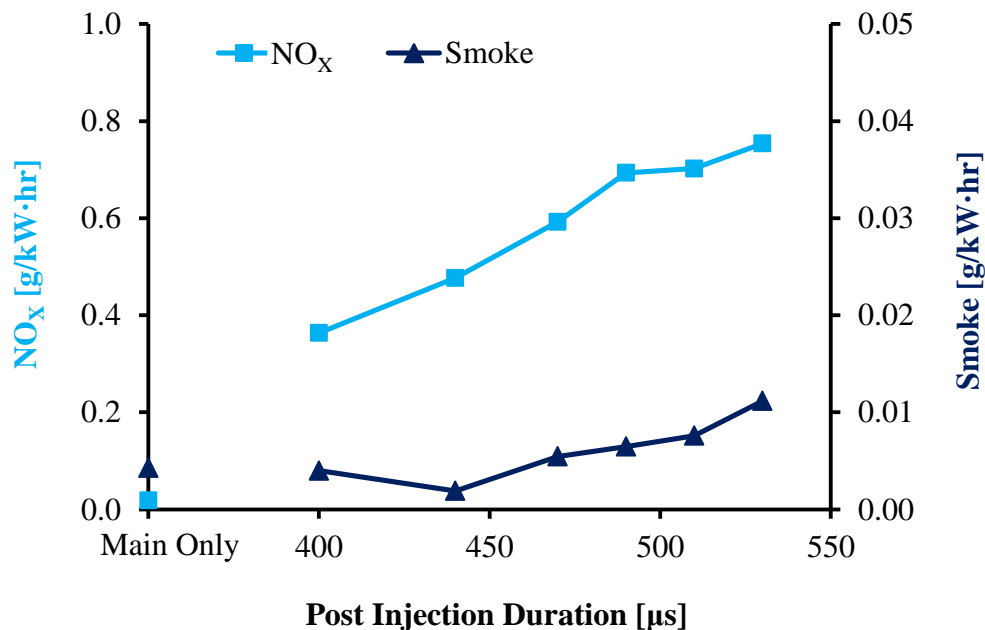


Figure 5-30: Effect of Butanol Post Injection Duration on NO_x and Smoke Emissions

The increased post injection duration reduced the THC and CO emissions as shown in Figure 5-31. The indicated emissions of CO and THC showed the same trends and the graphs are provided in Figure B-8. The reductions were accredited to the higher load conditions and the advanced combustion phasing of the main injection. Both effects led to higher flame temperatures that promoted complete combustion and reduced partial

combustion products such as CO and THC. At 8.9 bar IMEP, the THC emissions were relatively low, 73 ppmV, but the CO emissions were relatively high, 1707 ppmV.

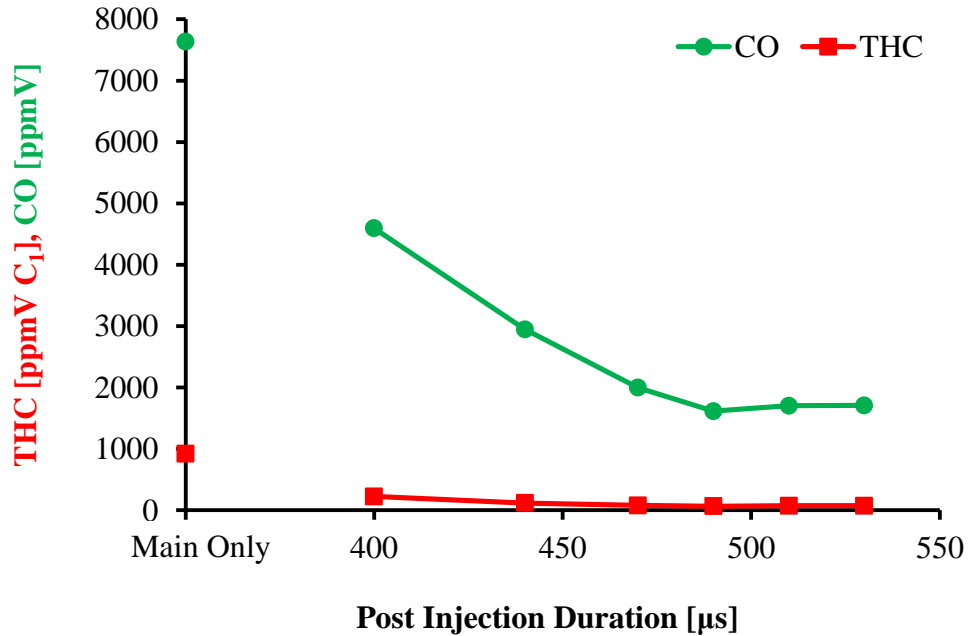


Figure 5-31: Effect of Butanol Post Injection Duration on CO and THC Emissions

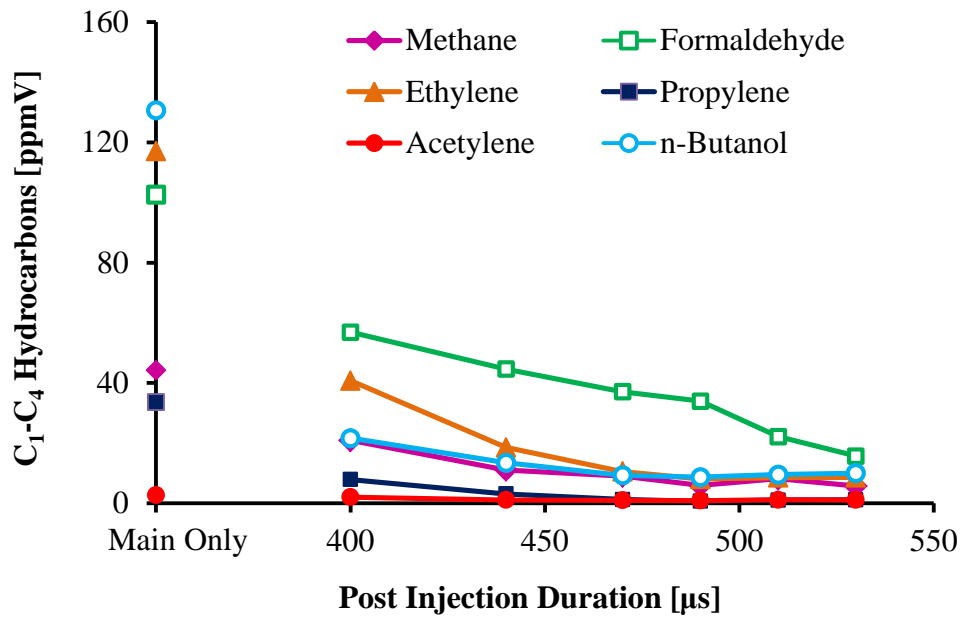


Figure 5-32: Effect of Butanol Post Injection Duration on Hydrocarbon Speciation

Analysis with an FTIR analyzer indicated that most of the hydrocarbons were light hydrocarbons and that there was very little unburned butanol fuel in the exhaust. The low amount of unburned butanol fuel indicated that the combustion was fairly efficient for the post injection. Formaldehyde was the most abundant species but all of the measured species were below 20 ppmV at 8.9 bar IMEP. Such levels would not be difficult to oxidize and remove with a diesel oxidation catalyst. Methane is a relatively stable species and may be more difficult to remove with a DOC but the methane levels were below 10 ppmV at 8.9 bar IMEP and were not a major concern.

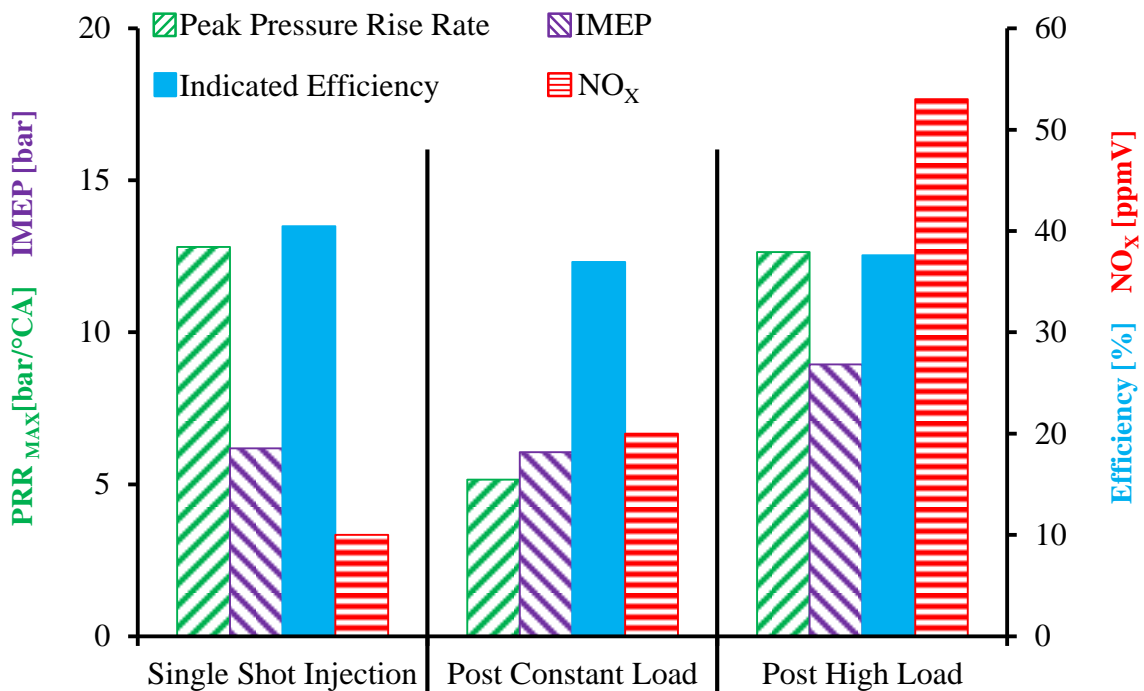


Figure 5-33: Comparison of Butanol Single Shot Injection and Post Injection

A summary of the results and a comparison with the single shot injection strategy are shown in Figure 5-33. The comparison demonstrated that, for a constant load of 6.1 bar IMEP, the post injection strategy effectively reduced the peak pressure rise rate from 12.8 to 5.2 bar/°CA. Furthermore, the results also showed that the engine load was increased from 6.1 to 8.9 bar IMEP for a constant peak pressure rise rate of 12.8 bar/°CA. Compared to the single shot strategy, the post strategy had a slightly reduced indicated

thermal efficiency and slightly increased NO_x emissions. The 8.9 bar IMEP level was not attainable with the single shot strategy due to excessive peak pressure rise rates so the slight efficiency and NO_x penalties for the post injection strategy were justified. However, further investigations were necessary to achieve the 14 bar IMEP target.

5.4 High Load Operation with Neat Butanol Fuel

Further investigations with a double post strategy were carried out to achieve high load operation at 14 bar IMEP. The previous results with a single post injection strategy indicated that an increased post injection duration caused an advanced combustion phasing for the main injection and resulted in an increased PRR. The test results also showed that the peak pressure rise rate always occurred during the combustion of the main injection and that the pressure rise was negative during the post injection event. With this in mind, the use of a double post injection strategy, with a relatively small main injection, was proposed. A smaller main injection provides leverage to offset the effect of the advanced combustion phasing of the main injection on the PRR. Additionally, the use of a very large first post injection was proposed because a large first post injection was expected to produce a significant amount of power without significantly affecting the peak pressure rise rate.

Two sets of tests were carried out. The purpose of the first set of tests was to carry out a duration sweep for the first post injection. The first post duration was gradually increased until a PRR of 10 bar/°CA ATDC was reached. At this point, a second set of tests was carried out where a second post injection was added and its duration was increased until the 14 bar IMEP target or the PRR limit of 17 bar/°CA were reached. Table 5-6 shows further details for the first set of tests. The injection pressure, air intake pressure, and intake oxygen were the same as in the previous tests; only the injection timing and injection duration were modified. The main and the first post injection timing were slightly advanced to allow for a longer expansion ratio and increased power output from the first post injection.

Table 5-6: Test Conditions for a Modified Butanol Single Post Injection Strategy

IMEP [bar]	Variable
Engine Speed [rpm]	1500
Air Intake Pressure [bar absolute]	1.9
Intake Oxygen [% V]	20.5
Test Fuel	n-Butanol
Fuel Injection Pressure [bar]	900
Main Injection Duration [μ s]	450
Main Injection Timing [$^{\circ}$ CA ATDC]	-22
1 st Post Injection Duration [μ s]	Sweep
1 st Post Injection Timing [$^{\circ}$ CA ATDC]	12

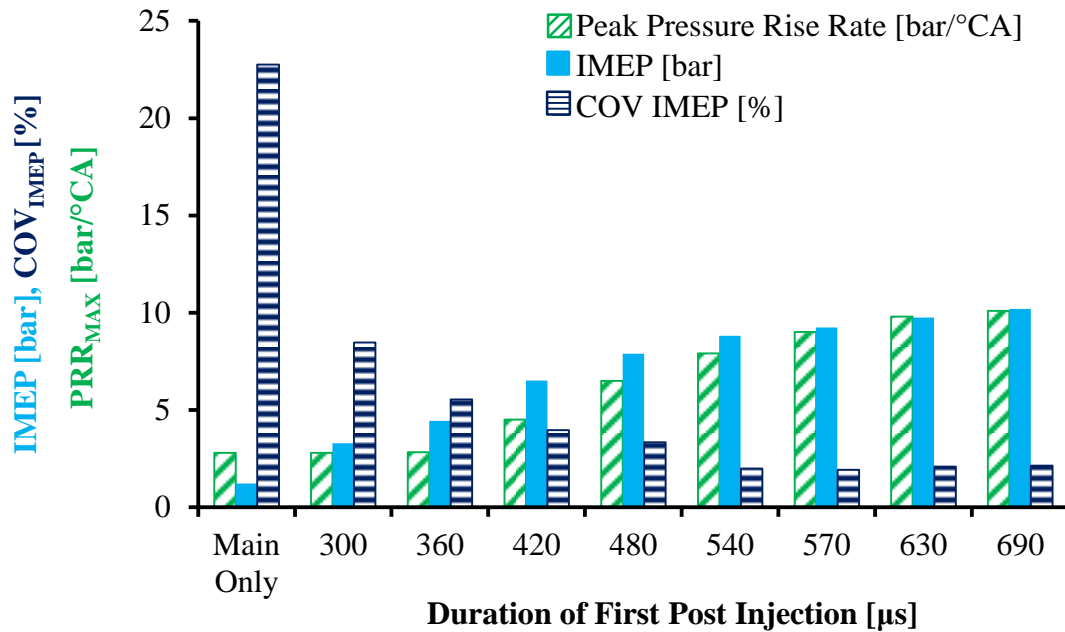
Figure 5-34: Effect of Modified Butanol Single Post Injection Strategy on PRR, IMEP, and COV_{IMEP}

Figure 5-34 shows that the new strategy, with a smaller main injection and a larger first post injection, allowed an IMEP of 10.2 bar to be achieved with a PRR of 10.1 $\text{bar}/^{\circ}\text{CA}$. This result represented a significant improvement compared to the previous attempts with the single post injection strategy that had a PRR of 12.8 $\text{bar}/^{\circ}\text{CA}$ for a load of 8.9 bar IMEP. The heat release traces in Figure 5-35 confirmed that the first post

injection advanced the combustion phasing of the main injection, as in the previous tests, but the effect was less significant since the main injection duration was reduced.

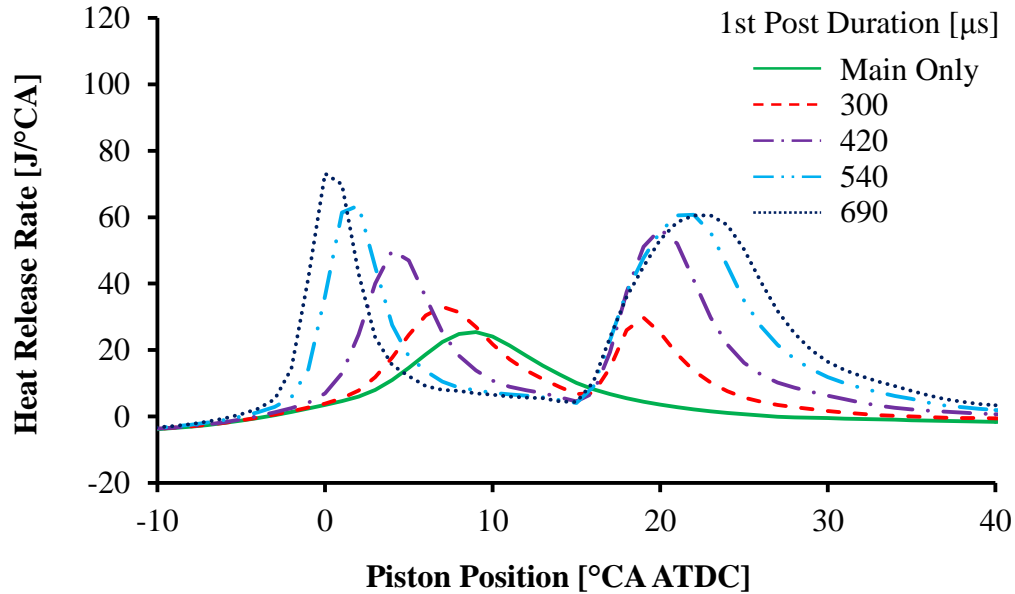


Figure 5-35: Effect of Modified Butanol Single Post Injection Strategy on HRR

The improved results were also attributed to the advanced injection phasing of the first post injection that extracted more power without increasing the PRR as shown by the flat or negative pressure slopes for the post injection in Figure 5-36. In addition to the reduced PRR, the new strategy also had a higher indicated thermal efficiency as demonstrated in Figure 5-37. The 690 μ s post duration achieved a 10.2 bar IMEP with an indicated efficiency of 40.3% and this was a significant increase compared to the previous tests that had an efficiency generally below 38% as previously shown in Figure 5-29. The increased thermal efficiency was accredited to the advanced injection phasing of the main injection and the first post injection and to higher flame temperatures, as suggested by the plot of the bulk gas temperatures in Figure 5-38. The peak bulk gas temperatures were higher compared to the previous tests shown in Figure 5-28.

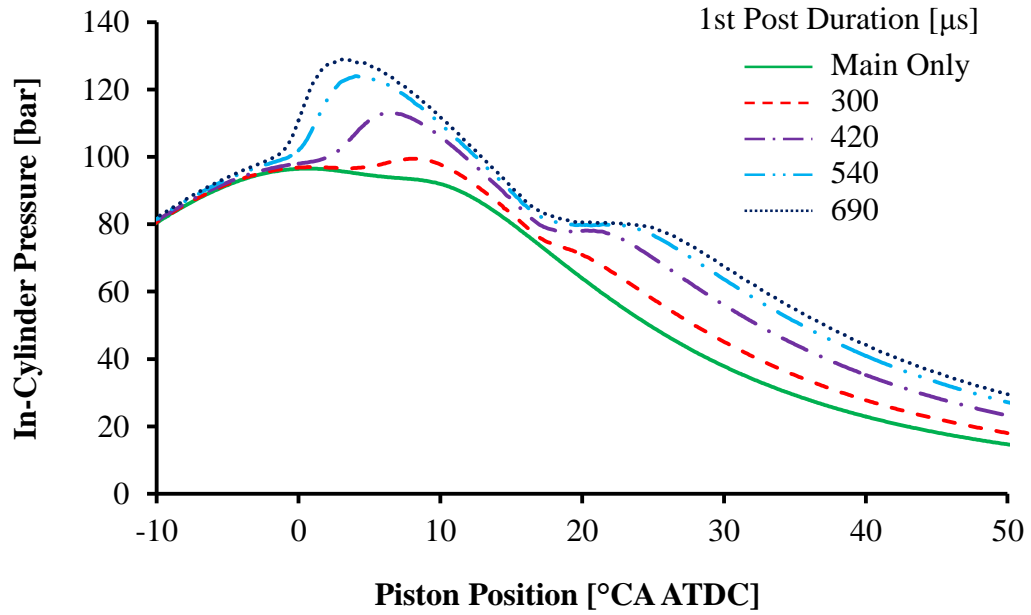


Figure 5-36: Effect of Modified Butanol Single Post Injection Strategy on In-Cylinder Pressure

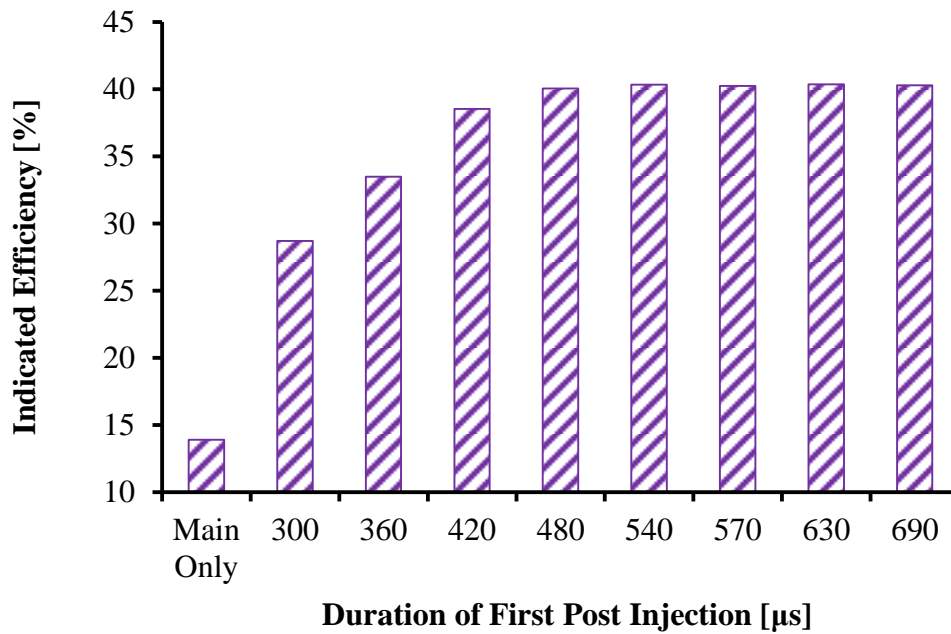


Figure 5-37: Effect of Modified Butanol Single Post Injection Strategy on Efficiency

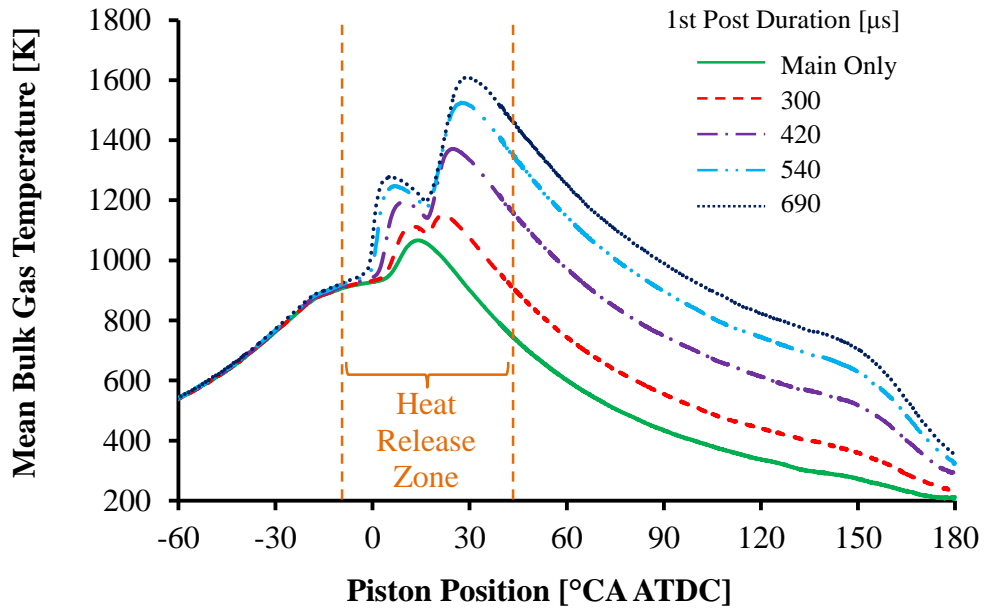


Figure 5-38: Effect of Modified Butanol Single Post Injection Strategy on Bulk Gas Temperature

The first set of tests focused on the IMEP and the PRR. For reference, the emissions results are given in the appendix in Figure B-9 to Figure B-12. To attain the 14 bar IMEP target, a second set of tests was carried out where a second post injection was added in an effort to produce more power. The test parameters for the second set of tests are shown in Table 5-7. A second post injection at 32°CA ATDC was added to the main and the first post injections and a post injection duration sweep was carried out for the second post injection.

The pertinent test data is presented in Figure 5-39. A load of 14.0 bar IMEP was achieved with a PRR of 14.8 bar/°CA. The targeted load and PRR were achieved due to the significant power generation from the first and the second post injections and a reduced PRR from the main injection compared to earlier tests. As seen in the heat release curves in Figure 5-40, the first post injection had a significant heat release while the heat release consistently increased for the second post injection as its injection duration was increased. The noticeable heat release profiles indicated that a considerable amount of power was generated by the post injections while the pressure traces in Figure

5-41 confirmed that the pressure rise was negative during the combustion of the post injections.

Table 5-7: Test Conditions for a Butanol Double Post Injection Strategy

IMEP [bar]	Variable
Engine Speed [rpm]	1500
Air Intake Pressure [bar absolute]	1.9
Intake Oxygen [% V]	20.5
Test Fuel	n-Butanol
Fuel Injection Pressure [bar]	900
Main Injection Duration [μ s]	450
Main Injection Timing [$^{\circ}$ CA ATDC]	-22
1 st Post Injection Duration [μ s]	570
1 st Post Injection Timing [$^{\circ}$ CA ATDC]	12
2 nd Post Injection Duration [μ s]	Sweep
2 nd Post Injection Timing [$^{\circ}$ CA ATDC]	32

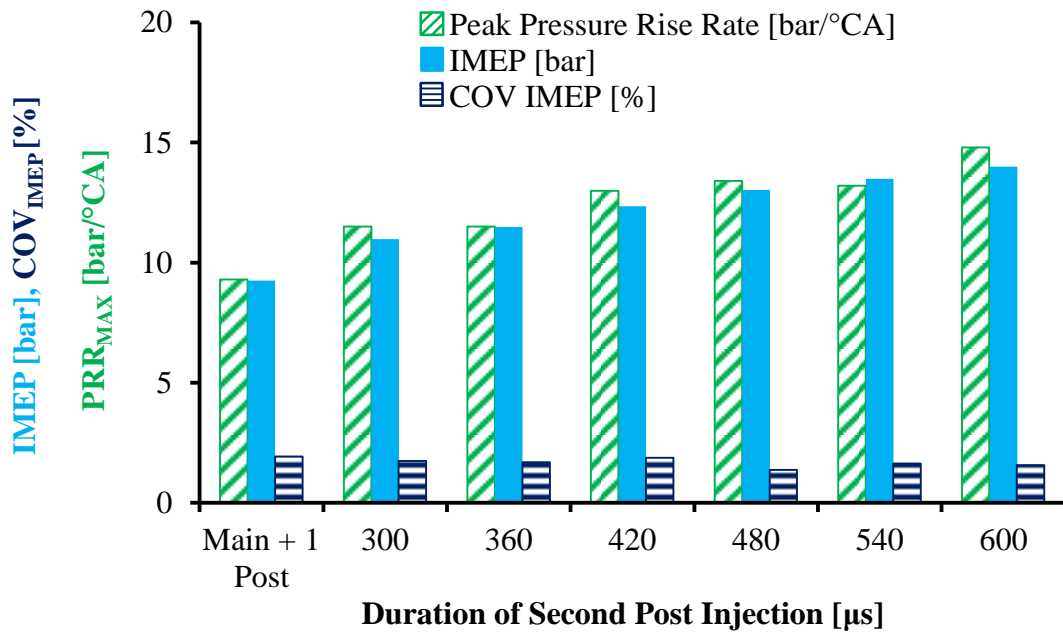


Figure 5-39: Effect of Butanol Double Post Injection Strategy on PRR, IMEP, COV_{IMEP}

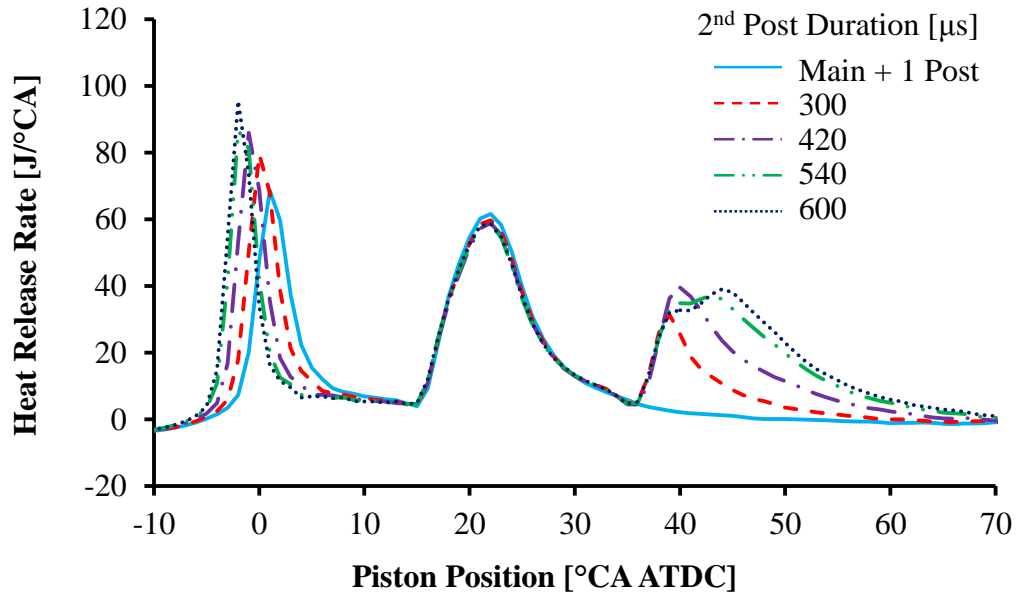


Figure 5-40: Effect of Butanol Double Post Injection Strategy on Heat Release

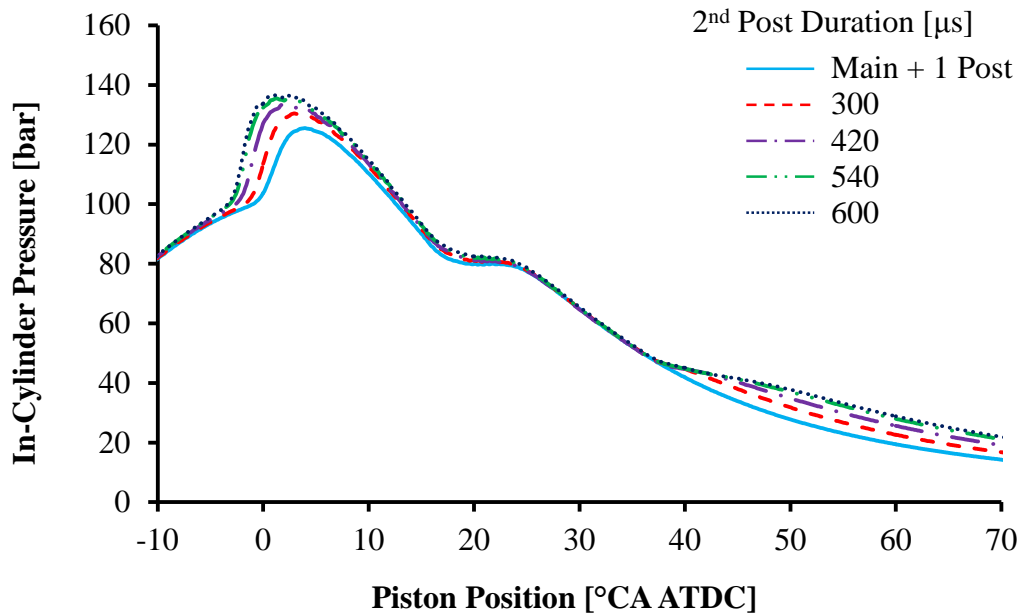


Figure 5-41: Effect of Butanol Double Post Injection Strategy on In-Cylinder Pressure

Although the targeted IMEP of 14 bar was achieved, the double post injection strategy did have some drawbacks. As witnessed in Figure 5-42, the indicated efficiency

reduced from 40.2 to 35.5% when the duration of the second post was increased. The reduced efficiency was caused by the relatively short expansion ratio, 6.8:1, for the second post injection compared an expansion ratio of 18.2:1 for the main and 14.7:1 for the first post injection. The same figure also showed that the exhaust gas temperature increased from 325°C to 530°C for larger second post injections. Higher exhaust gas temperatures can be desirable for heating up catalytic converters during cold start conditions and for maintaining high NO_x conversion efficiencies. Lean NO_x traps typically have improved operation in the region of 250-450°C while temperatures of 500°C and higher can be periodically required for purging unwanted sulfates from the LNT [83,90,99].

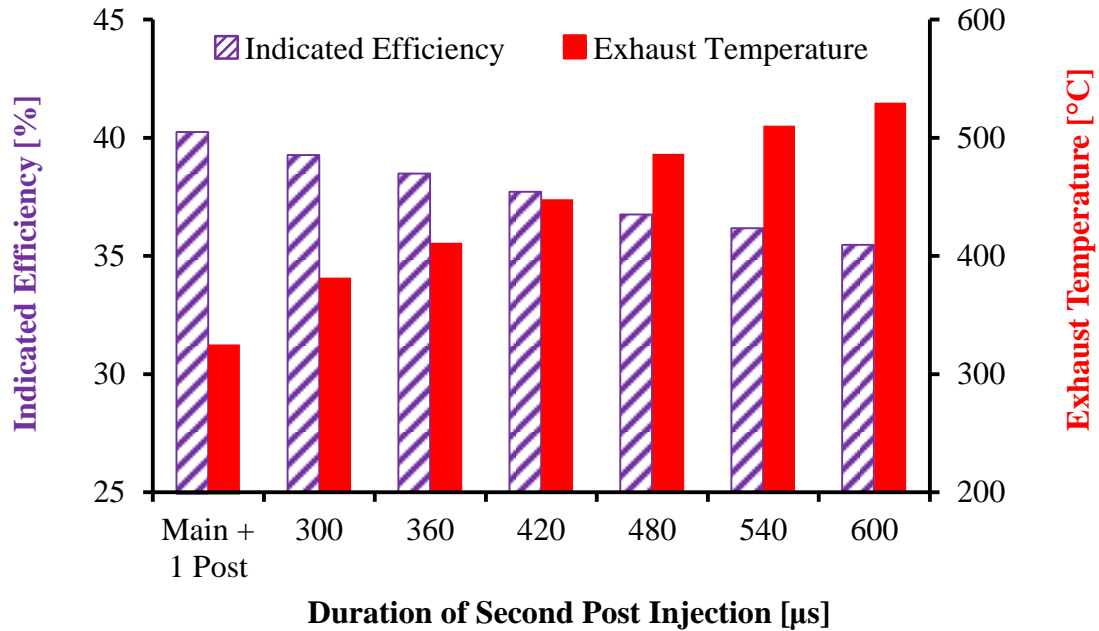


Figure 5-42: Effect of Butanol Double Post Injection Strategy on Efficiency and Exhaust Temperature

In addition to the reduced indicated thermal efficiency, there were also increased smoke emissions as illustrated in Figure 5-43. The smoke emissions increased substantially from 0.024 to 0.062 g/kW·hr (0.06 to 0.75 FSN) when the load was increased from 9.3 to 14.0 bar IMEP. Higher flame temperatures, as suggested by the

increased bulk gas temperatures in Figure 5-44, and a relatively short ignition delay for the second post injection led to an increased smoke formation rate. At the same time, the reduced oxygen availability for the second post injection led to a reduced soot oxidation rate. The indicated NO_x emissions were relatively high but fairly stable throughout the test, consistently in the region of 1.9 to 2.2 $\text{g/kW}\cdot\text{hr}$ (157 to 213 ppmV as shown in Figure B-13 in Appendix B). Consequently, the engine-out NO_x emissions were out of range for long breathing operation for these conditions.

The THC and CO emissions are shown in Figure 5-45. There was a substantial reduction of the CO emissions as the second post duration and the engine load were increased. Even the addition of a small second post injection, such as 300 μs , led to a significant CO reduction from 1474 to 708 ppmV. This observation implied that the second post injection was able to oxidize the CO produced by the main and the first post injections and that the second post injection did not produce much CO.

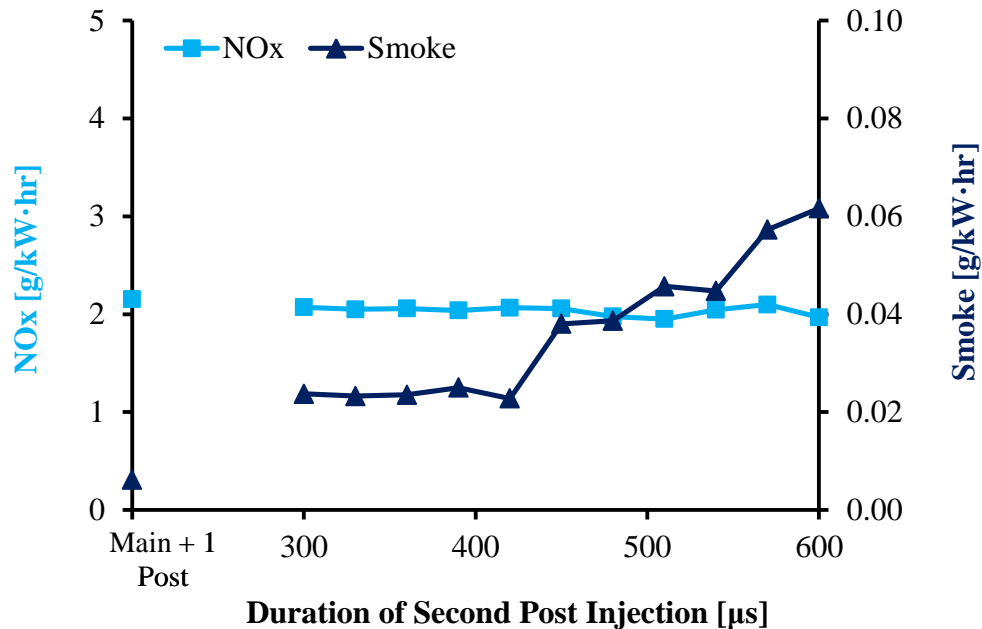


Figure 5-43: Effect of Butanol Double Post Injection Strategy on Indicated NO_x and Smoke Emissions

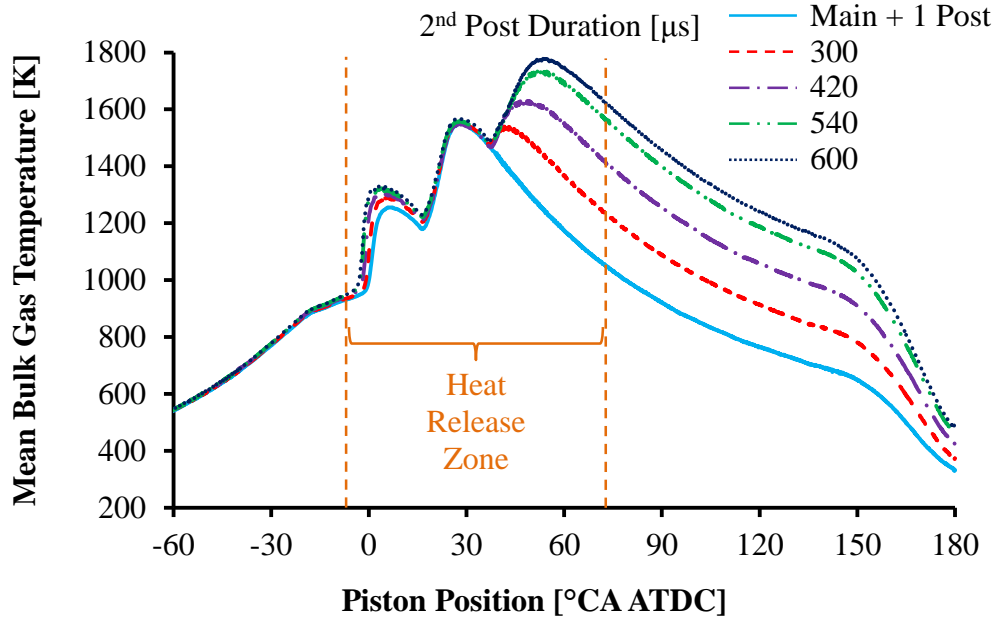


Figure 5-44: Effect of Butanol Double Post Injection Strategy on Bulk Gas Temperature

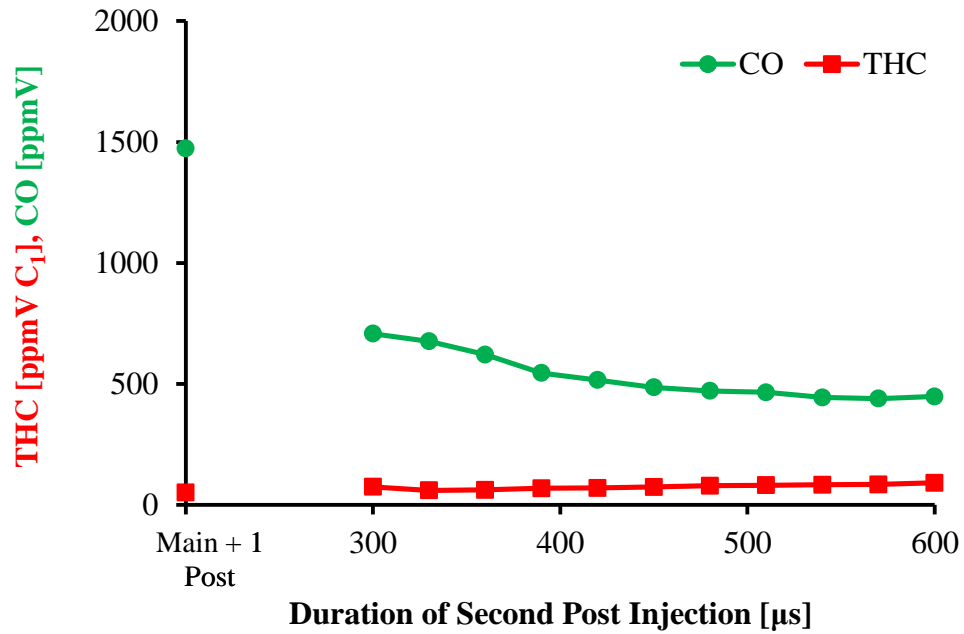


Figure 5-45: Effect of Butanol Double Post Injection Strategy on CO and THC

Conversely, the THC emissions increased from 51 to 92 ppmV as the second post injection duration was increased. The hydrocarbon speciation analysis in Figure 5-46 demonstrated that there was a slight increase in the unburned n-butanol emissions when the second post injection was added. On the other hand, there was a dramatic drop in the formaldehyde emissions. Considering the molar fraction of each species, the aggregate sum of the hydrocarbon species was lower but the THC emissions appeared to be higher because they were reported on a C₁ basis and because there was a slight increase for the longest chain hydrocarbon, unburned butanol (C₄).

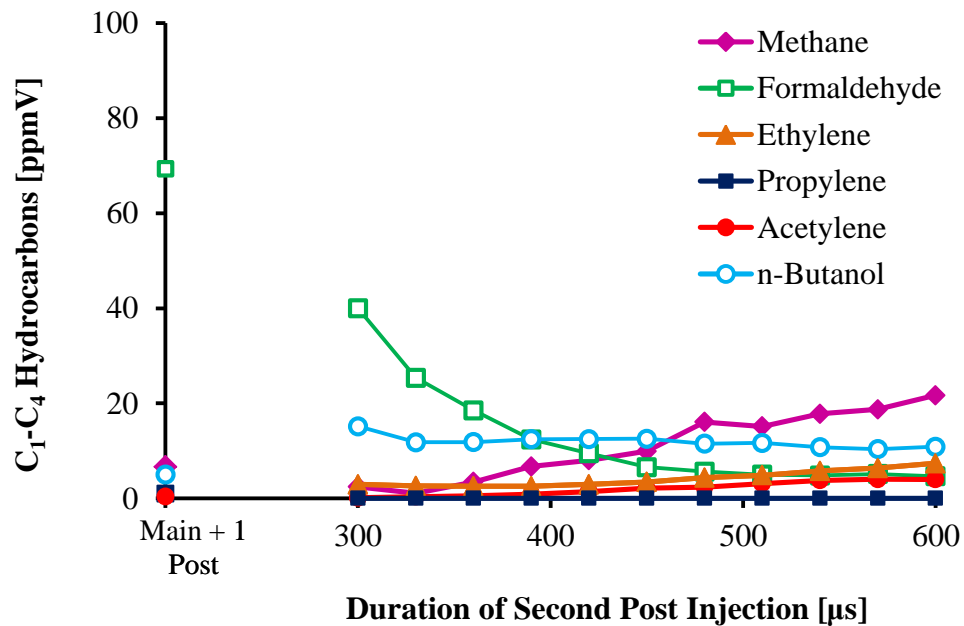


Figure 5-46: Effect of Butanol Double Post Injection Strategy on Light Hydrocarbons

To conclude, the double post injection strategy successfully achieved the 14 bar IMEP target without breaching the 17 bar/°CA PRR limit. This represented a major achievement because this engine load was not previously possible with the single shot injection strategy due to excessive peak pressure rise rates. However, there were some drawbacks to this strategy, such as increased smoke emissions and a reduced thermal efficiency. Nevertheless, butanol combustion without the use of EGR was demonstrated

at low, medium, and high load conditions and representative results were summarized for further analysis with the use of a long breathing LNT.

5.5 Chapter Summary for Long Breathing using Neat Butanol Fuel

Representative low, mid, and high load conditions for neat n-butanol combustion are summarized in Table 5-8. At low load conditions of 6 bar IMEP, single shot, single post, and double post injection strategies all achieved very low NO_x emissions, 32 ppmV or lower, that were suitable for a long breathing LNT. Each of the three low load strategies had benefits and drawbacks. For highest efficiency operation, the single shot strategy was the most suitable. The single post injection strategy was suitable for operation with a significantly reduced peak PRR and a slightly increased exhaust gas temperature. Finally, the double post strategy was a better choice for operation with increased exhaust gas temperatures, such as may be required for cold start conditions. Compared to long breathing operation with diesel fuel and EGR at low load conditions, the main advantage of the neat butanol strategy were the near zero smoke emissions and the relatively low NO_x emissions.

Medium load neat butanol combustion was achieved with multiple injection strategies. The single shot strategy was unable to achieve medium load conditions of 10 bar IMEP due to excessive PRR. The highest efficiency of 40.0% was achieved with a single post injection strategy. However, at this operating condition, the NO_x emissions were relatively high, 186 ppmV, and were slightly beyond the long breathing LNT range. For reduced NO_x emissions at this load level, the double post injection strategy was a better choice. The smoke emissions were also significantly lower compared to diesel fuel with EGR. A triple post injection strategy was also investigated for medium load operation and the results are shown in Appendix G. The triple post strategy had a substantially lower indicated thermal efficiency and did not provide any IMEP, peak pressure rise rate, and emission benefits compared to the double post strategy. The primary benefit of the triple post strategy was the moderately increased exhaust gas temperature which may be useful for cold start conditions.

Table 5-8: Representative Exhaust Gas Conditions with Neat Butanol

Type	Exhaust Conditions								
	IMEP bar	PRR _{MAX} bar/°CA	Efficiency [%]	CO ppmV	THC ppmV	NO _x ppmV	NO _x g/kW·hr	Smoke FSN	Temp °C
Butanol Single Shot	6.2	15.6	41.5	2471	169	16	0.313	0.0	208
Butanol Single Post	6.2	3.8	35.9	5020	309	32	0.663	0.0	234
Butanol Double Post	6.0	3.2	31.9	4356	1045	22	0.448	0.0	294
Butanol Single Post	10.0	9.7	40.0	1161	107	186	2.349	0.1	347
Butanol Double Post	10.0	15.3	32.9	1583	151	56	0.731	0.3	415
Butanol Double Post Tuned	10.0	17.2	36.9	1564	117	57	0.649	0.2	386
Butanol Double Post	14.0	14.8	35.5	427	97	213	1.968	0.7	529

For high load operation with neat butanol, only the double post strategy achieved the targeted load of 14 bar IMEP. At this operating condition, the NO_x emissions were 1.97 g/kW·hr (213 ppmV) and out of the long breathing LNT range. Thus, long breathing operation at butanol high load conditions proved to be a challenge. The NO_x emissions at high load were found to be lower compared to conventional diesel combustion but similar NO_x levels were obtained when diesel was used with EGR¹⁵.

Overall, neat butanol operation was achieved at low load, mid load, and high load conditions using a combination of single shot, single post, and double post injection strategies. Across all load ranges, the indicated NO_x emissions for neat butanol generally exceeded the EPA NO_x emission regulations for on-road heavy duty trucks. Thus, NO_x after-treatment may be required for potential vehicles with butanol fuel or with a fuel of similar properties to butanol. A long breathing LNT may be a suitable option since it can reduce the supplemental fuel consumption for low engine-out NO_x levels. With the gathered experimental data for the exhaust gas conditions from the engine tests, the next step was to quantify the potential energy saving benefits of a long breathing LNT compared to a conventional LNT.

¹⁵ The diesel fuel results with EGR were previously shown in Figure 4-1.

CHAPTER 6: LONG BREATHING LEAN NO_x TRAP

This chapter investigates the operation of a lean NO_x trap under the exhaust gas conditions equivalent to low load, medium load, and high load operation with neat n-butanol and with diesel and EGR. The investigation utilizes a numerical model of an LNT and the setup of the LNT catalyst model is presented. Experimental heated after-treatment flow bench tests are used to validate the numerical model. The numerical calculations are used to evaluate the potential energy savings of a long breathing LNT at different engine operating conditions.

6.1 Setup of the Lean NO_x Trap Numerical Model

In the previous chapters, representative exhaust gas conditions were summarized for low load, medium load, and high load operation with neat n-butanol and diesel fuels. The next step was to quantify the potential fuel consumption savings of the long breathing strategy at each engine load. Numerical models were utilized to carry out the investigation. Numerical models of an LNT were generated with AVL (Anstalt für Verbrennungskraftmaschinen List) FIRE and BOOST. A three dimensional (3D) lean NO_x trap model was created with AVL FIRE and a one dimensional (1D) model was created with AVL BOOST. To validate the models, experimental heated flow bench tests were carried out and the results were compared with the data from the numerical model.

For the 3D AVL FIRE model, the geometry of the LNT mesh, shown in Figure 6-1, was set to replicate the physical dimensions of the LNT catalyst that was used for the experimental flow bench tests. The model configuration consisted of a catalyst section, an inlet pipe, and an outlet pipe as shown in Figure 6-1. The default values were applied for the following meshing parameters: resolution, boundary, porosity, and interface. The AVL BOOST model was one dimensional and it did not require a mesh.

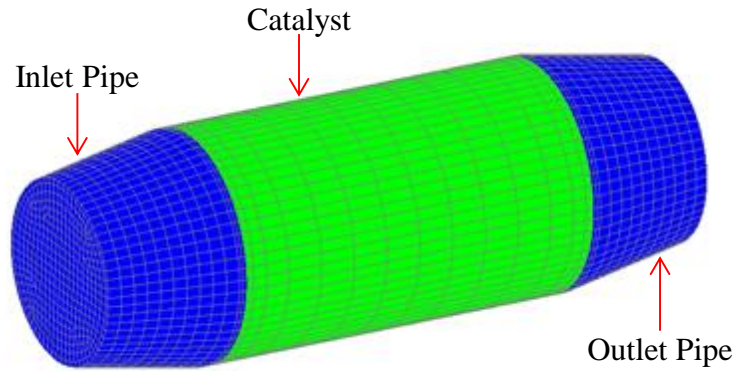


Figure 6-1: Three Dimensional LNT Mesh

For both models, the LNT catalyst was defined to be a square cell catalyst with a cell density of 400 cpsi and a wall thickness of 0.006 inch. The cell density was chosen to replicate the cell density of the physical catalyst sample used in the experimental tests while the wall thickness was chosen according to the common values found in literature [107,120]. The diameter of the catalyst was 44 mm and the length was 152 mm. The values were chosen based on the sample used for the experimental flow bench tests. The remaining variables were set to the default values. The key thermal and physical properties of the catalyst model are summarized in Table 6-1 and those of the physical LNT sample are given in Table 6-2.

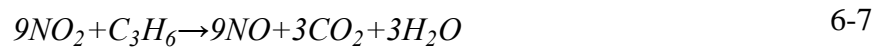
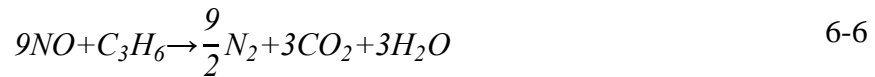
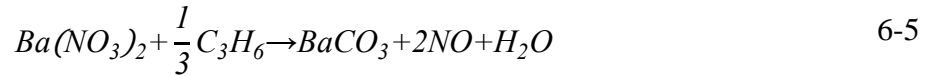
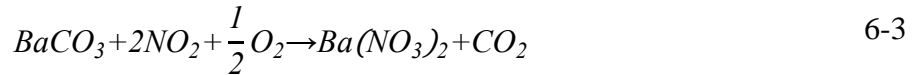
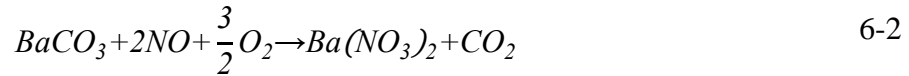
Table 6-1: Thermal and Physical Properties of the Numerical Model Catalyst

Diameter [mm]	44
Length [mm]	152
Volume [L]	0.231
Wall Thickness [inch]	0.006
Cells per Square Inch [cpai]	400
Density [kg/m ³]	450
Thermal Conductivity [W/m·K]	0.4
Specific Heat [J/kg·K]	1050

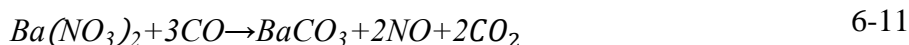
Table 6-2: Physical Properties of the Experimental Flow Bench Catalyst

Volkswagen Model Number	1K0-254-401-T
Diameter [mm]	44
Length [mm]	152
Volume [L]	0.231
Cells per Square Inch [cpsi]	400

The LNT ICVT Stuttgart model in AVL FIRE and BOOST with ash-core storage and regeneration models was used for modelling the chemical kinetics of the catalyst. The NO oxidation and the NO and NO₂ barium storage reactions shown in Equations 6-1 through 6-3 were activated to model the LNT storage cycle. The LNT regeneration cycle was modelled utilizing propene as a representative light hydrocarbon. The model included the oxidation reaction of propene as shown in Equation 6-4, the NO_x release reaction shown in Equation 6-5, and the NO and NO₂ reduction reactions in Equations 6-6 and 6-7.



The reactions shown in Equations 6-1 to 6-7 were used for the chemical kinetic modelling of the LNT catalyst. Additional chemical kinetics for carbon monoxide and hydrogen were included in the one dimensional model as shown in Equations 6-8 and 6-9. The water gas shift reaction, Equation 6-10, was used to simulate the conversion of carbon monoxide and water to hydrogen. Additional reactions were also included for the LNT regeneration cycle. Equations 6-11 and 6-12 were added to model the release of the nitrates from the LNT catalyst with CO and hydrogen as the reactants. Finally, the reduction reactions for NO, with hydrogen as the reducing agent, and for NO and NO₂, with CO as the reducing agent, were included as shown in Equations 6-13 to 6-15. The three dimensional model also had the functionality to simulate these reactions but the computational time for the 3D model was about ten to twenty times longer compared to the 1D model. To allow for a more reasonable computational time, only Equations 6-1 to 6-7 were used for the 3D model.



Both models assumed that the inlet pipe, the outlet pipe, and the catalyst substrate surfaces were well insulated and that there was no heat transfer to or from the system in the radial direction. Thus, adiabatic conditions were assumed at the system boundaries and the wall heat flux value was accordingly set to zero. The numerical model utilized a time step of 0.05 seconds but, to reduce the computational time, the calculated data was recorded every four time steps (every 0.2 seconds).

6.2 LNT Numerical Model Validation

A validation test was carried out between the experimental flow bench tests, the one dimensional model, and the three dimensional model. The tests were conducted at a common operating condition. The numerical calculations were carried out at a catalyst temperature of 300°C and a gas hourly space velocity (GHSV) of 32800 volumes per hour. The feed gas was dosed with 220 ppmV of NO. For the heated flow bench tests, there were slight fluctuations in the feed gas NO fraction from 200 to 220 ppmV. Furthermore, the catalyst temperature varied between 300°C and 320°C for the empirical tests. The tests were conducted for a NO_x storage cycle of 120 seconds; this duration was chosen since a typical LNT NO_x storage cycle is on the order of one minute [80].

The preliminary results are shown in Figure 6-2. The figure shows curves for the accumulated NO_x mass entering the LNT and exiting the LNT for the empirical test and the numerical calculations. There was a fairly good match between the 1D and the 3D models but the NO_x storage efficiency¹⁶ of both numerical models was lower than the storage efficiency of the empirical tests as illustrated in Figure 6-2. After 120 seconds of operation, the NO_x storage efficiencies of the numerical models were 69 to 70% while it was 76% for the empirical tests. The storage efficiency difference between the models and the empirical results suggested that the catalyst parameters for the model needed to be tuned. An iterative trial and error method was applied to tune the catalyst parameters. At this stage, the numerical modeling focused on the one dimensional model because the

¹⁶ The NO_x storage efficiency was calculated according to Equations 6-16 to 6-19. Nitric oxide was treated as nitrogen dioxide, according to the EPA rule.

difference between the one dimensional and three dimensional results was negligible as shown in Figure 6-2 and three dimensional results were not considered essential for this particular investigation.

$$\text{Storage Efficiency [\%]} = \frac{\text{NO}_x \text{ Stored [g]}}{\text{NO}_x \text{ Inflow [g]}} \times 100 \quad 6-16$$

$$\text{NO}_x \text{ Stored [g]} = \text{NO}_x \text{ Inflow [g]} - \text{NO}_x \text{ Outflow [g]} \quad 6-17$$

$$\text{NO}_x \text{ Inflow [g]} = (\text{NO Inflow [g]}) \times (46/30) \quad 6-18$$

$$\text{NO}_x \text{ Outflow [g]} = (\text{NO Outflow [g]}) \times (46/30) + \text{NO}_2 \text{ Outflow [g]} \quad 6-19$$

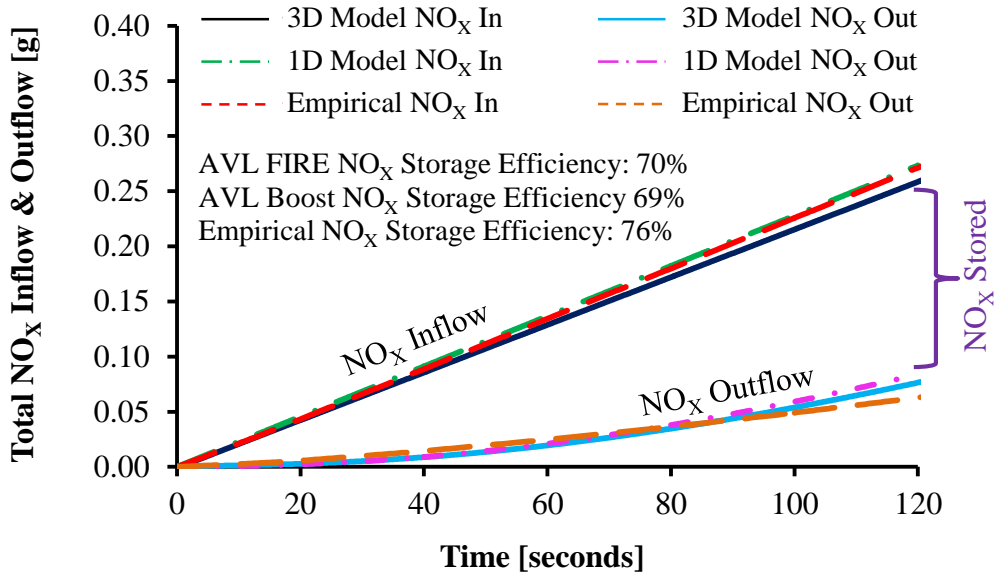


Figure 6-2: Validation Tests for the Numerical Models

Before tuning the numerical model, further heated flow bench tests were carried out to check the repeatability of the experimental results. The operating conditions for the additional experimental test are summarized in Table 6-3. The catalyst was heated to

a temperature of about 300°C which represented a common diesel exhaust gas temperature. The temperature was not uniform throughout the catalyst. The front of the catalyst had a temperature of 328°C and the rear of the catalyst had a temperature of 282°C¹⁷. The average catalyst temperature throughout the test was 315°C. The flow to the catalyst was adjusted to give an average gas hourly space velocity of 46170 volumes per hour using gas densities at standard temperature and pressure. These values of GHSV were chosen to be within the range commonly reported in literature [77,90,91]. The feed gas consisted of NO_x, oxygen, carbon dioxide, and balance nitrogen. The average NO_x, oxygen, and CO₂ concentrations are given in Table 6-3.

Table 6-3: Operating Conditions for Experimental Flow Bench Test

Storage Duration [s]	120
Average Catalyst Temperature [°C]	315
Standard Gas Hourly Space Velocity [1/h]	46170
Feed Gas NO _x [ppmV]	215
Feed Gas O ₂ [%V]	13.7
Feed Gas CO ₂ [%V]	8.3

The results of the additional experimental tests are shown in Figure 6-3. The empirical data exhibited good repeatability since the NO_x storage efficiency was consistently between 76.0 and 76.5%. The average NO_x storage efficiency for all three tests was calculated to be 76.2% while the coefficient of variation was only 0.3%. Despite the small sample size, the 95% confidence interval for the storage efficiency was within the narrow range of $76.2 \pm 0.5\%$.

The next step was to tune the catalytic coefficients of the 1D model under the average operating conditions shown in Table 6-3 to obtain a good correlation with the experimental data. In particular, the NO_x storage capacity of the LNT catalyst was increased from 0.013 mol/m² to 0.29 mol/m². This adjustment was made through

¹⁷ The catalyst temperature was measured by five equally spaced thermocouples. The ceramic substrate was drilled and the thermocouples were placed along the centreline of the longitudinal axis of the catalyst.

numerous trial and error iterations. The results with the tuned model are illustrated in Figure 6-4. The tuned model had a NO_x storage efficiency of 76.0% while the storage efficiency of the empirical investigation was 76.2% ± 0.5%. Thus, a good correlation was obtained between the model and the empirical data.

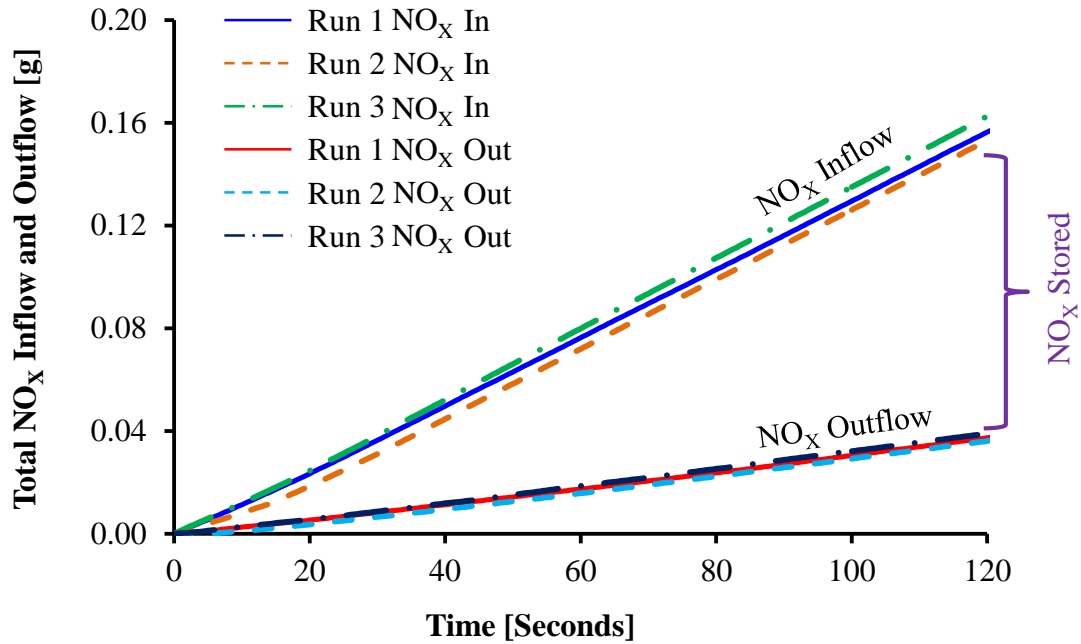


Figure 6-3: Repeatability Tests for the Empirical Flow Bench Tests

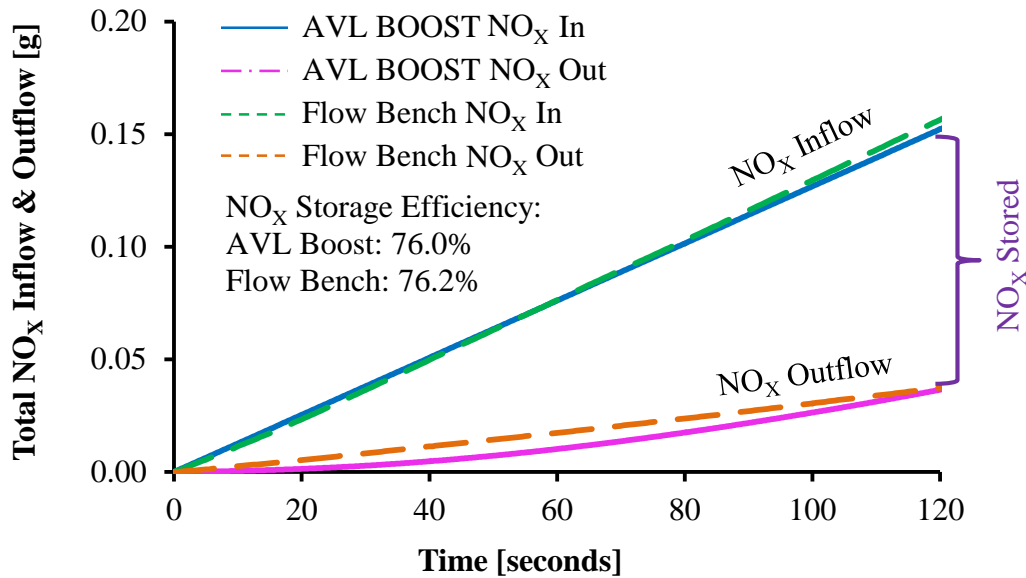


Figure 6-4: Comparison of 1D Model and Empirical Data

6.3 Quantification of Energy Savings for Long Breathing with Diesel and EGR

Strategies such as exhaust gas recirculation need to be applied to lower the engine-out NO_x emissions but the use of EGR will also impact the exhaust gas temperature and composition. The results in previous chapters indicated that the application of EGR also resulted in a fuel consumption penalty. Thus, a numerical investigation was conducted to determine if the potential fuel consumption savings of the long breathing LNT outweighed the fuel consumption penalty of EGR under real exhaust gas conditions at various engine loads. Representative exhaust gas conditions at different engine loads were obtained from the engine tests presented in Chapter 4. The exhaust conditions are summarized in Table 6-4. For the numerical calculations, the initial catalyst temperature and the feed gas temperature were set to the exhaust gas temperature shown in the table. The catalyst specifications of the 1D numerical model were described in the previous section.

Figure 6-5 shows a comparison of the NO_x storage efficiencies for conditions #1A to #4A, which represented low load diesel operation as shown in Table 6-4. Long breathing operation, with 54 to 94 ppmV of engine-out NO_x, consistently maintained a higher LNT NO_x storage efficiency compared to the conditions with 220 to 519 ppmV of NO_x. The data showed that the conventional LNT strategies maintained a NO_x storage efficiency of 80% or higher for only one to two minutes of storage. The long breathing LNT strategy with 54 ppmV of NO_x was able to maintain a NO_x storage efficiency greater than 80% for over 5 minutes. The primary reason for the improved performance of the long breathing strategy was the slower saturation rate of the LNT as shown in Figure 6-6. The long breathing condition with 54 ppmV of NO_x exhibited an LNT saturation of 23.9% after one hour of storage. The same saturation level was reached after only 5.65 minutes for conventional operation with 519 ppmV of NO_x. High levels of saturation effectively reduced the amount of available NO_x storage sites within the catalyst and the NO_x storage efficiency.

Table 6-4: Exhaust Gas Conditions for Diesel Combustion with EGR

Test #	Type	IMEP	Intake O ₂	Exhaust						
				CO	THC	NO _x	Smoke	O ₂	CO ₂	Temp
		bar	%V	ppmV	ppmV	ppmV	FSN	%V	%V	°C
1A	Conventional High NO _x	6.2	18.8	162	15	519	0.2	12.4	6.0	277
2A	Conventional Mid NO _x	6.2	16.7	322	29	220	0.3	10.1	7.6	281
3A	Long Breathing	6.1	15.2	611	58	94	0.7	8.7	9.1	283
4A	Long Breathing	6.1	14.0	1147	96	54	1.3	7.3	10.0	285
5B	Conventional High NO _x	10.2	18.7	58	9	743	0.2	11.7	6.5	316
6B	Conventional Mid NO _x	10.3	16.6	171	8	224	1.0	8.9	8.6	327
7B	Long Breathing	10.3	15.2	359	16	101	1.9	7.1	9.9	337
8B	Long Breathing	10.3	14.8	443	21	77	2.2	6.7	10.1	337
9C	Conventional High NO _x	14.5	18.9	32	6	829	0.3	11.5	6.6	352
10C	Conventional Mid NO _x	14.9	16.6	121	3	219	0.7	8.2	9.1	375
11C	Long Breathing	14.8	15.5	284	6	113	1.7	6.8	10.0	382
12C	Long Breathing	14.6	15.0	607	9	72	3.1	6.1	10.6	388

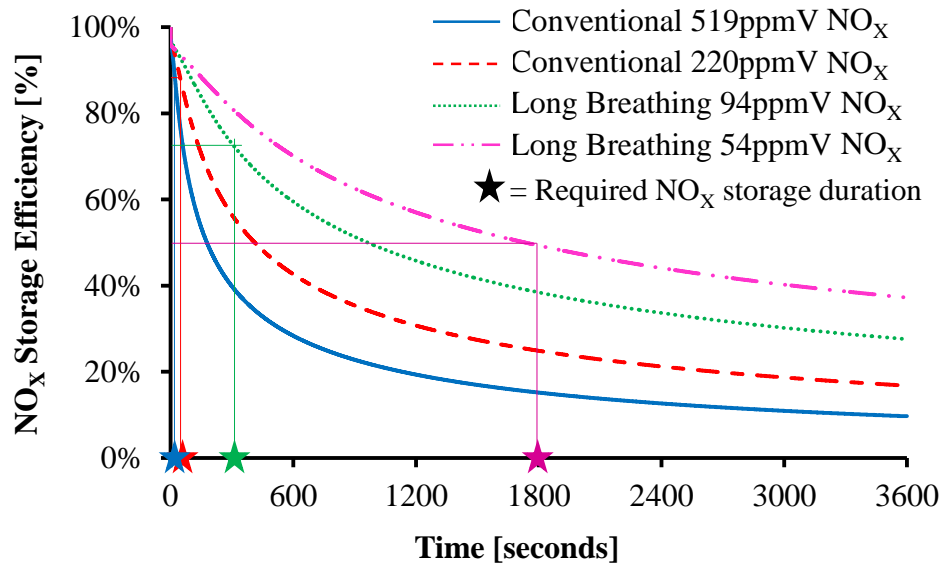
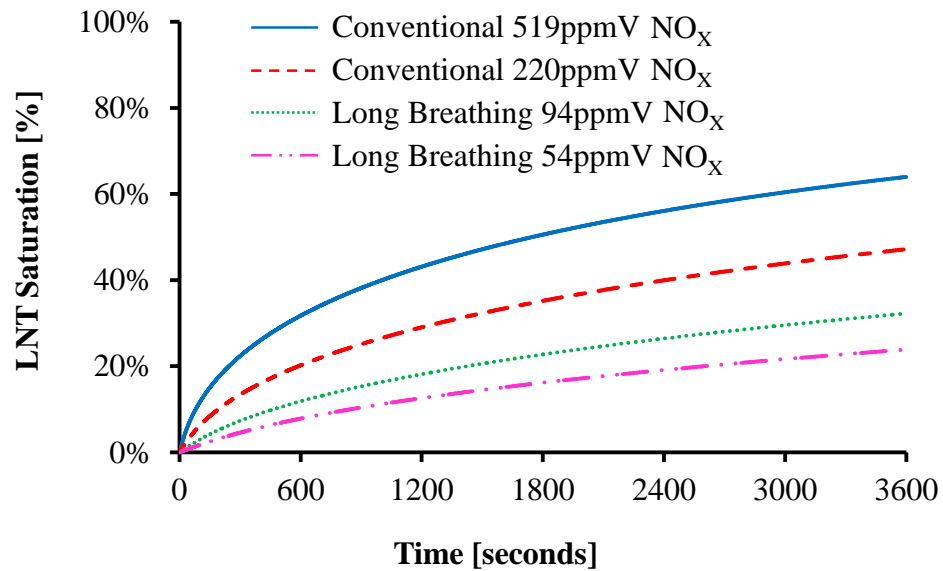
Figure 6-5: NO_x Storage Efficiency for Low Load Diesel Conditions

Figure 6-6: LNT Saturation for Low Load Diesel Conditions

The next part of the investigation focused on calculating the combined fuel consumption of the engine and the after-treatment system to quantify the potential energy savings of the long breathing technique. The first step was to determine the required

NO_x storage duration at each operating condition according to the selected NO_x emission target of 0.2 g/kW·hr. The selected NO_x target was moderately lower than the current (2010) EPA heavy duty on-road truck emission standard of 0.2 g/hp·hr (0.267 g/kW·hr). This target was chosen to account for the use of indicated power instead of brake power to calculate the NO_x emissions.

The required NO_x conversion efficiency was calculated based on the engine-out indicated NO_x emissions for each condition as shown in Figure 6-7. The figure illustrated that the indicated engine-out NO_x emissions were relatively high for the conventional strategies with 5.72 and 1.96 g/kW·hr of NO_x and this implied that the conventional strategies required a NO_x conversion efficiency of 96.5% and 89.8%, respectively, from the after-treatment system. The required NO_x conversion efficiencies were much lower for the long breathing conditions; 73.1% for the 0.74 g/kW·hr (94ppmV) NO_x condition and 48.9% for the 0.39 g/kW·hr (54 ppmV) NO_x condition.

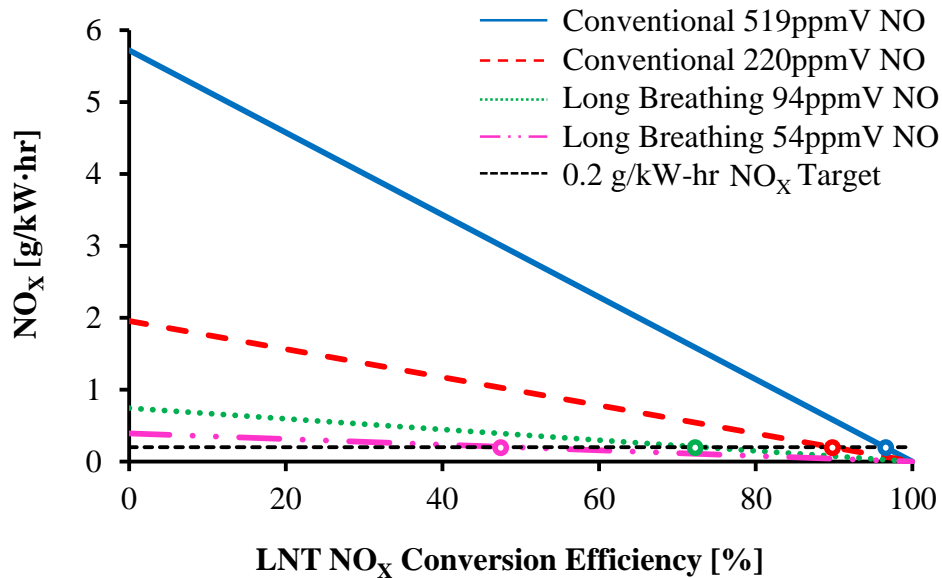


Figure 6-7: Required NO_x Conversion Efficiency for Low Load Diesel

The required NO_x conversion efficiencies were used to determine the required NO_x storage duration. An assumption was made that the NO_x conversion efficiency was

equal to the NO_x storage efficiency and that 100% of the stored NO_x were reduced to N₂ during the regeneration cycle. This assumption was used to simplify the analysis since the LNT regeneration and NO_x reduction cycles were not the focus of the present study. The required storage duration for each low load condition is shown in Figure 6-8. The conventional strategies required a NO_x storage duration of 3.4 to 40.0 seconds at these conditions while the required NO_x storage duration was in the range of 298.2 to 1835.2 seconds for the long breathing strategies.

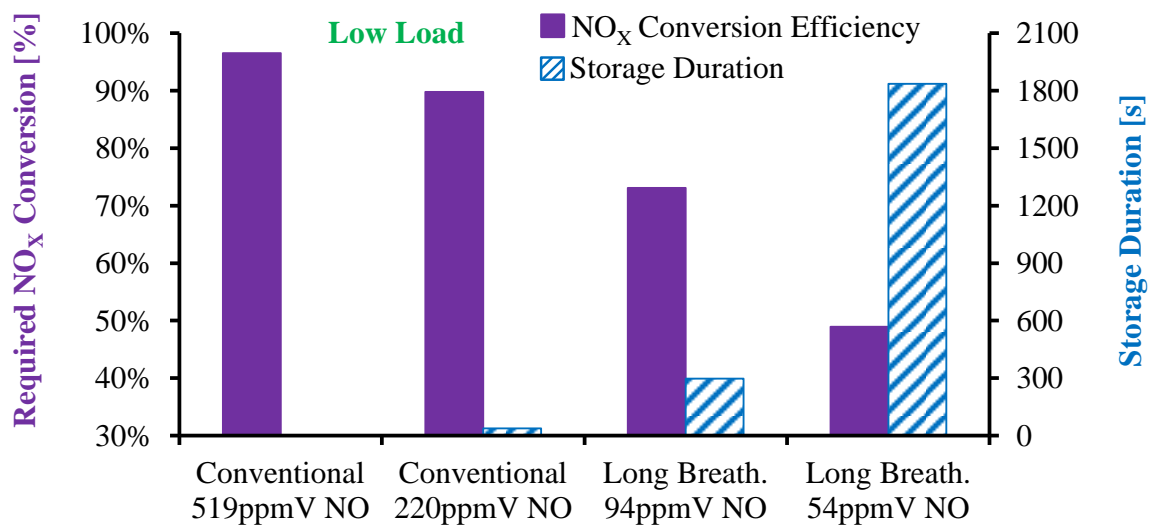


Figure 6-8: Storage Duration & Required NO_x Conversion Efficiency at Low Load

The results from the numerical model were used to obtain the NO_x mass stored within the LNT for each condition. However, the volume of the catalyst in the numerical model was based on the catalyst used in the after-treatment flow bench tests and it was significantly smaller than the catalyst volume required for the test engine. Thus, the stored NO_x mass for the numerical model catalyst was multiplied by a proportionality factor to obtain the expected stored NO_x mass for the engine catalyst. The calculation of the proportionality factor is shown in Appendix E. The results for the stored NO_x mass are given in Table 6-5. The data outlined that the conventional strategies had a much lower mass of NO_x stored within the LNT, caused by the substantially shorter NO_x storage duration.

Table 6-5: Stored NO_x Mass for Low Load Diesel Conditions

Strategy	IMEP [bar]	NO _x [ppmV]	NO _x [g/kW·hr]	Required NO _x Conversion Efficiency [%]	Storage Duration [s]	Stored NO _x Model [g]	Stored NO _x Engine [g]
1A Conventional	6.2	519	5.72	96.5%	3.4	0.010	0.167
2A Conventional	6.2	220	1.96	89.8%	40.0	0.048	0.771
3A Long Breathing	6.1	94	0.74	73.1%	298.2	0.124	1.997
4A Long Breathing	6.1	54	0.39	48.9%	1835.2	0.293	4.728

Table 6-6: Supplemental LNT Fuel Consumption for Low Load Diesel Conditions

Strategy	NO _x [ppmV]	Supplemental Fuel Mass [g]	Storage Duration [s]	Regeneration Duration [s]	Regeneration Frequency [# per hour]	Supplemental Fuel Rate [g/s]
1A Conventional	519	0.159	3.4	1.0	818.2	0.036
2A Conventional	220	0.581	40.0	5.0	80.0	0.013
3A Long Breathing	94	1.067	298.2	10.0	11.7	0.003
4A Long Breathing	54	2.605	1835.2	30.0	1.9	0.001

Table 6-7: Supplemental Fuel Penalty for Low Load Diesel Conditions

Strategy	NO _x [ppmV]	Supplemental Fuel Rate [g/s]	Engine Fuel [g/s]	Combined Fuel [g/s]	Engine ISFC [g/kW·hr]	Combined ISFC [g/kW·hr]	Fuel Penalty [%]
1A Conventional	519	0.036	0.767	0.803	179.4	187.8	4.67
2A Conventional	220	0.013	0.773	0.786	180.3	183.3	1.67
3A Long Breathing	94	0.003	0.772	0.775	181.9	182.6	0.38
4A Long Breathing	54	0.001	0.763	0.764	181.1	181.5	0.25

The total mass of supplemental fuel was calculated based on the addition of the stoichiometric amount of fuel required to provide an excess air ratio (λ) of 0.9 and the stoichiometric amount of fuel required to reduce the stored NO_x mass shown in Table 6-5. Propylene, with a carbon to hydrogen ratio of 1 to 2 (similar to diesel fuel), was assumed as a representative hydrocarbon for NO_x reduction. The calculated amount of fuel was further multiplied by a factor of 1.5 since the amount of fuel used in practice was expected to exceed the stoichiometric amount.

The supplemental fuel consumption results are tabulated in Table 6-6. The charts showed that the long breathing strategy needed a larger mass of fuel per regeneration cycle as a result of the higher NO_x mass stored per storage cycle. However, the supplemental fuel consumption rate was also a function of the regeneration frequency as shown in Equations 6-20 and 6-21. The regeneration duration was estimated according to the values given in Table 6-8.

Table 6-8: Regeneration Duration as a Function of Storage Duration

Storage Duration [s]	Regeneration Duration [s]
<1	0.5
1-5	1.0
5-20	3.0
20-60	5.0
60-300	10.0
300-600	20.0
>600	30.0

$$\text{Regeneration Frequency} = \frac{3600 \text{ [s/hr]}}{\text{Storage Duration [s]} + \text{Regeneration Duration [s]}} \quad 6-20$$

$$\text{Supplmnt. Fuel Rate [g/s]} = \frac{\text{Supplmnt. Fuel Mass [g]}}{\text{Storage Duration [s]} + \text{Regen. Duration [s]}} \quad 6-21$$

The calculated values for the regeneration frequency and supplemental fuel flow rate are shown in Table 6-6. The results indicated that the long breathing strategies had a substantially lower supplemental fuel consumption rate than the conventional strategies. The long breathing conditions required a supplemental fuel flow rate of 1.4 to 3.4 mg/s while the conventional conditions required a rate of 12.9 to 36.1 mg/s. The reduced supplemental fuel rate for the long breathing strategies was a result of the infrequent LNT regeneration cycles.

Further calculations were required to determine the combined fuel consumption of the engine and the LNT. The results for the combined fuel consumption and for the supplemental fuel penalty are provided in Table 6-7 and Figure 6-9. The use of conventional LNT strategies led to a supplemental fuel penalty of 1.7 to 4.7% that was caused by the relatively frequent requirement for fuel-rich regeneration. The use of EGR resulted in significantly reduced engine-out NO_x emissions and markedly reduced the supplemental fuel consumption penalty of the long breathing strategies to the range of 0.25 to 0.38%. The results indicated that, although the ISFC of the engine was slightly lower for the conventional strategies, the long breathing strategies had a significant reduction in the combined fuel consumption. These findings confirmed the supplemental energy savings of the long breathing LNT for low load diesel conditions.

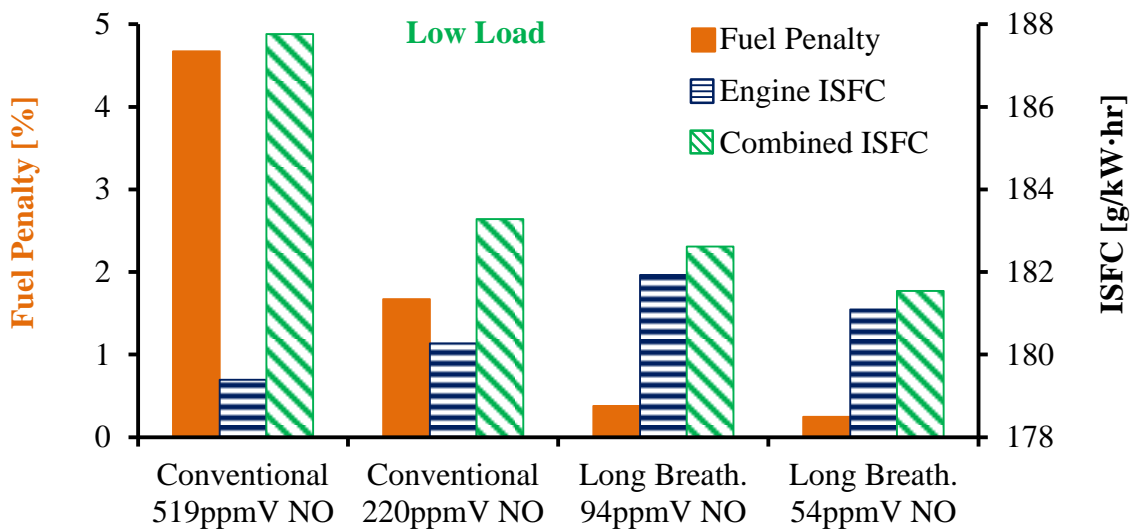


Figure 6-9: Long Breathing Energy Savings for Low Load Diesel Conditions

The results for medium load conditions at 10 bar IMEP are shown in Figure 6-10 and Table 6-9 to Table 6-11. The same calculation procedure was followed as for the low load conditions. The calculations indicated that the same trends were generally observed at mid load conditions. The indicated engine-out NO_x emissions were relatively high for the conventional strategies. Thus, relatively high NO_x conversion efficiencies and relatively short NO_x storage durations were required as shown in Figure 6-10 and Table 6-9. The data in Table 6-10 established that the extended NO_x storage duration of the long breathing strategies occasioned less frequent fuel-rich regenerations and reduced the supplemental fuel flow rate.

The combined ISFC of the engine and the supplemental fuel for the LNT regeneration is shown in Table 6-11 and Figure 6-11. The calculations verified that the long breathing LNT strategy reduced the overall fuel consumption and the fuel penalty. The use of conventional LNT strategies resulted in a lower ISFC from the engine but the frequent requirement for fuel-rich regenerations led to a 1.1 to 6.3% fuel consumption penalty. The fuel penalty for the long breathing conditions was substantially lower, in the range of 0.23 to 0.31%, and led to a reduced combined ISFC for the long breathing strategies as illustrated in Figure 6-11. These results highlighted the benefits of the long breathing LNT strategy at medium load conditions.

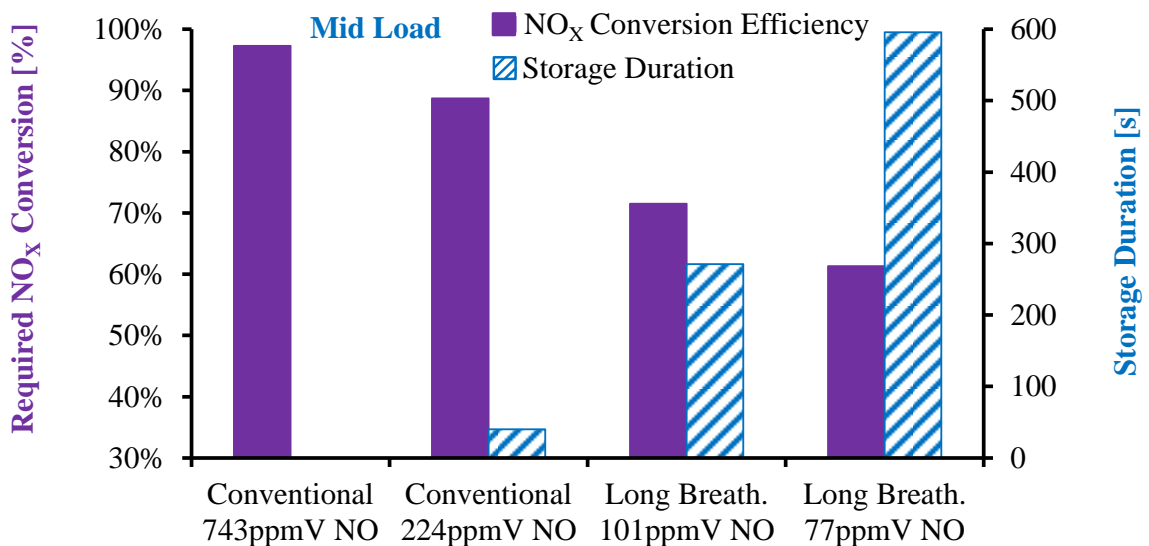


Figure 6-10: Storage Duration & Required NO_x Conversion Efficiency at Mid Load

Table 6-9: Stored NO_x Mass for Mid Load Diesel Conditions

Strategy	IMEP [bar]	NO _x [ppmV]	NO _x [g/kW·hr]	Required NO _x Conversion Efficiency [%]	Storage Duration [s]	Stored NO _x Model [g]	Stored NO _x Engine [g]
5B Conventional	10.2	743	7.37	97.3%	0.6	0.003	0.043
6B Conventional	10.3	224	1.77	88.7%	40.2	0.048	0.780
7B Long Breathing	10.3	101	0.70	71.5%	271.4	0.118	1.911
8B Long Breathing	10.3	77	0.52	61.3%	596.0	0.170	2.742

Table 6-10: Supplemental LNT Fuel Consumption for Mid Load Diesel Conditions

Strategy	NO _x [ppmV]	Supplemental Fuel Mass [g]	Storage Duration [s]	Regeneration Duration [s]	Regeneration Frequency [# per hour]	Supplemental Fuel Rate [g/s]
5B Conventional	743	0.095	0.6	0.5	3272.7	0.086
6B Conventional	224	0.733	40.2	5.0	79.7	0.016
7B Long Breathing	101	1.247	271.4	10.0	12.8	0.004
8B Long Breathing	77	2.041	596.0	20.0	5.8	0.003

Table 6-11: Supplemental Fuel Penalty for Mid Load Diesel Conditions

Strategy	NO _x [ppmV]	Supplemental Fuel Rate [g/s]	Engine Fuel [g/s]	Combined Fuel [g/s]	Engine ISFC [g/kW·hr]	Combined ISFC [g/kW·hr]	Fuel Penalty [%]
5B Conventional	743	0.086	1.372	1.458	194.4	206.6	6.29
6B Conventional	224	0.016	1.424	1.440	200.0	202.3	1.14
7B Long Breathing	101	0.004	1.430	1.434	201.1	201.7	0.31
8B Long Breathing	77	0.003	1.428	1.431	200.2	200.7	0.23

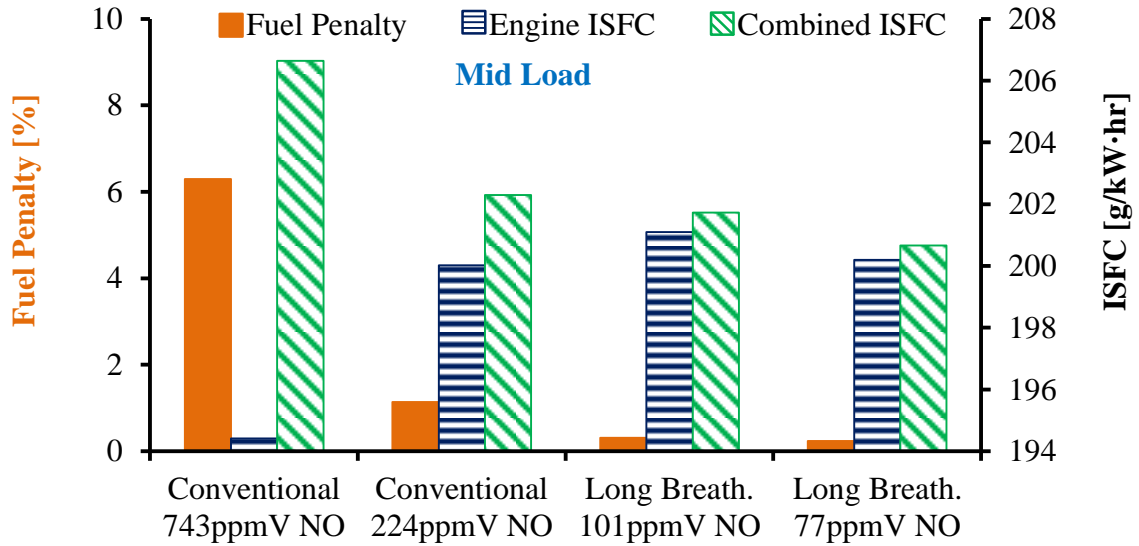


Figure 6-11: Long Breathing Energy Savings for Mid Load Diesel Conditions

The results for high load conditions, at 14 bar IMEP, are given in Table 6-12 to Table 6-14. The results were mostly consistent with the data for low and mid load conditions. The data in Table 6-12 and Figure 6-12 signified that higher engine-out NO_x required higher NO_x conversion efficiencies with shorter NO_x storage durations for conventional LNT strategies. Lower engine-out NO_x led to longer NO_x storage durations and lower supplemental fuel flow rates for the long breathing strategies.

However, there were a few key differences at high load conditions. The data in Table 6-14 and Figure 6-13 showed that the fuel consumption penalty was 0.4 to 5.8% for conventional LNT operation and 0.23 to 0.33% for long breathing LNT operation. Consequently, the supplemental energy savings of the LNT were not enough to offset the increased fuel consumption from the engine as illustrated in Figure 6-13. The combined ISFC for the conventional LNT strategies was calculated to be in the range of 198.3 to 206.4 g/kW·hr while the combined ISFC for the long breathing strategies was in the range of 197.5 to 201.0 g/kW·hr. The considerable overlap between the ISFC values for conventional and for long breathing operation implied that the effectiveness of the long breathing LNT strategy was reduced at high load conditions. The data in Table 6-14 suggested that the lowest combined ISFC occurred for a NO_x range of 113 to 219 ppmV.

Table 6-12: Stored NO_x Mass for High Load Diesel Conditions

Strategy	IMEP [bar]	NO _x [ppmV]	NO _x [g/kW·hr]	Required NO _x Conversion Efficiency [%]	Storage Duration [s]	Stored NO _x Model [g]	Stored NO _x Engine [g]
9C Conventional	14.5	829	7.92	97.5%	0.6	0.003	0.047
10C Conventional	14.9	219	1.61	87.6%	39.4	0.046	0.740
11C Long Breathing	14.8	113	0.76	73.7%	193.2	0.097	1.572
12C Long Breathing	14.6	72	0.47	57.8%	683.6	0.172	2.772

Table 6-13: Supplemental LNT Fuel Consumption for High Load Diesel Conditions

Strategy	NO _x [ppmV]	Supplemental Fuel Mass [g]	Storage Duration [s]	Regeneration Duration [s]	Regeneration Frequency [# per hour]	Supplemental Fuel Rate [g/s]
9C Conventional	829	0.122	0.6	0.5	3272.7	0.111
10C Conventional	219	0.373	39.4	5.0	81.1	0.008
11C Long Breathing	113	1.368	193.2	10.0	17.7	0.007
12C Long Breathing	72	3.348	683.6	30.0	5.0	0.005

Table 6-14: Supplemental Fuel Penalty for High Load Diesel Conditions

Strategy	NO _x [ppmV]	Supplemental Fuel Rate [g/s]	Engine Fuel [g/s]	Combined Fuel [g/s]	Engine ISFC [g/kW·hr]	Combined ISFC [g/kW·hr]	Fuel Penalty [%]
9C Conventional	829	0.111	1.924	2.035	195.1	206.4	5.76
10C Conventional	219	0.008	2.038	2.046	197.5	198.3	0.41
11C Long Breathing	113	0.007	2.017	2.024	196.8	197.5	0.33
12C Long Breathing	72	0.005	2.029	2.034	200.5	201.0	0.23

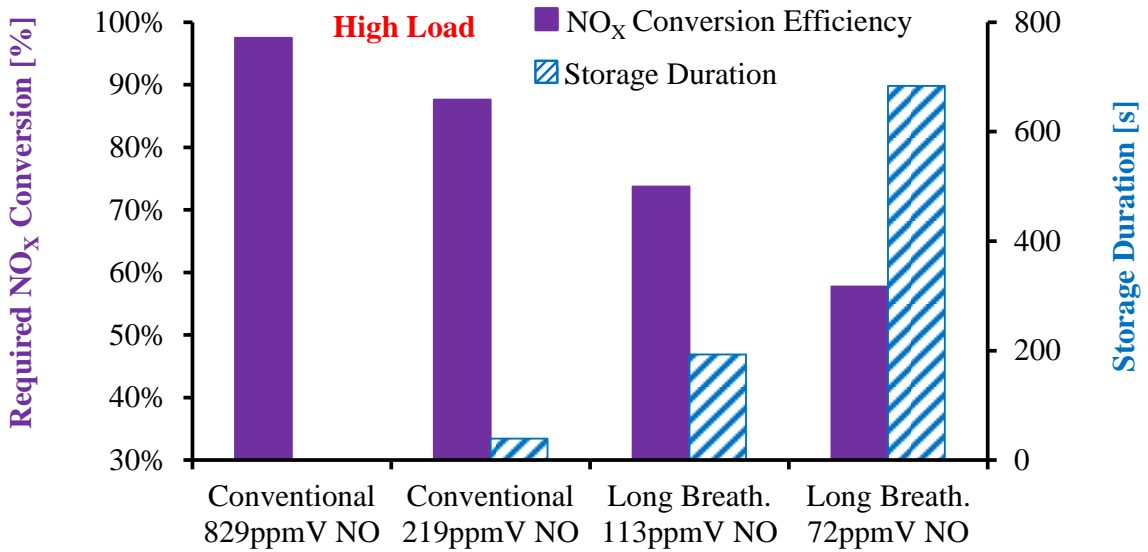


Figure 6-12: Storage Duration & Required NO_x Conversion Efficiency at High Load

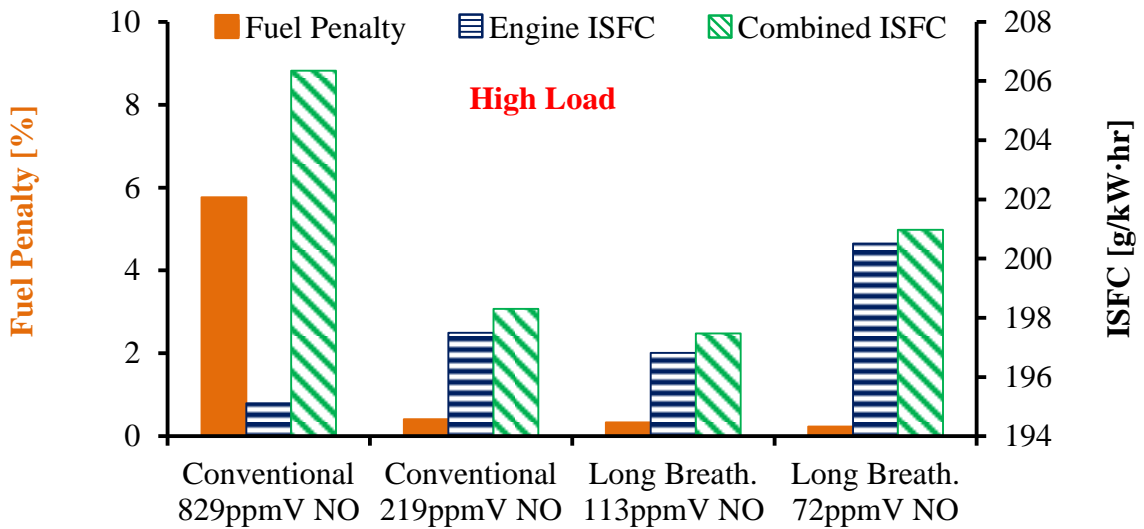


Figure 6-13: Long Breathing Energy Savings for High Load Diesel Conditions

To summarize, engine tests were conducted with diesel fuel and EGR and the engine exhaust data was combined with a numerical model of an LNT after-treatment

system to quantify the effects of the long breathing strategy on the supplemental fuel penalty and the combined fuel consumption of the engine and the LNT. The results indicated that the long breathing strategy significantly prolonged the NO_x storage duration and reduced the fuel-rich regeneration frequency, which led to supplemental fuel savings at all tested conditions. The use of the long breathing strategy also decreased the combined fuel consumption of the engine and the LNT at low and medium loads, 6 to 10 bar IMEP. However, the long breathing technique increased the combined fuel consumption of the LNT and the engine at high load conditions of 14 bar IMEP. Furthermore, the engine tests indicated that the long breathing strategy led to a smoke emission penalty at high load conditions. Therefore, the long breathing strategy was mostly recommended for low and medium loads while further tests were required to justify its use at high loads.

6.4 Quantification of Energy Savings for Long Breathing with Neat Butanol

The long breathing strategy with the use of diesel fuel and EGR resulted in smoke emission penalties at all conditions, but most prominently at high load. Therefore, the use of long breathing with neat butanol fuel was investigated to mitigate the smoke emission penalties. The low, medium, and high load exhaust gas conditions from the engine tests¹⁸ are summarized in Table 6-15. The engine test data was combined with a 1D numerical LNT model. The chemical reaction equations and the simulation parameters, such as the gas hourly space velocity and the time step, were consistent with the values utilized for the long breathing LNT simulations with diesel fuel and EGR.

The results for the LNT performance at low load neat n-butanol exhaust gas conditions are given in Figure 6-14, Figure 6-15, and Table 6-16 to Table 6-18. All of the low load conditions were favourable for the use of a long breathing LNT strategy. The engine-out NO_x levels were consistently below 32 ppmV even without the use of EGR. The low engine-out NO_x led to fairly low required NO_x conversion efficiencies and relatively long NO_x storage cycles as shown in Figure 6-14 and Table 6-16.

¹⁸ The neat butanol engine tests were previously shown in Chapter 5.

Table 6-15: Exhaust Conditions for Neat Butanol Combustion

Test #	Type	IMEP	Intake O ₂	Exhaust						
				CO	THC	NO _x	Smoke	O ₂	CO ₂	Temp
		bar	% V	ppmV	ppmV	ppmV	FSN	% V	% V	°C
13D	Butanol Single Shot	6.2	20.5	2471	169	16	0.0	15.6	3.4	208
14D	Butanol Single Post	6.2	20.5	5020	309	32	0.0	15.4	3.3	234
15D	Butanol Double Post	6.0	20.6	4356	1045	22	0.0	14.5	4.0	294
16E	Butanol Single Post	10.0	20.4	1161	107	186	0.1	12.3	5.8	347
17E	Butanol Double Post	10.0	20.6	1583	151	56	0.3	11.2	6.6	415
18E	Butanol Double Post Tuned	10.0	20.2	1564	117	57	0.2	11.5	6.4	386
19F	Butanol Double Post High Load	14.0	20.4	427	97	213	0.7	7.6	10.1	529

Table 6-16: Stored NO_x Mass for Low Load Butanol

Strategy	IMEP bar	NO _x [ppmV]	NO _x [g/kW·hr]	Required NO _x Conversion Efficiency [%]	Storage Duration [s]	Stored NO _x Model [g]	Stored NO _x Engine [g]
13D Single Shot	6.2	16	0.31	36.2%	17151.0	0.604	9.746
14D Single Post	6.2	32	0.66	69.9%	1104.8	0.150	2.427
15D Double Post	6.0	22	0.45	55.4%	2390.6	0.177	2.853

Table 6-17: Supplemental LNT Fuel Consumption for Low Load Butanol

Strategy	NO _x [ppmV]	Supplemental Fuel Mass [g]	Storage Duration [s]	Regeneration Duration [s]	Regeneration Frequency [# per hour]	Supplemental Fuel Rate [g/s]
13D Single Shot	16	10.978	17151.0	30.0	0.2	0.0006
14D Single Post	32	8.967	1104.8	30.0	3.2	0.0079
15D Double Post	22	8.767	2390.6	30.0	1.5	0.0036

Table 6-18: Supplemental Fuel Penalty for Low Load Butanol

Strategy	NO _x [ppmV]	Supplemental Fuel Rate [g/s]	Engine Fuel [g/s]	Combined Fuel [g/s]	Engine ISFC [g/kW·hr]	Combined ISFC [g/kW·hr]	Fuel Penalty [%]
13D Single Shot	16	0.0006	1.138	1.139	262.0	262.1	0.06
14D Single Post	32	0.0079	1.295	1.303	303.3	305.2	0.61
15D Double Post	22	0.0036	1.495	1.498	341.3	342.1	0.24

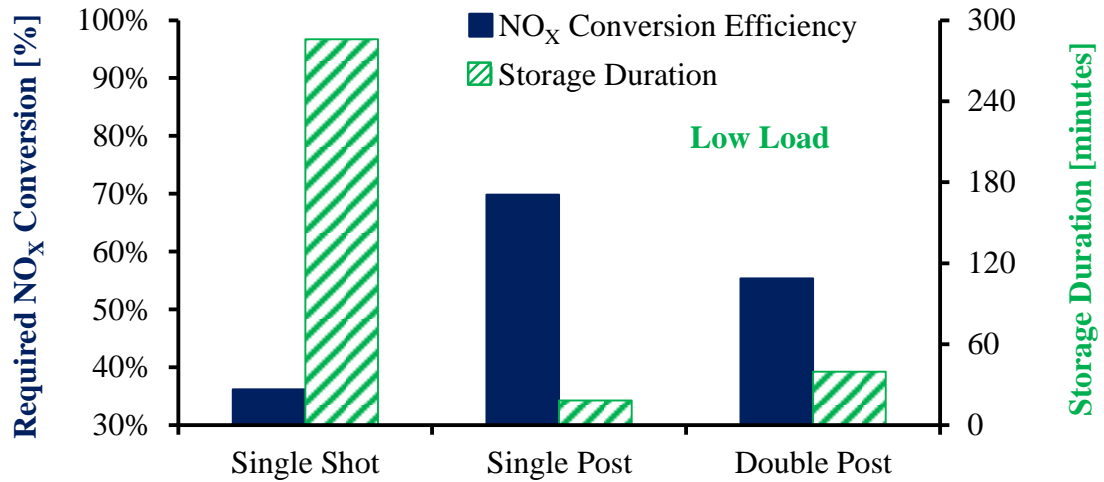
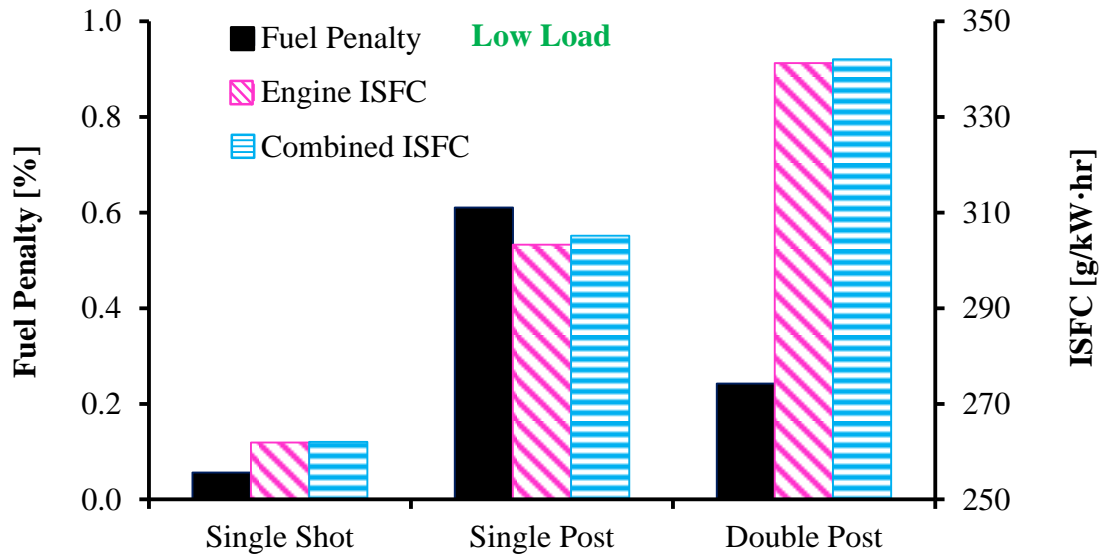
Figure 6-14: NO_x Storage Duration for Low Load Butanol

Figure 6-15: LNT Fuel Consumption Penalty for Low Load Butanol

The single shot strategy resulted in the longest NO_x storage duration, over four hours long, but the single post and double post injection strategies also had relatively long NO_x storage durations, in the range of 18 to 39 minutes. The extended duration of the NO_x storage cycle resulted in a substantial amount of NO_x stored within the LNT, 2.8 to 9.8 grams, as indicated in Table 6-16. As a result, the calculations in Table 6-17

signified that more fuel was required to convert the stored NO_x compared to diesel tests shown in the previous section.

Nonetheless, the required supplemental fuel rate was ultra-low because of the long storage cycle and the infrequent need for LNT regeneration. The extended NO_x storage duration resulted in a supplemental fuel penalty below 0.61% for all of the investigated low load conditions and the effect of the supplemental fuel on the combined ISFC was almost negligible as supported by the data in Table 6-18 and Figure 6-15. This data confirmed that neat n-butanol combustion at low load conditions was particularly suitable for a long breathing LNT strategy. Although the supplemental fuel penalty was ultra-low for all three low load conditions, the single shot strategy was the most desirable since it resulted in a significantly lower combined ISFC.

The results for medium and high load operation with neat n-butanol are given in Figure 6-16, Figure 6-17, and Table 6-19 to Table 6-21. At mid load conditions, the engine test results demonstrated that the single post injection strategy generated increased engine-out NO_x emissions that required a fairly high NO_x conversion efficiency and a relatively short NO_x storage duration. The use of a double post injection strategy was able to reduce the engine-out NO_x emissions to a level suitable for long breathing operation and led to an extended NO_x storage cycle as illustrated in Figure 6-16. The data in Table 6-20 demonstrated that the relatively long NO_x storage cycle for the double post strategies led to a less frequent requirement for fuel-rich regeneration and a reduced supplemental fuel consumption rate. As a result, the fuel consumption penalty for the double post injection strategies was 0.48 to 0.56% compared to 1.97% for the single post injection strategy as shown in Table 6-21.

However, the data in Table 6-21 and Figure 6-17 indicated that the ISFC from the engine was significantly lower for the single post injection strategy. The supplemental fuel consumption savings of the long breathing LNT with the double post injection strategies were not enough to overcome the increased fuel consumption from the engine. Thus, these results suggested that the single shot post injection strategy with a conventionally short NO_x storage duration was preferred for neat n-butanol combustion at mid load conditions.

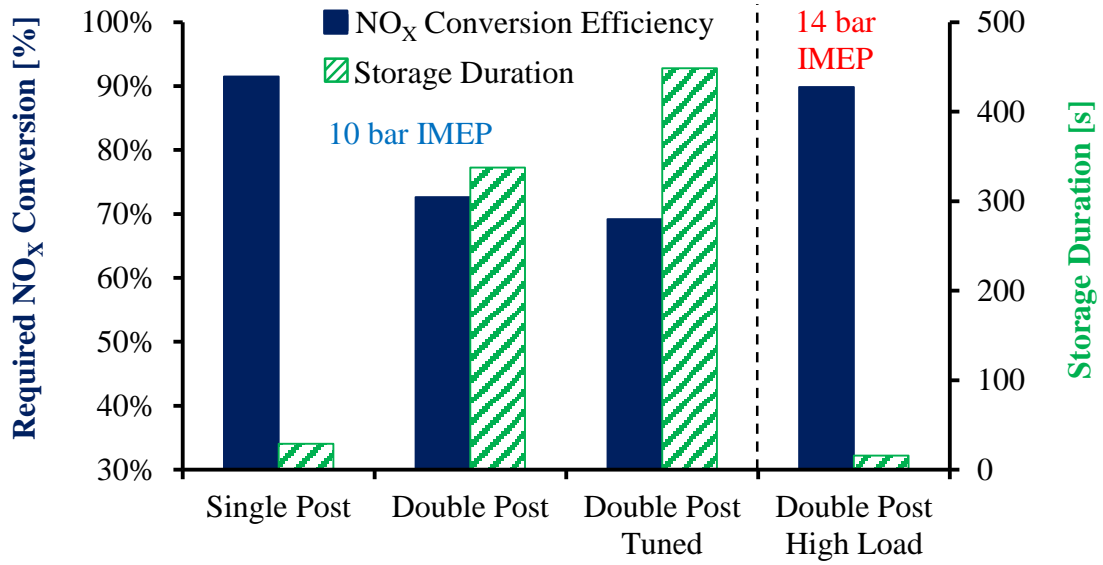


Figure 6-16: NO_x Storage Duration for Mid and High Load Butanol

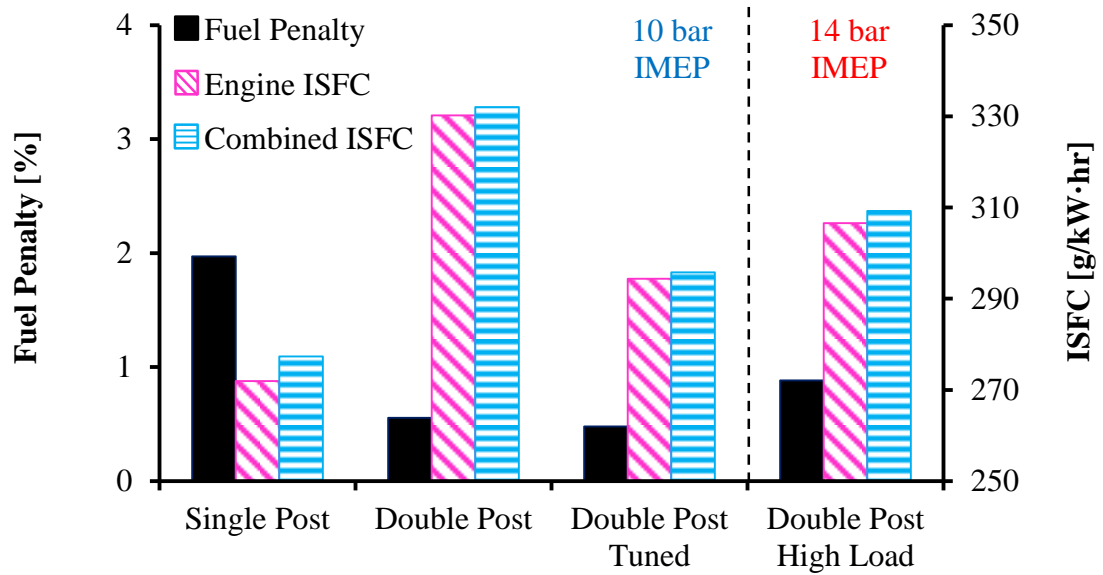


Figure 6-17: LNT Fuel Consumption Penalty for Mid and High Load Butanol

Table 6-19: Stored NO_x Mass for Mid & High Load Butanol

Strategy	IMEP [bar]	NO _x [ppmV]	NO _x [g/kW·hr]	Required NO _x Conversion Efficiency [%]	Storage Duration [s]	Stored NO _x Model [g]	Stored NO _x Engine [g]
16E Single Post	10.0	186	2.35	91.5%	29.2	0.030	0.487
17E Double Post	10.0	56	0.73	72.6%	337.4	0.083	1.344
18E Double Post Tuned	10.0	57	0.65	69.2%	448.2	0.107	1.730
19F Double Post	14.0	213	1.97	89.8%	16.0	0.019	0.300

Table 6-20: Supplemental LNT Fuel Consumption for Mid & High Load Butanol

Strategy	IMEP [bar]	NO _x [ppmV]	Supplemental Fuel Mass [g]	Storage Duration [s]	Regeneration Duration [s]	Regeneration Frequency [# per hour]	Supplemental Fuel Rate [g/s]
16E Single Post	10.0	186	1.264	29.2	5.0	105.3	0.0370
17E Double Post	10.0	56	4.515	337.4	20.0	10.1	0.0126
18E Double Post Tuned	10.0	57	4.605	448.2	20.0	7.7	0.0098
19F Double Post	14.0	213	0.491	16.0	3.0	189.5	0.0258

Table 6-21: Supplemental Fuel Penalty for Mid & High Load Butanol

Strategy	IMEP [bar]	NO _x [ppmV]	Supplemental Fuel Rate [g/s]	Engine Fuel [g/s]	Combined Fuel [g/s]	Engine ISFC [g/kW·hr]	Combined ISFC [g/kW·hr]	Fuel Penalty [%]
16E Single Post	10.0	186	0.0370	1.8754	1.9124	272.0	277.3	1.97
17E Double Post	10.0	56	0.0126	2.2750	2.2877	330.2	332.1	0.56
18E Double Post Tuned	10.0	57	0.0098	2.0504	2.0602	294.4	295.8	0.48
19F Double Post	14.0	213	0.0258	2.9279	2.9537	306.6	309.3	0.88

High load operation at 14 bar IMEP for neat n-butanol was only achieved with the double post injection strategy. Long breathing LNT operation at high load conditions for neat n-butanol was not achieved because the engine-out NO_x level of 213 ppmV was outside the range of a long breathing LNT. The fairly high amount of engine-out NO_x required a relatively high NO_x conversion efficiency and a relatively short NO_x storage cycle as shown in Figure 6-16. Further tests are required to demonstrate long breathing with neat n-butanol at high load. Thus, the analysis indicated that long breathing with neat butanol reduced the combined fuel consumption of the engine and the LNT only at low load conditions.

6.5 Chapter Summary for Supplemental Fuel Savings with Long Breathing

The results of this chapter focused on quantifying the supplemental energy savings of the long breathing LNT strategy. The long breathing strategy was conducted with diesel fuel and EGR and with neat butanol fuel. Engine test data from previous chapters was combined with a numerical LNT model to analyze the supplemental fuel consumption of the LNT and the overall fuel consumption of the engine and the LNT. The investigation was conducted at engine loads of 6, 10, and 14 bar IMEP.

A summary of the results for the diesel fuel investigations is presented in Table 6-22. The results showed that long breathing LNT operation reduced the supplemental fuel penalty and the combined fuel consumption of the engine and the LNT at low and medium load conditions. The use of the long breathing strategy did not provide fuel economy benefits at high load conditions and resulted in significantly increased smoke emissions, over 3 FSN. Thus, the use of the long breathing strategy did not appear to be suitable at high load operation under the tested conditions and hardware limitations.

The long breathing LNT results with neat n-butanol are tabulated in Table 6-23. The results established that long breathing was particularly suitable for low load operation with neat butanol fuel. The use of long breathing resulted in ultra-low supplemental fuel penalties, as low as 0.06%, with ultra-low smoke emissions, less than 0.04 FSN. However, long breathing with neat butanol at medium load conditions was not

justified since the use of a conventional LNT resulted in an overall lower combined fuel consumption for the engine and the LNT. At high load conditions, the engine-out NO_x emissions were out of range for long breathing. Therefore, long breathing with neat butanol fuel was restricted to low load operation for the tested conditions.

The engine tests were conducted at steady state conditions and at three different load levels, ranging from 6 to 15 bar IMEP. Future work is recommended to conduct engine tests at more load levels and under transient operation to determine the effect of the long breathing strategy under conditions representative of real world driving. Furthermore, to avoid the uncertainty of the numerical LNT model results, future work is proposed to integrate an LNT into the engine exhaust system to get empirical data for the long breathing LNT directly from the engine tests.

Table 6-22: Long Breathing Results for Combustion with Diesel Fuel and EGR

Test Strategy	IMEP [bar]	CO [ppmV]	THC [ppmV]	Smoke [FSN]	NO _x [g/kW·hr]	NO _x Conversion [%]	Storage Duration [s]	Regen. Frequency [per hour]	Combined Fuel [g/kW·hr]	Fuel Penalty [%]
1A Conventional	6.2	162	15	0.213	5.72	96.5%	3.4	818.2	187.8	4.67
2A Conventional	6.2	322	29	0.317	1.96	89.8%	40.0	80.0	183.3	1.67
3A Long Breath.	6.1	611	58	0.698	0.74	73.1%	298.2	11.7	182.6	0.38
4A Long Breath.	6.1	1147	96	1.342	0.39	48.9%	1835.2	1.9	181.5	0.25
5B Conventional	10.2	58	9	0.249	7.37	97.3%	0.6	3272.7	206.6	6.29
6B Conventional	10.3	171	8	0.953	1.77	88.7%	40.2	79.6	202.3	1.14
7B Long Breath.	10.3	359	16	1.884	0.70	71.5%	271.4	12.8	201.7	0.31
8B Long Breath.	10.3	443	21	2.174	0.52	61.3%	596.0	5.8	200.7	0.23
9C Conventional	14.5	32	6	0.336	7.92	97.5%	0.6	3272.7	206.4	5.76
10C Conventional	14.9	121	3	0.718	1.61	87.6%	39.4	81.1	198.3	0.41
11C Long Breath.	14.8	284	6	1.740	0.76	73.7%	193.2	17.7	197.5	0.33
12C Long Breath.	14.6	607	9	3.050	0.47	57.8%	683.6	5.0	201.0	0.23

Table 6-23: Summary of Long Breathing Results for Neat n-Butanol Combustion

Test Strategy	IMEP [bar]	CO [ppmV]	THC [ppmV]	Smoke [FSN]	NO _x [g/kW·hr]	NO _x Conversion [%]	Storage Duration [s]	Regen. Frequency [per hour]	Combined Fuel [g/kW·hr]	Fuel Penalty [%]
13D Single Shot	6.2	2471	169	0.020	0.31	36.2%	17151.0	0.2	262.1	0.06
14D Single Post	6.2	5020	309	0.009	0.66	69.9%	1104.8	3.2	305.2	0.61
15D Double Post	6.3	4356	1045	0.032	0.45	55.4%	2390.6	1.5	342.1	0.24
16E Single Post	10.0	1161	107	0.085	2.35	91.5%	29.2	105.3	277.3	1.97
18E Double Post	10.0	1564	117	0.190	0.65	69.2%	448.2	7.7	295.8	0.48
19F Double Post	14.0	427	97	0.745	1.97	89.8%	16.0	189.5	309.3	0.88

CHAPTER 7: ACTIVE CONTROL OF THE EXHAUST GAS TEMPERATURE AND COMPOSITION TO AID LNT PERFORMANCE

This chapter presents the development of post injection strategies for exhaust gas management. The desirable exhaust gas conditions for the LNT storage and regeneration cycles are described. Data is shown to demonstrate the effects of the post injection quantity, the post injection timing, the engine load, the combustion phasing, the intake oxygen, and low temperature combustion on the exhaust gas temperature and composition. Suitable strategies for the control of the exhaust gas temperature and composition are demonstrated.

7.1 The Purpose of Exhaust Gas Management

The previous chapter solely focused on the challenges related to extending the NO_x storage process. The NO_x storage process usually requires catalyst temperatures in the range of 250 to 500°C for higher storage efficiency [78,83]. The LNT regeneration process is also crucial for improved performance of the LNT. As described in the literature review section, the LNT regeneration process requires fuel-rich exhaust conditions. Under fuel-rich conditions, the stored nitrates are released from the LNT and are reduced to nitrogen. Although there may be variations which depend on the catalyst formulation, the NO_x conversion efficiency is generally higher when the catalyst temperatures are in the range of 250 to 450°C [77,83,125].

There is also a periodic and less frequent need for a fuel-rich desulfation process to purge any stored sulfates. The desulfation process normally takes place at higher temperatures, typically exceeding 500°C [90]. As a result, for improved performance, the LNT catalyst needs to be within a certain temperature range for the NO_x storage, regeneration, and desulfation cycles. However, lean-burn compression ignition engines can have a wide range of exhaust gas temperatures which may not be suitable for the LNT. Thus, there is a need to actively maintain the exhaust gas temperature within a suitable window for the LNT storage, regeneration, and desulfation processes.

Consequently, studies were carried out to develop in-cylinder post injection strategies for active management of the exhaust gas temperature.

Typical fuel-lean exhaust is suitable for the LNT storage cycle but the LNT periodically requires fuel-rich exhaust gas conditions for the regeneration and desulfation processes. Thus, there is a periodic need for supplemental fuel to be dosed into the exhaust. The supplemental fuel is generally provided by in-cylinder post injection or by the direct injection of fuel into the exhaust stream [80,126]. The supplemental fuel is typically a hydrocarbon fuel since it is readily available on-board a vehicle. Direct injection of fuel into the exhaust has several disadvantages, including the need for additional hardware, such as exhaust injectors and fuel lines. The direct injection of fuel into the exhaust represents a fuel consumption penalty since it cannot contribute to engine power. Therefore, studies were conducted to develop post injection strategies for increased production of desirable NO_x reducing agents.

In addition to a hydrocarbon fuel, species like light hydrocarbons, carbon monoxide, and hydrogen can be utilized as efficient NO_x reducing agents. For this reason, the post injection studies included the use of Fourier transform infrared spectroscopy analysis to quantify the presence of light hydrocarbon species in the exhaust. Reactive light hydrocarbons, such as propylene and ethylene, were preferred as reducing agents, as opposed to methane which has a relatively low reactivity. As described in the literature review, the presence of hydrogen can enhance the LNT performance during the regeneration and desulfation processes. As a result, a hydrogen mass spectrometer was used to measure the quantity of hydrogen in the exhaust. The effects of carbon monoxide on LNT regeneration have also been reported in literature and the studies demonstrated that a carbon monoxide reducing agent performed similar to hydrogen at a catalyst temperature of 300°C [127].

Therefore, a primary purpose of this investigation was to develop post injection strategies for the in-cylinder production of hydrogen, carbon monoxide, and reactive light hydrocarbon species. In particular, the effects of the post injection quantity, the post injection timing, the engine load, the combustion phasing, the intake oxygen, and low temperature combustion were investigated. An understanding of the effects of these

parameters on the exhaust gas temperature and on the formation of hydrogen, carbon monoxide, and light hydrocarbons could be valuable for the development of effective and energy efficient LNT after-treatment.

7.2 Effects of Post Injection Duration and Timing on Exhaust Temperature and Composition

Engine tests were carried out to investigate the ability of a post injection to control the exhaust gas conditions through control of the post injection timing and quantity. The tests were carried out at two different baseline loads: 5.8 bar IMEP and 9.9 bar IMEP. These loads refer to the IMEP generated by the main injection only. The main injection in each case was a single shot injection close to compression TDC as shown in Figure 7-1. The main injection timing and duration were constant throughout the tests to provide stable and repeatable background conditions for the post injection duration sweep. As a result, the changes to the exhaust gas conditions were attributed solely to the effects of the post injection.

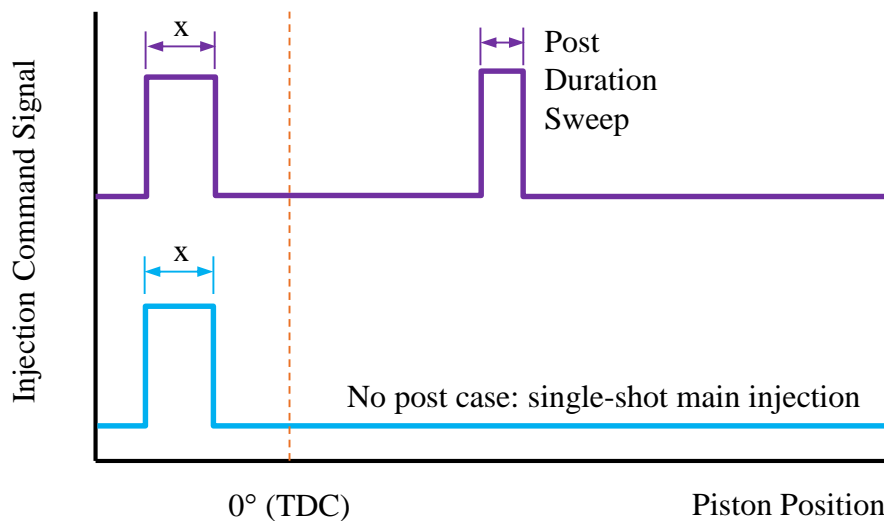


Figure 7-1: Comparison between Baseline Single Shot Injection and Post Injection

The test conditions for the post injection tests are shown in Table 7-1. The main injection timing and duration were kept constant and a post injection duration and timing sweep was carried out according to the ranges shown in the table. All of the tests were conducted with ultra-low sulfur diesel fuel whose properties were previously given in Table 2-2. The fuel injection pressure and the air intake pressure were fixed throughout the tests. EGR was used to reduce the intake oxygen to 16.5% and to reduce the engine-out NO_x emissions.

Table 7-1: Diesel Post Injection Duration Test Matrix

IMEP [bar]	5.8	9.9
Engine Speed [rpm]	1500	1500
Air Intake Pressure [bar absolute]	1.3	1.9
Intake Oxygen [% V]	16.5	16.5
Test Fuel	Diesel	Diesel
Fuel Injection Pressure [bar]	900	1200
Main Injection Duration [μ s]	490	590
Main Injection Timing [$^{\circ}$ CA ATDC]	-7.6	-7.0
Post Injection Duration [μ s]	200 to 400	200 to 400
Post Injection Timing [$^{\circ}$ CA ATDC]	30 to 100	30 to 100

The effect of the post injection timing on the heat release rate is illustrated in Figure 7-2 for the 9.9 bar IMEP condition. The curves showed that early post injections produced a large heat release and that the heat release gradually declined as the post injection timing was retarded so that a distinct heat release was not observed for post injections later than 50 $^{\circ}$ CA ATDC. The effect of the post injection duration, at a fixed post injection timing of 30 $^{\circ}$ CA ATDC, on the heat release is shown in Figure 7-3. The heat release curves demonstrated that larger post injections produced a higher heat release peak. On the contrary, the data in Figure 7-4 showed that a heat release peak was not observed for late post injections at 100 $^{\circ}$ CA ATDC regardless of its duration. Consequently, the results in Figure 7-5 revealed that there was a significant increase in the exhaust gas temperature when the post injection timing was between 30 and 50 $^{\circ}$ CA

ATDC and that the exhaust temperature was mostly unaffected by the use of late post injections at 70 to 100°CA ATDC.

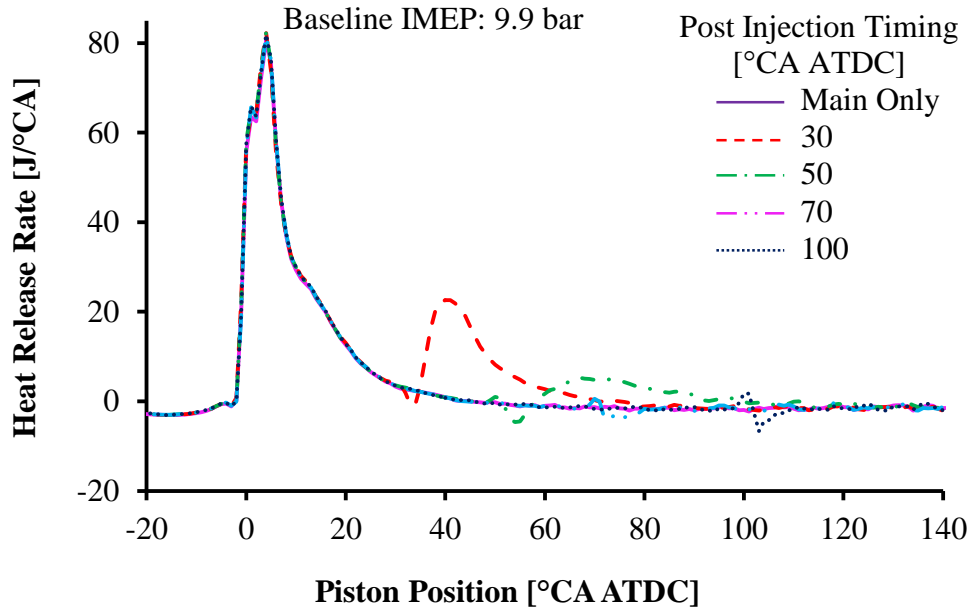


Figure 7-2: Effect of Post Injection Timing on Heat Release Rate

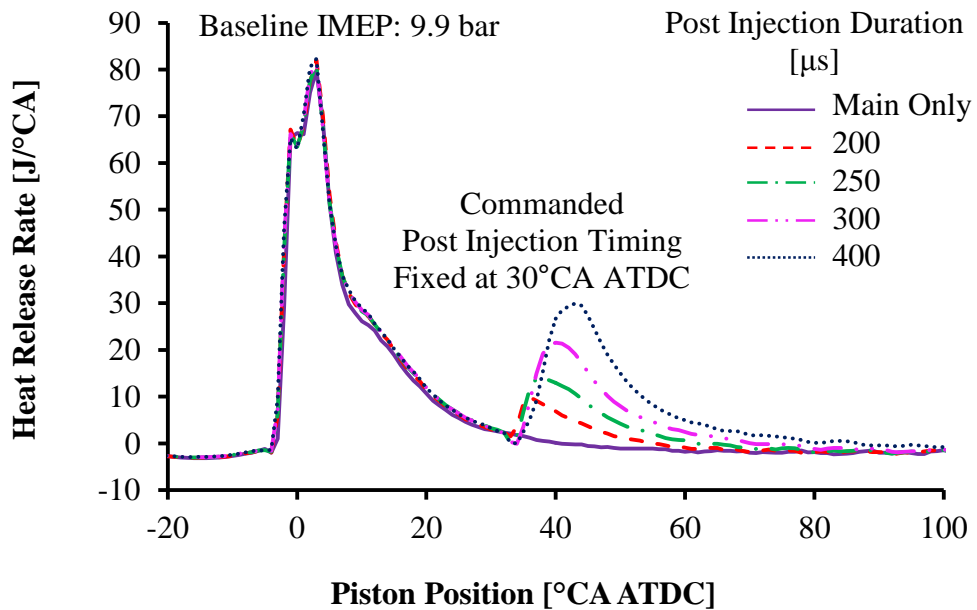


Figure 7-3: Effect of Post Injection Duration at 30°CA ATDC on the HRR

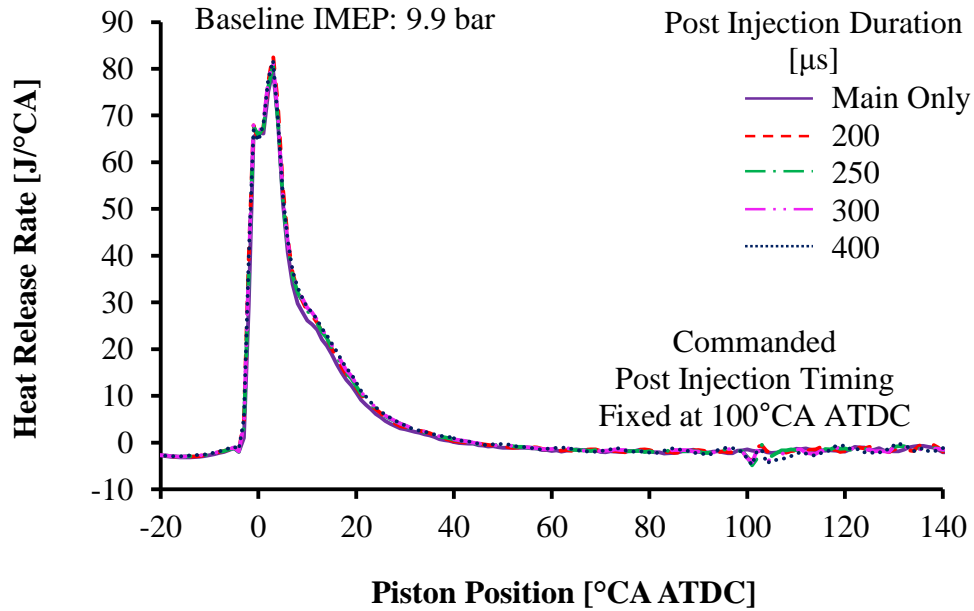


Figure 7-4: Effect of Post Injection Duration at 100°CA ATDC on the HRR

The results in Figure 7-5 showed that the baseline exhaust gas temperature, without a post injection, was 290°C and an early post injection of 200 μs increased the exhaust temperature to over 340°C. For early post injection between 30 and 50°CA ATDC, a progressive increase of the post injection duration to 400μs raised the exhaust gas temperature above 525°C. In contrast to these results, the use of late post injection, 70°CA ATDC and later, did not have a meaningful impact on the exhaust gas temperature as illustrated in Figure 7-5. For late post injections, the exhaust gas temperature remained below 358°C even when the post injection duration was increased to 400 μs. Such a minor exhaust gas temperature increase would not be meaningful for exhaust gas temperature control. Therefore, this data indicated that exhaust gas temperature control was more suitable for relatively early post injections, such as 30 to 50°CA ATDC for the tested conditions.

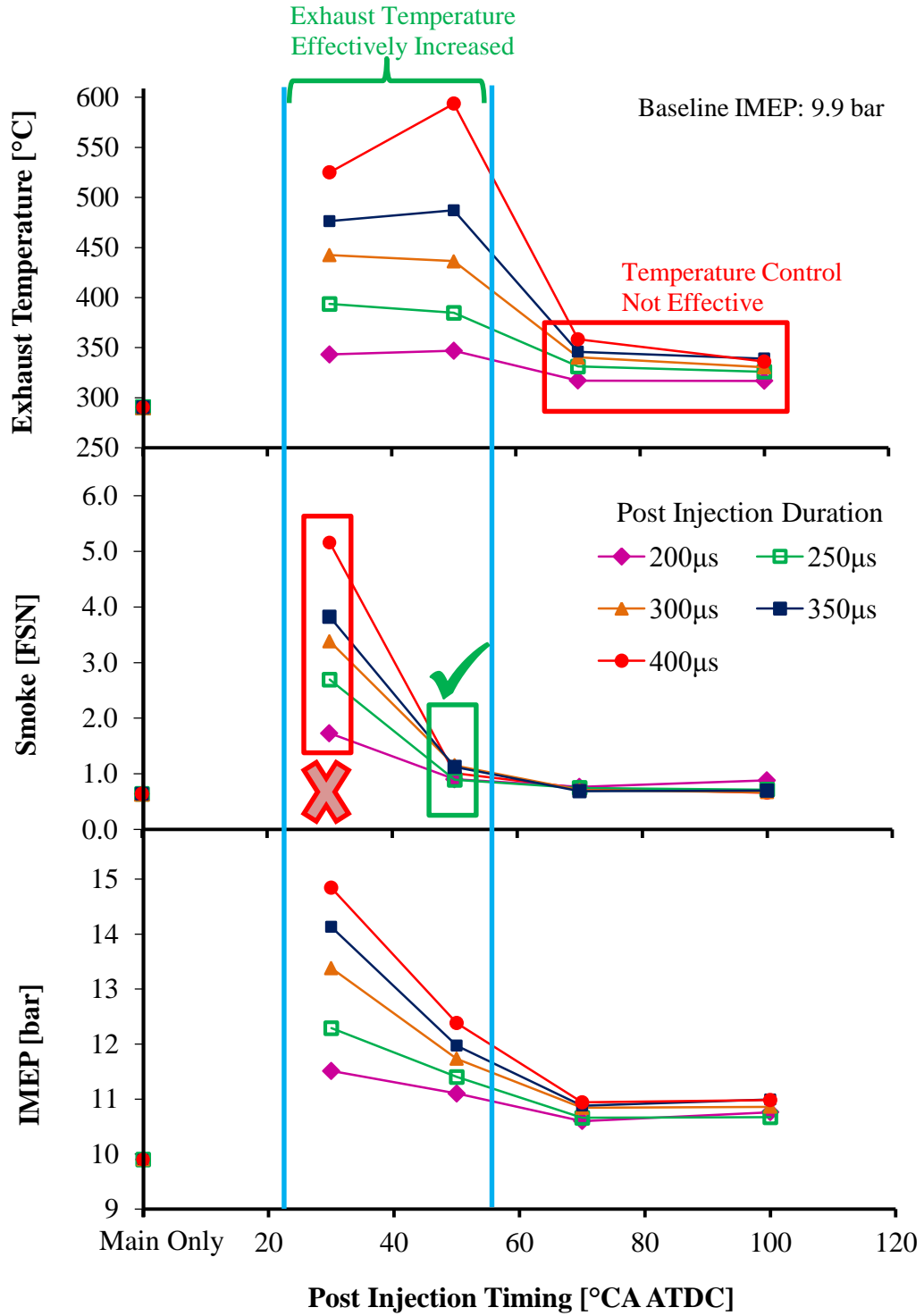


Figure 7-5: Post Injection Quantity and Timing vs. Exhaust Temperature (9.9 bar)

The results in Figure 7-5 also showed that the smoke emissions substantially increased by the addition of a post injection at 30°CA ATDC and that the smoke emissions significantly reduced when the post injection timing was delayed from 30 to 50°CA ATDC. This result indicated that the post injection at 50°CA ATDC did not contribute to a net formation of smoke and suggested that a post injection at 50°CA ATDC, for the tested conditions, can be used for effective management of the exhaust temperature without a smoke penalty. One drawback of delaying the post injection from 30 to 50°CA ATDC was the reduced power output, as illustrated by the IMEP data in Figure 7-5, which suggested that there was a slight fuel penalty.

Overall, the test data demonstrated that there was an optimal range for exhaust gas temperature control. The optimal timing within this range was dependant on whether the maximum fuel efficiency or the minimum smoke emissions were required. For maximum engine power output, the results showed that an earlier post injection, such as 30°CA ATDC, was more suitable and that a slightly delayed post injection, 50°CA ATDC for the tested conditions, was more appropriate for smoke emission reduction.

A second set of tests with a load of 5.8 bar IMEP were carried out as previously shown in Table 7-1. The overall trends for the 9.9 and the 5.8 bar test conditions in Figure 7-5 and Figure 7-6 were generally similar. There was an increase in the IMEP, the exhaust gas temperature, and the smoke emissions with a post injection at 30°CA ATDC. The late post injections at 70°CA ATDC and beyond did not increase the exhaust gas temperature or the IMEP relative to the single shot baseline. The heat release traces for the 5.8 bar IMEP case, illustrated by the graphs in Figure C-1 and Figure C-2 in Appendix C, showed similar trends to the heat release traces for the 9.9 bar IMEP tests in Figure 7-3 and Figure 7-4.

However, the data in Figure 7-6 illustrated that the post injection at 50°CA ATDC did not maintain an elevated exhaust temperature, in contrast to the results shown in Figure 7-5 at 9.9 bar IMEP. Thus, the results in Figure 7-6 suggested that the optimal post injection timing range for exhaust gas temperature management was narrower for the 5.8 bar test condition. As a consequence, a suitable post injection timing with high exhaust gas temperatures and low smoke emissions was not found for the low load test.

Therefore, a low load post injection timing sweep with a finer increment size was conducted to determine a suitable post injection timing. Details of the test conditions are given in Table 7-2.

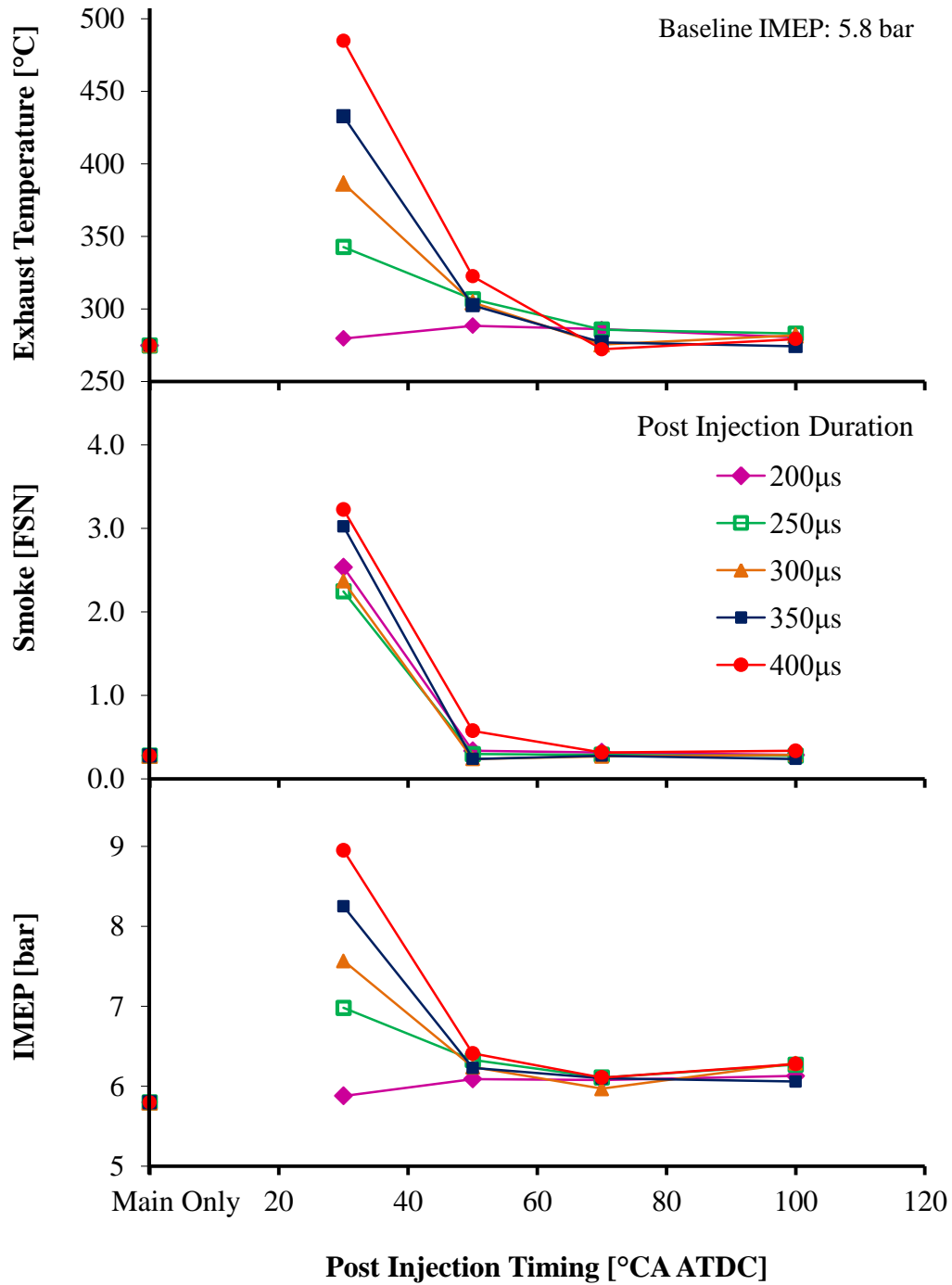


Figure 7-6: Post Injection Quantity and Timing vs. Exhaust Temperature (5.8 bar)

Table 7-2: Test Conditions for Post Injection Timing Sweep at 6.1 bar IMEP

Baseline IMEP [bar]	6.1
Engine Speed [rpm]	1500
Air Intake Pressure [bar absolute]	1.3
Intake Oxygen [% V]	16.5
Test Fuel	Diesel
Fuel Injection Pressure [bar]	900
Main Injection Duration [μ s]	465
Main Injection Timing [$^{\circ}$ CA ATDC]	-7
Post Injection Duration [μ s]	300
Post Injection Timing [$^{\circ}$ CA ATDC]	30 to 100

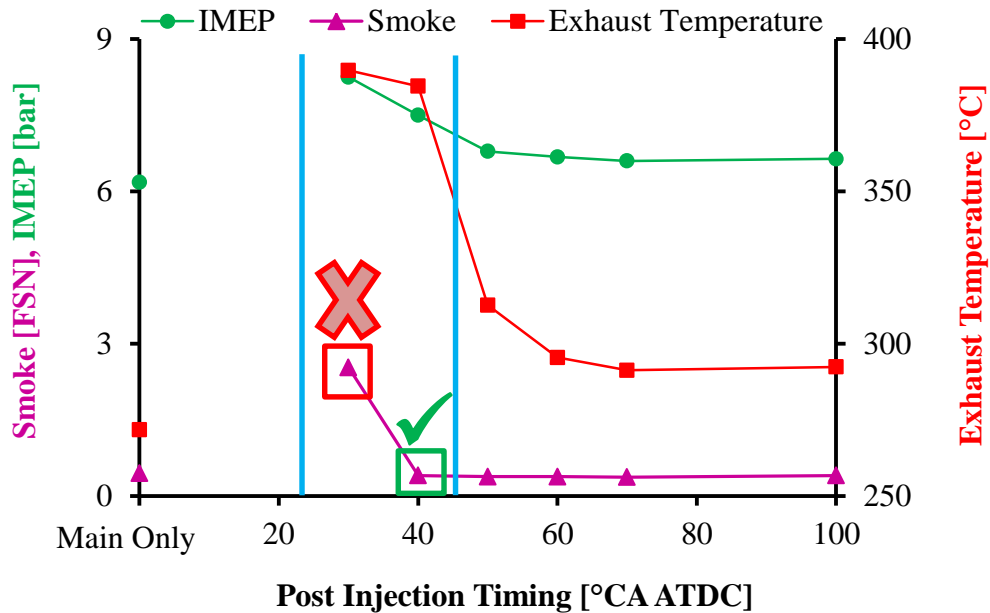


Figure 7-7: Effect of Post Injection Timing on Exhaust Temperature (6.1 bar)

The results of the low load post injection timing sweep are shown in Figure 7-7. The same overall patterns were noticed as in Figure 7-6 but the finer post injection timing increment revealed that the exhaust gas temperature was relatively high from 30 to 40 $^{\circ}$ CA ATDC. This was a significant result because there was a considerable reduction in the smoke emissions when the post injection was delayed from 30 to 40 $^{\circ}$ CA ATDC. Based on this discovery, the optimal post injection timing range, for the exhaust gas

temperature increase, was from 30 to 40°C CA ATDC. For optimal exhaust gas temperature control with minimal smoke emissions, the preferred timing was at the later stages of this range and this was consistent with the conclusions made for higher load conditions at 9.9 bar in Figure 7-5.

Overall, the results in Figure 7-5 to Figure 7-7 demonstrated the use of post injection strategies for the active control of the exhaust gas temperature. The results presented in these figures established that a wide range of exhaust gas temperatures were achieved by varying the post injection duration of early post injections, such as 30 to 50°C CA ATDC. A graphical summary of the effect of the post injection timing and duration on the exhaust gas temperature is shown in Figure 7-8 and Figure 7-9.

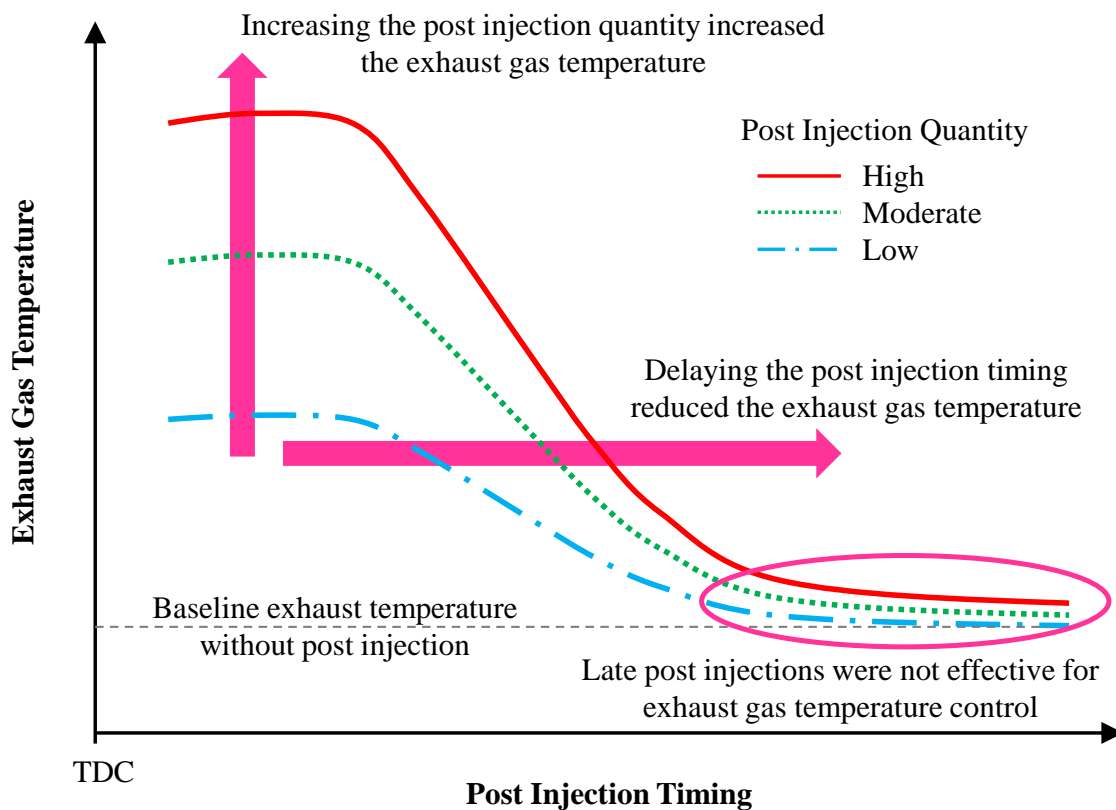


Figure 7-8: Exhaust Temperature Control via Post Injection Duration & Timing


Maximum Exhaust Gas Temperature	High	High	High	Moderate	Low
Sensitivity of Exhaust Temperature to Post Injection Duration	High	High	High	Moderate	Negligible
Engine-out Smoke Emissions	High	Moderate	Low	Low	Low
IMEP Contribution of Post Injection	High	Moderate	Moderate	Low	Negligible
Post Injection Timing	Too Early	Optimal	Optimal	Too Late	Too Late
Reduction in Exhaust Gas Temperature, IMEP, & Smoke 					
	TDC		Post Injection Timing		BDC

Figure 7-9: Optimal Post Injection Timing for Exhaust Temperature Control

The effect of the post injection timing and duration on the production of desirable NO_x reducing agents is shown in Figure 7-10. The results demonstrated that a suitable post injection timing range for the production of hydrogen and carbon monoxide was between 30 and 70°CA ATDC and that the highest hydrogen and carbon monoxide yields were generally observed at 50°CA ATDC. The trends for hydrogen and carbon monoxide were generally consistent with each other. The matching patterns suggested that these species were formed by the same reaction mechanisms, such as the partial oxidation reaction or the steam reforming reaction. The trend for the total hydrocarbons was unmistakably different from the trend for hydrogen and carbon monoxide. The total hydrocarbon emissions continually increased as the post injection timing was delayed.

A hydrocarbon speciation analysis was performed for further clarification as presented in Figure 7-11. The results of the hydrocarbon speciation revealed that the initial increase in the total hydrocarbon emissions was caused by increased light hydrocarbons and this trend was consistent with the hydrogen and carbon monoxide trends. However, the peak production of reactive light hydrocarbons like propylene coincided with the peak production of methane. The formation of methane was

undesirable since methane is not useful for after-treatment and it is a potent greenhouse gas which is difficult to eliminate with exhaust catalysts.

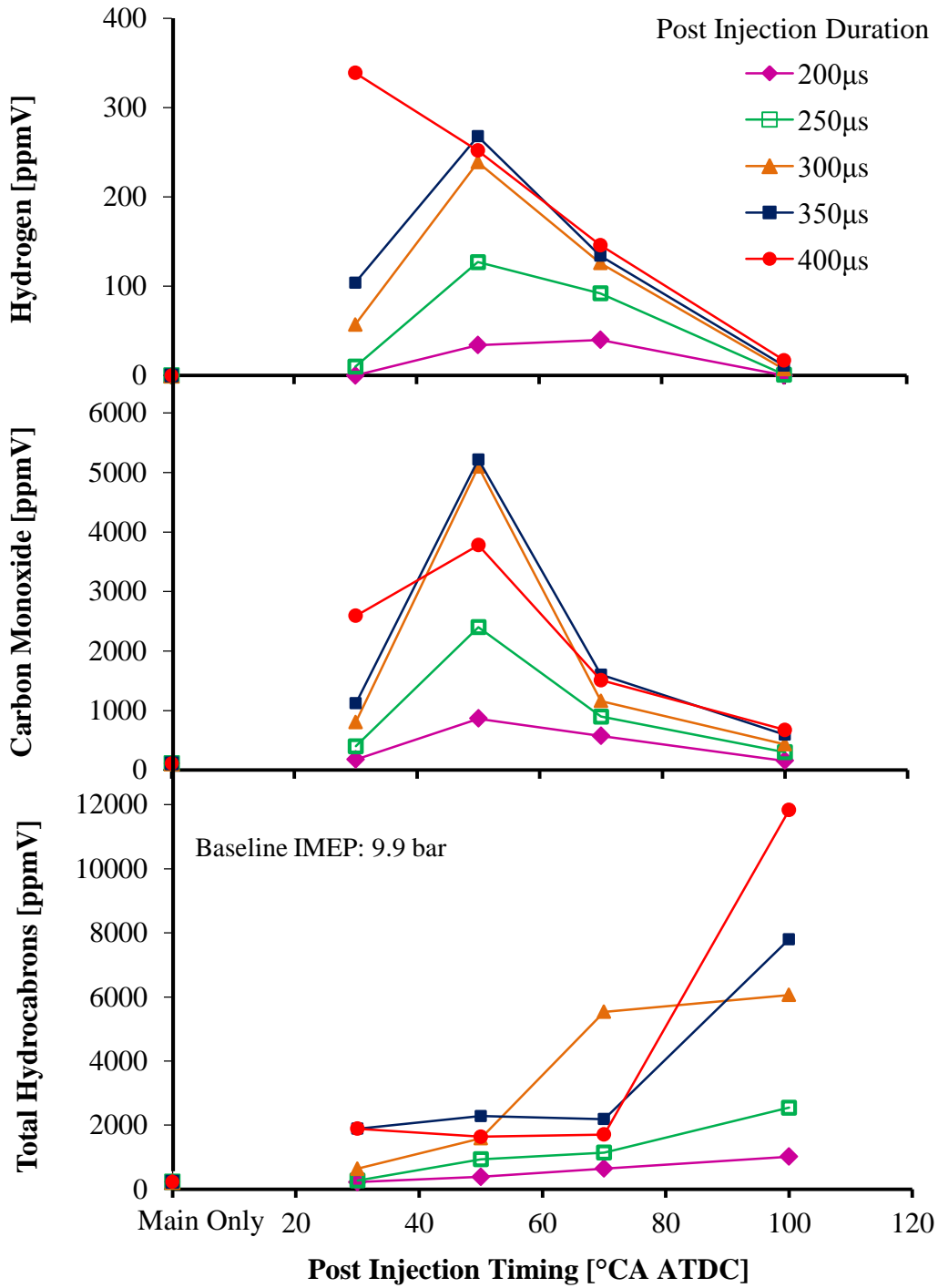


Figure 7-10: Effect of Post Injection on the Formation of NO_x Reducing Agents (9.9 bar)

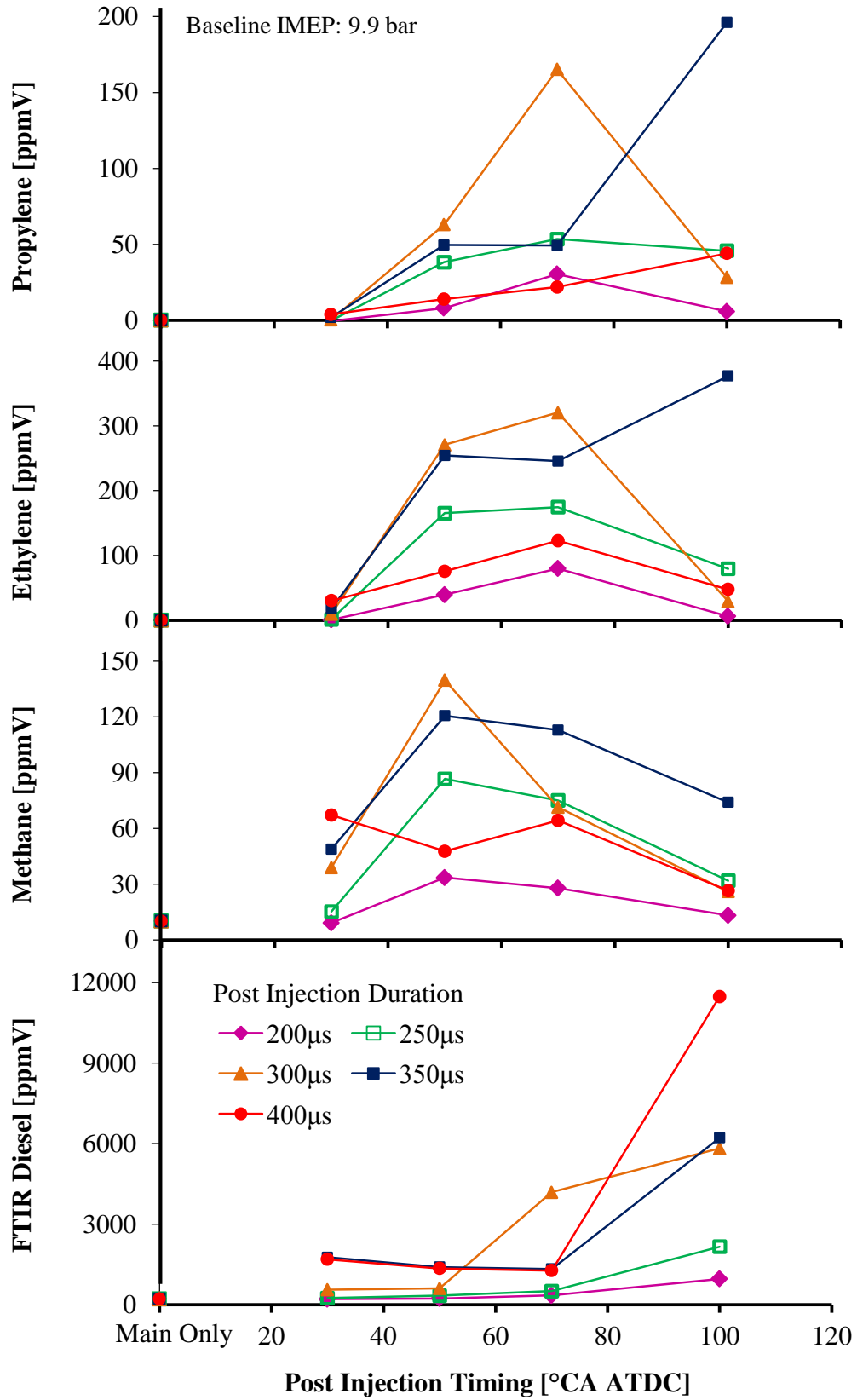


Figure 7-11: Effect of Post Injection on Hydrocarbon Speciation (9.9 bar)

Figure 7-11 further illustrated that the light hydrocarbon emissions generally dropped when the post injection was delayed to 100°CA ATDC while the unburned diesel fuel hydrocarbons dramatically increased. The high unburned fuel emissions and the low yield of light hydrocarbons provided further evidence against the use of very late post injections.

For reference, the test results for the NO_x emissions are provided in Figure 7-12. In general, the use of a post injection reduced the indicated NO_x emissions. The reduction of the indicated NO_x emissions was caused by a combination of an increased engine power output and a reduction of the raw engine-out NO_x emissions. The reduction of the raw NO_x emissions was partially accredited to the reduced oxygen atmosphere and the increased production of hydrogen and other NO_x reducing agents that may provide suitable conditions for in-cylinder NO_x reduction.

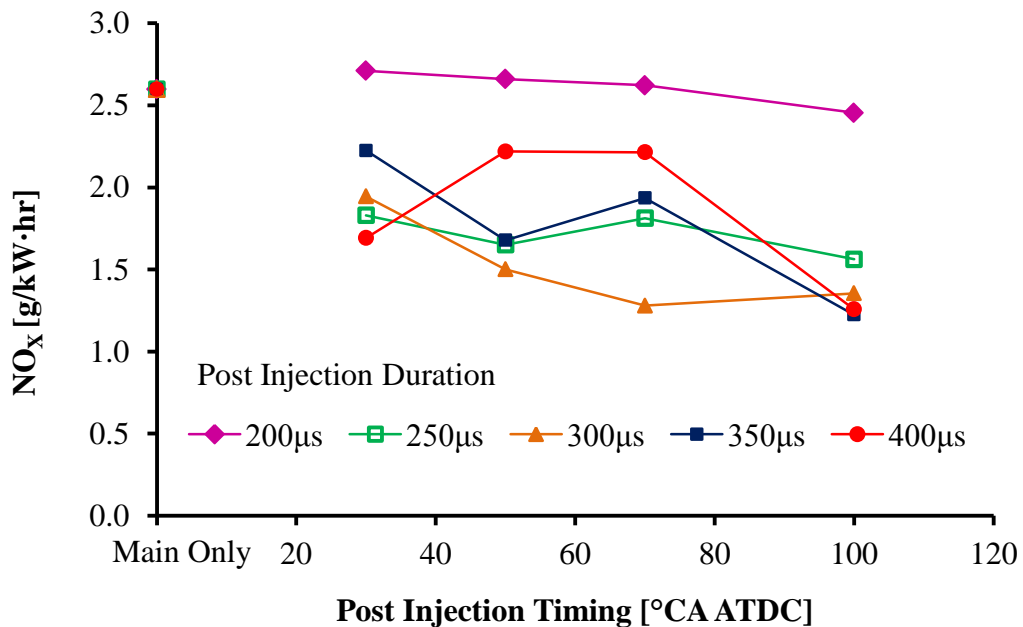


Figure 7-12: Effect of Post Injection Quantity and Timing on NO_x (9.9 bar)

Based on the data shown in Figure 7-10 and Figure 7-11, the optimal post injection timing for the production of desirable NO_x reducing agents was 50 to 70°CA

ATDC for these test conditions. These conditions yielded over 300 ppmV of ethylene, over 150 ppmV of hydrogen and propylene, and over 0.5% of carbon monoxide. However, the production of these desirable species also resulted in a methane emission penalty. Further tests were carried out at low load conditions, 5.8 and 6.1 bar IMEP, to confirm these patterns. The results for the 5.8 bar and 6.1 bar IMEP tests are provided in Figure C-3 to Figure C-7 in Appendix C. The results generally showed the same trends as at 9.9 bar IMEP. One exception was that the highest yield of hydrogen, CO, and light hydrocarbons at low load conditions was achieved at a post injection timing of 40 to 60°CA ATDC, which was slightly earlier compared to the 9.9 bar condition.

A graphical summary of the effect of the post injection timing on the production of hydrogen and other desirable NO_x reducing agents is shown in Figure 7-13. The results demonstrated that a very early post injection, relatively close to TDC, was not suitable for the production of desirable NO_x reducing agents. A slightly delayed post injection resulted in increased production of these species and, for the tested conditions, the maximum yield was reached when the post injection timing was in the region of 50°CA ATDC. Thus, the post injection timing range for the peak yield of NO_x reducing agents was slightly retarded compared to the optimal post injection timing range for exhaust gas temperature control, which indicated that the two goals of increasing the exhaust gas temperature and obtaining an increased yield of NO_x reducing agents were not reached simultaneously.

Hydrogen	Low	Moderate	High	Moderate	Low
Carbon Monoxide	Low	Moderate	High	High	Moderate
Propylene, Ethylene	Low	Moderate	High	Moderate	Low
Methane	Low	Moderate	High	Moderate	Low
Heavy Hydrocarbons	Low	Moderate	Moderate	Moderate	High
Post Injection Timing	Too Early	Not-Optimal	Optimal	Not-Optimal	Too Late

TDC
BDC
Post Injection Timing

Figure 7-13: Optimal Post Injection Timing for NO_x Reducing Agents

7.3 Effects of Engine Load and Combustion Phasing on Exhaust Temperature and Composition

The results in the previous section indicated that the optimal post injection timing for exhaust gas management was dependent on the engine operating conditions. Thus, the effects of the engine IMEP and the combustion phasing on the optimal post injection timing were investigated. The effects of the intake oxygen were also investigated and the data is shown in subsequent sections of this chapter.

Table 7-3: Test Conditions for Engine Load and Combustion Phasing Study

	Early Low Load	Delayed Low Load	High Load
Main Injection IMEP [bar]	6.0	6.0	14.7
Main Injection CA50 [°CA ATDC]	5	9	9
Fuel Injection Pressure [bar]	1200	1200	1200
Main Injection Timing [°CA ATDC]	-5	-1	-3
Main Injection Duration [μ s]	385	405	900
Post Injection Timing [°CA ATDC]	30 to 130	30 to 130	30 to 130
Post Injection Duration [μ s]	300	300	300
Air Intake Pressure [bar absolute]	1.3	1.3	2.5
Intake Oxygen [% volume]	16.5	16.5	16.5
Test Fuel	Diesel	Diesel	Diesel

Three different test conditions were utilized to investigate the effect of the engine load and the combustion phasing as shown in Table 7-3. The baseline engine load and the combustion phasing refer specifically to the main injection while the post injection was allowed to generate additional IMEP beyond the baseline level to determine the power producing capability of the post injection. Two distinct engine loads were used for this investigation; a relatively low IMEP of 6 bar and a relatively high IMEP of 14.7 bar. The combustion phasing was characterized by the crank angle of 50% heat released (CA50) from the main injection. The CA50 was at 5°CA ATDC for the early low load condition while the high load and the delayed low load conditions had a CA50 of 9°CA ATDC. The commanded main injection duration and timing were fixed. The post

injection duration was maintained at $300\mu\text{s}$ while the post injection timing was varied from 30 to 130°CA ATDC .

The in-cylinder pressure traces are shown in Figure 7-14 for a post injection at 30°CA ATDC . The cylinder pressure traces showed that the high load condition produced a much higher peak in-cylinder pressure than the two low load conditions. The increased peak pressure at high load was a product of the higher intake air pressure and the increased energy released from combustion. The delayed low load condition had the lowest peak pressure. The pressure during the expansion stroke, from 20 to 60°CA ATDC , was slightly higher for the delayed low load condition, compared to the early low load condition, because of the delayed combustion phasing.

The post injection was difficult to visualize from the in-cylinder pressure traces but it was more easily identified on the apparent heat release diagrams in Figure 7-15. The heat release rate graphs clearly demonstrated that there was a distinct heat release for the post injection at 30°CA ATDC for all three conditions, suggesting that the post injection combustion was effective at this post injection timing regardless of the engine load and the combustion phasing.

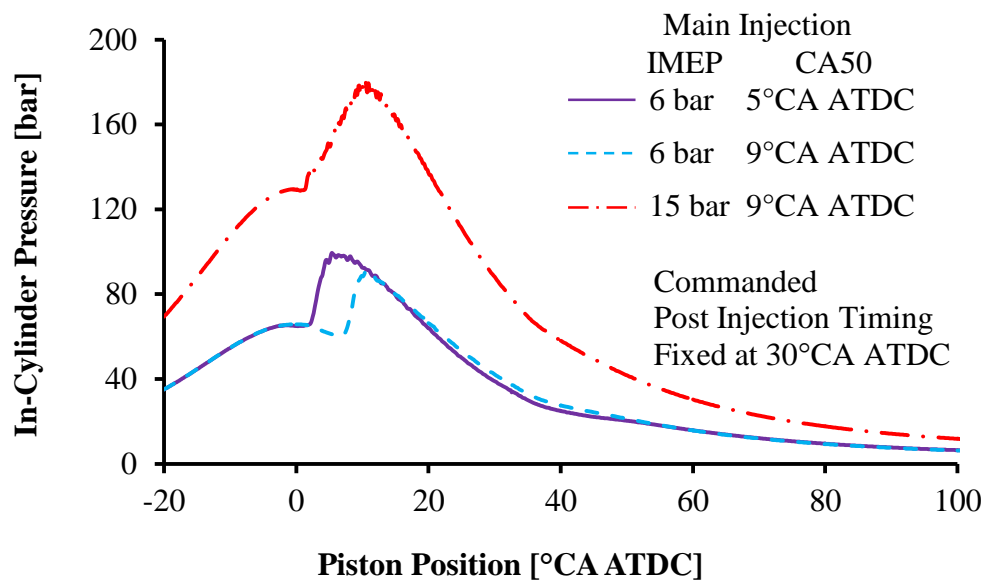


Figure 7-14: In-cylinder Pressure for Post Injection at 30°CA ATDC

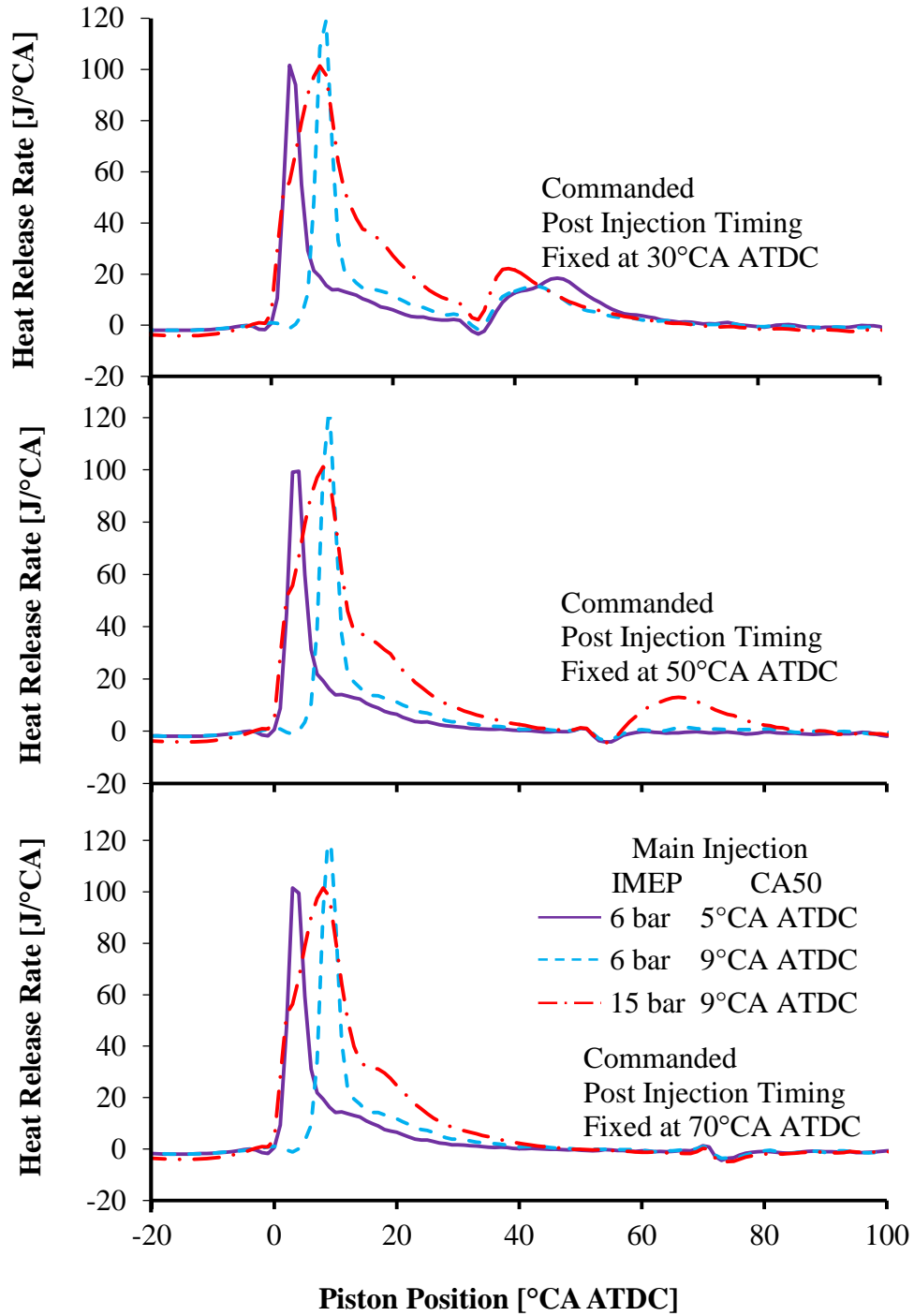


Figure 7-15: HRR Comparison for Post Injection at 50° & 70°CA ATDC

Conversely, the results in Figure 7-15 demonstrated that only the high load condition produced a visible heat release when the post injection timing was delayed to

50°CA ATDC and that a heat release peak was not visible for either of the two low load conditions regardless of the combustion phasing. When the post injection was delayed to 70°CA ATDC, a heat release rate peak was not observed for any of the three conditions. Thus, the effect of the engine load was established to be more significant for intermediate post injections, such as at 50°CA ATDC for the tested conditions.

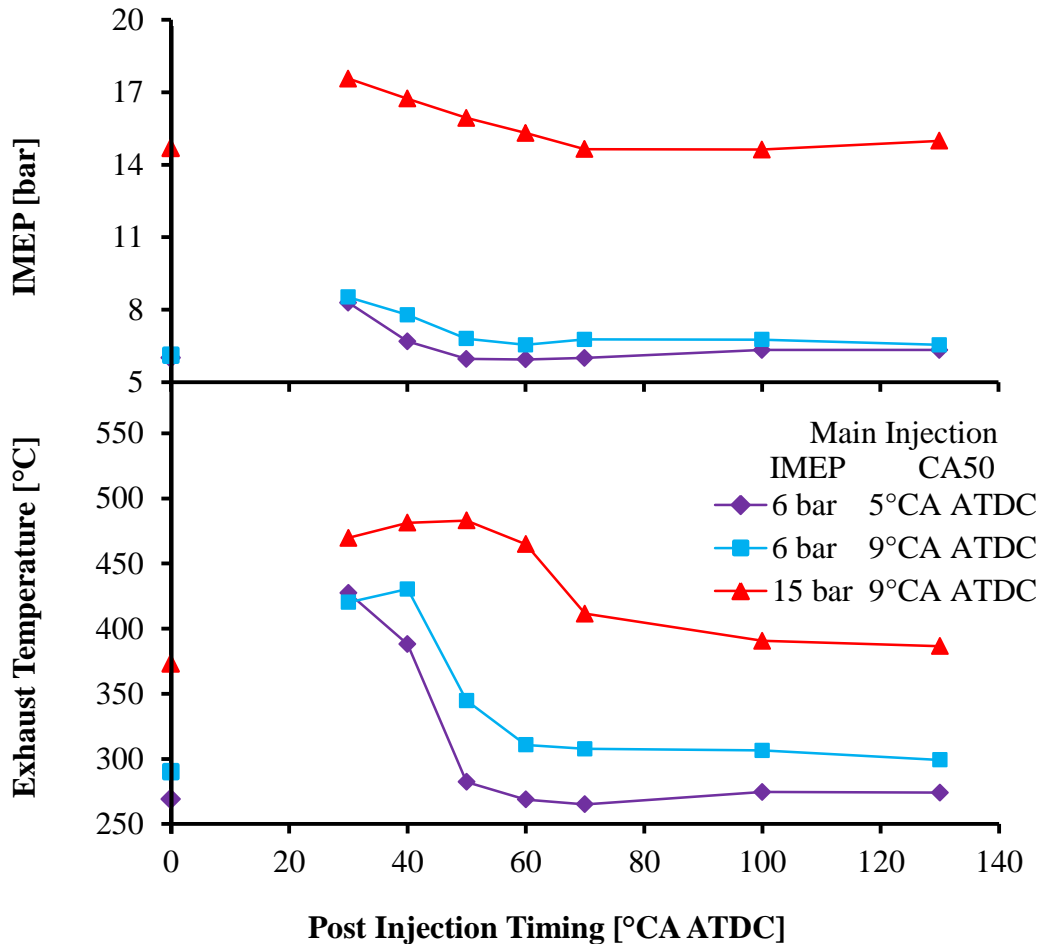


Figure 7-16: Effect of Engine Load on IMEP and Exhaust Temperature

The IMEP and the exhaust gas temperature results in Figure 7-16 were consistent with the heat release rate results in the previous two figures. In general, the effect of the engine load was greater than the effect of the combustion phasing on the exhaust gas temperature. The IMEP and the exhaust gas temperature were significantly increased by

an early post injection at 30°CA ATDC for all load conditions. When the post injection timing was delayed to 50°CA ATDC, the data revealed that the exhaust gas temperature dropped significantly for the two low load conditions.

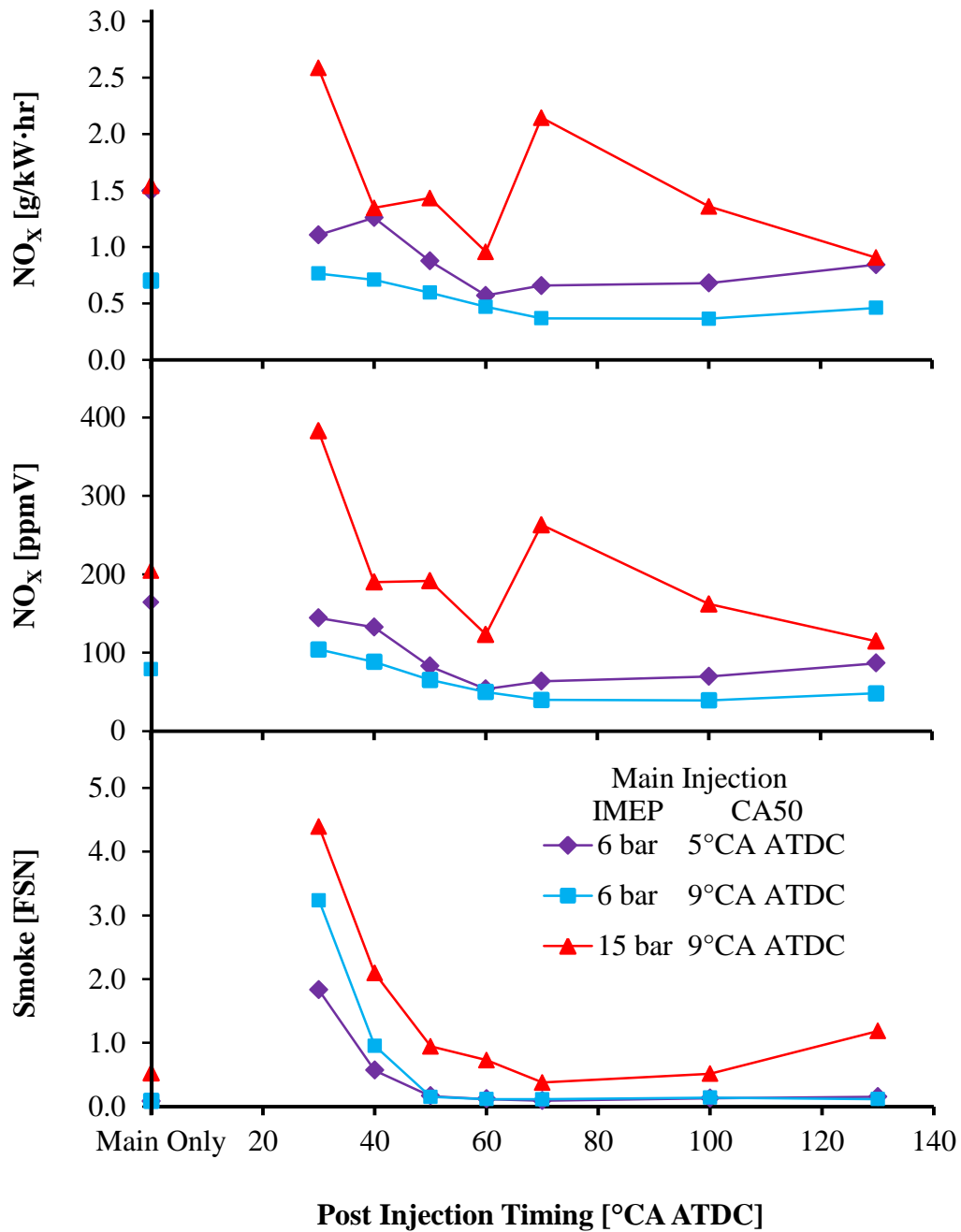


Figure 7-17: Effect of Engine Load on NO_x and Smoke Emissions

In contrast, the exhaust gas remained at elevated temperatures for the high load condition even when the post injection was delayed to 60°CA ATDC. When the post injection timing was delayed to 70°CA ATDC or later, the effects of the post injection on the exhaust gas temperature were negligible for all load conditions as illustrated in Figure 7-16. Therefore, the effect of the engine load on the exhaust gas temperature was the greatest at intermediate post injection timings, between 50 to 60°CA ATDC for the tested conditions.

The effects of the combustion phasing and the engine load on the nitrogen oxide and the smoke emissions are illustrated in Figure 7-17. The indicated and the volumetric fraction NO_x emissions showed similar trends for all three conditions; there was generally a slight NO_x reduction when a post injection was utilized. The NO_x emissions increased when the engine load was increased but the combustion phasing only had a slight effect on the NO_x emissions. Therefore, the engine load generally had a greater effect than the combustion phasing on the NO_x emissions. The increased NO_x emissions were attributed to the higher flame temperatures at high load conditions.

Figure 7-17 also illustrated that the engine load had a meaningful effect on the smoke emissions. The smoke emissions were consistently higher when the engine load was increased, especially for very early post injections. Figure 7-18 shows the mean bulk gas temperatures during the post injection combustion. The data showed that early post injections and high load conditions had the highest bulk gas temperatures, which was an indication of hotter flame temperatures during combustion and of higher smoke formation rates. The increased smoke emissions were also attributed to the reduced in-cylinder oxygen availability and the reduced soot oxidation at higher engine loads.

The data in Figure 7-16 and Figure 7-17 confirmed that the preferred post injection timing for exhaust gas temperature management was slightly advanced for lower engine loads. For both low load conditions, the most suitable post injection timing was at 40°CA ATDC since the exhaust temperature was high and the smoke emissions were relatively low. Thus, the combustion phasing did not affect the optimal post injection timing for exhaust temperature management at these conditions. On the other

hand, the most suitable post injection timing was in the range of 50 to 60°CA ATDC for high load conditions.

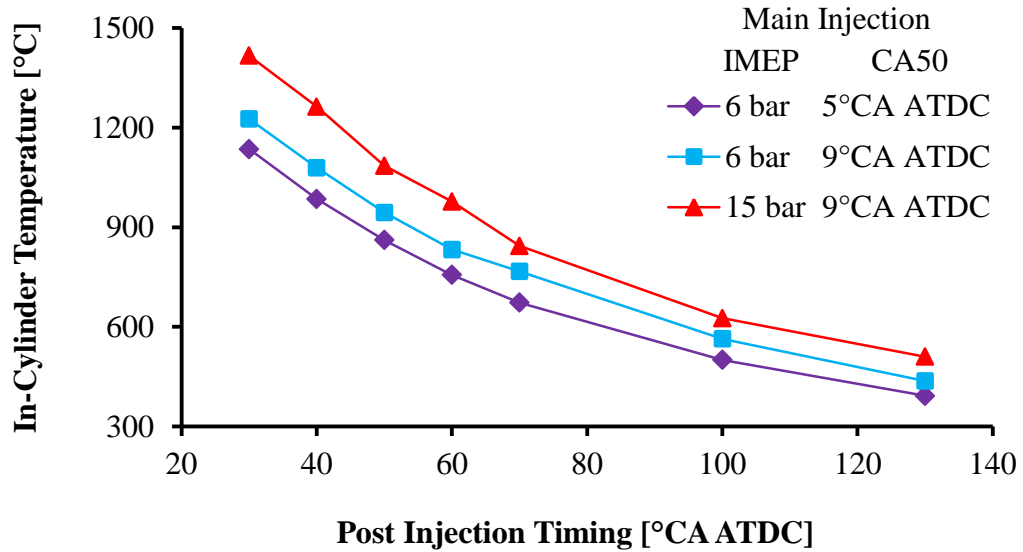


Figure 7-18: Engine Load & Combustion Phasing vs. Post Bulk Gas Temperature

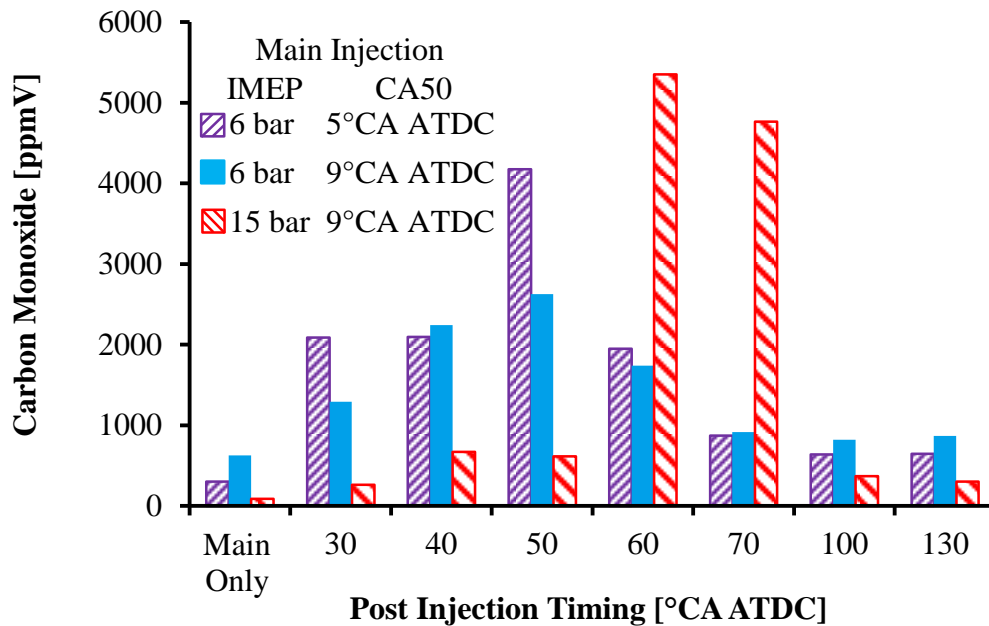


Figure 7-19: Effect of Engine Load and Combustion Phasing on CO Emission

The effects of the engine load and the combustion phasing on the exhaust gas composition are presented in Figure 7-19 to Figure 7-22. The effect on the exhaust carbon monoxide is shown in Figure 7-19 and the data indicated that the combustion phasing did not produce a meaningful impact. The trend for the two low load conditions was the same, the peak CO was reached at 50°CA ATDC, and the absolute values were generally similar, regardless of the combustion phasing. The effect of the engine load was more significant since the peak carbon monoxide emissions were delayed to 60°CA ATDC and the carbon monoxide emissions remained very high when the post injection was delayed to 70°CA ATDC at high load conditions.

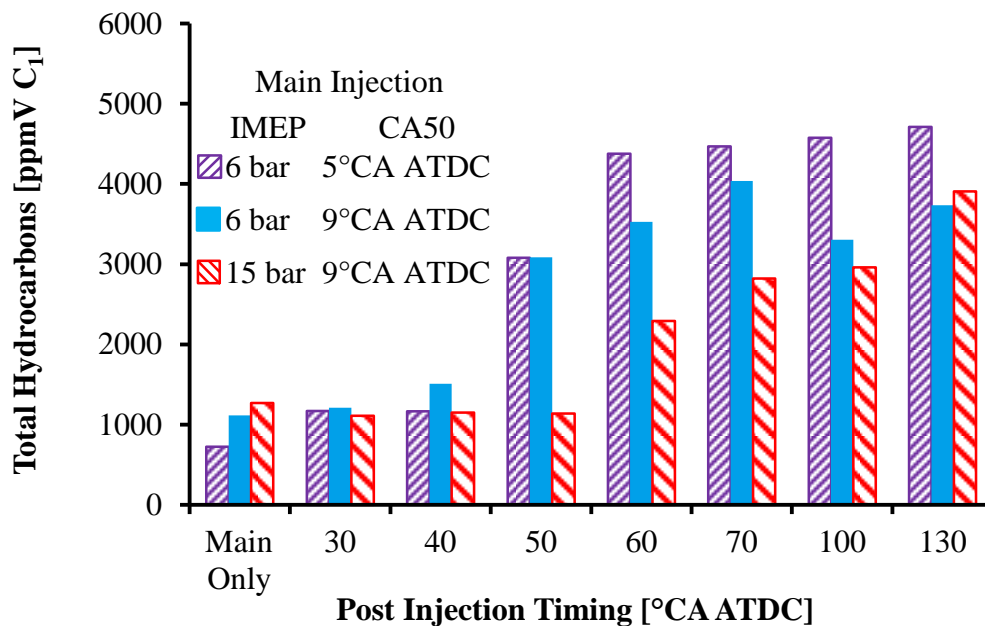


Figure 7-20: Effect of Engine Load and Post Timing on THC Emission

A similar plot for the total hydrocarbons emissions is provided in Figure 7-20. All three conditions displayed a similar trend with respect to the effect of the post injection timing on the THC emissions; the total hydrocarbon emissions generally increased when the post injection timing was delayed. The effect of the combustion phasing was not consistent. For early post injections, the delayed combustion phasing resulted in slightly higher total hydrocarbon emissions but, for late post injections, the

advanced combustion phasing led to higher THC emissions. The engine load did not appear to have a meaningful impact on the THC emissions for early post injections but higher load condition produced less THC when the post injection was between 50 to 100°CA ATDC. For late post injections, the reduced THC emissions at higher load were attributed to higher in-cylinder temperatures, as shown in Figure 7-18, which helped to promote the oxidation of the post injection fuel.

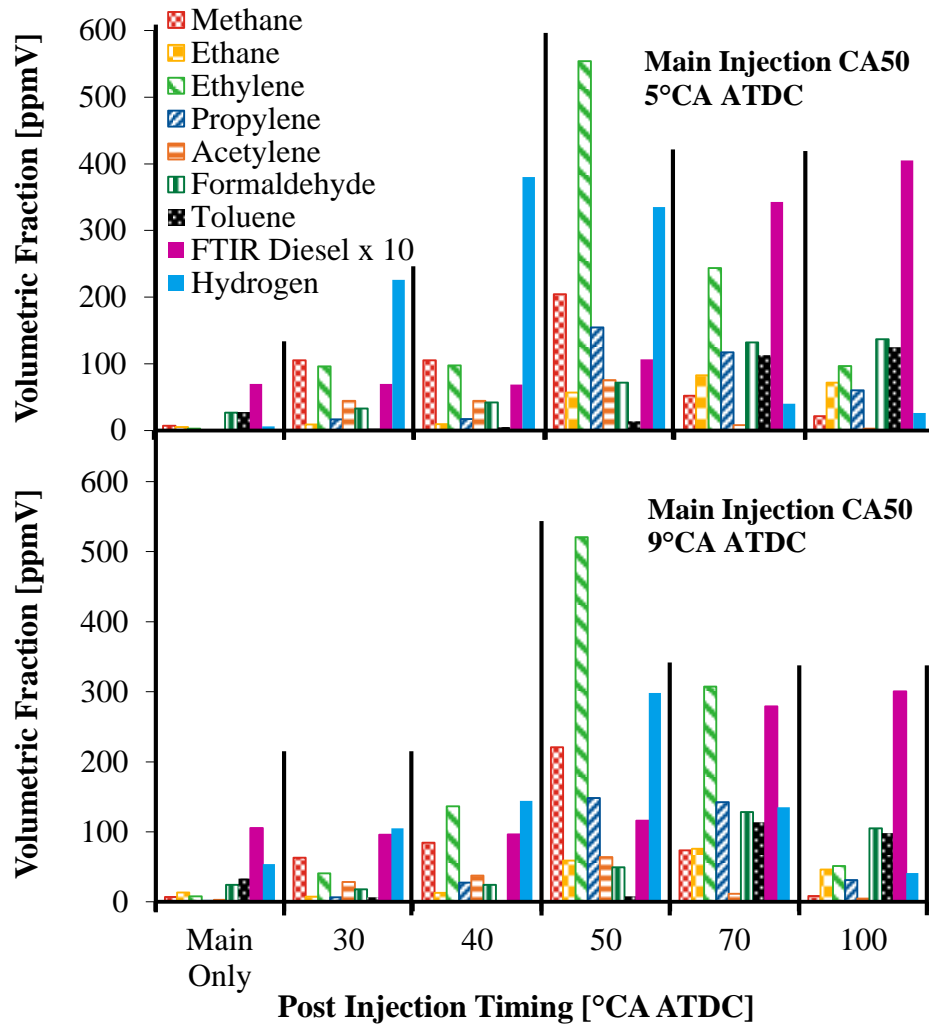


Figure 7-21: Exhaust Gas Speciation for Low Engine Load

Figure 7-21 shows the hydrocarbon speciation for the two low load conditions and Figure 7-22 shows the hydrocarbon speciation for the high load condition. Additionally, the hydrogen was measured by a mass spectrometer and the measurement results are included in these figures. The results in Figure 7-21 demonstrated that the effect of the combustion phasing on the hydrocarbon speciation was negligible at these test conditions since the same trends were observed for both low load conditions.

The light hydrocarbons were negligible without a post injection and there was a slight increase when an early post injection was added. The peak light hydrocarbons were at a post injection timing of 50°CA ATDC and methane, ethylene, and propylene were found to be the most abundant light hydrocarbon species, regardless of the combustion phasing. The delay of the post injection, to 70°CA ATDC and beyond, slightly increased the toluene and formaldehyde emissions but reduced the light hydrocarbons. The presence of toluene and formaldehyde suggested that the post injection fuel was undergoing reaction kinetics even when the post injection timing was very late. The speciation analysis also confirmed that late post injections were characterized by a large fraction of unburned fuel hydrocarbons.

The combustion phasing seemed to have a minor effect on the hydrogen yield. The early low load condition had a slightly higher yield of hydrogen for early post injections while the delayed low load condition had a slightly higher yield of hydrogen for late post injections. However, the peak hydrogen yield was obtained with a post injection timing of 40 to 50°CA ATDC for both low load conditions. In general, the post injection timing for the peak production of hydrogen and reactive light hydrocarbons matched the post injection timing for the peak production of carbon monoxide. Hence, the preferred post injection timing for the in-cylinder production of desirable NO_x reducing agents was found to be independent of the main injection combustion phasing for these test conditions.

The results of the hydrocarbon speciation and the hydrogen yield for the 14.7 bar IMEP condition are presented in Figure 7-22. The results revealed that the engine load had a significant effect on the light hydrocarbon yield. At high engine load, the light hydrocarbon emissions and the hydrogen yield were insignificant for post injections from

30 to 50°C_A ATDC, in contrast to the low load results that exhibited the peak light hydrocarbons and hydrogen emissions at 50°C_A ATDC. Instead, the peaks at high engine load were observed to be at a post injection timing of 60 to 70°C_A ATDC. Similar to low load, the most abundant species at high load were ethylene, propylene, methane, and formaldehyde. There was a dramatic drop in the light hydrocarbon and the hydrogen yield when the post injection timing was delayed to 100°C_A ATDC and most of the hydrocarbons consisted of unburned fuel. The post injection timing range for the peak production of hydrogen and reactive light hydrocarbons overlapped with the post injection timing range for the peak production of carbon monoxide as shown in Figure 7-19 and Figure 7-22. Overall, the test results indicated that the engine load had a bigger impact than the combustion phasing on the exhaust gas management.

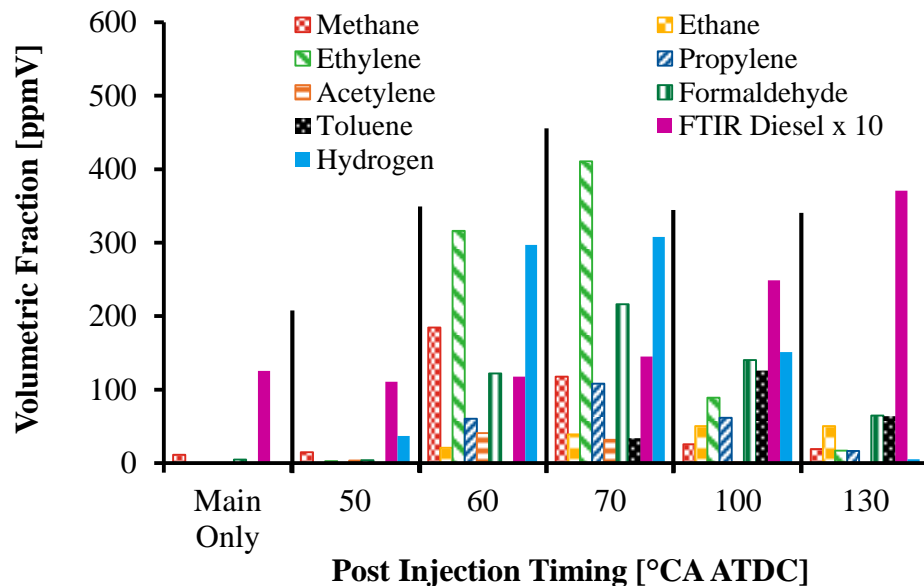


Figure 7-22: Exhaust Gas Speciation for High Engine Load (14.7 bar IMEP)

7.4 Effects of Intake Oxygen and Low Temperature Combustion on Exhaust Temperature and Composition

The effects of the intake oxygen and low temperature combustion on the post injection characteristics were investigated according to the test matrix shown in Table

7-4. The tests were carried out at three different intake oxygen quantities: 20.7 percent by volume (%V), 16.5%V, and 9.5%V. The intake oxygen was controlled by adjusting the opening of the EGR control valve and the backpressure valve. The main injection combustion phasing and IMEP were similar for all three tests. The post injection duration was maintained constant and a post injection timing sweep was carried out for the three sets of tests. A higher fuel injection pressure was used for the LTC test to reduce the smoke emissions during the EGR sweep that was carried out to reach LTC. The results in Appendix H showed that the fuel injection pressure did not affect the optimal post injection timing for control of the exhaust gas temperature and composition.

Table 7-4: Test Conditions for the Intake Oxygen Study

	No EGR	Moderate EGR	LTC
Fuel	Diesel	Diesel	Diesel
Intake Oxygen [% Volume]	20.7	16.5	9.5
Air Intake Pressure [bar absolute]	1.3	1.3	2.0
Main Injection IMEP [bar]	5.9	6.1	5.5
Main Injection CA50 [°CA ATDC]	5	5	5
Fuel Injection Pressure [bar]	900	900	1200
Main Injection Timing [°CA ATDC]	-6.5	-7	-6
Main Injection Duration [μs]	530	465	465
Post Injection Timing [°CA ATDC]	20 to 130	30 to 130	20 to 130
Post Injection Duration [μs]	300	300	250

Figure 7-23 illustrates the effect of the intake oxygen quantity on the exhaust gas temperature and the engine IMEP. The trends were generally independent of the intake oxygen since the exhaust gas temperature increased for early post injections and dropped as the post injection timing was delayed for all three cases. However, the absolute values of the exhaust gas temperature were greatly dependant on the intake oxygen. The LTC condition consistently generated the lowest exhaust gas temperature and the post

injection failed to provide a significant exhaust temperature increase relative to the main injection. The reduced oxygen availability for LTC prevented effective oxidation of the post injection fuel and resulted in relatively low exhaust gas temperatures.

Conversely, an early post injection significantly increased the exhaust gas temperature for the two sets of tests with higher intake oxygen. The data also demonstrated that the condition with 20.7% V generated noticeably higher exhaust gas temperatures when the post injection was in the region of 50 to 70°CA ATDC. This pattern was attributed to the higher oxygen availability that enabled improved oxidation of retarded post injections. The trends for the IMEP generally followed the same trends as the exhaust gas temperature. These results insinuated that LTC conditions were not suitable for exhaust gas temperature control and that high intake oxygen levels provided a wider post injection timing range for active management of the exhaust gas temperature.

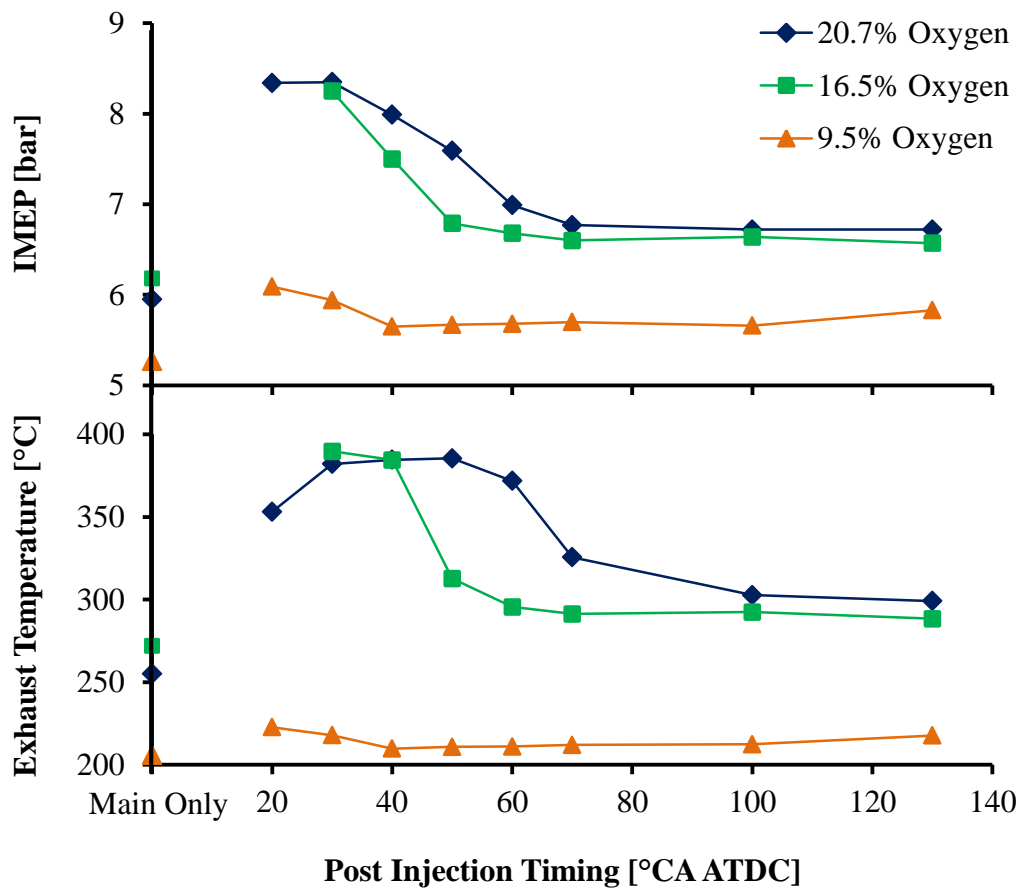


Figure 7-23: Effect of Intake Oxygen on IMEP and Exhaust Temperature

The effect of the intake oxygen concentration on the NO_x emissions is illustrated in Figure 7-24. A significant reduction of the NO_x emissions was observed when the intake oxygen was reduced. The impact of the intake oxygen was much more crucial than the impact of the post injection timing. Calculations indicated that the NO_x emissions were reduced by a factor of 100 when the intake oxygen was reduced from 20.7%V to 9.5%. Such a large reduction was magnitudes greater than the NO_x reduction by the post injection for any of the tested conditions. Despite such large differences between the NO_x emissions at different intake oxygen levels, the overall trends with regards to the effect of the post injection timing on the NO_x emissions were the same.

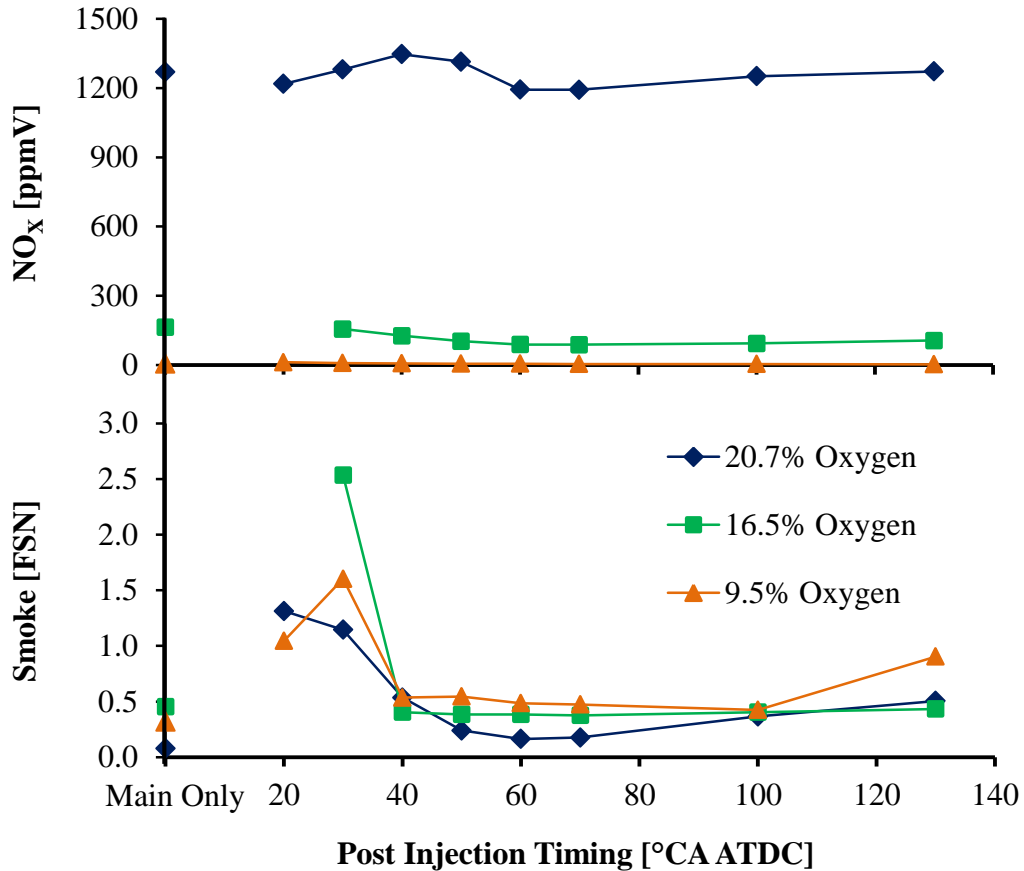


Figure 7-24: Effect of Oxygen on NO_x and Smoke Emissions

Likewise, the effect of the post injection timing on the smoke emissions was consistent. At each condition, the smoke emissions increased when a very early post injection was used and the smoke emissions drastically dropped when the post injection timing was delayed to 40°CA ATDC and later. In general, the smoke emissions were the highest when medium EGR was used, caused by the combination of high temperature combustion and very low in-cylinder oxygen availability. The reduced smoke emissions for very high or very low intake oxygen levels could be beneficial for advancing the post injection timing for exhaust gas temperature control, which would allow more power to be produced by the post injection as shown in Figure 7-23.

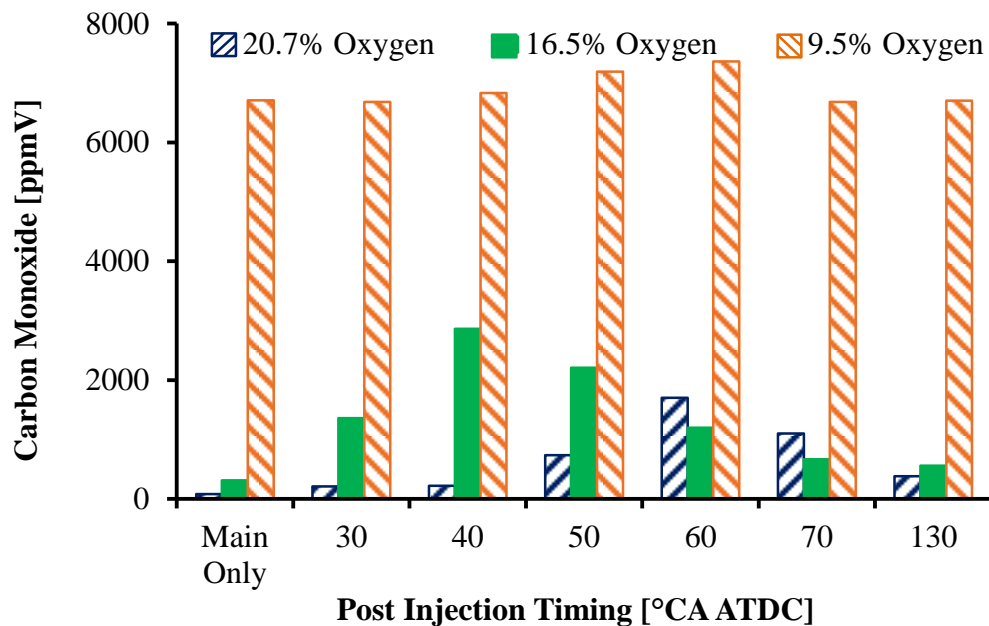


Figure 7-25: Effect of Oxygen on Carbon Monoxide Emissions

The data in Figure 7-25 showed that the intake oxygen had a major effect on the carbon monoxide emissions. The baseline carbon monoxide from the main injection exceeded 6000 ppmV for the LTC test. When an early post injection was added, there was a slight decrease in the carbon monoxide with LTC but the overall quantity remained above 6000 ppmV throughout the post injection timing sweep. This result signified that the use of a post injection was not required for the production of carbon monoxide under

low temperature combustion. The use of a post injection was more meaningful for the tests with higher intake oxygen since the formation of carbon monoxide was sensitive to the post injection timing as shown in Figure 7-25.

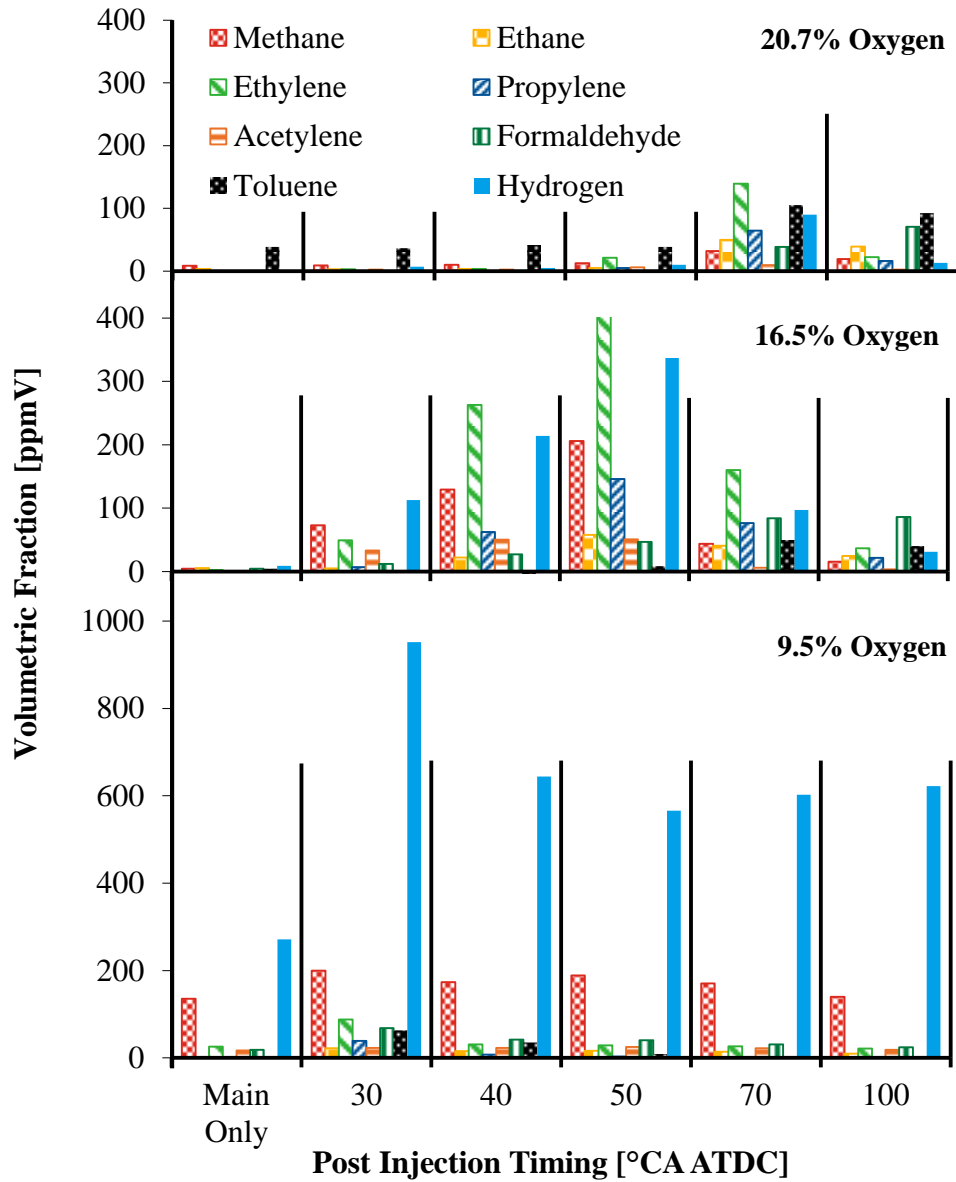


Figure 7-26: Effect of Oxygen on Hydrocarbon Speciation

The hydrocarbon speciation and the hydrogen yield results are illustrated in Figure 7-26. With regards to the hydrocarbon speciation, large differences were observed between the low and high temperature combustion conditions. With low temperature combustion at 9.5%V intake oxygen, methane was the most abundant light hydrocarbon at all post injection timings and the quantity of more reactive light hydrocarbons was relatively insignificant. This result was undesirable since methane is not suitable for NO_x reduction. In contrast, the most abundant light hydrocarbons were ethylene, propylene, and methane when the intake oxygen was 16.5%V but the formation of these species was sensitive to the post injection timing. When the intake oxygen was 20.7%V, toluene was generally the most abundant species and all of the light hydrocarbons remained relatively low throughout the post injection timing sweep. The results in Figure 7-26 implied that moderately reduced intake oxygen levels, in the region of 16.5%V, were more suitable for the production of light hydrocarbons for NO_x reduction. For reference, the effect of the intake oxygen on the total hydrocarbon emissions is shown in Figure C-8.

The hydrogen yield was also significantly affected by the intake oxygen and by low temperature combustion. Figure 7-26 shows that with 20.7%V intake oxygen, the peak hydrogen yield was marginal and never exceeded 100 ppmV. The hydrogen yield increased, up to 337 ppmV, when moderate EGR was applied to reduce the intake oxygen to 16.5%V. At 16.5%V intake oxygen, the hydrogen formation was very sensitive to the post injection timing. When the intake oxygen was reduced to 9.5% to achieve LTC, the hydrogen yield increased dramatically. For LTC, noticeable levels of hydrogen were generated without a post injection and the addition of a post injection further increased the hydrogen yield. The peak hydrogen was obtained for the earliest post injection timing but the hydrogen yield remained relatively high throughout the post injection timing sweep. These trends established that a high yield of hydrogen was obtained with low intake oxygen and LTC despite the relatively low in-cylinder temperatures.

An EGR sweep (intake oxygen sweep) was carried out to further investigate the effects of the intake oxygen. The test conditions for the EGR sweep are shown in Table 7-5. The tests were carried out at constant load conditions by adjusting the main injection

duration throughout the EGR sweep. The main injection combustion phasing was also kept constant by adjusting the main injection timing. The commanded post injection duration was maintained at 300 μ s and the post injection timing was fixed at 40 $^{\circ}$ CA ATDC. The fuel injection pressure was increased compared to previous tests to reduce the impact of EGR on the smoke emissions.

Table 7-5: Test Conditions for Intake Oxygen Sweep Study

IMEP [bar]	6.0
Fuel	Diesel
Intake Oxygen [% Volume]	Sweep
Air Intake Pressure [bar absolute]	1.9
Main Injection CA50 [$^{\circ}$ CA ATDC]	9
Fuel Injection Pressure [bar]	1500
Main Injection Timing [$^{\circ}$ CA ATDC]	-5 to 0
Main Injection Duration [μ s]	370 to 480
Post Injection Timing [$^{\circ}$ CA ATDC]	40
Post Injection Duration [μ s]	300

The results for the NO_x and the smoke emissions are given in Appendix C in Figure C-9. As expected, the classical NO_x-smoke trade-off was observed when the intake oxygen was reduced from 20.4 to 11.7%V under high temperature combustion conditions. A further reduction in oxygen led to low temperature combustion with simultaneously low NO_x and smoke emissions. These trends have been previously explained in the literature review section for a single shot injection strategy. The data in Figure C-9 confirmed that these trends were also valid when a post injection was utilized. The results for the exhaust temperature are shown in Appendix C in Figure C-10. The results confirmed the trends observed in the previous figures in this chapter. The exhaust gas temperature continually reduced as the intake oxygen was reduced despite constant load conditions. This result validated the conclusion that LTC conditions were not

suitable for exhaust gas temperature control due to the inability to generate high exhaust temperatures.

Previous results demonstrated that LTC was particularly suitable for the generation of CO and hydrogen, but was not suitable for the formation of reactive light hydrocarbons. The data in Figure 7-27 and Figure 7-28 confirmed these trends. The carbon monoxide emissions increased as the intake oxygen was reduced and low temperature combustion resulted in a yield of 1.3%V of carbon monoxide. The hydrogen yield also increased to 0.37%V when the intake oxygen was reduced to 9.5%V. Such high quantities of CO and hydrogen would be expected to improve the LNT regeneration performance as discussed in the literature review. Figure 7-27 further illustrated that the effect of LTC was greater than the effect of the intake oxygen. There was a fairly linear increase in the CO and hydrogen as the intake oxygen was reduced from 20.4 to 11.7%V under high temperature combustion. However, CO and hydrogen increased exponentially when the intake oxygen was reduced from 11.7 to 9.5%V under the LTC combustion regime. Thus, the combination of low intake oxygen and LTC provided particularly suitable reaction kinetics for the in-cylinder formation of hydrogen and carbon monoxide.

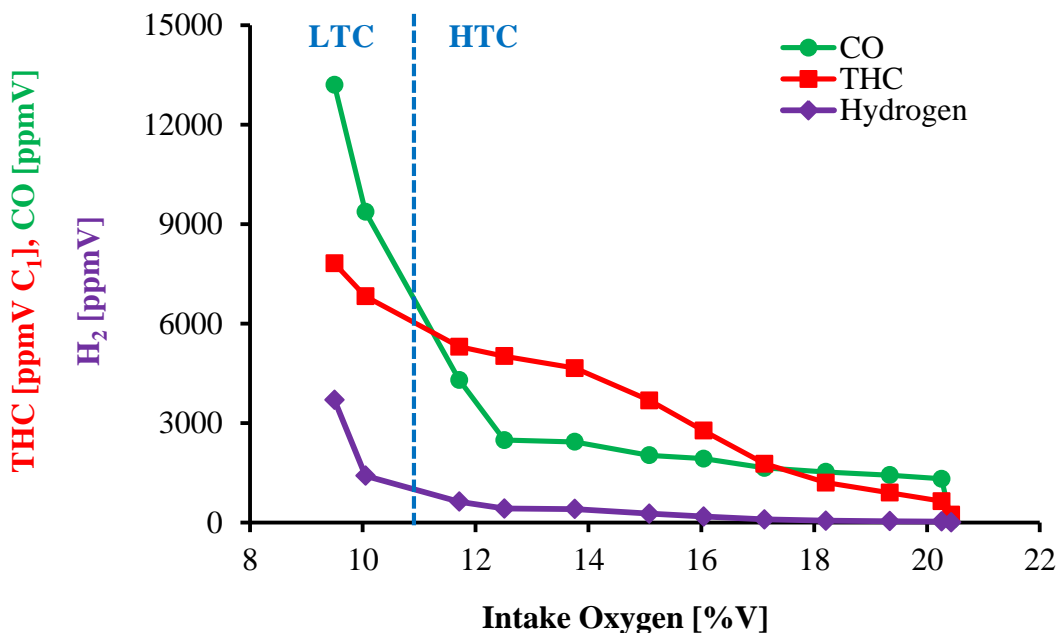


Figure 7-27: Effect of Intake Oxygen Sweep on H₂, CO, and THC

The hydrocarbon speciation results are given in Figure 7-28. The trends were consistent with the previous test results. All of the light hydrocarbon species increased as the intake oxygen was reduced under high temperature combustion. However, there was an abrupt and significant reduction of most light hydrocarbons when the intake oxygen was further reduced to the low temperature combustion region; only methane continued to increase. These test results suggested that LTC reaction kinetics were not effective for the formation of reactive light hydrocarbons like propylene and ethylene. Moreover, there was a methane emission penalty for the production of hydrogen and carbon monoxide via LTC.

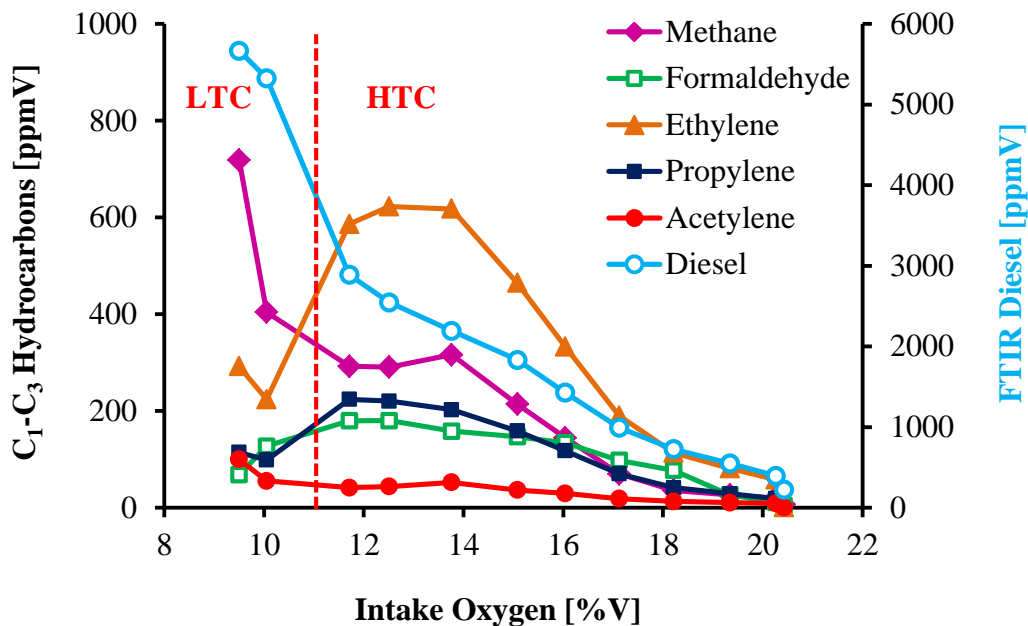


Figure 7-28: Effect of Intake Oxygen Sweep on Hydrocarbon Speciation

An additional post injection timing sweep was conducted under LTC conditions as shown in Table 7-6. The purpose of the test was to produce a higher yield of hydrogen compared to the previous test results. The fuel injection pressure was increased to 1500 bar, the post injection duration was increased to 300 μ s, the intake oxygen was reduced to 9.1%, and the combustion phasing was delayed to 9 $^{\circ}$ CA ATDC. The IMEP was within the same range as previous tests. For reference, the NO_x and smoke emission results are

given in Figure C-11 in the appendix. The results showed that the smoke and the NO_x emissions were ultra-low throughout the post injection timing sweep, providing a confirmation of LTC.

Table 7-6: Test Conditions for LTC Post Injection Sweep Study

IMEP [bar]	5.3 – 6.4
Fuel	Diesel
Intake Oxygen [% Volume]	9.1
Air Intake Pressure [bar absolute]	1.9
Main Injection CA50 [°CA ATDC]	9
Fuel Injection Pressure [bar]	1500
Main Injection Timing [°CA ATDC]	-5
Main Injection Duration [μs]	480
Post Injection Timing [°CA ATDC]	Sweep
Post Injection Duration [μs]	300

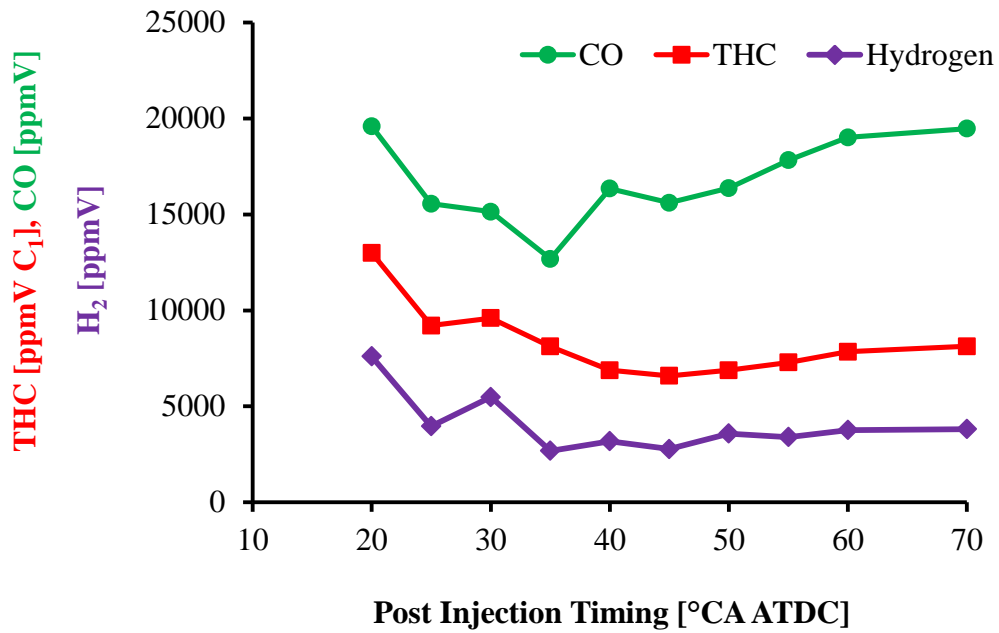


Figure 7-29: Effect of LTC Post Injection Timing Sweep on H₂, CO, and THC

The results in Figure 7-29 showed that the increased fuel injection, the lower intake oxygen with LTC, and the delayed combustion phasing increased the yield of hydrogen, carbon monoxide, and total hydrocarbons. An early post injection produced the highest yield with 1.96%V of carbon monoxide, 0.76%V of hydrogen, and 1.3%V of total hydrocarbons. Such a high yield of carbon monoxide and hydrogen would benefit the LNT regeneration and desulfation processes.

The hydrocarbon speciation results are illustrated in Figure 7-30. Methane was revealed to be the most abundant light hydrocarbon throughout the post injection timing sweep and this was consistent with the previous results in Figure 7-26. The peak yield of 0.30% of methane was achieved with the earliest post injection timing, confirming the elevated methane emission penalty for hydrogen formation. The results in Figure 7-30 also showed that the use of early post injections significantly increased the formation of ethylene, up to 0.19% V. The ethylene yield represented a significant increase compared to the previous results. The large yield of ethylene would be useful for after-treatment devices. In summary, the use of LTC with reduced intake oxygen and a relatively early post injection achieved the highest yield of hydrogen, carbon monoxide, and ethylene but at the cost of increased methane emissions.

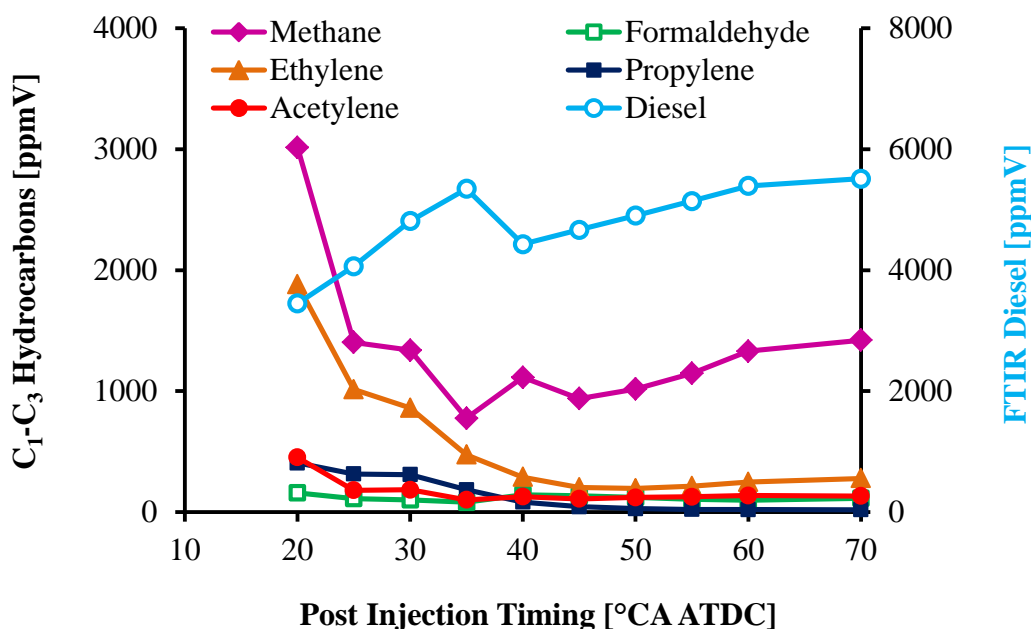


Figure 7-30: Effect of LTC Post Injection Timing Sweep on Hydrocarbon Speciation

7.5 Chapter Summary for Exhaust Gas Management

Exhaust after-treatment devices achieve optimal performance at selected operating conditions. The lean NO_x trap, in particular, has specific temperature ranges for improved performance of NO_x storage, regeneration, and desulfation processes. Furthermore, the use of hydrogen, carbon monoxide, and light hydrocarbons as NO_x reducing agents can help improve the NO_x conversion efficiency of the LNT. However, diesel exhaust gas temperatures can vary widely and the presence of H₂, CO, and light hydrocarbons is generally scarce in the lean-burn exhaust of conventional diesel engines. Thus, post injection strategies for active exhaust gas control were developed to provide suitable conditions for enhancing the performance of an LNT after-treatment system. The experiments in this chapter investigated the effects of the post injection timing and duration, the engine load, the combustion phasing, the intake oxygen, and low temperature combustion on the exhaust gas management.

The tests results demonstrated that the exhaust gas temperature was effectively controlled by adjusting the post injection duration of early post injections. A suitable post injection timing for exhaust gas temperature control was identified based on reducing the effect of the post injection on the smoke emissions. The results showed that the suitable post injection timing was relatively early in the expansion stroke and that it was slightly retarded when the engine load was increased. Relatively high amounts of intake oxygen were preferred for exhaust gas temperature control. Therefore, the results concluded that post injections can be utilized to control the exhaust temperature and to potentially improve the performance of an LNT after-treatment system without a significant impact on the smoke emissions.

The post injection timing and duration, the intake oxygen, and the use of LTC were crucial factors for the in-cylinder production of desirable NO_x reducing agents. In particular, a post injection timing sweep indicated that very early post injections with low intake oxygen and low temperature combustion produced increased yields of H₂, CO, and ethylene. Under these conditions, the hydrogen yield reached 0.76% V, carbon monoxide reached 1.96% V, and ethylene reached 0.19% V. The main drawback of this strategy was the relatively high methane, up to 0.30% V. Based on these results, a conclusion was

reached that LNT performance could be potentially improved by using low intake oxygen, low temperature combustion, and an early post injection to produce high yields of hydrogen, carbon monoxide, and light hydrocarbons like propylene for the LNT regeneration process. Future work is recommended to quantify the potential benefits of the exhaust temperature and composition control strategies on the storage, regeneration, and desulfation processes of an LNT.

CHAPTER 8: CONCLUSIONS AND FUTURE WORK

This chapter provides a summary of the main research results and the pertinent conclusions that derived from those results. Recommendations for future research are also provided.

8.1 Long Breathing LNT with Diesel Fuel and EGR

A novel long breathing technique was devised to extend the NO_x storage cycle of the LNT and to lower the supplemental fuel consumption compared to conventional strategies with relatively short NO_x storage cycles. Engine tests were carried out with diesel fuel and EGR at a broad range of engine load conditions, ranging from 6 to 15 bar IMEP. The application of EGR reduced the engine-out NO_x emissions to a range of 0.4 to 0.8 g/kW·hr (50 to 100 ppmV), which was suitable for the long breathing strategy.

The data from the engine tests were combined with a numerical LNT after-treatment model to determine the supplemental fuel penalty and the combined fuel consumption from the engine and the LNT. The results revealed that the use of the long breathing LNT strategy resulted in an extended NO_x storage cycle that led to less frequent fuel-rich regeneration cycles and reduced supplemental fuel consumption at all tested conditions. The long breathing method was found to be more effective at low load conditions of 6 bar IMEP. The use of long breathing reduced the supplemental fuel penalty from a range of 1.7 to 4.7% to a range of 0.2 to 0.4% and reduced the fuel consumption from a range of 183.3-187.8 g/kW·hr to a range of 181.5-182.6 g/kW·hr.

Long breathing at medium load conditions, 10 bar IMEP, was also suitable since the net supplemental fuel savings of the long breathing LNT outweighed the slightly increased fuel consumption from the engine. For high load operation at 14 bar IMEP, long breathing had a negligible effect on the overall fuel consumption because of the increased fuel consumption from the engine. High load conditions also resulted in a noticeable smoke emission penalty when long breathing was used with EGR.

8.2 High Load Operation with Neat Butanol Fuel

Engine tests were carried out to determine suitable exhaust gas conditions for long breathing operation with the direct injection of neat n-butanol in a lean-burn compression ignition engine. A load sweep with a single shot fuel injection strategy was conducted for neat n-butanol combustion and the results were compared to diesel fuel combustion. The results confirmed that neat n-butanol combustion offered significant reductions for the NO_x and smoke emissions throughout the load sweep. However, excessive peak pressure rise rates, such as $17 \text{ bar}/^\circ\text{CA}$ and higher, limited the butanol load sweep to below 7 bar IMEP while the diesel fuel tests achieved loads above 10 bar IMEP with peak pressure rise rates below $7 \text{ bar}/^\circ\text{CA}$. Further neat butanol tests were required to demonstrate high load operation, at 14 bar IMEP, with a tolerable peak pressure rise rate, below $17 \text{ bar}/^\circ\text{CA}$.

Neat butanol tests with delayed single shot injection, pilot injection, and post injection strategies were conducted at constant load conditions to investigate the impact on the peak pressure rise rate. The results determined that the post injection strategy provided the greatest reduction of the peak pressure rise rate at constant load conditions. However, high load operation was challenging to achieve with a single post injection because the use of a large post injection advanced the combustion phasing of the main injection and caused increased peak pressure rise rates. Additional single post injection, double post injection, and triple post injection strategies were investigated and the results revealed that the double post injection strategy was the most suitable for high load operation for the tested conditions. The use of the double post injection strategy achieved a load of 14 bar IMEP with a peak pressure rise rate below $15 \text{ bar}/^\circ\text{CA}$.

8.3 Long Breathing LNT with Neat Butanol Fuel

The use of long breathing with neat n-butanol fuel was investigated. Exhaust gas data from the engine tests were combined with a numerical LNT model. The results indicated that the long breathing strategy was especially appropriate for low load conditions with neat n-butanol. Low load operation, at 6 bar IMEP, exhibited extremely

low engine-out NO_x emissions that allowed prolonged NO_x storage cycles, extending over four hours in certain instances, with ultra-low supplemental fuel penalties of 0.06 to 0.61%.

Long breathing operation extended the NO_x storage cycle and reduced the supplemental fuel consumption at medium load conditions of 10 bar IMEP. However, the supplemental fuel savings were far inferior to the increased fuel consumption from the engine for long breathing operation. Thus, the long breathing strategy was not suitable for medium load operation with neat n-butanol for the tested conditions. Long breathing with neat butanol was not demonstrated at high load conditions, such as 14 bar IMEP, due to the relatively high engine-out NO_x emissions of 1.97 g/kW·hr that were outside the range for long breathing.

8.4 Active Control of the Exhaust Gas Temperature and Composition

The performance of a lean NO_x trap is sensitive to the exhaust gas temperature while the presence of species such as hydrogen, carbon monoxide, and light hydrocarbons can improve the LNT regeneration and desulfation performance. Post injection strategies were developed for active control of the exhaust gas temperature and composition. A post injection strategy was successfully implemented for active management of the exhaust gas temperature through control of the duration of relatively early post injections, such as 20 to 50°CA ATDC. However, the use of relatively early post injections also increased the smoke emissions. A suitable post injection timing was discovered that allowed effective management of the exhaust temperature while mitigating the effect on the smoke emissions. Relatively high amounts of intake oxygen, 16.5 to 20.7%V for the tested conditions, were preferred for exhaust gas temperature control.

In contrast, the combination of low temperature combustion, low intake oxygen (such as 9.5%V), and an early post injection led to an exponential increase of desirable NO_x reducing agents like hydrogen, carbon monoxide, and ethylene. A hydrogen yield of 0.76%V, a carbon monoxide yield of 1.96%V, and an ethylene yield of 0.19%V with

low NO_x and smoke emissions were demonstrated. These results established that high yields of hydrogen were obtained with low temperature combustion despite the relatively low in-cylinder temperatures. However, this strategy increased the methane emissions, up to 0.30% V for the tested conditions. Medium intake oxygen levels, such as 16.5% V, were also suitable for the production of desirable NO_x reducing agents but the formation of these species was sensitive to the post injection timing.

8.5 Recommendations for Future Work

Future work is proposed to determine if the use of higher fuel injection pressures and higher intake air pressures would promote the use of long breathing operation at high load conditions with diesel fuel and EGR since higher fuel injection and air intake pressures may reduce the smoke emission penalty. Engine tests with an LNT integrated into the exhaust are advised to confirm the numerical calculation results and to remove the effects of the uncertainty of the numerical model results. Additionally, the use of a broader range of lean-burn CI test engines is recommended to verify the repeatability of the long breathing results across a broader range of experimental setups.

For long breathing with neat butanol, the use of in-cylinder gas sampling is proposed to help explain the phenomenon of the advanced combustion phasing of the main injection due to the increased duration of the post injection. Analysis of the residual gas composition would also be beneficial. Further neat butanol studies with a pilot injection are recommended with a higher compression ratio engine, such as 20:1 or higher. An engine with a higher compression ratio may achieve adequate in-cylinder temperatures for auto-ignition of a butanol pilot injection, which can potentially reduce the peak pressure rise rates and improve the overall fuel consumption compared to the use of multiple post injections.

Additional tests are proposed to investigate the use of EGR with the use of a single post injection strategy at medium load conditions and with the use of a double post injection strategy at high load conditions for neat butanol tests. The use of EGR with neat butanol may allow for reduced engine-out NO_x emissions that may justify the use of

the long breathing strategy at medium and high load conditions like 10 bar IMEP and higher. The use of n-butanol fuel for LNT regeneration is also proposed for future work. Experimental tests with the after-treatment flow bench are recommended to determine the suitability of neat n-butanol as a NO_x reducing agent and to compare the results to the use of diesel fuel, carbon monoxide, and hydrogen.

The active exhaust gas management strategies were demonstrated with diesel fuel and similar tests are proposed with other fuels, for example butanol or blended fuels. The use of different fuels may give different trends, particularly with regards to the effects of the post injection on the formation of hydrogen, carbon monoxide, and light hydrocarbons. Investigations are also recommended to compare the use of the in-cylinder post injection strategies and the use of exhaust fuel injections with catalytic reactors to determine the more fuel efficient method for the production of hydrogen, carbon monoxide, and light hydrocarbons. Additional engine tests are suggested to determine the potential benefits of active exhaust gas management on the NO_x storage, regeneration, and desulfation processes of an LNT.

REFERENCES

1. Heywood, J.B., “Internal Combustion Engine Fundamentals”, McGraw-Hill Book Company, Singapore, 1988.
2. Stone, R. “Introduction to Internal Combustion Engines”, SAE International, Warrendale, Pennsylvania, USA, 2012.
3. Airgas, “Safety Data Sheet: Nitric Oxide”, 2014, 001039.
4. Bruckdorfer, R., “The Basics about Nitric Oxide”, *Molecular Aspects of Medicine* 26 (2005) 3–31, 2005.
5. Weinberger, B., Laskin, D.L., Heck, D.E., and Laskin, J.D., “The Toxicology of Inhaled Nitric Oxide”, *Toxicological Sciences* 59 (1) 5–16, 2001, doi: 10.1093/toxsci/59.1.5.
6. Airgas, “Safety Data Sheet: Nitrogen Dioxide”, 2014, 001041.
7. Miller, O.I., Celermajer, D.S., Deanfield, J.E., and Macrae, D.J., “Guidelines for the Safe Administration of Inhaled Nitric Oxide”, *Archives of Disease in Childhood* 70 F47-F49, 1994.
8. New Jersey Department of Health and Senior Services, “Hazardous Substance Fact Sheet: Nitrogen Dioxide”, 2000, CAS Number 10102-44-0.
9. US Department of Transportation, “Recent Examinations of Mobile Source Air Toxics: Change in Heavy-Duty Truck Emission Standards, 1988 – 2010”, 2010.
10. Johnson, T., “Vehicular Emissions in Review”, *SAE Int. J. Engines* 6 (2) 699-715, 2013, doi:10.4271/2013-01-0538.
11. California Environmental Protection Agency Air Resources Board, “Technology Assessment: Lower NO_x Heavy-Duty Diesel Engines”, Draft, 2015, url: http://www.arb.ca.gov/msprog/tech/techreport/diesel_tech_report.pdf, Accessed: 29 February 2016.
12. State of California Air Resources Board, “Evaluating Technologies and Methods to Lower Nitrogen Oxide Emissions from Heavy-Duty Vehicles”, Agenda Item No. 13-6-1, 2013.

13. US Department of Transportation, "2017 and Later Model Year Light-Duty Vehicle Greenhouse Gas Emissions and Corporate Average Fuel Economy Standards; Final Rule", Federal Register 77 (199) 62623–63200, 2012.
14. Andersen, P., Ballinger, T., Bennett, C., and Lafyatis, D., "Development and System Application of an Ultra Low Loaded Precious Metal Catalyst Technology on LEV2 Vehicles," SAE Technical Paper 2004-01-1271, 2004, doi:10.4271/2004-01-1271.
15. US Department of Energy, "Fact #716: February 27, 2012 Diesels are More than Half of New Cars Sold in Western Europe", 2012.
16. Chen, S., "Simultaneous Reduction of NO_x and Particulate Emissions by Using Multiple Injections in a Small Diesel Engine", SAE Technical Paper 2000-01-3084, 2000, doi:10.4271/2000-01-3084.
17. Tanin, K., Wickman, D., Montgomery, D., Das, S. et al., "The Influence of Boost Pressure on Emissions and Fuel Consumption of a Heavy-Duty Single-Cylinder D.I. Diesel Engine", SAE Technical Paper 1999-01-0840, 1999, doi:10.4271/1999-01-0840.
18. Flynn, P., Hunter, G., Durrett, R., Farrell, L. et al., "Minimum Engine Flame Temperature Impacts on Diesel and Spark-Ignition Engine NO_x Production," SAE Technical Paper 2000-01-1177, 2000, doi:10.4271/2000-01-1177.
19. Ladommatos, N., Abdelhalim, S., Zhao, H., and Hu, Z., "The Dilution, Chemical, and Thermal Effects of Exhaust Gas Recirculation on Diesel Engine Emissions - Part 1: Effect of Reducing Inlet Charge Oxygen", SAE Technical Paper 961165, 1996, doi:10.4271/961165.
20. Ladommatos, N., Abdelhalim, S., Zhao, H., and Hu, Z., "The Dilution, Chemical, and Thermal Effects of Exhaust Gas Recirculation on Diesel Engine Emissions - Part 2: Effects of Carbon Dioxide", SAE Technical Paper 961167, 1996, doi:10.4271/961167.
21. Ladommatos, N., Abdelhalim, S., Zhao, H., and Hu, Z., "The Dilution, Chemical, and Thermal Effects of Exhaust Gas Recirculation on Diesel Engine Emissions - Part 3: Effects of Water Vapour", SAE Technical Paper 971659, 1997, doi:10.4271/971659.

22. Ladommatos, N., Abdelhalim, S., Zhao, H., and Hu, Z., “The Dilution, Chemical, and Thermal Effects of Exhaust Gas Recirculation on Diesel Engine Emissions - Part 4: Effects of Carbon Dioxide and Water Vapour”, SAE Technical Paper 971660, 1997, doi:10.4271/971660.
23. Kreso, A., Johnson, J., Gratz, L., Bagley, S. et al., “A Study of the Effects of Exhaust Gas Recirculation on Heavy-Duty Diesel Engine Emissions”, SAE Technical Paper 981422, 1998, doi:10.4271/981422.
24. Kohketsu, S., Mori, K., Sakai, K., and Hakozaiki, T., “EGR Technologies for a Turbocharged and Intercooled Heavy-Duty Diesel Engine”, SAE Technical Paper 970340, 1997, doi:10.4271/970340.
25. Baert, R., Beckman, D., and Veen, A., “Efficient EGR Technology for Future HD Diesel Engine Emission Targets”, SAE Technical Paper 1999-01-0837, 1999, doi:10.4271/1999-01-0837.
26. Verbeek, R., van Aken, M., and Verkiel, M., “DAF Euro-4 Heavy Duty Diesel Engine with TNO EGR system and CRT Particulates Filter”, SAE Technical Paper 2001-01-1947, 2001, doi:10.4271/2001-01-1947.
27. Zheng, M., Reader, G.T., and Hawley, J.G., “Diesel Engine Exhaust Gas Recirculation – A Review on Advanced and Novel Concepts”, *Energy Conversion and Management* 45 (2004): 883-900, 2004.
28. Alriksson, M. and Denbratt, I., “Low Temperature Combustion in a Heavy Duty Diesel Engine Using High Levels of EGR”, SAE Technical Paper 2006-01-0075, 2006, doi:10.4271/2006-01-0075.
29. Zheng, M., Asad, U., Reader, G.T., Tan, Y., and Wang, M., “Energy Efficiency Improvement Strategies for a Diesel Engine in Low-temperature Combustion”, *International Journal of Energy Research* 33 8–28, 2009, doi: 10.1002/er.1464.
30. de Ojeda, W., Zoldak, P., Espinosa, R., and Kumar, R., “Development of a Fuel Injection Strategy for Diesel LTC”, SAE Technical Paper 2008-01-0057, 2008, doi:10.4271/2008-01-0057.
31. Han, S., Kim, J., and Bae, C., “Effect of Air–Fuel Mixing Quality on Characteristics of Conventional and Low Temperature Diesel Combustion”, *Applied Energy* 119 (2014) 454–466, 2014, doi:10.1016/j.apenergy.2013.12.045.

32. Zheng, M. and Kumar, R., “Implementation of Multiple-Pulse Injection Strategies to Enhance the Homogeneity for Simultaneous Low-NO_x and -Soot Diesel Combustion”, *International Journal of Thermal Sciences* 48 (2009) 1829–1841, 2009, doi:10.1016/j.ijthermalsci.2009.02.009.
33. Pickett, L. and Siebers, D., “Non-Sooting, Low Flame Temperature Mixing-Controlled DI Diesel Combustion”, *SAE Technical Paper* 2004-01-1399, 2004, doi:10.4271/2004-01-1399.
34. Asad, U. and Zheng, M., “EGR Oxidation and Catalytic Fuel Reforming for Diesel Engines”, *Proceedings of the ASME Internal Combustion Engine Division 2008 Spring Technical Conference ICES2008-1684* 87-97, 2008, doi:10.1115/ICES2008-1684.
35. Zheng, M., Asad, U., Kumar, R., Reader, G. et al., “An Investigation of EGR Treatment on the Emission and Operating Characteristics of Modern Diesel Engines”, *SAE Technical Paper* 2007-01-1083, 2007, doi:10.4271/2007-01-1083.
36. Hountalas, D., Kouremenos, D., Binder, K., Schwarz, V. et al., “Effect of Injection Pressure on the Performance and Exhaust Emissions of a Heavy Duty DI Diesel Engine”, *SAE Technical Paper* 2003-01-0340, 2003, doi:10.4271/2003-01-0340.
37. Fulton, B. and Leviticus, L., “Variable Injection Timing Effects on the Performance and Emissions of a Direct Injection Diesel Engine”, *SAE Technical Paper* 932385, 1993, doi:10.4271/932385.
38. Hardy, W. and Reitz, R., “An Experimental Investigation of Partially Premixed Combustion Strategies Using Multiple Injections in a Heavy-Duty Diesel Engine”, *SAE Technical Paper* 2006-01-0917, 2006, doi:10.4271/2006-01-0917.
39. Zheng, M., Li, T., and Han, X., “Direct Injection of Neat n-Butanol for Enabling Clean Low Temperature Combustion in a Modern Diesel Engine”, *Fuel* 142 28-37, 2015, doi:10.1016/j.fuel.2014.10.075.
40. Yanai, T., Han, X., Wang, M., Reader, G. et al., “Clean Combustion in a Diesel Engine Using Direct Injection of Neat n-Butanol”, *SAE Technical Paper* 2014-01-1298, 2014, doi:10.4271/2014-01-1298.

41. Liu, H., Li, S., Zheng, Z., et al, "Effects of n-Butanol, 2-Butanol, and Methyl Octynoate Addition to Diesel Fuel on Combustion and Emissions over a Wide Range of Exhaust Gas Recirculation (EGR) Rates", *Applied Energy* 112 246-256, 2013, doi:10.1016/j.apenergy.2013.06.023.
42. Chen, Z., Liu, J., Wu, Z., and Lee, C., "Effects of Port Fuel Injection (PFI) of n-Butanol and EGR on Combustion and Emissions of a Direct Injection Diesel Engine", *Energy Conversion and Management* 76 725-731, 2013, doi:10.1016/j.enconman.2013.08.030.
43. Maurya, R.K., and Agarwal, A.K., "Experimental Study of Combustion and Emission Characteristics of Ethanol Fuelled Port Injected Homogeneous Charge Compression Ignition (HCCI) Combustion Engine", *Applied Energy* 88 (4) 1169-1180, 2011, doi:10.1016/j.apenergy.2010.09.015.
44. Han, X., Zheng, M., and Wang, J., "Fuel Suitability for Low Temperature Combustion in Compression Ignition Engines", *Fuel* 109 336-349, 2013, doi:10.1016/j.fuel.2013.01.049.
45. Lee, J., Choi, S., Lee, J., Shin, S. et al., "Emission Reduction using a Close Post Injection Strategy with a Modified Nozzle and Piston Bowl Geometry for a Heavy EGR Rate", *SAE Technical Paper* 2012-01-0681, 2012, doi:10.4271/2012-01-0681.
46. Hotta, Y., Inayoshi, M., Nakakita, K., Fujiwara, K. et al., "Achieving Lower Exhaust Emissions and Better Performance in an HSDI Diesel Engine with Multiple Injection", *SAE Technical Paper* 2005-01-0928, 2005, doi:10.4271/2005-01-0928.
47. Desantes, J., Arrègle, J., López, J., and García, A., "A Comprehensive Study of Diesel Combustion and Emissions with Post-injection", *SAE Technical Paper* 2007-01-0915, 2007, doi:10.4271/2007-01-0915.
48. Desantes, J., Bermudez, V., Garcia, A., Linares, W. et al., "An Investigation of Particle Size Distributions with Post Injection in DI Diesel Engines", *SAE Technical Paper* 2011-01-1379, 2011, doi:10.4271/2011-01-1379.

49. Nimodia, S., Senthilkumar, K., Halbe, V., Ghodke, P. et al., "Simultaneous Reduction of NO_x and Soot Using Early Post Injection", SAE Technical Paper 2013-26-0055, 2013, doi:10.4271/2013-26-0055.
50. Park, Y. and Bae, C., "Effects of Single and Double Post Injections on Diesel PCCI Combustion", SAE Technical Paper 2013-01-0010, 2013, doi:10.4271/2013-01-0010.
51. de Ojeda, W., Zoldak, P., Espinosa, R., and Kumar, R., "Development of a Fuel Injection Strategy for Partially Premixed Compression Ignition Combustion", SAE Int. J. Engines 2(1):1473-1488, 2009, doi:10.4271/2009-01-1527.
52. Storey, J.M., Lewis Sr., S.A., West, B.H., Huff, S.P., et al, "Hydrocarbon Species in the Exhaust of Diesel Engines Equipped with Advanced Emission Control Devices", Final Report CRC Project No. AVFL-10b-2, 2005.
53. Jeftić, M., Asad, U., Han, X., Xie, K., et al, "An Analysis of the Production of Hydrogen and Hydrocarbon Species by Diesel Post Injection Combustion", Proceedings of the ASME 2011 Internal Combustion Engine Division Fall Technical Conference ICEF2011-60135, 2011, doi:10.1115/ICEF2011-60135.
54. Yao, M., Wang, H., Zheng, Z., and Yue, Y., "Experimental Study of n-Butanol Additive and Multi-injection on HD Diesel Engine Performance and Emissions", Fuel 89 (9) 2191-2201, 2010, doi:10.1016/j.fuel.2010.04.008.
55. West, B., Huff, S., Parks, J., Swartz, M. et al., "In-Cylinder Production of Hydrogen During Net-Lean Diesel Operation", SAE Technical Paper 2006-01-0212, 2006, doi:10.4271/2006-01-0212.
56. Gekas, I., Vressner, A., and Johansen, K., "NO_x Reduction Potential of V-SCR Catalyst in SCR/DOC/DPF Configuration Targeting Euro VI Limits from High Engine NO_x Levels", SAE Technical Paper 2009-01-0626, 2009, doi:10.4271/2009-01-0626.
57. Grossale, A., Nova, I., and Tronconi, E., "Study of a Fe-zeolite-based System as NH₃-SCR Catalyst for Diesel Exhaust Aftertreatment", Catalysis Today 136 (2008) 18-27, 2008, doi:10.1016/j.cattod.2007.10.117.
58. Prikhodko, V.Y., Pihl, J.A., Lewis Sr., S.A., and Parks II, J.E., "Effect of Hydrocarbon Emissions from PCCI-Type Combustion on the Performance of

- Selective Catalytic Reduction Catalysts”, Proceedings of the ASME 2011 Internal Combustion Engine Division Fall Technical Conference, 2011 ICEF2011-60129, 2011, doi:10.1115/ICEF2011-60129.
59. Miller, W., Klein, J., Mueller, R., Doelling, W. et al., “The Development of Urea-SCR Technology for US Heavy Duty Trucks”, SAE Technical Paper 2000-01-0190, 2000, doi:10.4271/2000-01-0190.
60. Oha, J. and Lee, K., “Spray Characteristics of a Urea Solution Injector and Optimal Mixer Location to Improve Droplet Uniformity and NO_x Conversion Efficiency for Selective Catalytic Reduction”, Fuel 119 (2014) 90–97, 2014, doi:10.1016/j.fuel.2013.11.032.
61. Brandenberger, S., Kröcher, O., Tissler, A., and Althoff, R., “The State of the Art in Selective Catalytic Reduction of NO_x by Ammonia Using Metal-Exchanged Zeolite Catalysts”, Catalysis Reviews: Science and Engineering 50 (4) 492-531, 2008, doi:10.1080/01614940802480122.
62. Madia, G., Koebel, M., Elsener, M., and Wokaun, A., “The Effect of an Oxidation Precatalyst on the NO_x Reduction by Ammonia SCR”, Industrial and Engineering Chemistry Research 41 (15) 3512-3517, 2002, doi:10.1021/ie0200555.
63. Devarakonda, M., Parker, G., Johnson, J., Strots, V. et al., “Model-Based Estimation and Control System Development in a Urea-SCR Aftertreatment System”, SAE Int. J. Fuels Lubr. 1(1):646-661, 2009, doi:10.4271/2008-01-1324.
64. Folić, M., Lemus, L., Gekas, I., and Vressner, A., “Selective Ammonia Slip Catalyst Enabling Highly Efficient NO_x Removal Requirements of the Future”, US Department of Energy, Directions in Engine-Efficiency and Emissions Research Conference, 2010, Detroit, MI.
65. Chen, X., Currier, N., Yezerets, A., and Kamasamudram, K., “Mitigation of Platinum Poisoning of Cu-Zeolite SCR Catalysts”, SAE Int. J. Engines 6(2):856-861, 2013, doi:10.4271/2013-01-1065.
66. Cavataio, G., Jen, H., Girard, J., Dobson, D. et al., “Impact and Prevention of Ultra-Low Contamination of Platinum Group Metals on SCR Catalysts Due to DOC Design”, SAE Int. J. Fuels Lubr. 2(1):204-216, 2009, doi:10.4271/2009-01-0627.

67. Jen, H., Girard, J., Cavataio, G., and Jagner, M., “Detection, Origin and Effect of Ultra-Low Platinum Contamination on Diesel-SCR Catalysts”, *SAE Int. J. Fuels Lubr.* 1(1):1553-1559, 2009, doi:10.4271/2008-01-2488.
68. Kamasamudram, K., Henry, C., Yezerets, A., “N₂O Emissions from 2010 SCR Systems”, US Department of Energy, Directions in Engine-Efficiency and Emissions Research Conference, 2011, Detroit, MI.
69. Smith, M., Depcik, C., Hoard, J., Bohac, S. et al., “The Effects of CO, H₂, and C₃H₆ on the SCR Reactions of an Fe Zeolite SCR Catalyst”, SAE Technical Paper 2013-01-1062, 2013, doi:10.4271/2013-01-1062.
70. Levin, M. and Baker, R., “Co-fueling of Urea for Diesel Cars and Trucks”, SAE Technical Paper 2002-01-0290, 2002, doi:10.4271/2002-01-0290.
71. Cummins Filtration, “Diesel Exhaust Fluid (DEF) Q&A”, 2009, MB10033-Rev10.
72. Hirata, K., Masaki, N., Ueno, H., and Akagawa, H., “Development of Urea-SCR System for Heavy-Duty Commercial Vehicles”, SAE Technical Paper 2005-01-1860, 2005, doi:10.4271/2005-01-1860.
73. ScienceLab.com, “Urea Material Safety Data Sheet”, 2013, 57-13-6.
74. Adelman, K., Soeger, N., and Pauly, T., “Advanced Metal-Oxide based SCR Catalysts”, US Department of Energy, Directions in Engine-Efficiency and Emissions Research Conference, 2010, Detroit, MI.
75. Forzatti, P., Lietti, L., Nova, I., and Tronconi, E., “Diesel NO_x Aftertreatment Catalytic Technologies: Analogies in LNT and SCR Catalytic Chemistry”, *Catalysis Today* 151 (3-4) 202–211, 2010, doi:10.1016/j.cattod.2010.02.025.
76. Castoldi, L., Lietti, L., Nova, I., Matarrese, R., et al., “Alkaline- and Alkaline-Earth Oxides based Lean NO_x Traps: Effect of the Storage Component on the Catalytic Reactivity”, *Chemical Engineering Journal* 161 (3) 416–423, 2010 doi:10.1016/j.cej.2009.10.065.
77. Dou, D. and Balland, J., “Impact of Alkali Metals on the Performance and Mechanical Properties of NO_x Adsorber Catalysts”, SAE Technical Paper 2002-01-0734, 2002, doi:10.4271/2002-01-0734.

78. Theis, J., Ura, J., Goralski, C., Jen, H. et al., “The Effect of Ceria Content on the Performance of a NO_x Trap”, SAE Technical Paper 2003-01-1160, 2003, doi:10.4271/2003-01-1160.
79. West, B., Huff, S., Parks, J., Lewis, S. et al., “Assessing Reductant Chemistry During In-Cylinder Regeneration of Diesel Lean NO_x Traps”, SAE Technical Paper 2004-01-3023, 2004, doi:10.4271/2004-01-3023.
80. Parks, J., West, B., Swartz, M., and Huff, S., “Characterization of Lean NO_x Trap Catalysts with In-Cylinder Regeneration Strategies”, SAE Technical Paper 2008-01-0448, 2008, doi:10.4271/2008-01-0448.
81. Parks, J., Watson, A., Campbell, G., and Epling, B., “Durability of NO_x Absorbers: Effects of Repetitive Sulfur Loading and Desulfation”, SAE Technical Paper 2002-01-2880, 2002, doi:10.4271/2002-01-2880.
82. Kočí, P., Marek, M., Kubíček, M., Maunulad, T., et al., “Modelling of Catalytic Monolith Converters with Low- and High-Temperature NO_x Storage Compounds and Differentiated Washcoat”, Chemical Engineering Journal 97 (2-3) 131–139, 2004, doi:10.1016/S1385-8947(03)00151-7.
83. Theis, J., Ura, J., Li, J., Surnilla, G. et al., “NO_x Release Characteristics of Lean NO_x Traps During Rich Purges”, SAE Technical Paper 2003-01-1159, 2003, doi:10.4271/2003-01-1159.
84. Kočí, P., Plát, F., Štěpánek, J., Bártová, Š., et al., “Global Kinetic Model for the Regeneration of NO_x Storage Catalyst with CO, H₂ and C₃H₆ in the Presence of CO₂ and H₂O”, Catalysis Today 147S S257–S264, 2009, doi:10.1016/j.cattod.2009.07.036.
85. Olsson, L., Fredriksson, M., and Blint, R.J., “Kinetic Modeling of Sulfur Poisoning and Regeneration of Lean NO_x Traps”, Applied Catalysis B: Environmental 100 (1-2) 31–41, 2010, doi:10.1016/j.apcatb.2010.07.004.
86. Johnson, T., “Diesel Emission Control in Review”, SAE Technical Paper 2006-01-0030, 2006, doi:10.4271/2006-01-0030.
87. West, B. and Sluder, C., “NO_x Adsorber Performance in a Light-Duty Diesel Vehicle”, SAE Technical Paper 2000-01-2912, 2000, doi:10.4271/2000-01-2912.

88. Matsumoto, S., Ikeda, Y., Suzuki, H., Ogai, M., et al., “NO_x Storage-Reduction Catalyst for Automotive Exhaust with Improved Tolerance Against Sulfur Poisoning”, *Applied Catalysis B: Environmental* 25 (2-3) 115–124, 2000, doi:10.1016/S0926-3373(99)00124-1.
89. Theis, J., Ura, J., and McCabe, R., “The Effects of Sulfur Poisoning and Desulfation Temperature on the NO_x Conversion of LNT+SCR Systems for Diesel Applications”, *SAE Int. J. Fuels Lubr.* 3(1):1-15, 2010, doi:10.4271/2010-01-0300.
90. Monroe, D. and Li, W., “Desulfation Dynamics of NO_x Storage Catalysts”, *SAE Technical Paper* 2002-01-2886, 2002, doi:10.4271/2002-01-2886.
91. Epling, W.S., Campbell, L.E., Yezerets, A., Currier, N.W., et al., “Overview of the Fundamental Reactions and Degradation Mechanisms of NO_x Storage/Reduction Catalysts”, *Catalysis Reviews: Science and Engineering* 46 (2) 163-245, 2007, doi:10.1081/CR-200031932.
92. United States Environmental Protection Agency, “Heavy-Duty Engine and Vehicle Standards and Highway Diesel Fuel Sulfur Control Requirements”, EPA420-F-00-057, December 2000.
93. Taniguchi, M., Uenishi, M., Tan, I., Tanaka, H. et al., “Thermal Properties of the Intelligent Catalyst”, *SAE Technical Paper* 2004-01-1272, 2004, doi:10.4271/2004-01-1272.
94. Kaneeda, M., Iizuka, H., Higashiyama, K., Kuroda, O. et al., “Improvement of Thermal Resistance for Lean NO_x Catalyst”, *SAE Technical Paper* 2003-01-1166, 2003, doi:10.4271/2003-01-1166.
95. Jeftić, M., and Zheng, M., “Lean NO_x Trap Supplemental Energy Savings with a Long Breathing Strategy,” *Proceedings of the Institution of Mechanical Engineers, Part D: Journal of Automobile Engineering*, 227 (3): 400-408, 2013.
96. Jeftić, M., “A Long Breathing Lean NO_x Trap for Diesel After-treatment Supplemental Energy Reduction”, University of Windsor, 2011.
97. Burch, R. and Coleman, M., “An Investigation of Promoter Effects in the Reduction of NO by H₂ under Lean-burn Conditions”, *Journal of Catalysis* 208 (2) 435-447, 2002, doi:10.1006/jcat.2002.3596.

-
98. Kong, Y., Crane, S., Patel, P., and Taylor, B., "NO_x Trap Regeneration with an On-Board Hydrogen Generation Device", SAE Technical Paper 2004-01-0582, 2004, doi:10.4271/2004-01-0582.
 99. Poulston, S. and Rajaram, R., "Regeneration of NO_x Trap Catalysts", *Catalysis Today* 81 (4) 603-610, 2003, doi:10.1016/S0920-5861(03)00158-5.
 100. Tsolakis, A. and Megaritis, A., "Catalytic Exhaust Gas Fuel Reforming for Diesel Engines - Effects of Water Addition on Hydrogen Production and Fuel Conversion Efficiency", *International Journal of Hydrogen Energy* 29 (13) 1409-1419, 2004, doi:10.1016/j.ijhydene.2004.01.001.
 101. Tsolakis, A., Megaritis, A., and Yap, D., "Application of Exhaust Gas Fuel Reforming in Diesel and Homogeneous Charge Compression Ignition (HCCI) Engines Fuelled with Biofuels", *Energy* 33 (3) 462-470, 2008, doi:10.1016/j.energy.2007.09.011.
 102. Tsolakis, A., Megaritis, A., and Wyszynski, M.L., "Low Temperature Exhaust Gas Fuel Reforming of Diesel Fuel", *Fuel* 83 (13) 1837-1845, 2004, doi:10.1016/j.fuel.2004.03.012.
 103. Holladay, J.D., Hu, J., King, D.L., and Wang, Y., "An Overview of Hydrogen Production Technologies", *Catalysis Today* 139 (4) 244-260, 2009, doi:10.1016/j.cattod.2008.08.039.
 104. Parvary, M., Jazayeri, S.H., Taeb, A., Petit, C., et al., "Promotion of Active Nickel Catalysts in Methane Dry Reforming Reaction by Aluminum Addition", *Catalysis Communications* 2 (11-12) 357-362, 2001, doi:10.1016/S1566-7367(01)00060-7.
 105. Joo, O.S. and Jung, K.D., "CH₄ Dry Reforming on Alumina-Supported Nickel Catalyst", *Bull. Korean Chem. Soc.* 23 (8) 1149-1153, 2002.
 106. Kang, I. and Bae, J., "Autothermal Reforming Study of Diesel for Fuel Cell Application", *Journal of Power Sources* 159 (2) 1283-1290, 2006, doi:10.1016/j.jpowsour.2005.12.048.
 107. EFS, "EFS 8532 IPoD Coil Injector Power Module", 2012, V2.0 20-06-2012.
 108. National Instruments, "NI PXI-8110 User Manual", 2010, 372655D-01.

109. National Instruments, “Multifunction RIO: NI R Series Multifunction RIO User Manual”, 2009, 370489G-01.
110. Kistler Instrument Corporation, “Type 5010B Dual Mode Charge Amplifier with Piezotron® Operating Mode”, 2009, 5010B_000-387a-07.09.
111. Gurley Precision Instruments, “Gurley Series 9X25 Rotary Incremental Encoders”, 2006, 606.
112. SMC Corporation, “Electro-Pneumatic Regulator Electronic Vacuum Regulator”, 2010, OZ 12450SZ.
113. Parker Hannifin Corporation, “K Series Process Control Valves”, 2008, PCV-1/USA 2.5M 10/04 FP.
114. Innospec Fuel Specialties LLC, “Safety Data Sheet OLI-9070.x”, 2015, 10555.
115. National Instruments, “Using the LabVIEW Shared Variable”, 2012, url: <http://www.ni.com/white-paper/4679/en/>, Accessed: 17 May 2016.
116. V&F Analyse und Messtechnik Ges.M.B.H Instrumentation and Environmental Technology, “Technical Description Hydrogen Monitoring System”, 2005, Version 2/02.
117. AVL, “Maintenance Guide AVL 415S Smoke Meter G002”, 2011, AT2483E, Rev.04.
118. MKS Instruments, “MKS Type MultiGas™ Analyzer Models 2030, 2031 and 2032 Hardware Manual”, 2006, 134987-P1 Rev B 09/06.
119. Sassi, A., Noirot, R., Rigaudeau, C., and Belot, G., “Influence of Catalyst Support Geometry and Wall Thickness on NO_x Trap Desulfation: Rich/Lean Wobbling Strategies and Hexagonal Cell supports for High SO₂ Selectivity during Desulfation”, *Topics in Catalysis* 30/31 (1–4) 267-272, 2004, doi:10.1023/B:TOCA.0000029761.68907.96.
120. Lafossas, F.A., Manetas, C., Mohammadi, A., Kalogirou, M., et al., “Sulfation and Lean/Rich Desulfation of a NO_x Storage Reduction Catalyst: Experimental and Simulation Study”, *International Journal of Engine Research* 16 (2) 197–212, 2015, doi: 10.1177/1468087414526188.
121. Busch, S., Zha, K., and Miles, P.C., “Investigations of Closely Coupled Pilot and Main Injections as a Means to Reduce Combustion Noise in a Small Bore Direct

- Injection Diesel Engine”, *International Journal of Engine Research* 16 (1): 13-22, 2015, doi: 10.1177/1468087414560776.
122. Yoon, S.J., Park, B., Park, J., and Park, S., “Effect of Pilot Injection on Engine Noise in a Single Cylinder Compression Ignition Engine”, *International Journal of Automotive Technology* 16 (4): 571-579, 2015, doi:10.1007/s12239-015-0058-6.
123. Geckler, S., Tomazic, D., Scholz, V., Whalen, M. et al., “Development of a Desulfurization Strategy for a NO_x Adsorber Catalyst System”, *SAE Technical Paper* 2001-01-0510, 2001, doi:10.4271/2001-01-0510.
124. Hodjati, S., Semelle, F., Moral, N., Bert, C. et al., “Impact of Sulphur on the NO_x Trap Catalyst Activity-Poisoning and Regeneration Behaviour”, *SAE Technical Paper* 2000-01-1874, 2000, doi:10.4271/2000-01-1874.
125. Rohr, F., Kattwinkel, P., Kreuzer, T., Müller, W. et al., “NO_x-Storage Catalyst Systems Designed to Comply with North American Emission Legislation for Diesel Passenger Cars”, *SAE Technical Paper* 2006-01-1369, 2006, doi:10.4271/2006-01-1369.
126. Zheng, M. and Reader, G.T., “Energy Efficiency Analyses of Active Flow Aftertreatment Systems for Lean Burn Internal Combustion Engines”, *Energy Conversion and Management* 45 (15-16): 2473–2493, 2004, doi:10.1016/j.enconman.2003.11.006.
127. Choi, J-S., Partridge, W.P., and Daw, C.S., “Spatially Resolved In-situ Measurements of Transient Species Breakthrough During Cyclic, Low-temperature Regeneration of a Monolithic Pt/K/Al₂O₃ NO_x Storage-Reduction Catalyst”, *Applied Catalysis A: General* 293: 24-40, 2005, doi:10.1016/j.apcata.2005.06.025.

APPENDIX A: DERIVATION OF THE HEAT RELEASE RATE EQUATION

The following shows the derivation for the apparent heat release rate equation which was utilized for the heat release rate graphs.

Let $\frac{dQ}{dCA}$ be the apparent heat release rate

where :

Q = thermal (heat) energy [J]

CA = crank angle [°]

from the balance of the internal energy :

$$\Delta U = \Delta Q + \Delta W$$

where :

W = piston boundary work [J]

assuming that there are no heat losses:

$$\Delta U = Q_{in} - W_{out}$$

consider a differential quantity with respect to the crank angle :

$$\frac{dQ}{dCA} = \frac{dU}{dCA} + \frac{dW}{dCA} \quad (\text{B-1})$$

for piston boundary work, assume the pressure is constant

over a differential change in the volume so that:

$$\frac{dW}{dCA} = p \frac{dV}{dCA} \quad (\text{B-2})$$

where :

p = in-cylinder pressure [Pa]

V = in-cylinder volume [m^3]

assuming an ideal gas as the working fluid:

$$pV = mRT$$

where :

m = in-cylinder working fluid mass [kg]

R = specific gas constant [J/kg·K]

T = mean bulk gas in-cylinder temperature [K]

with respect to a differential change in the crank angle:

$$p \frac{dV}{dCA} + V \frac{dp}{dCA} = mR \frac{dT}{dCA} \quad (\text{B-3})$$

assuming constant specific heat over a differential change in temperature :

$$\frac{dU}{dCA} = mC_V \frac{dT}{dCA} \quad (\text{B-4})$$

and

$$c_V = \frac{R}{\gamma - 1} \quad (\text{B-5})$$

where:

c_V = specific heat at constant volume [J/kg·K]

γ = specific heat ratio [-]

substitute (2), (3), (4), (5) into (1):

$$\frac{dQ}{dCA} = \left[\frac{mR}{\gamma - 1} \right] \left[\frac{1}{mR} \right] \left[p \frac{dV}{dCA} + V \frac{dp}{dCA} \right] + p \frac{dV}{dCA}$$

simplifying:

$$\frac{dQ}{dCA} = \left[\frac{1}{\gamma - 1} \right] \left[p \frac{dV}{dCA} + V \frac{dp}{dCA} + (\gamma - 1)p \frac{dV}{dCA} \right]$$

$$\frac{dQ}{dCA} = \left[\frac{1}{\gamma - 1} \right] \left[p \frac{dV}{dCA} + V \frac{dp}{dCA} + p\gamma \frac{dV}{dCA} - p \frac{dV}{dCA} \right]$$

$$\frac{dQ}{dCA} = \left[\frac{1}{\gamma - 1} \right] \left[V \frac{dp}{dCA} + p\gamma \frac{dV}{dCA} \right] \quad (\text{B-6})$$

APPENDIX B: ADDITIONAL NEAT BUTANOL TEST RESULTS

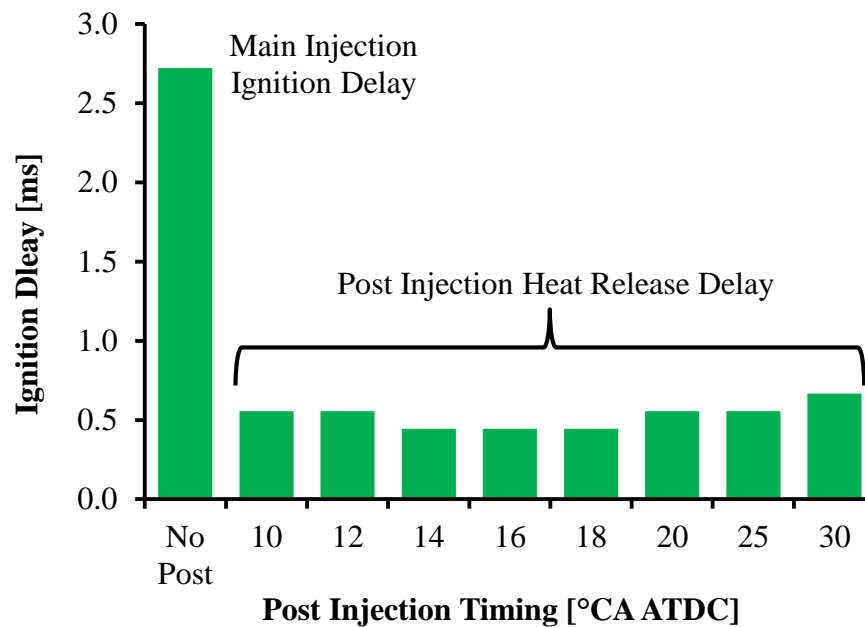


Figure B-1: Comparison of Butanol Main and Post Injection Ignition Delay

The test conditions shown in Table B-1 pertain to the results shown in Figure B-2 to Figure B-6.

Table B-1: Test Conditions for Broad Range Butanol Post Injection Timing Sweep

IMEP [bar]	6.1
Engine Speed [rpm]	1500
Air Intake Pressure [bar absolute]	1.9
Intake Oxygen [% V]	20.5
Test Fuel	n-Butanol
Fuel Injection Pressure [bar]	900
Main Injection Duration [μ s]	Variable
Main Injection Timing [°CA ATDC]	-15
Pilot Injection Duration [μ s]	300
Pilot Injection Timing [°CA ATDC]	10 to 50

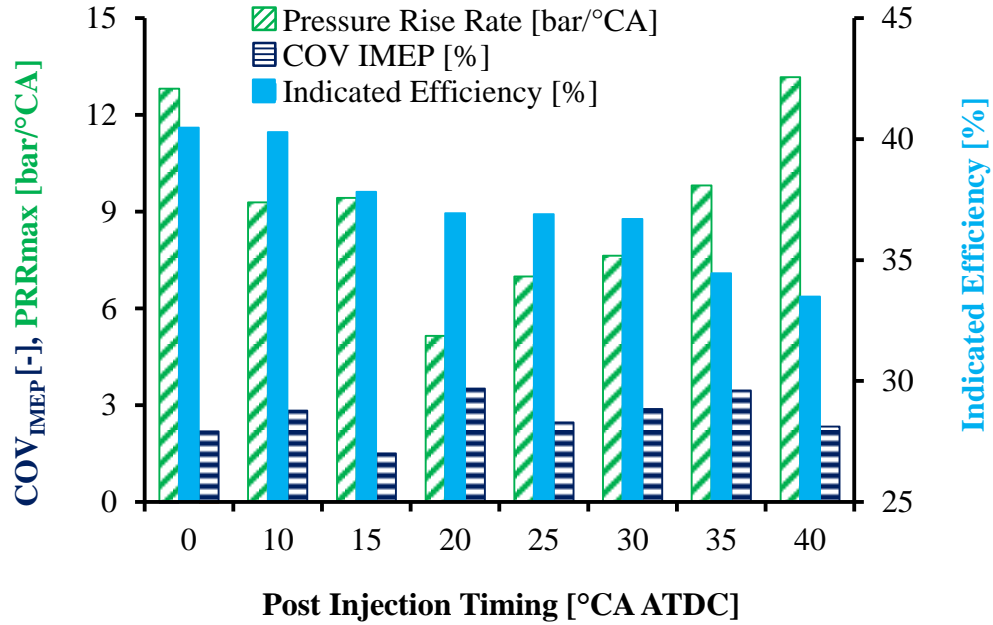


Figure B-2: Butanol Post Injection Timing vs. PRR, COV_{IMEP}, and Efficiency

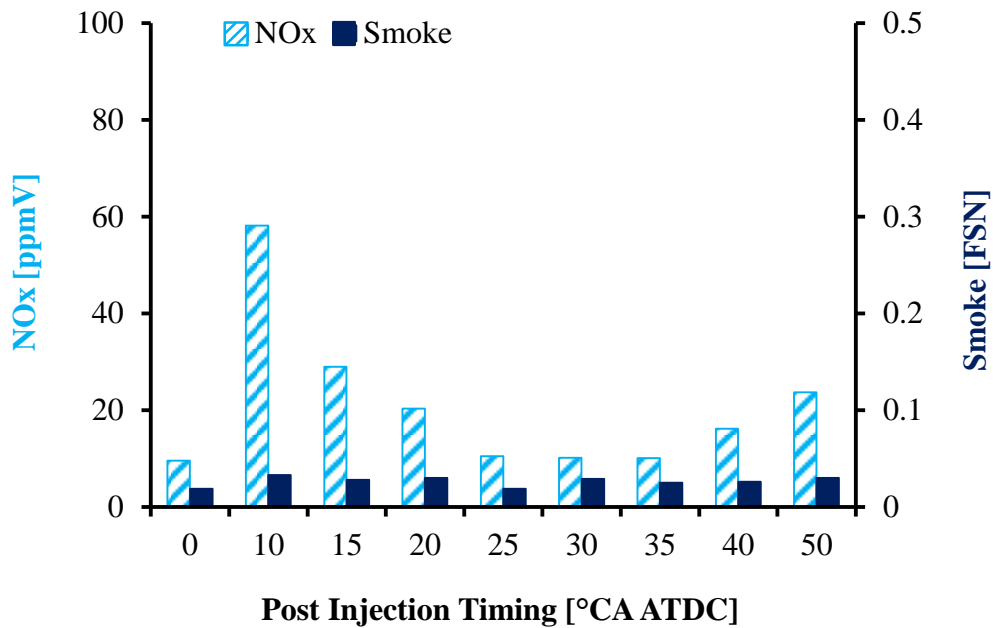


Figure B-3: Effect of Butanol Post Injection Timing on NO_x and Smoke Emissions

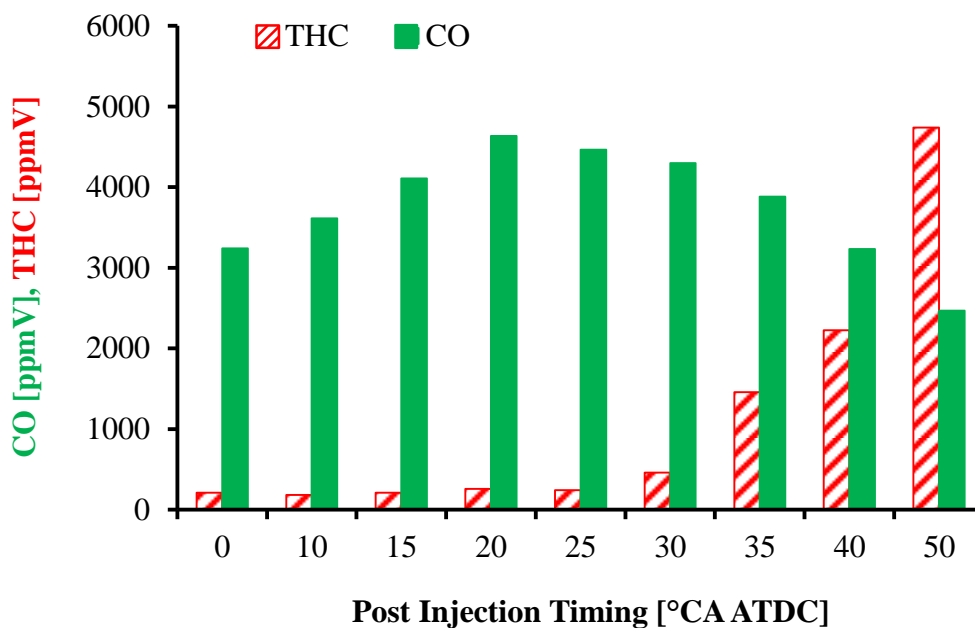


Figure B-4: Effect of Butanol Post Injection Timing on CO and THC Emissions

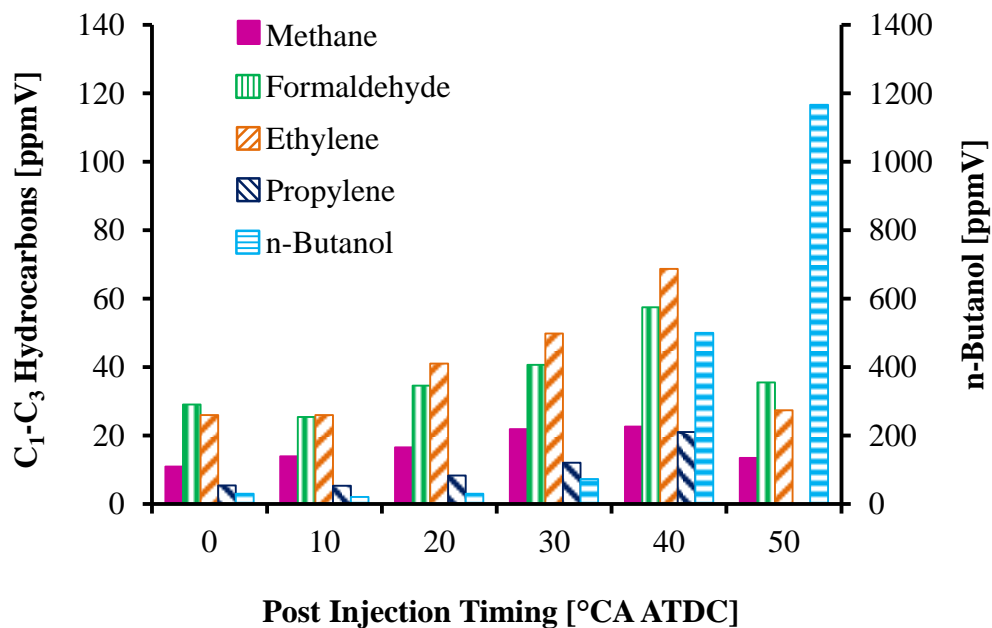


Figure B-5: Effect of Butanol Post Injection Timing on Hydrocarbon Speciation

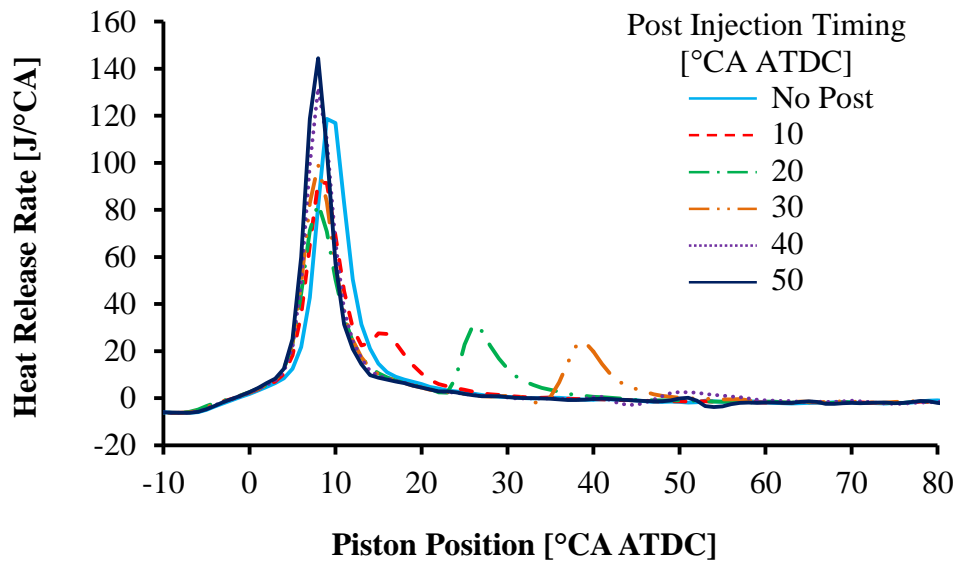


Figure B-6: Effect of Butanol Post Injection Timing on Heat Release Rate

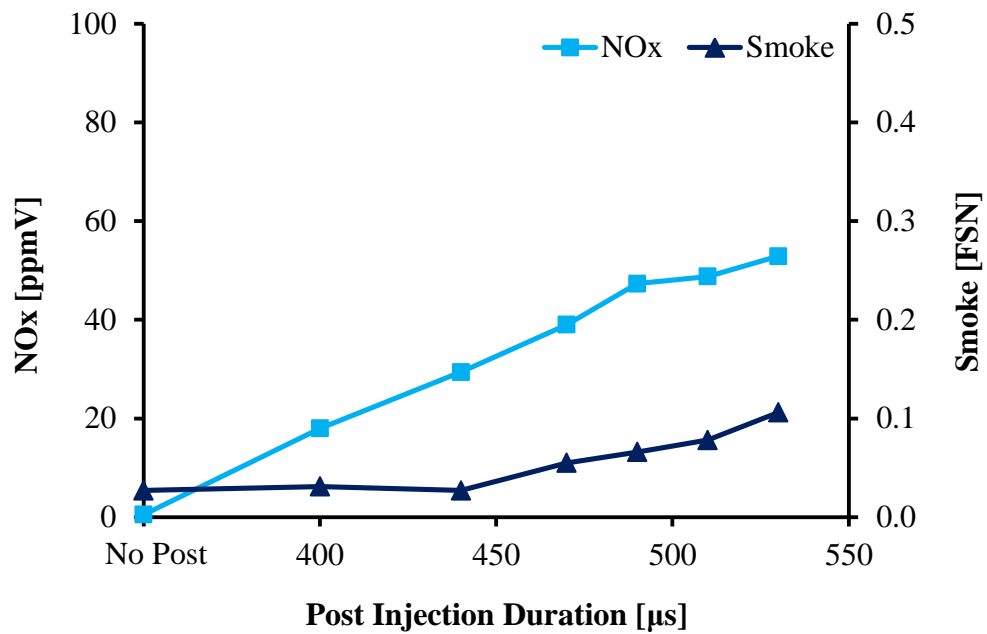


Figure B-7: Effect of Butanol Post Injection Duration on NO_x and Smoke Fractions

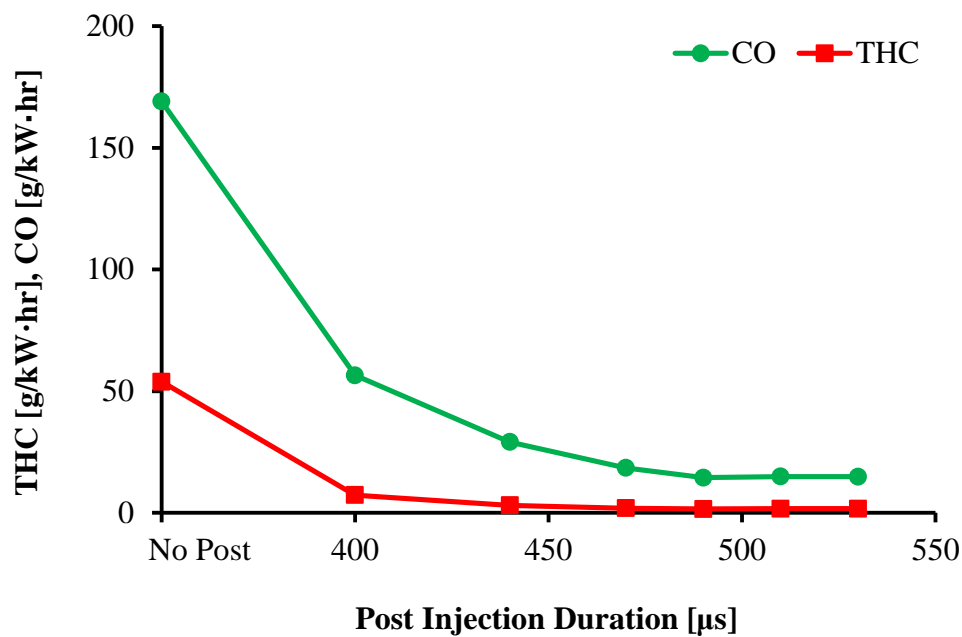


Figure B-8: Effect of Butanol Post Injection Duration on Indicated CO and THC

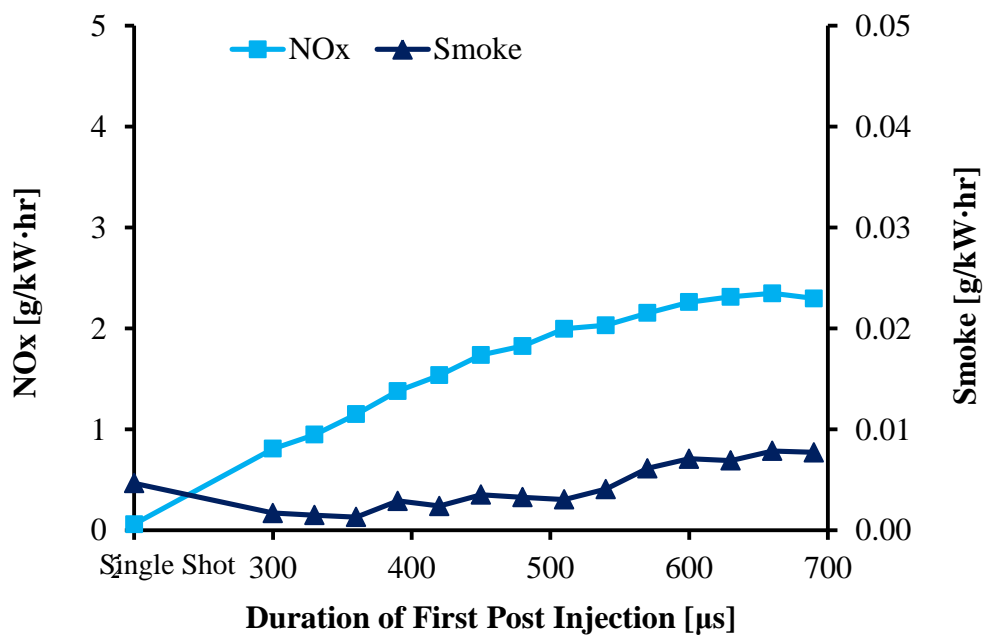


Figure B-9: Effect of Modified Butanol Single Post Injection Strategy on Indicated NO_x and Smoke Emissions

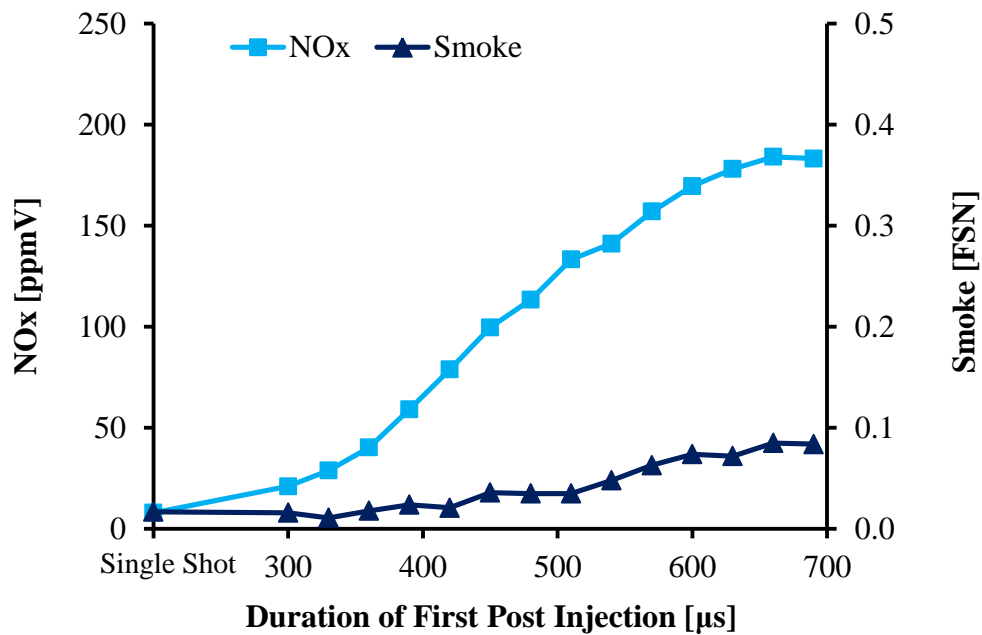


Figure B-10: Effect of Modified Butanol Single Post Injection Strategy on Raw NO_x and Smoke Emissions

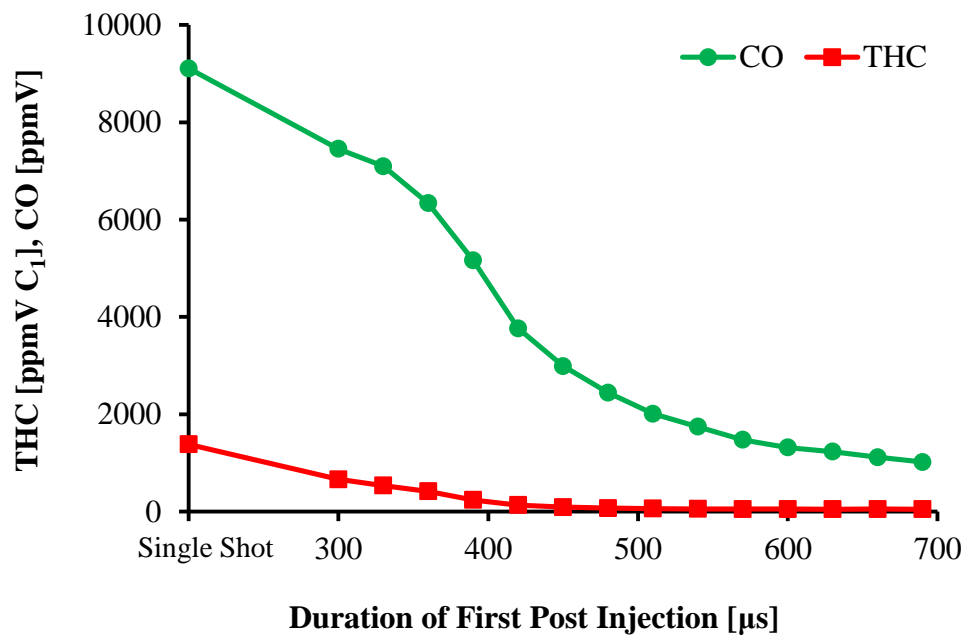


Figure B-11: Effect of Modified Butanol Single Post Injection Strategy on CO and THC

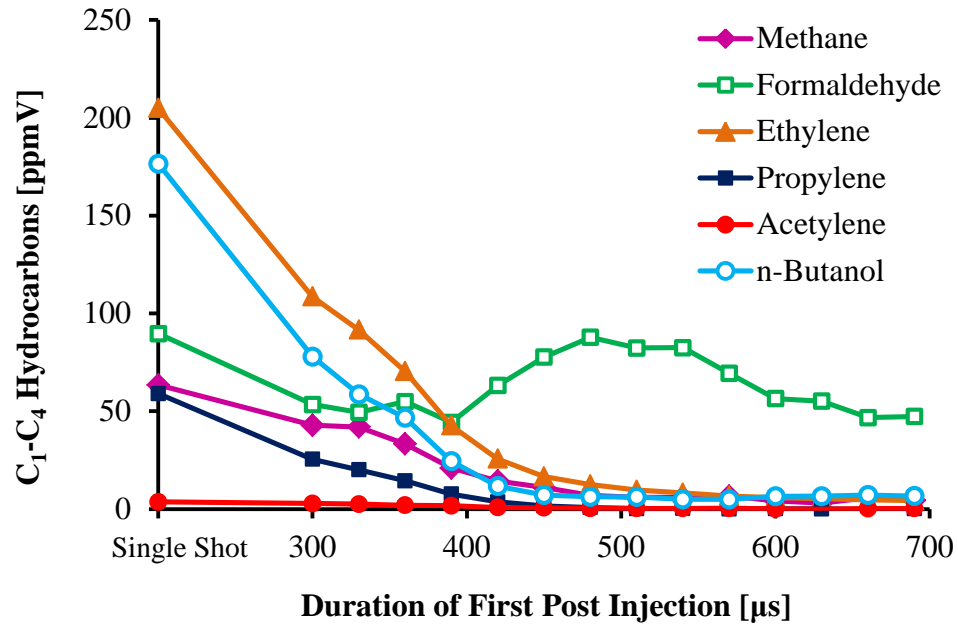


Figure B-12: Effect of Modified Butanol Single Post Injection Strategy on Light Hydrocarbons

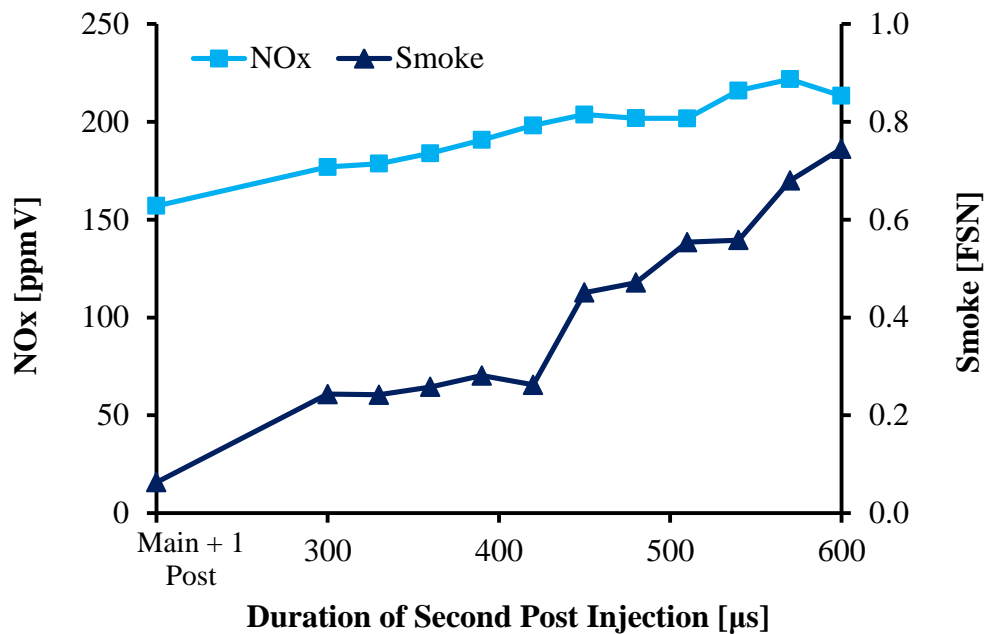


Figure B-13: Effect of Butanol Double Post Injection Strategy on NO_x and Smoke

APPENDIX C: ADDITIONAL EXHAUST GAS MANAGEMENT RESULTS

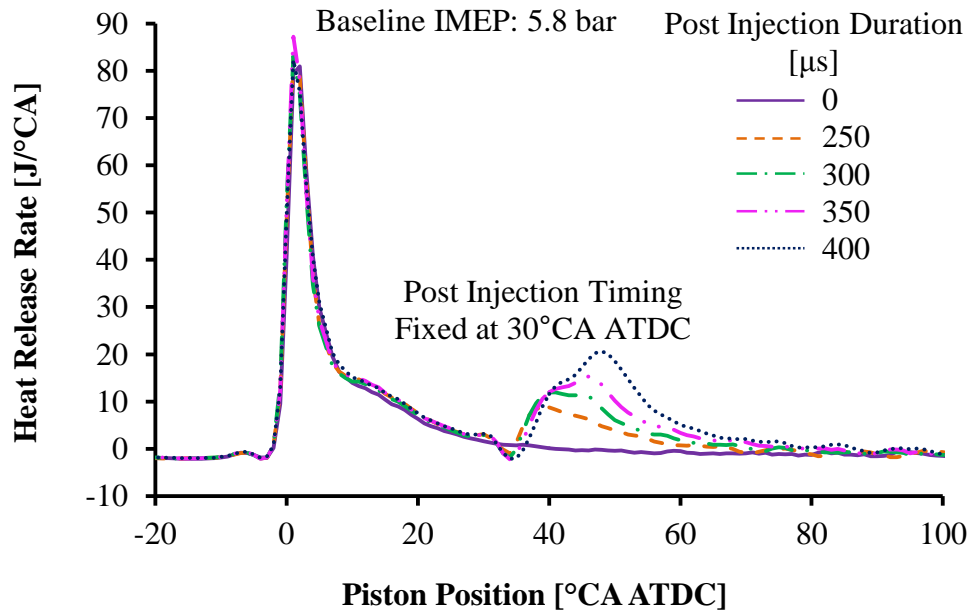


Figure C-1: Duration of Early Post Injection vs. HRR (5.8 bar)

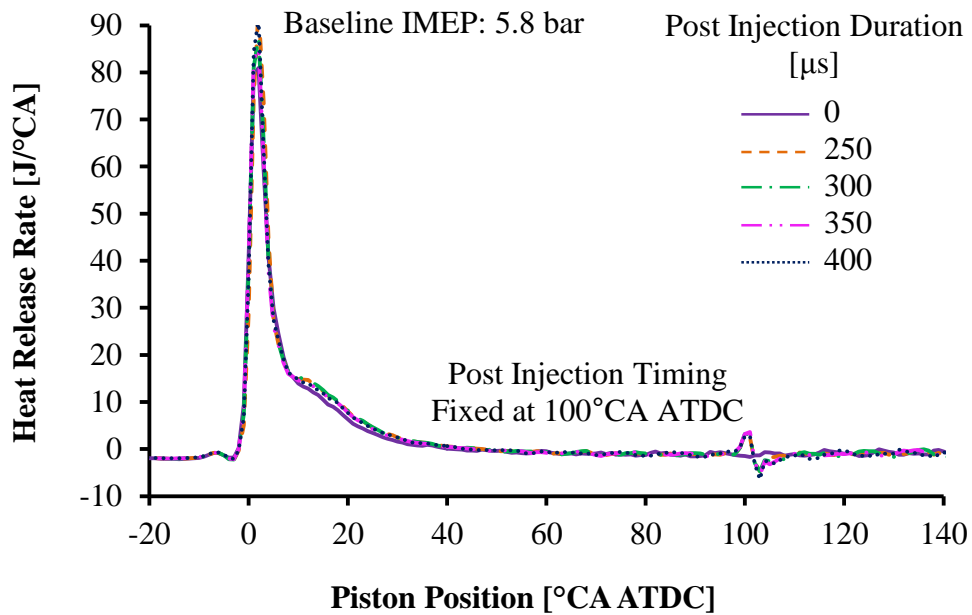
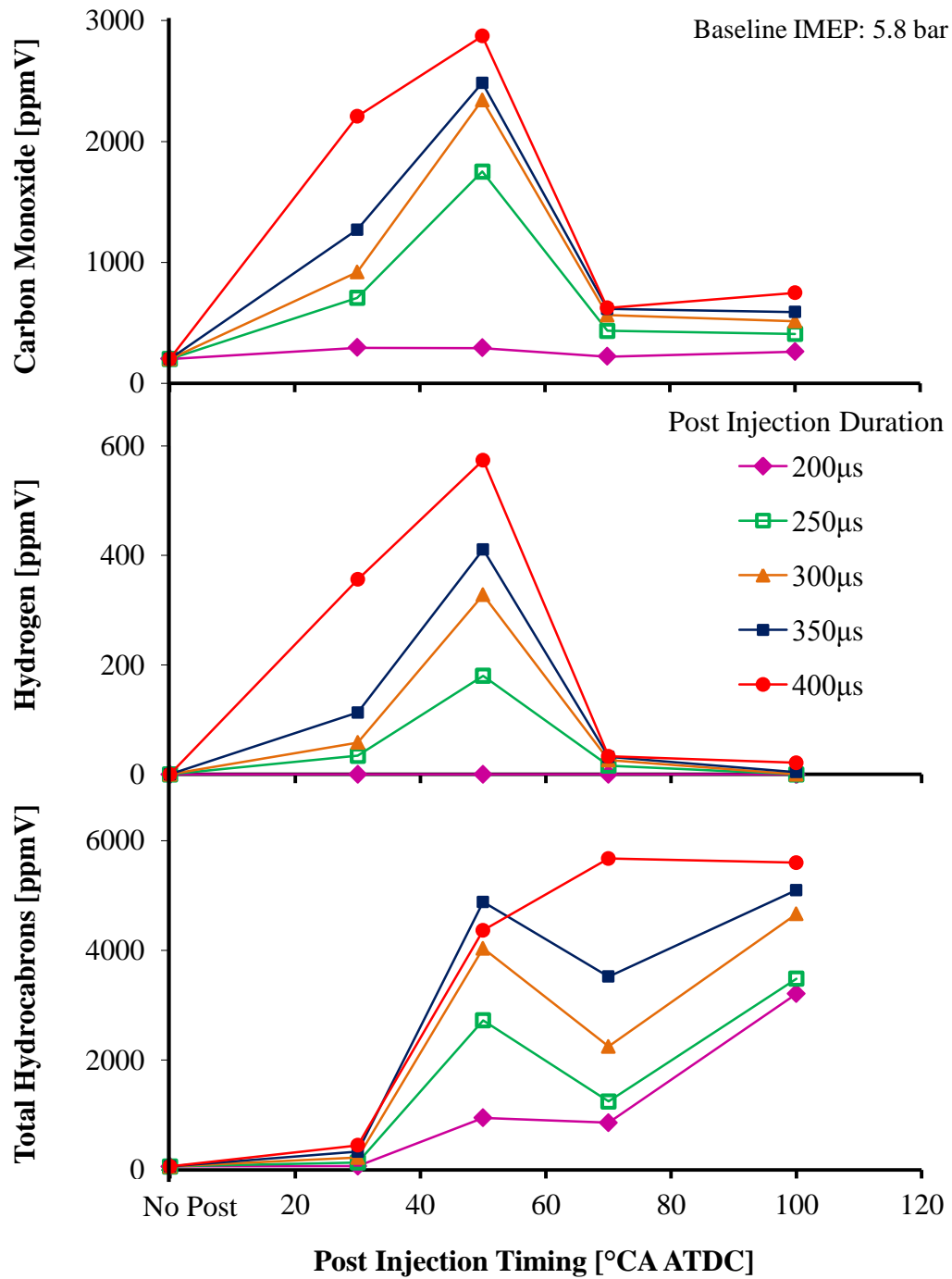


Figure C-2: Duration of Late Post Injection vs. HRR (5.8 bar)

Figure C-3: Post Injection Duration and Timing vs. NO_x Reducing Agents (5.8bar)

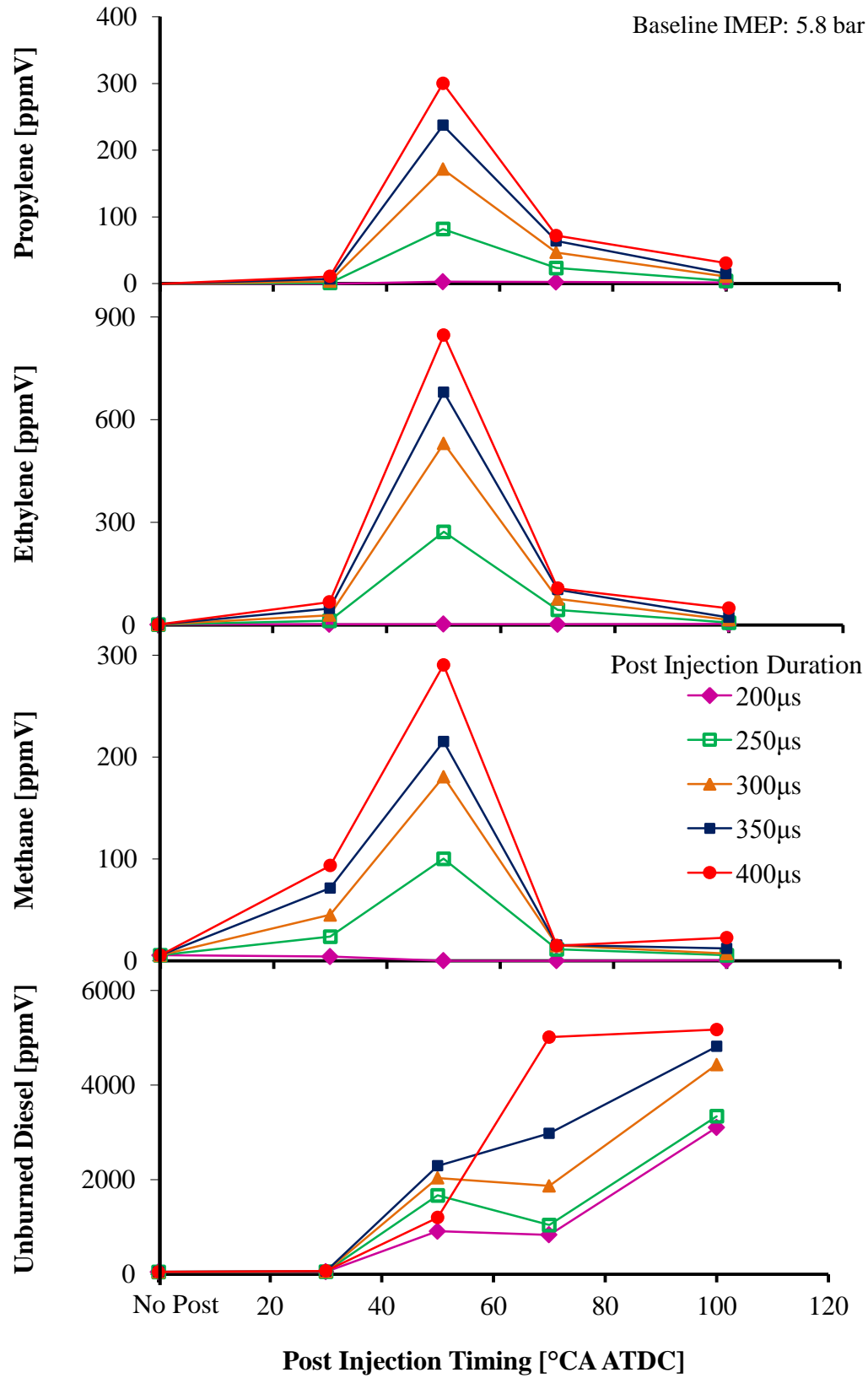


Figure C-4: Post Injection Duration & Timing vs. Hydrocarbon Speciation (5.8 bar)

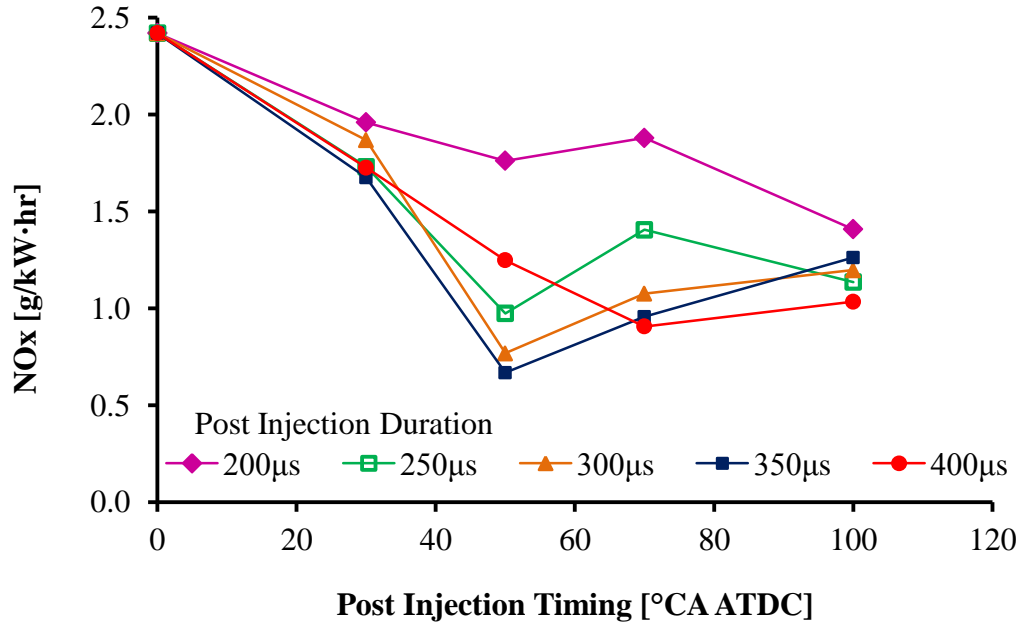


Figure C-5: Effect of Post Injection Quantity and Timing on NO_x (5.8bar)

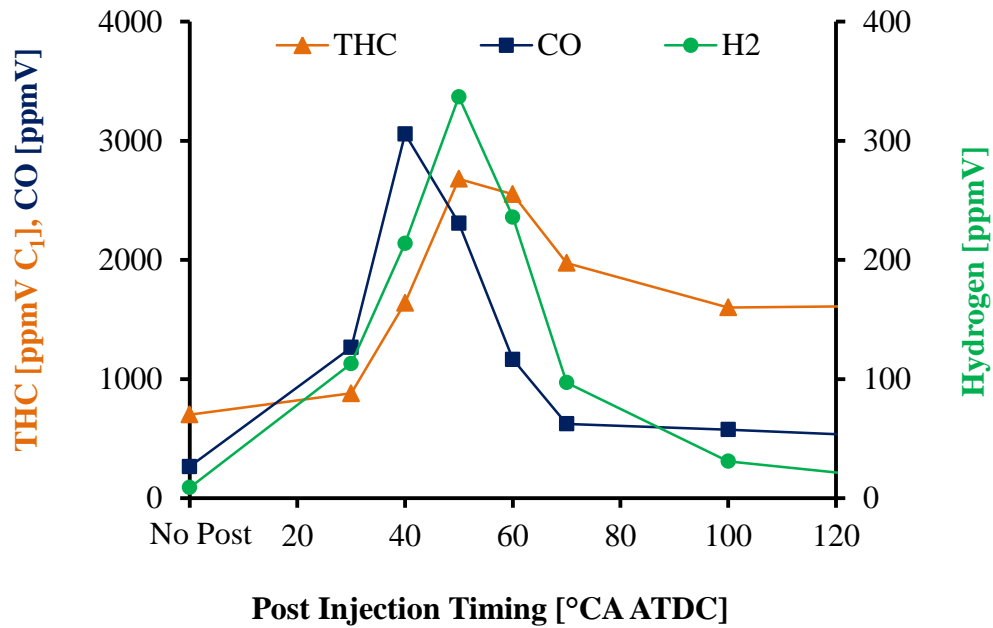


Figure C-6: Effect of Post Injection Timing on THC, CO, H₂ (6.1 bar)

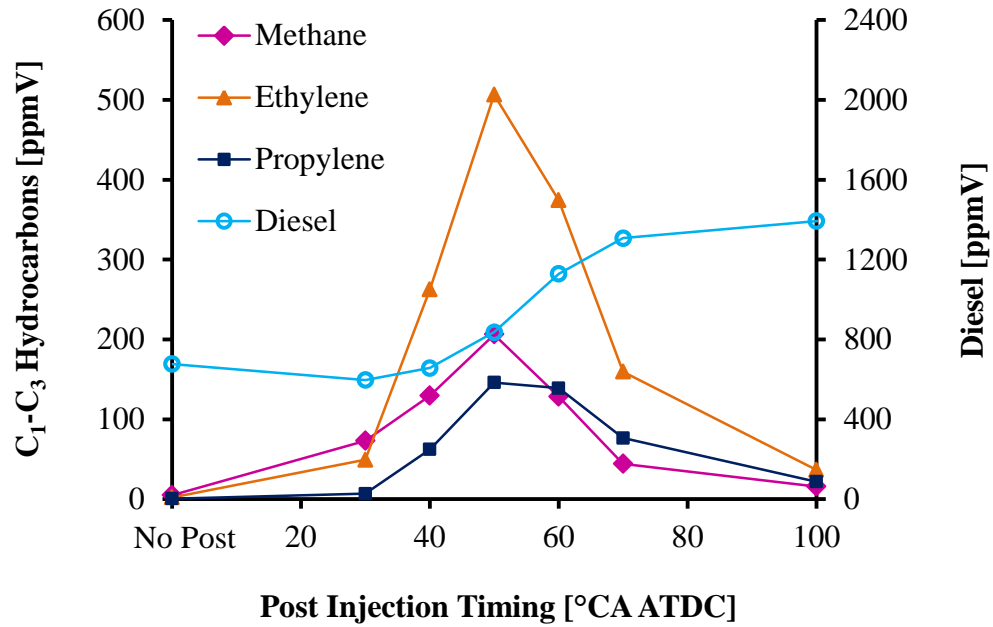


Figure C-7: Effect of Post Injection Timing on Hydrocarbon Speciation (6.1 bar)

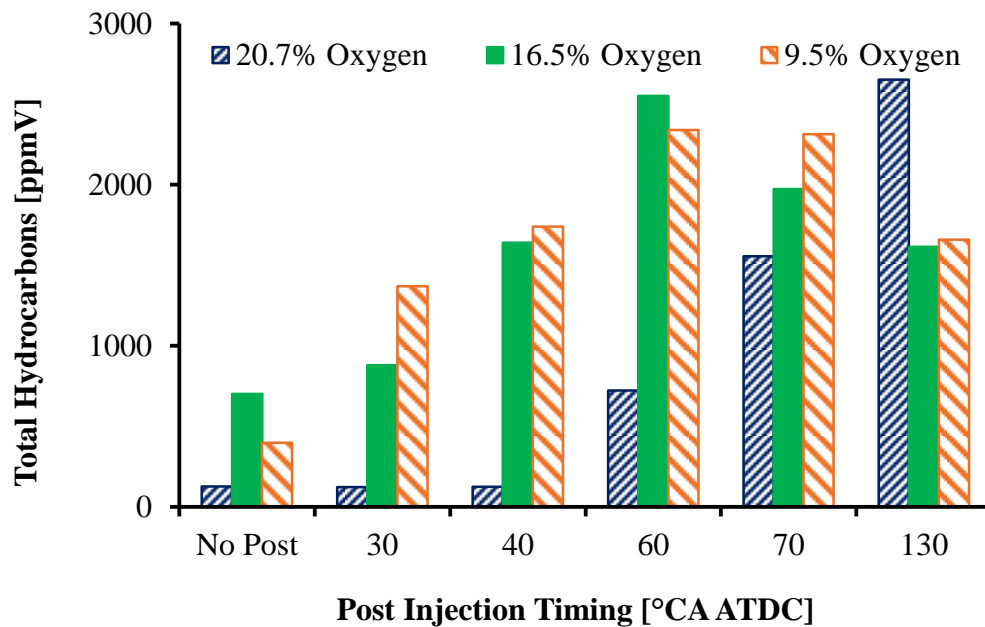


Figure C-8: Effect of Intake Oxygen on Total Hydrocarbon Emissions

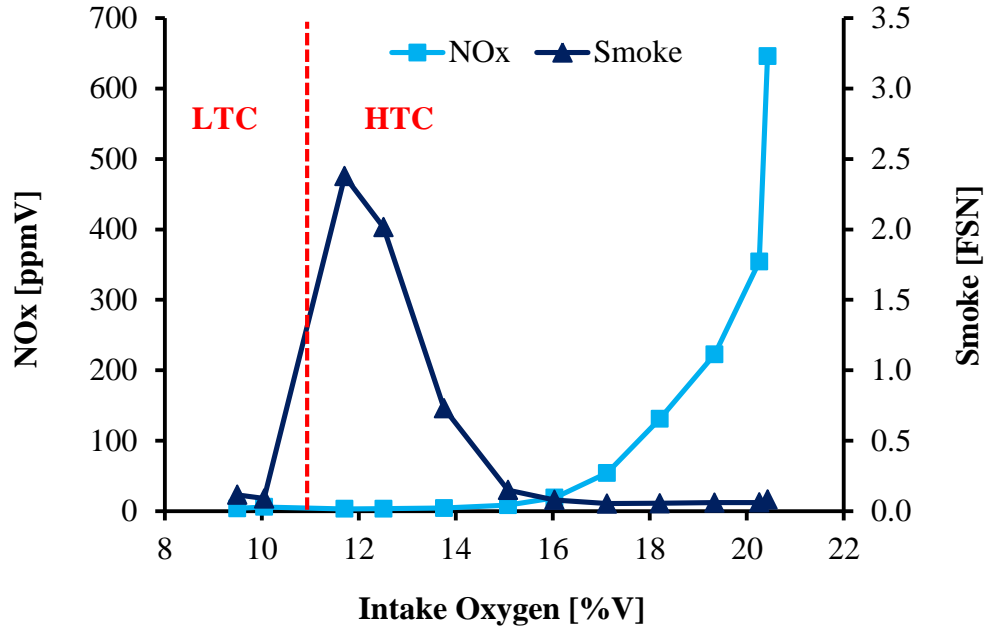


Figure C-9: Effect of Intake Oxygen Sweep on NO_x and Smoke Emissions

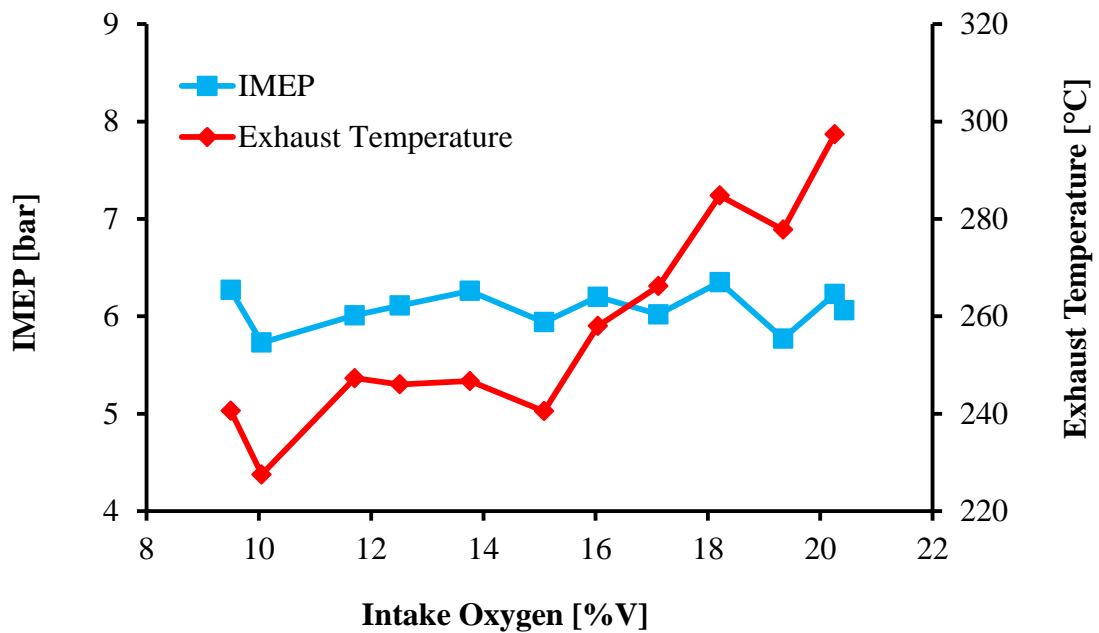


Figure C-10: Effect of Intake Oxygen Sweep on the Exhaust Temperature

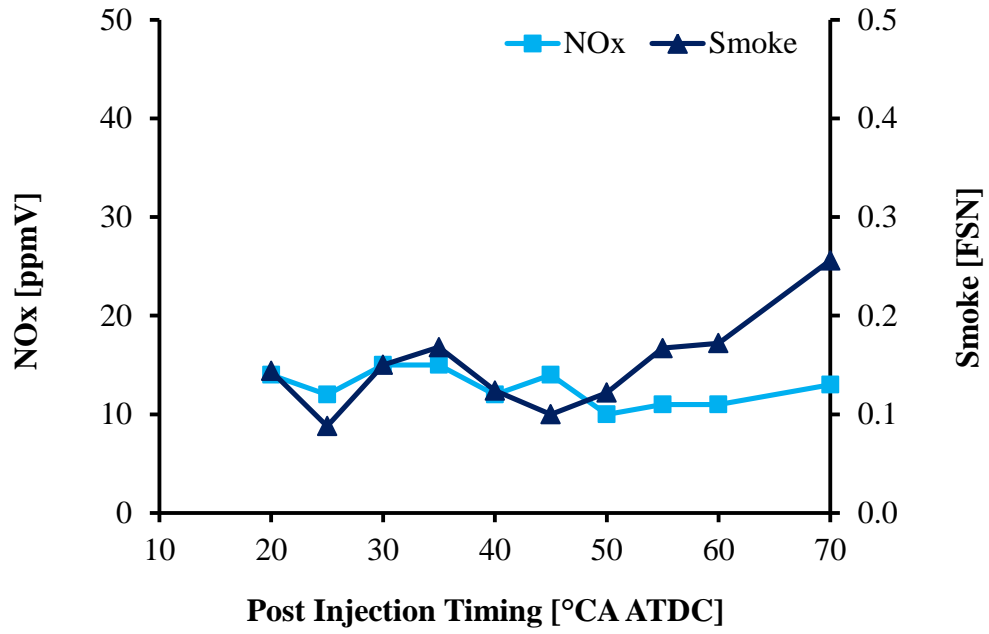


Figure C-11: Effect of LTC Post Injection Timing Sweep on NO_x and Smoke

APPENDIX D: ADDITIONAL FIGURES FOR EXPERIMENTAL SETUP

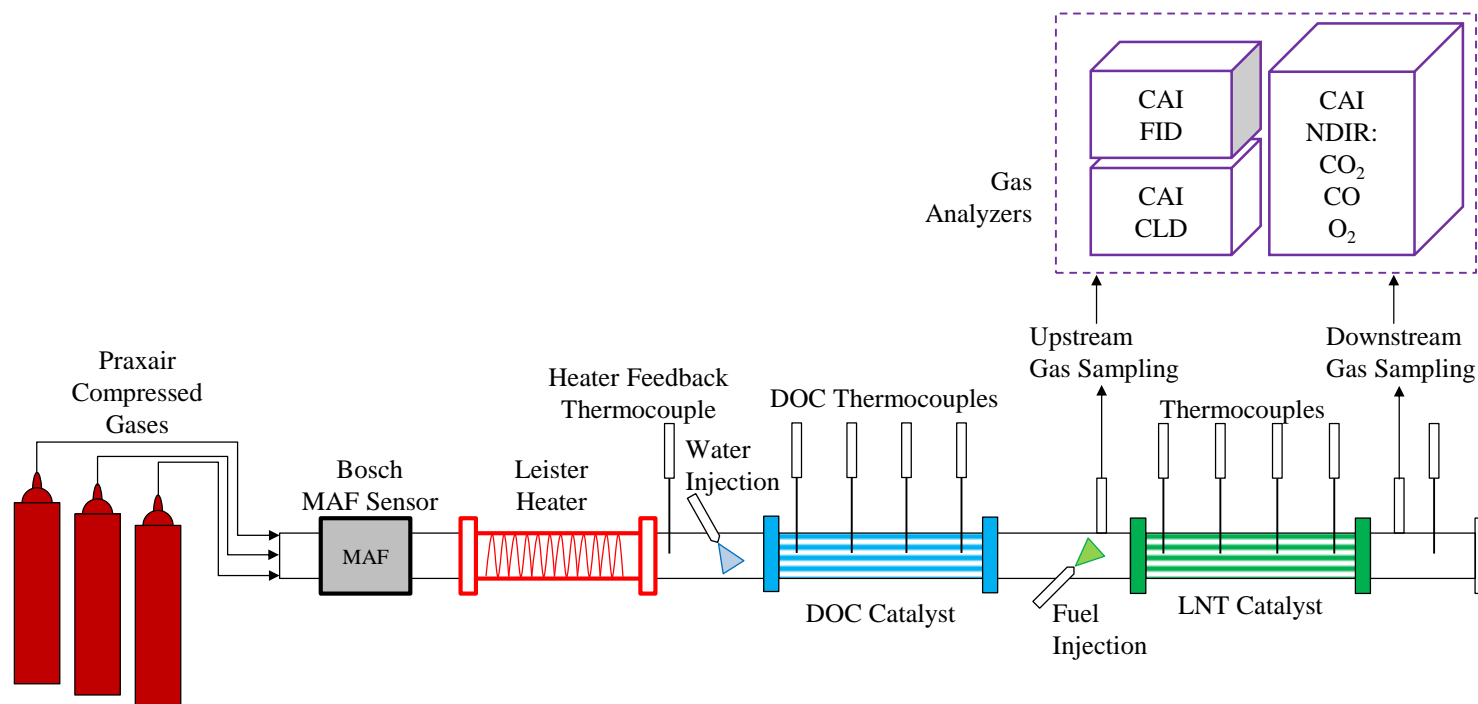


Figure D-1: Schematic Diagram of the After-treatment Flow Bench

APPENDIX E: PROPORTIONALITY FACTOR CALCULATION

The volume of the catalyst that was used for the numerical calculations was smaller than the required catalyst volume for the test engine. The numerical model had a catalyst that was the same volume (0.231 L) as the catalyst that was used for the heated after-treatment flow bench tests, which was used to tune the model and was sized according to the flow specifications of the heated flow bench. Thus, a proportionality factor was calculated based on the volume of the numerical model catalyst and the required catalyst volume for the test engine. The calculation procedure is outlined below.

Based on the test conditions from the engine tests, the maximum engine exhaust flow rate was 56 g/s. This mass flow rate was converted to a volumetric flow rate as shown below in Equation E-1. The density of the exhaust gas was assumed to be 1.2 kg/m³, based on the sea level air density at 15°C. This assumption was reasonable because the major constituents of the exhaust gas and of air are nitrogen and oxygen. Based on this density and the mass flow rate, the corresponding volumetric exhaust flow rate was calculated to be 168000 litres per hour.

$$56 \frac{\text{g}}{\text{s}} \times \frac{3600 \text{ s}}{1 \text{ hr}} \times \frac{1 \text{ m}^3}{1.2 \text{ kg}} \times \frac{1000 \text{ L}}{1 \text{ m}^3} \times \frac{1 \text{ kg}}{1000 \text{ g}} = \frac{168000 \text{ L}}{1 \text{ hr}} \quad \text{E-1}$$

The numerical model utilized a gas hourly space velocity of 45000 volumes per hour. This gas hourly space velocity value was chosen to be within the range commonly reported in literature [77,90,91]. Therefore, the required catalyst volume for the test engine was calculated as shown in Equation E-2. The required catalyst volume for the test engine was determined to be 3.73 L, which gave a catalyst volume to engine displacement volume ratio of 1.87 as shown in Equation E-3. The calculated volume ratio of 1.87 was within the range reported in literature [123,124]. Finally, the proportionality factor of the engine catalyst and the model catalyst was calculated by Equation E-4 and found to be 16.1. Thus, the stored NO_x mass for the numerical catalyst was multiplied by 16.1 to obtain the expected stored NO_x mass for the engine catalyst.

$$\frac{168000 L}{1 hr} \times \frac{1 hr}{45\,000 \text{ catalyst volumes}} = 3.73 L \quad \text{E-2}$$

$$\frac{\text{Engine Catalyst Volume}}{\text{Engine Displacement Volume}} = \frac{3.73}{1.998} = 1.87 \quad \text{E-3}$$

$$\frac{\text{Engine Catalyst Volume}}{\text{Model Catalyst Volume}} = \frac{3.73}{0.231} = 16.1 \quad \text{E-4}$$

APPENDIX F: DEFINITION OF TERMS

The terms low load, medium or mid load, and high load are used throughout the thesis. These are relative terms that are used for convenience. The quantitative values attached to these terms are defined as shown in Table F-1. Similarly, the terms early, intermediate, and late post injection are used throughout the text and are broadly defined as shown in Table F-2.

Table F-1: Definition of Different Load Levels

Load Description	IMEP [bar]
Low	0 to 6
Medium	6 to 12
High	>12

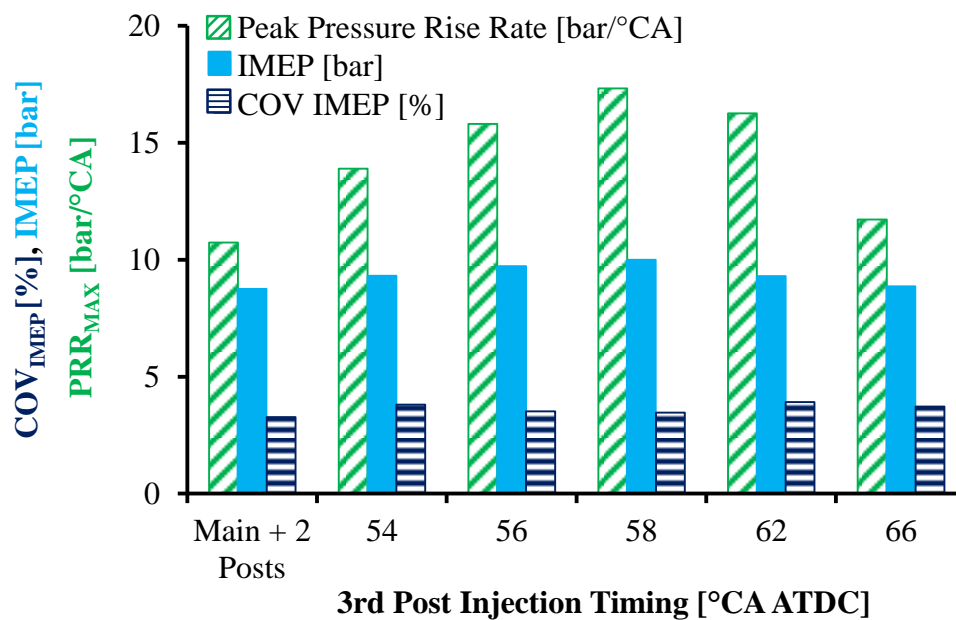
Table F-2: Definition of Post Injection Timing Descriptions

Post Injection Timing Description	Commanded Injection Timing [°CA ATDC]
Early	0 to 50
Intermediate	50 to 70
Late	>70

APPENDIX G: TRIPLE POST INJECTION STRATEGY WITH NEAT BUTANOL FUEL

Table G-1: Test Conditions for Butanol Triple Post Injection Duration Sweep

IMEP [bar]	Variable
Engine Speed [rpm]	1500
Air Intake Pressure [bar absolute]	1.9
Intake Oxygen [% V]	20.5
Test Fuel	n-Butanol
Fuel Injection Pressure [bar]	900
Main Injection Duration [μ s]	520
Main Injection Timing [$^{\circ}$ CA ATDC]	-18
1 st Post Injection Duration [μ s]	420
1 st Post Injection Timing [$^{\circ}$ CA ATDC]	20
2 nd Post Injection Duration [μ s]	380
2 nd Post Injection Timing [$^{\circ}$ CA ATDC]	40
3 rd Post Injection Duration [μ s]	300
3 rd Post Injection Timing [$^{\circ}$ CA ATDC]	Sweep

Figure G-1: Effect of Butanol Third Post Injection Timing on IMEP, PRR, p_{MAX}

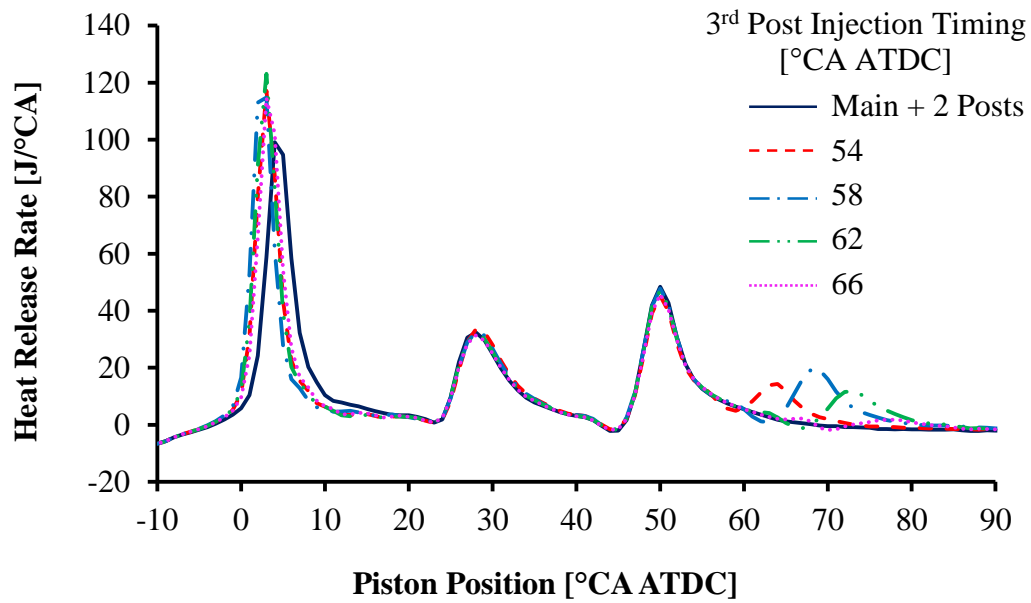


Figure G-2: Effect of Butanol Third Post Injection Timing on Heat Release

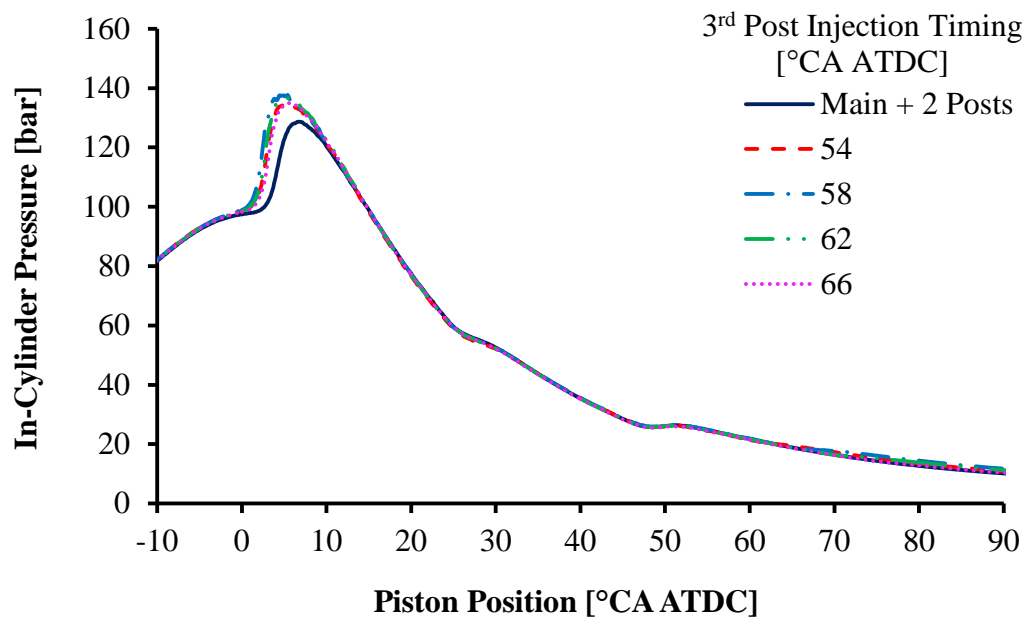


Figure G-3: Effect of Butanol Third Post Injection Timing on In-Cylinder Pressure

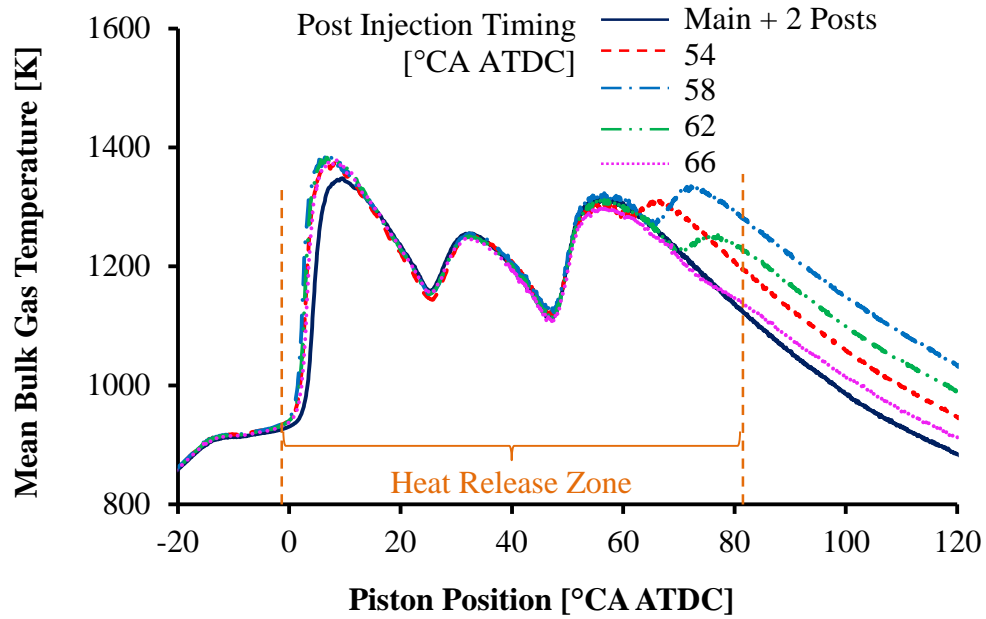


Figure G-4: Effect of Butanol Third Post Injection Timing on Bulk Gas Temperature

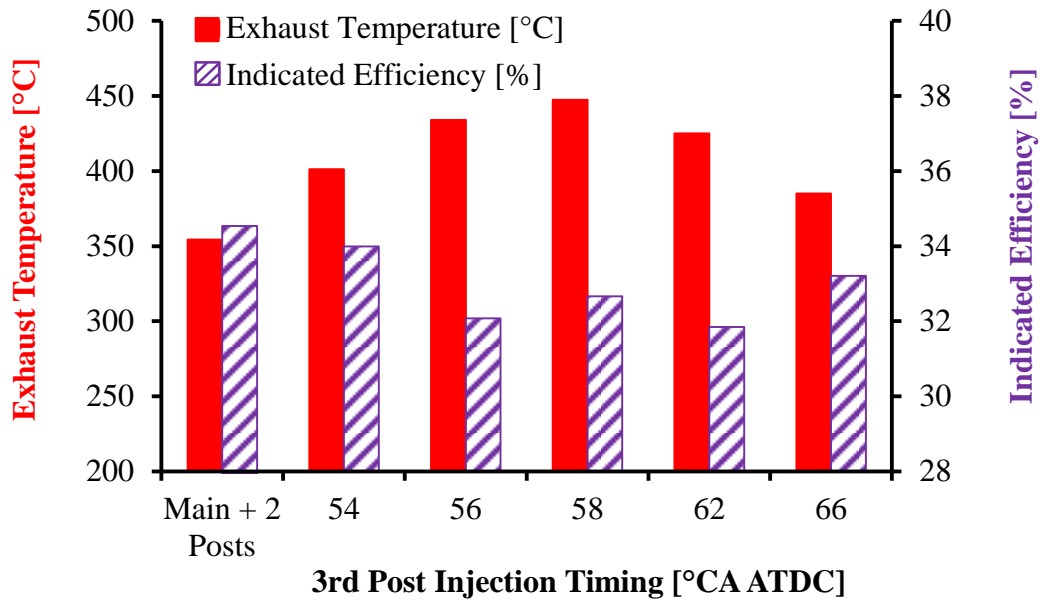


Figure G-5: Effect of Butanol Third Post Injection Timing on Exhaust Temperature and Efficiency

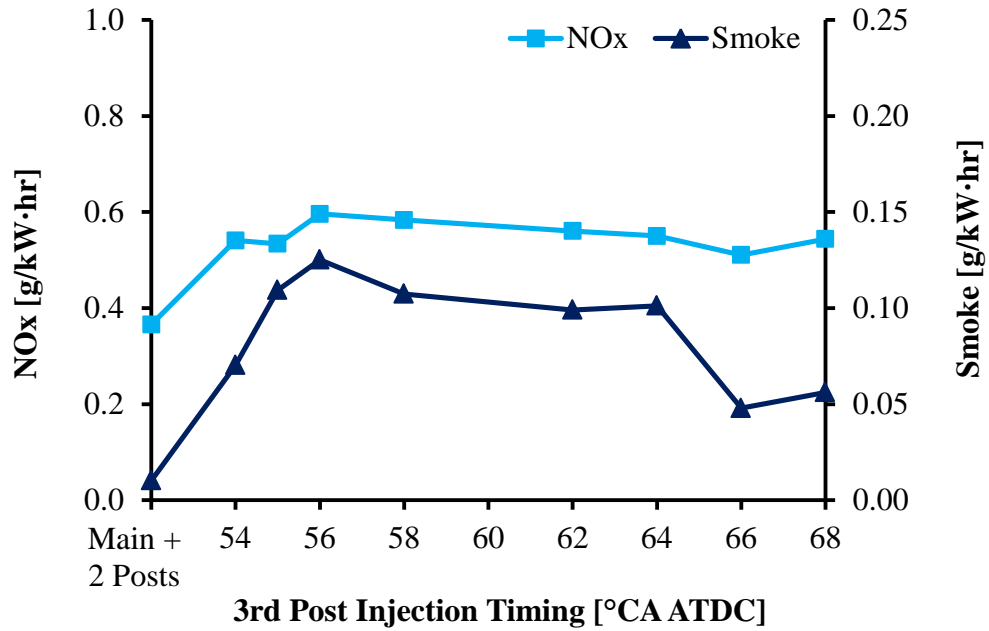


Figure G-6: Effect of Butanol Third Post Injection Timing on Indicated NO_x and Smoke

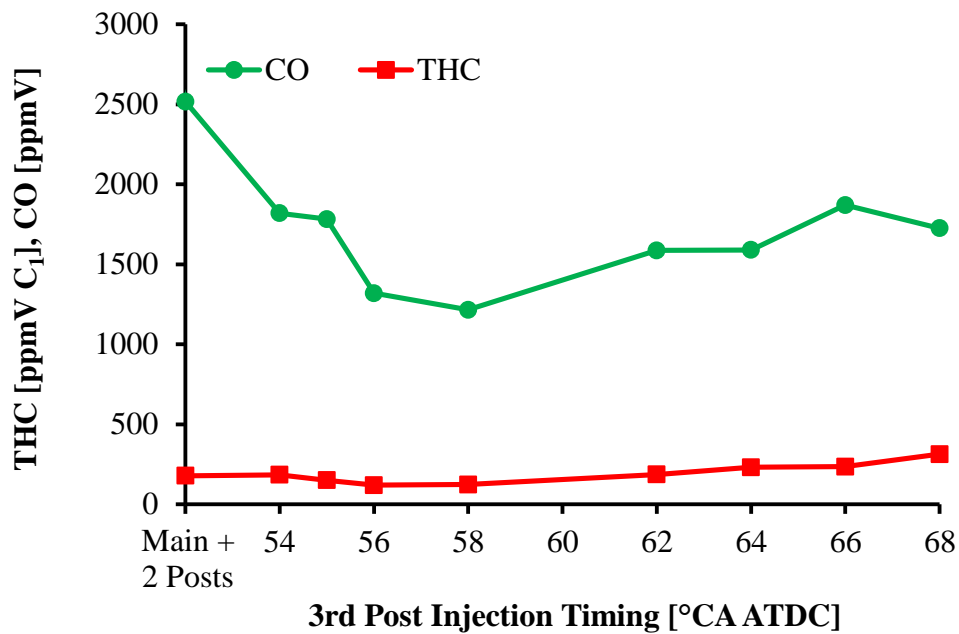


Figure G-7: Effect of Butanol Third Post Injection Timing on CO and THC

Table G-2: Tabulated Data for Butanol Multiple Post Injection Strategies

Injection Strategy	Pressure			COV _{IMEP} [%]	Indicated Efficiency [%]	NO _x [ppmV]	Smoke [FSN]	CO [ppmV]	THC [ppmV]
	IMEP [bar]	Rise Rate [bar/°CA]	p _{MAX} [bar]						
Single Shot	6.2	12.8	123.2	2.2	40.5	10	0.019	3239	210
Single Post	8.9	12.6	133.3	1.3	37.6	53	0.106	1707	73
Double Post	9.0	7.3	122.7	4.3	35.0	43	0.190	2908	268
Double Post High Load	10.1	17.2	134.0	4.3	36.9	52	0.190	1574	117
Triple Post	10.0	17.3	138.5	3.5	32.7	59	0.894	1215	124

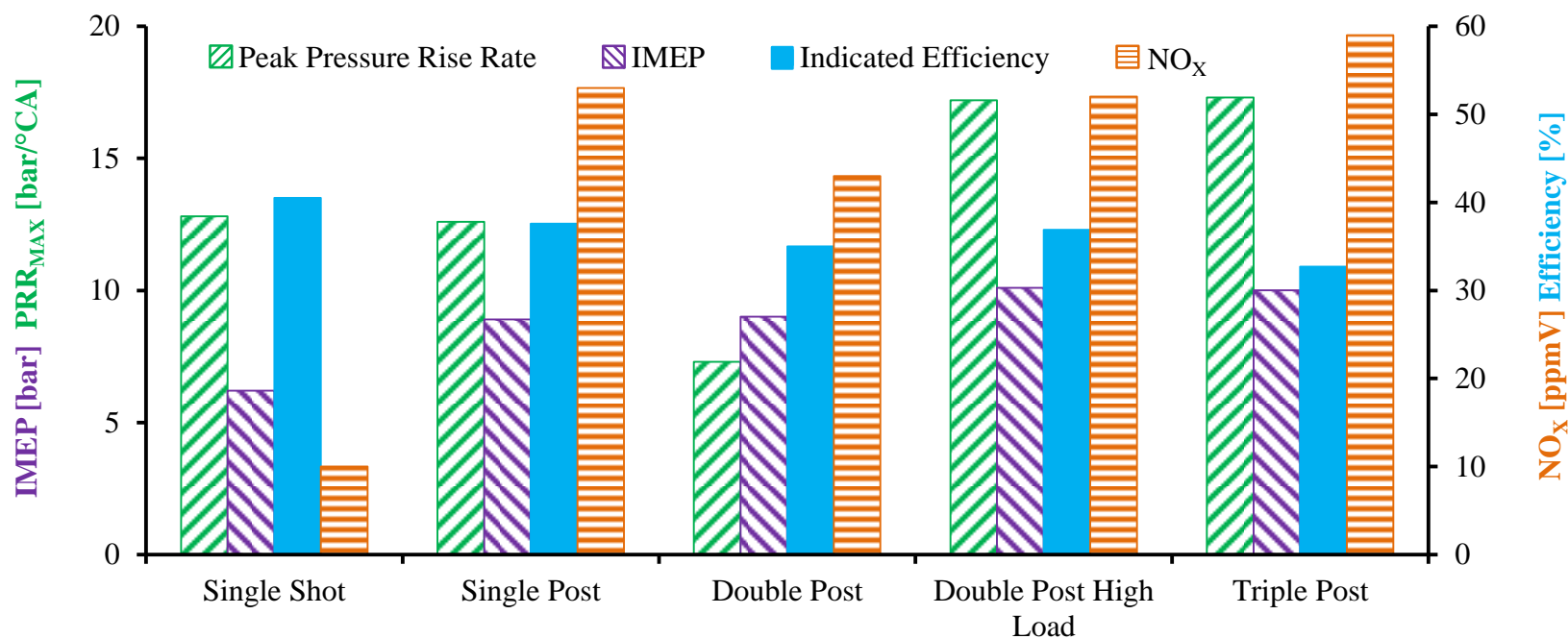


Figure G-8: Comparison of Butanol Multiple Post Injection Strategies

APPENDIX H: EFFECTS OF FUEL INJECTION PRESSURE ON EXHAUST TEMPERATURE AND COMPOSITION

Table H-1: Test Conditions for Injection Pressure Study

	Low Load Low Pressure	Low Load High Pressure	High Load Low Pressure	High Load High Pressure
Test Fuel	Diesel	Diesel	Diesel	Diesel
Main Injection IMEP [bar]	6	6	14.7	14.7
Fuel Injection Pressure [bar]	900	1200	1200	1500
Main Injection CA50 [°CA ATDC]	5	5	9	9
Main Injection Timing [°CA ATDC]	-7	-5	-3	-2
Main Injection Duration [μ s]	465	385	900	840
Post Injection Timing [°CA ATDC]	30 - 130	30 - 130	30 - 130	30 - 130
Post Injection Duration [μ s]	300	300	300	300
Air Intake Pressure [bar absolute]	1.3	1.3	2.5	2.5
Intake Oxygen [% volume]	16.5	16.5	16.5	16.5

An investigation was carried out to determine the effect of injection pressure on the exhaust gas temperature and composition. Four different operating conditions were used for this investigation as outlined in Table H-1. A pair of tests were done at a baseline IMEP of 6 bar with injection pressures of 900 to 1200 bar and another pair of tests were done at a 14.7 bar baseline IMEP with injection pressures of 1200 to 1500 bar. To achieve the same baseline IMEP, the main injection duration was reduced when the injection pressure was increased. The main injection timing was adjusted to maintain a constant combustion phasing for both low load conditions and for both high load conditions. The post injection duration was 300 μ s for all four tests, resulting in more injected fuel for higher injection pressures. The effects of fuel pressure wave actions within the common rail were not studied.

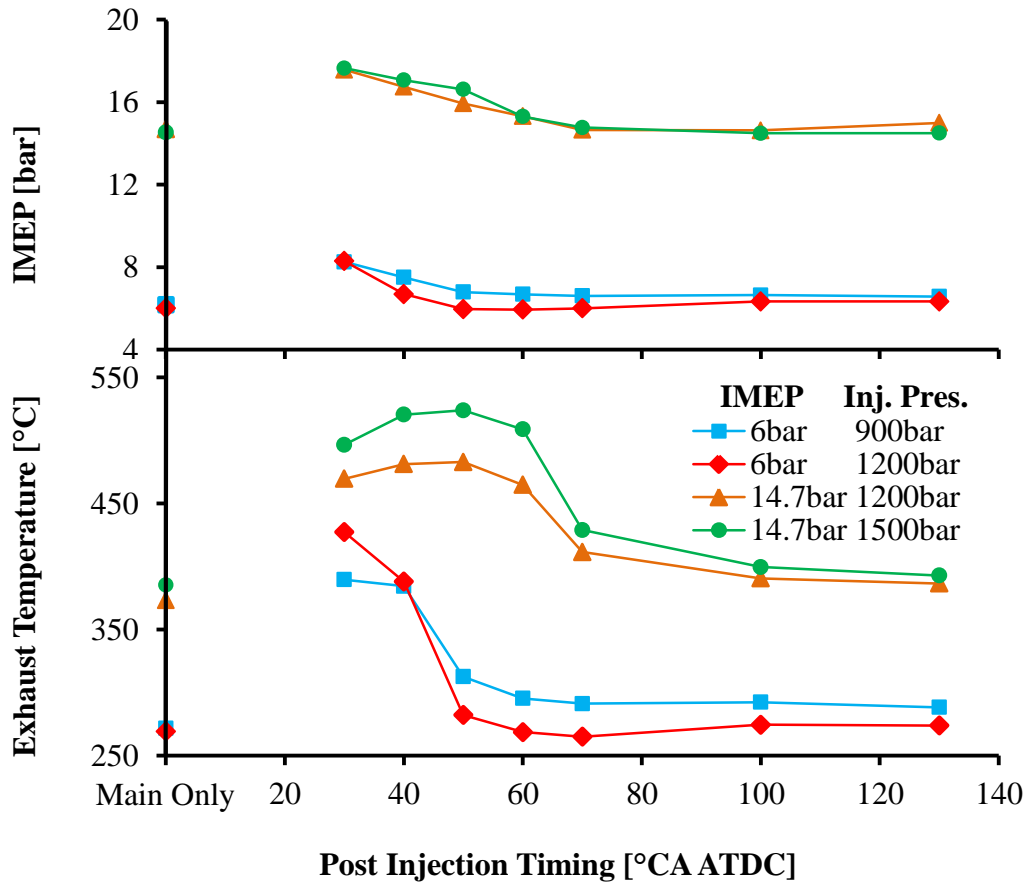


Figure H-1: Effect of Injection Pressure on IMEP and Exhaust Temperature

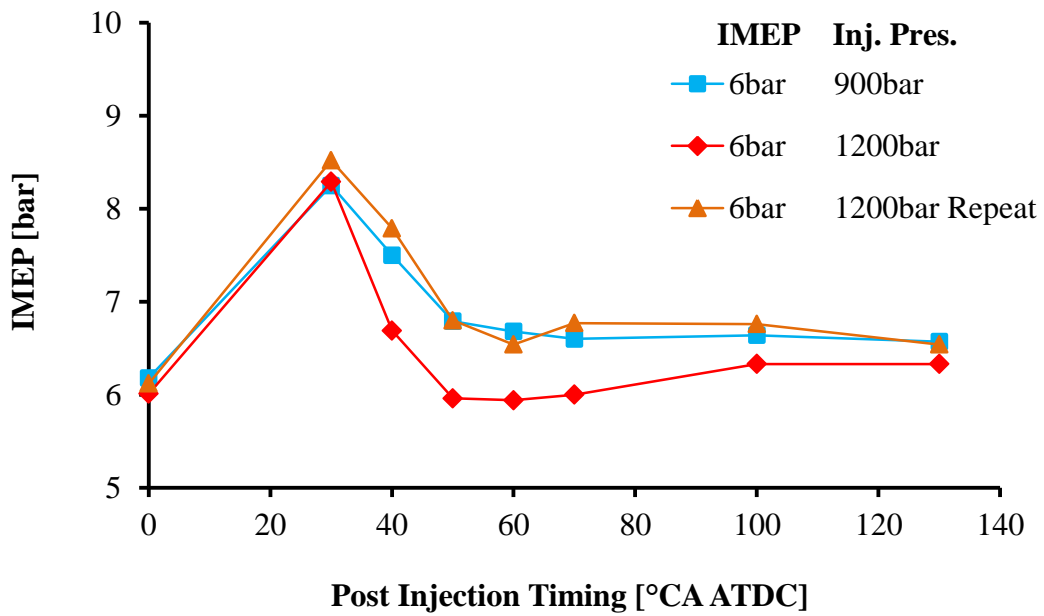


Figure H-2: Repeatability Test for Effect of Injection Pressure on IMEP

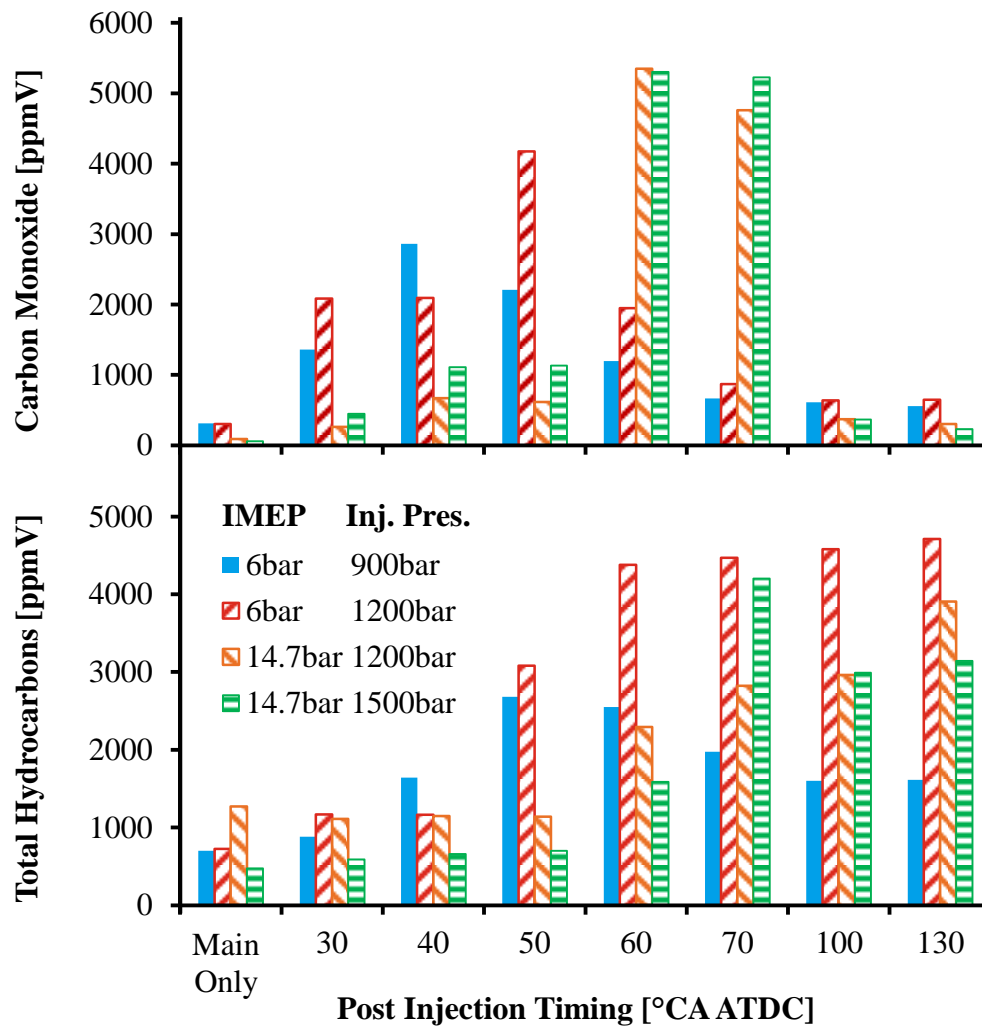


Figure H-3: Effect of Injection Pressure on CO and THC Emissions

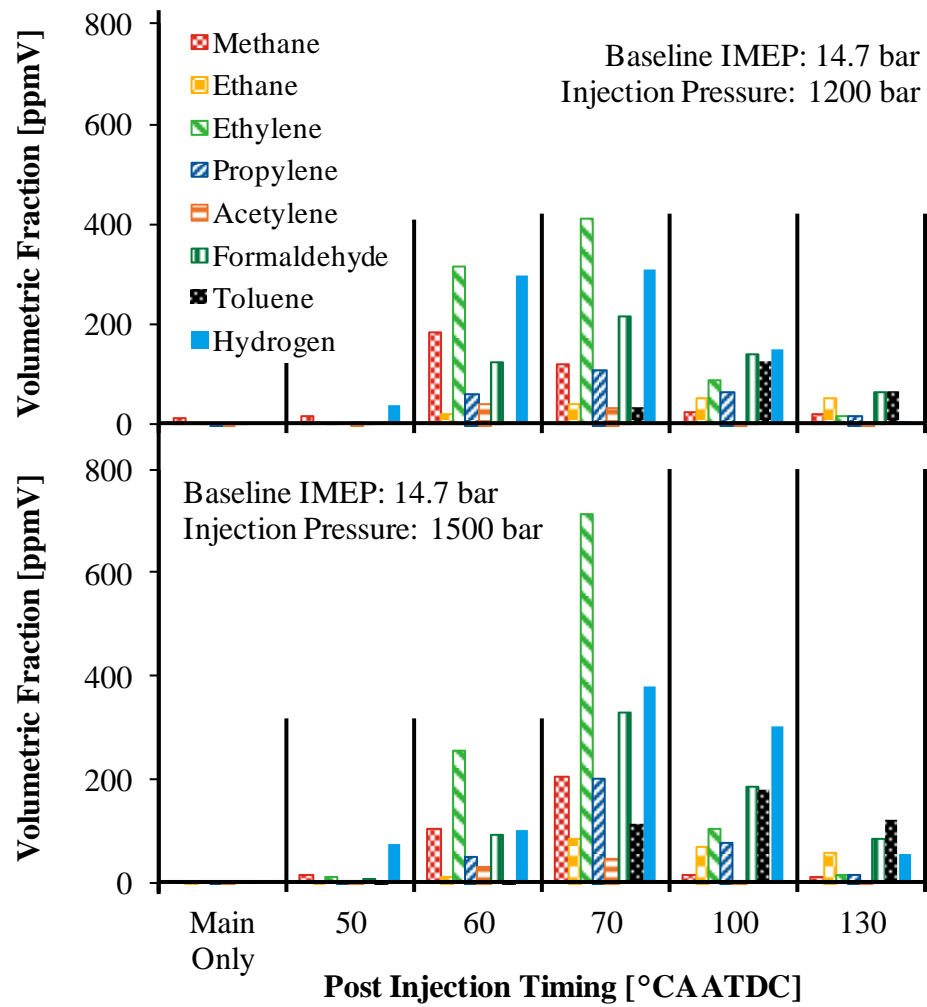


Figure H-4: Effect of Injection Pressure on Hydrocarbon Speciation (14.7 bar)

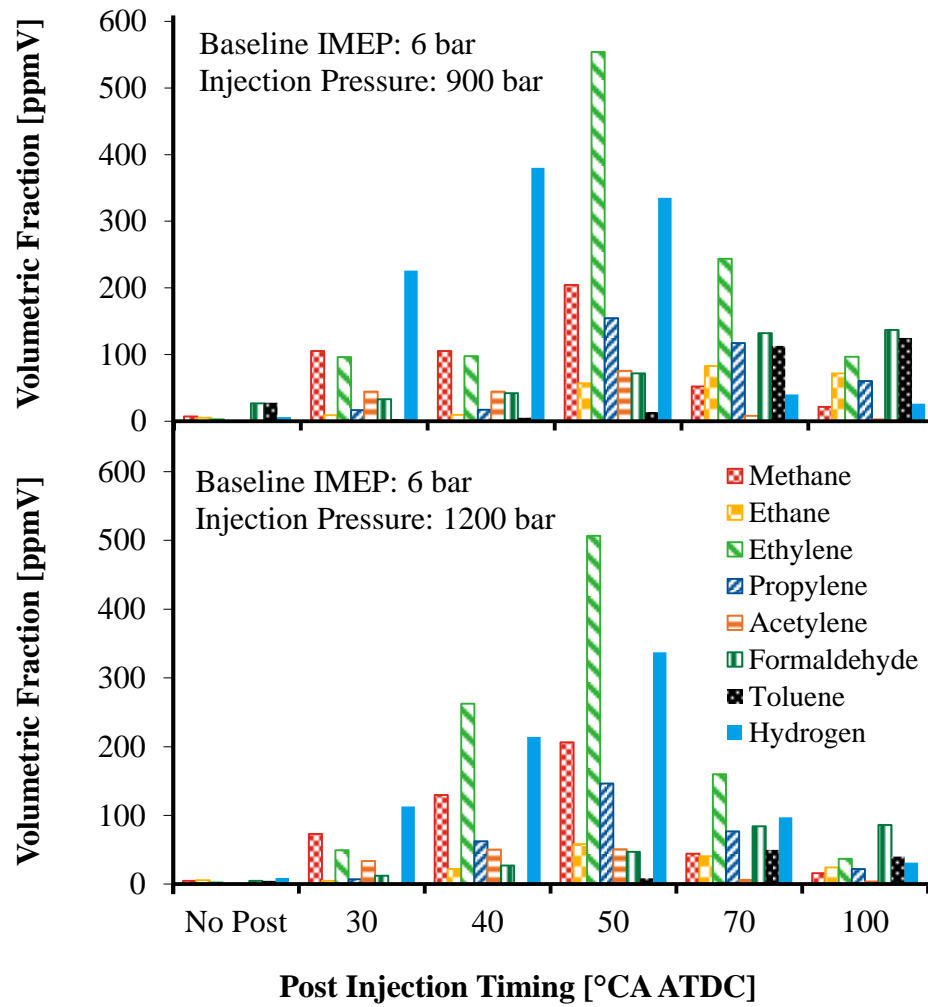


Figure H-5: Effect of Injection Pressure on Hydrocarbon Speciation (6 bar)

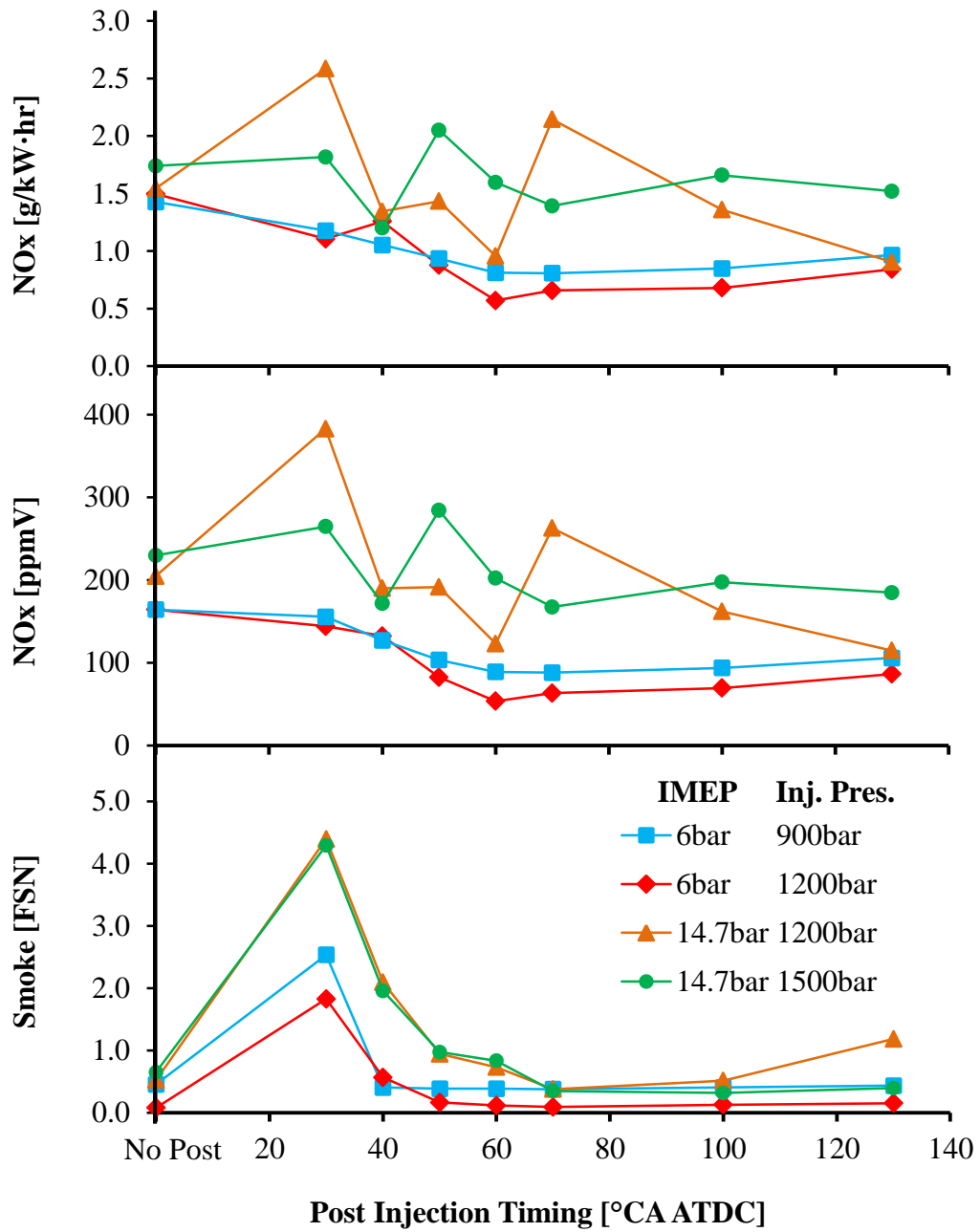


Figure H-6: Effect of Injection Pressure on NO_x and Smoke Emissions

LIST OF AUTHORED AND CO-AUTHORED PUBLICATIONS

Articles Published in Refereed Journals

1. **Jeftić, M.**, Yang, Z., Reader, G.T., and Zheng, M., “Fuel Efficiency Analysis and Peak Pressure Rise Rate Improvement for Neat n-Butanol Injection Strategies”, Proceedings of the Institution of Mechanical Engineers, Part D: Journal of Automobile Engineering (Article in Press), 16 Pages, 2016.
2. **Jeftić, M.**, and Zheng, M., “Post Injection Strategy for the Reduction of the Peak Pressure Rise Rate of Neat n-Butanol Combustion”, Journal of Engineering for Gas Turbines and Power (Article in Press), 9 Pages, 2016.
3. **Jeftić, M.**, and Zheng, M., “A study of the Effect of Post Injection on Combustion and Emissions with Premixing Enhanced Fueling Strategies”, Journal of Applied Energy 157: 861-870, 2015.
4. **Jeftić, M.**, and Zheng, M., “Lean NO_x Trap Supplemental Energy Savings with a Long Breathing Strategy,” Proceedings of the Institution of Mechanical Engineers, Part D: Journal of Automobile Engineering, 227 (3): 400-408, 2013.
5. **Jeftić, M.**, Yu, S., Han, X., Reader, G.T, Wang, M., and Zheng, M., “Effects of Postinjection Application with Late Partially Premixed Combustion on Power Production and Diesel Exhaust Gas Conditioning,” Journal of Combustion, vol. 2011, Article ID 891096, 9 pages, 2011.

Papers in Refereed International Conference Proceedings

6. **Jeftić, M.**, Tjong, J., Reader, G.T., Wang, M., et al., "Combustion and Exhaust Gas Speciation Analysis of Diesel and Butanol Post Injection," SAE Technical Paper 2015-01-0803, 13 Pages, 2015.
7. **Jeftić, M.**, Asad, U., Han, X., Xie, K., Yu, S., Wang, M., and Zheng, M., "An Analysis of the Production of Hydrogen and Hydrocarbon Species by Diesel Post Injection Combustion," ICEF2011-60135, Proceedings of the ASME Internal

Combustion Engine Division Fall Technical Conference, 9 Pages, 2011, Morgantown, WV.

8. **Jeftić, M.**, Yu, S., Chen, X., Xu, X., Wang, M., Zheng, M., "Diesel Active-Flow Aftertreatment Control on a Heated Flow Bench," IMECE2010-39057, Proceedings of the ASME International Mechanical Engineering Congress and Exposition, 7 Pages, 2010, Vancouver, BC.
9. Gao, T., **Jeftić, M.**, Bryden, G., Reader, G.T., Tjong, J., Zheng, M., "Heat Release Analysis of Clean Combustion with Ethanol Ignited by Diesel in a High Compression Ratio Engine", SAE Technical Paper 2016-01-0766, 11 Pages, 2016.
10. Asad, U., Mendoza, A., Xie, K., **Jeftić, M.**, Wang, M., and Zheng, M., "Speciation Analysis of Light Hydrocarbons and Hydrogen Production during Diesel Low Temperature Combustion," ICEF2011-60130, Proceedings of the ASME Internal Combustion Engine Division Fall Technical Conference, 10 Pages, 2011, Morgantown, WV.
11. Yu, S., Xie, K., Han, X., **Jeftić, M.**, Gao, T., and Zheng, M., "A Preliminary Study of the Spark Characteristics for Unconventional Cylinder Charge with Strong Air Movement," ICEF2011-60132, Proceedings of the ASME Internal Combustion Engine Division Fall Technical Conference, 10 Pages, 2011, Morgantown, WV.

Papers in Non-Refereed Conference Proceedings

12. **Jeftić, M.**, Gao, T., and Zheng, M., "Post Injection Strategies for Increased Power Output of Neat n-Butanol Combustion in a Compression Ignition Engine", Proceedings of Combustion Institute – Canadian Section Spring Technical Meeting, 6 Pages, 2016, Waterloo, ON.
13. **Jeftić, M.**, Yang, Z., Ting, D., and Zheng, M., "An Investigation of the Optimal Post Injection Timing for Diesel Engine Exhaust After-treatment", Proceedings of

Combustion Institute – Canadian Section Spring Technical Meeting, 6 Pages, 2014, Windsor, ON.

14. **Jeftić, M.**, and Zheng, M., “Investigation of Lean NO_x Trap Storage Characteristics and Exhaust Fuel Reformer Performance with AVL FIRE,” Proceedings of the AVL AST User Conference, 13 Pages, 2013, Graz, Austria.
15. **Jeftić, M.**, Asad, U., Tjong, J., Wang, M., Reader, G.T., and Zheng, M., “Ultra-low NO_x with Diesel Enhanced Premixed Combustion and a Long-breathing Lean NO_x Trap Strategy,” Proceedings of the Global Emissions Congress, 13 Pages, 2011, Ann Arbor, MI.
16. **Jeftić, M.**, Meng, Z., Xu, X., and Zheng, M., “Heated Flow Bench Test for Aftertreatment Control,” Proceedings of Combustion Institute – Canadian Section Spring Technical Meeting, 8 Pages, 2010, Ottawa, ON.

Patents Accepted for Evaluation

17. Zheng, M., Yu, S., **Jeftić, M.**, and Wang, M., “In-Cylinder Temperature Measurement with Thermocouple and RTD via Multi-Hole Ceramic Spark Plug Adapter”, Chinese Patent No. 201620078311.4, 2016.
18. de Ojeda, W., Zheng, M., Han, X., **Jeftić, M.**, and Wang, M., “Long Breathing Lean NO_x Trap with Low Pressure Exhaust Gas Recirculation Loop”, U.S. Patent and Trademark Office, U.S. Patent & Trademark Office, US20150113961 A1, 2013.

Selected Poster Presentations

19. **Jeftić, M.**, and Zheng, M., "Post Injection Characterization", NSERC CREATE Program for Clean Combustion Engines, Combustion Summer School, 2015, Windsor, ON.

20. **Jeftić, M.**, Gao, T., and Xie, X., "Diesel Injector Characterization", NSERC CREATE Program for Clean Combustion Engines, Combustion Summer School, 2014, Toronto, ON.
21. **Jeftić, M.**, "Clean Diesel Combustion and Emission Control", Annual General Meeting: ORF-RE: Green Auto Power Train, 2012, Windsor, ON.
22. **Jeftić, M.**, Gao, T., Yu, S., Asad, U., Han, X., Xie, K., Zhang, X., Mendoza, A., Wang, M., Reader, G.T., Chen, X., and Zheng, M., "Theme 2: Diesel and Diesel-Electric Power Train," Annual General Meeting: ORF-RE: Green Auto Power Train, 2010, Waterloo, ON.
23. **Jeftić, M.**, Asad, U., Han, X., Tan, T., Rajaei, N., Lin, F., Kumar, R., Wang, M., "Second Generation Biofuels for Sustainable Transportation," Auto21 Annual Conference, 2009, Hamilton, ON.
24. **Jeftić, M.**, Asad, U., Han, X., Tan, Y., Rajaei, N., Lin, F., Kumar, R., and Wang, M., "Enabling Biodiesel Fuel Use for Sustainable Mobility," Auto21 HQP Colloquium, 2009, Windsor, ON.
25. Gao, T., Divekar, P., **Jeftić, M.**, Xie, K., Han, X., Yu, S., Asad, U., Haggith, D., and Wang, M., "Flexible Operation of HCCI Combustion using Intelligent Control," Auto21 Annual Conference, 2011, Ottawa, ON.
26. Divekar, P., Lin, F., Gao, T., Han, Q., Han, X., **Jeftić, M.**, Mendoza, A., Xie, K., Zhang, X., Asad, U., Kumar, R., Mulenga, C., Wang, M., and Yu, S., "Clean Diesel Engine Technologies: Past, Present, Future and Beyond," 10th Year Canada Research Chairs - Thinking Ahead for a Strong Future Conference Series: Ontario Region, 2010, Toronto, ON.
27. Han, X., Asad, U., Tan, Y., Rajaei, N., Lin, F., **Jeftić, M.**, Kumar, R., and Wang, M., "Flexible Operation of HCCI Combustion Using Intelligent Control," Auto21 Annual Conference, 2009, Hamilton, ON.

VITA AUCTORIS

Marko Jeftić was born in Tuzla, Yugoslavia in 1985. In early childhood, he immigrated with his parents to Windsor, Canada. After completing his high school studies at Riverside Secondary School in Windsor, Ontario, he attended the University of Windsor's mechanical engineering program. He received his Bachelor's Degree of Applied Science with Distinction in 2007. Marko joined the Clean Diesel research group as a graduate student at the University of Windsor in 2009. He received his Master of Applied Science degree in 2011.